INTERNATIONAL DOCTORAL
SCHOOL OF THE USC

Javier
López Vázquez

PhD Thesis

Analytical Assessment of the Impact of Microplastics, Perfluoroalkylated Substances, and Related Chemicals on Human and Environmental Health

Santiago de Compostela, 2023

Doctoral Programme in Chemical Science and Technology

ESCOLA DE DOUTORAMENTO
INTERNACIONAL DA USC

TESE DE DOUTORAMENTO

ANALYTICAL ASSESSMENT OF THE IMPACT OF MICROPLASTICS, PERFLUOROALKYLATED SUBSTANCES, AND RELATED CHEMICALS ON HUMAN AND ENVIRONMENTAL HEALTH

Javier López Vázquez

Directores: Mª del Rosario Rodil Rodríguez

José Benito Quintana Álvarez

PROGRAMA DE DOUTORAMENTO EN CIENCIA E TECNOLOXÍA QUÍMICA

SANTIAGO DE COMPOSTELA

2023

DECLARATION OF INTERESTS

I herein declare that I have no known competing financial interests or personal relationships that could influence the work reported in this tesis.

ATTRIBUTIONS TO THE FIGURES

All original figures and charts included in this Thesis were prepared by myself using the following softwares ChemDraw® (21.0.0.28 version), Adobe® Illustrator (26.2.1 version), Statgraphics® Centurion 18 (18.1.14 version), Origin® (8.5.0 version), Grapher® (16.9.3 version), Microsoft® PowerPoint® (2309 version), BioRender® and Freepik®.

INSTITUTIONAL ACKNOWLEDGEMENTS

I would like to express my gratitude to Agilent for providing access to LC-ESI-MS/MS instrumentation and technical assistance, to Restek for the kind gift of the Biphenyl column used to determine the metabolites of phthalate esters in the bioaccessibility analyses, to "Centro de Supercomputación de Galicia (CESGA)" for the use of their computational resources for screening data processing and to Applus Norcontrol S.L.U. for the collaborative work carried out in the AMBAR project.

FUNDING

This thesis would not be possible without the financial support of the following institutions:

- Xunta de Galicia, Consellería de Cultura, Educación e Universidades (ref. ED431C 2021/06).
- Ministerio de Ciencia, Innovación y Universidades - Agencia Estatal de Investigación, MCIN/AEI/ 10.13039/501100011033 (ref. CTM2017-84763-C3-R-2, co-funded by the European Regional Development Fund / Fondo Europeo de Desenvolvemento Rexional (ERDF/FEDER); PID2020-117686RB-C32; CTM2017-90980-REDT; and TED2021-129200B-C41, funded through NextGeneration/PRTR funds).
- Axencia Galega de Innovación (GAIN) - Xunta de Galicia (ref. 001_IN853D-2022).

AGRADECEMENTOS

O camiño que culminou na realización desta tese de doutoramento foi unha viaxe de descubrimento, aprendizaxe e crecemento persoal e académico. Durante anos, tiven o privilexio de mergullarme nun mundo de coñecemento e exploración, e esta tese é o resultado dese compromiso e esforzo.

Chegados a este punto, só quero expresar o meu sincero agradecemento a todas as persoas que, de maior ou menor maneira, colaboraron no éxito que hoxe me permite escribir esta tese. Sabendo que é imposible mencionar a todas as persoas ás que me gustaría agradecer, desexo que saiban que a súa axuda e apoio non foron esquecidos durante este percorrido.

En primeiro lugar, agradecer aos meus directores de tese José Benito Quintana Álvarez e Mª del Rosario Rodil Rodríguez (**Tito** e **Charo**) pola súa orientación experta, apoio constante e paciencia infinita. Os seus valiosos consellos e coñecementos foron fundamentais para conseguir os obxectivos fixados e dar forma a esta investigación.

Gustaríame agradecerlle tamén a **Rafael** que me acollese no grupo de investigación (ChromChem), que sería a miña segunda casa durante un lustro. Grazas a **Isaac** e **María** cos que tiven o gusto de compartir espazo de traballo e incluso traballar con eles xa sexa envolvéndome nalgún proxecto ou impartindo docencia. Moitas grazas a **Rosa** por estar sempre ao pé do canón para botarme(nos) unha man cando era preciso, pola paciencia, axuda e as bromas diarias.

Botando unha vista atrás aos meus inicios, eu comecei a finais do 2018 con ilusión e ganas de mergullarme neste mundo que é a investigación e non tiven unha mellor benvida no laboratorio que coñecer aos meus primeiros compañeiros cos que faríamos unha piña. Graciñas **Leti** fuches e eres un apoio moi grande durante esta etapa e non podería agradecerche en palabras todo o que fixeches por min. Grazas pola túa predisposición a axudar sempre ós demais, por ser un exemplo a seguir e incluso tivemos a oportunidade de compartir proxecto e mesa xuntos. Gazas **Gabi** e por partida dobre con esa volta recente ao laboratorio, déchesme unha calurosa benvida e un apoio importante durante o desenrolo da mesma cando máis o necesitaba e que aínda segues facendo. Grazallas, **Beni** por ser o meu primeiro compañeiro de mesa, polas anécdotas da túa experiencia durante a tese e por botarme unha man cando estaba tan perdido ao comezo. Agradecer tamén a **Iria**, **Sara** e **Vero** coas que tiven o pracer de traballar e compartir pausas para café que tan necesarias eran.

Co paso do tempo chegaron novos compañeiros cos que faríamos un novo grupo novamente unido e con moi bo ambiente co que traballar e desconectar. Agradecer en primeiro lugar a **Andrea** pola súa enerxía coa que contaxiaba a todo o laboratorio e ao seu compañeiro de aventuras, **Miguel** porque sempre serei o seu casual favorito. Gracias **Vicky** por estar aí e ser máis cunha compañeira de laboratorio, por escoitarme e darme consellos. Grazas **Sandra** polas risas e conversas traballando no laboratorio e nos descansos. Agradecer a **Xiana** e **Mauricio** as boas conversas na hora do café que facían máis ameno o día a día. Por último, á sangue nova con **Carlos** que comeza o camiño, solo dicirche que mires sempre cara adiante e que nada te pare. Aínda que non me quero esquecer tampouco de **Tania** o teu tempo polo laboratorio foi curto, pero cargado de boas experiencias e que incluso chegamos a compartir traballo de forma satisfactoria, espero que che vaia ben na túa nova aventura.

Me gustaría agradecer también a **Manel Miró** y su grupo por su acogida en Mallorca para realizar mi primera estancia, fue un placer trabajar con vosotros y me llevo muy buenos recuerdos de esa ciudad y la gente. Moltes graciès.

There are also people outside Spain I want to give thanks too. Obrigado Professor **Vítor Vilar** and **Francisca Moreira** for supporting me in Porto, knowing another country, another

city, another lab and that allowed me to get to know people with whom I would collaborate in the future.

A la familia que se elige desde pequeño como son los incombustibles **Porto** y **Vidu** con los que tantas aventuras hemos pasado y las que nos quedan por vivir juntos, la desconexión en Lugo sin vosotros no sería la misma y aunque nos veamos solo los findes, sabemos que nos tenemos ahí para lo que sea. Si juntamos en la ecuación a **María** y **Raquel** son risas aseguradas. Mención especial para **Marcos**, amigo, hermano y actualmente, familia, un orgullo ser padrino de tu hijo y aunque nos separen miles de quilómetros, siempre nos ponemos al día cuando podemos. A mis pilares fundamentales fuera de casa, como son don **Iago**, gracias por esas tardes de liberar tensión por el trabajo, ya sabes que eres como un hermano para mí y don **Ángel** muchos momentos juntos que nos hacen estar muy unidos, aunque estemos en diferentes puntos, pero a la mínima que podemos siempre hacemos una escapadita para Madrid y nos ponemos al día.

Á miña familia que tanto me apoiou en todas as miñas etapas da vida dende a distancia por aquel ano 2012. Grazas **papá** e **mamá** pola educación, valores e consellos que me distedes, sen vos todo isto que logrei ata o de agora non sería posible e sempre vos estarei agradecido.

E, por último, á persoa máis importante e pilar fundamental, o meu irmán **Miguel**. Inseparables dende que viñen ao mundo e un apoio crucial na miña vida. Nunca me cansarei de darche ás grazas, gracias por todo o que fas e fixeches por min, por estar aí tanto nos bos e malos momentos. Aínda que non falemos tanto como deberíamos pola distancia, sabes que eres como un pai para min e sen dúbida, a miña gran sorte na vida.

Moitas grazas a esas persoas coas que coñecín e que foron un apoio moi importante durante este último ano.

Grazas.

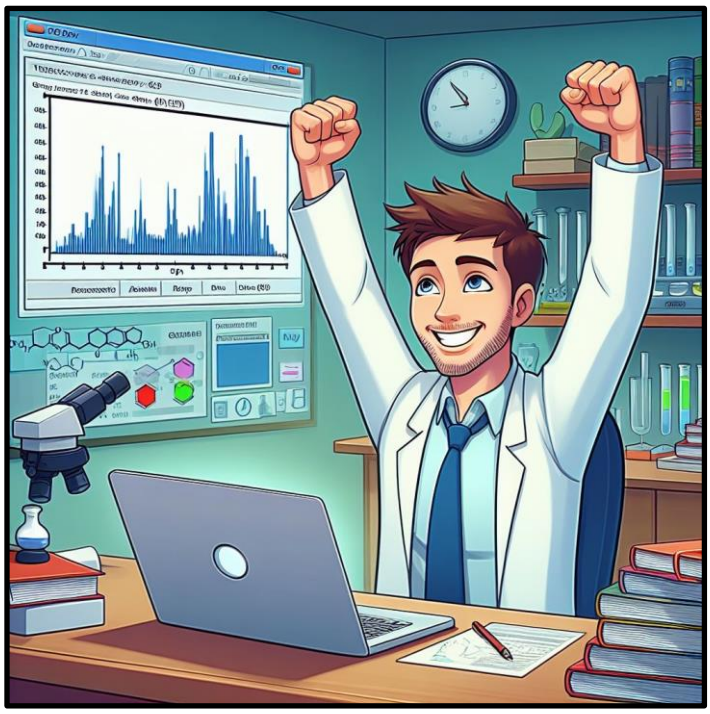

“One of my goals is to learn more than is absolutely necessary.”

-Jules Verme-

INDEX

INDEX

ABBREVIATIONS

ABBREVIATIONS

A

Accelerated solvent extraction - ASE
Acrylonitrile butadiene styrene - ABS
Advanced oxidation process - AOP
Analysis of variance - ANOVA
Atmospheric pressure chemical ionization - APCI
Attenuated total reflection - ATR
Average daily intake - ADI

B

Bioaccessible fraction - BF
Bioaccessibility Research Group of Europe - BARGE
Benzylbutyl phthalate - BzBP
Bisphenol A - BPA
Boron-doped diamond - BDD
Bovine serum albumin - BSA
Brominated flame retardant - BFR
Butylated hydroxytoluene - BHT

C

Cellulose acetate - CA
Certified reference material - CRM
Chemical oxygen demand - COD
Collision energy - CE
Cone voltage - CV
Contaminant of emerging concern - CEC

D

Daily intake - DI
Data-dependent acquisition - DDA
Data-independent acquisition - DIA
Dichloromethane - DCM
Diethyl phthalate - DEP
Di(2-ethylhexyl) phthalate - DEHP
Di(2-propylheptyl) phthalate - DPHP
Dimethyl phthalate - DMP
Dimethyl sulfoxide - DMSO
Diisobutyl phthalate - DiDP
Diisodecyl phthalate - DiDP
Diisononyl phthalate - DiNP
Dynamic Multiple Reaction Monitoring (dMRM)
Di-n-butyl phthalate - DnBP
Di-n-octyl phthalate - DnOP
Dispersive liquid-liquid microextraction - DLLME
Dissolved organic carbon - DOC
Drinkwater treatment plant - DWTP

E

Electrochemical advanced oxidation process - EAOP
European Food Safety Authority - EFSA
Electron ionization - EI
Electrospray ionization - ESI
European Commission - EC
European Council for Plasticisers and Intermediates - ECPI
European Chemicals Agency - ECHA
Ethanol - EtOH
Ethyl acetate - AcOEt
Ethylene-vinyl acetate - EVA
2-Ethylhexyl salicylate - EHS

F

Fed organic estimation human simulation test - FOREhST
Fluorotelomer sulfonate - FTSA
Fluorooctane sulfonamide - FOSA
Fluorooctane sulfonamidoethanol - FOSE
Fluoro-1-octanesulfonamidoacetic acid - FOSAA
Fluorotelomer carboxylic acid - FTCA
Fluorotelomer unsaturated carboxylic acid - FTUCA
Fourier-transform infrared spectroscopy - FTIR

G

Gas chromatography - GC
Gastrointestinal tract - GIT

H

Hexabromocyclodecane - HBCD
Hexafluoropropylene oxide dimer acid - HFPO-DA / Gen X
High-density polyethylene - HDPE
High-resolution mass spectrometry - HRMS
High-water mark - HWM
Hydrogen evolution reaction - HER
Hydrophilic-Lipophilic Balance - HLB

I

ICIS Chemical Business - ICB
Instrumental limit of quantification- iLOQ
Internal standard - IS
Ion mobility spectrometry - IMS

J

JAMSTEC microplastic-sediment separator - JAMSS

L

Limit of detection - LOD
Limit of quantification - LOQ
Liquid chromatography - LC
Liquid-liquid extraction - LLE
Low-density polyethylene - LDPE
Low-water mark - LWM

M

Marine Strategy Framework Directive - MSFD
Mass spectrometry - MS
Mass spectrometry in tandem - MS/MS
Methanol - MeOH
Method limit of quantification - mLOQ
Microplastic - MP
Microplastics-separator design approach - µSEP
Microwave - MW
Milli-Q® water - MQ
Monobenzyl phthalate - MBzP
Monobutyl phthalate - MBP
Monoethyl phthalate - MEP
Mono-(2-ethyl-5-carboxylpentyl) phthalate - MECPP
Mono-(2-ethylhexyl) phthalate - MEHHP
Mono-(2-ethyl-5-oxohexyl) phthalate - MEOHP
Mono-(hydroxyisononyl) phthalate - MHINP
Monomethyl phthalate - MMP
Munich Plastic Sediment Separator - MPSS

N

Nanofiltration concentrate - NF
National Institute of Standards and Technology - NIST
National Oceanic and Atmospheric Administration - NOAA
N-methyl-N-(trimethylsilyl) trifluoroacetamide - MSTFA
N-octanol-water distribution coefficients - D_{ow}
Nondispersive infrared detector - NDIR

O

Organisation for Economic Co-operation and Development - OECD
Organochlorine pesticide - OCP
Organophosphate flame retardant - OPFR
Oxygen evolution reaction - OER

P

Phthalic acid ester - PAE
Per- and polyfluoroalkyl substance - PFAS
Perfluoroalkyl carboxylic acid - PFCA
Perfluoroalkyl chain length - PCL
Perfluorobutanoic acid - PFBA
Perfluorobutane sulfonic acid - PFBS
Perfluorodecanoic acid - PFDA
Perfluorodecane sulfonic acid - PFDS
Perfluorododecanoic acid - PFDoA
Perfluorododecanesulfonic acid - PFDoS
Perfluoroethanesulfonic acid - PFEtS
Perfluoroheptanoic acid - PFHpA
Perfluoroheptanesulfonic acid - PFHpS
Perfluorohexanoic acid - PFHxA
Perfluorohexane sulfonic acid - PFHxS
Perfluoromethanesulfonic acid - PFMS

P

Perfluorononanoic acid - PFNA
Perfluorononanesulfonic acid - PFNS
Perfluorooctanoic acid - PFOA
Perfluorooctane amido betaine - PFOAB
Perfluorooctane sulfonate - PFOS
Perfluorooctane sulfonamidoacetate - PFOSAA
Perfluoropentanoic acid - PFPeA
Perfluoropentanesulfonic acid - PFPeS
Perfluoropropanoic acid - PFPrA
Perfluoropropanesulfonic acid - PFPrS
Perfluorosulfonic acid - PFSA
Perfluorotetradecanoic acid - PFTeDA
Perfluorotridecanoic acid - PFTrDA
Perfluorotridecanesulfonate - PFTrDS
Perfluoroundecanoic acid - PFUdA
Perfluoroundecanesulfonic acid - PFUdS
Peroxide-cured ethylene propylene diene monomer - EPDM
Persistent organic pollutant - POP
Physiologically based extraction test - PBET
Polyamide - PA
Polybrominated diphenyl ether - PBDE
Polycarbonate - PC
Polychlorinated biphenyl - PCB
Polycyclic aromatic hydrocarbon - PAH
Polydimethylsiloxane - PDMS
Polyethylene - PE
Polyethylene terephthalate - PET
Polymethyl methacrylate - PMMA
Polyoxymethylene - POM
Polypropylene - PP
Polystyrene - PS
Polytetrafluoroethylene - PTFE
Polyurethane - PU
Polyvinyl alcohol - PVA
Polyvinyl chloride - PVC
Principal component analysis - PCA

Q

Quantitative nuclear magnetic resonance - qNMR
Quality control - QC

R

Reference dose - RfD
Registration, Evaluation, Authorisation and Restriction of Chemicals - REACH
Relative recoveries - RR
Relative standard deviation - RSD
Retention index - RI
Retention time - RT
Reverse osmosis concentrate - RO

R

Room temperature - RT

S

Sediment-Microplastic Isolation - SMI
Selected-ion monitoring mode - SIM
Selected reaction monitoring - SRM
Signal to noise - S/N
Simulation of the human intestinal microbial ecosystem - SHIME
Solid-phase extraction - SPE
Solid-phase micro extraction - SPME
Standard Methods for the Examination of Water and Wastewater - SMEWW
Styrene-divinylbenzene - SDB

T

Tetrabromobisphenol A - TBBPA
Tetrahidrofuran - THF
Thermal extraction desorption - TED
Thermogravimetric analysis - TGA
Time-of-flight - TOF
Tolerable daily intake - TDI
Toluene - Tol
Total oxidizable precursor assay - TOPA
Trifluoroacetic acid - TFA
Triple quadrupole - QqQ
Tris(2-chloroethyl) phosphate - TCEP
Tris(1-chloro-2-propyl) phosphate - TCPP
Tris(1,3-dichloro-2-propyl) phosphate - TDCPP

U

Unified BARGE method - UBM
Ultra-high performance liquid chromatography - UHPLC
Ultrapure water - UPW
Ultrasonic solvent extraction - USE
United States Environmental Protection Agency - USEPA
Ultraviolet radiation - UV
Urban wastewater after secondary treatment - UWW

V

Visual stochastic network embedding - viSNE

W

Wastewater treatment plant - WWTP
Weak anion exchange - WAX

LIST OF FIGURES

LIST OF FIGURES

LIST OF TABLES

LIST OF TABLES

ABSTRACT

ABSTRACT

In today's world, given the extensive production and widespread use of plastics in our society, it is essential to fully grasp the potential risks they pose to both human health and the environment. Therefore, the detection of microplastics (MPs) and their associated contaminants assumes a pivotal role in uncovering their potential effects. MPs have the capability to sorb from the surrounding environment and transport these (hazardous) chemicals and many others which are intentionally added to plastic to improve their properties (i.e. plastic additives) or during synthesis (e.g. monomers). This raises the concern of their potential introduction into our food and water supply, thus constituting a direct threat to human health but also to aquatic organisms. The detection of these minute particles and their associated plastic-related chemicals is imperative for mitigating the ecological repercussions of their presence in freshwater and marine environments. Consequently, there is a pressing need for dependable methodologies to identify and quantify MPs and the related chemical compounds.

In this context, advancements in sample preparation, such as density separation for isolating MPs from environmental matrices, coupled with analytical techniques like nuclear magnetic resonance (NMR) are of interest. On the other hand, liquid chromatography-high-resolution mass spectrometry (LC-HRMS), and gas chromatography (GC)-HRMS systems, have enabled the detection of a multitude of compounds associated with MPs, either plastic-related chemicals or substances sorbed to them from the surrounding environment.

Besides MPs themselves and the many classes of plastic-related chemicals, this thesis also considers per- and poly-fluoroalkylated substances (PFAS), not only because they can be associated to plastic polymers (e.g. polytetrafluoroethylene or sorbed from the environment to MPs), but also because of their environmental persistence and recent regulatory concerns.

Therefore, this thesis considers several aspects on the determination of MPs, PFAS and plastic-related chemicals in the environment. This involves the development of a novel density separation and NMR quantification method. Additionally, the research conducted aims to identify compounds associated with MPs exposed to the marine environment. In the subsequent phase, the study delves into the assessment of phthalate acid esters (PAEs) and bisphenol A (BPA) associated to MPs introduction into both human and environmental organisms, by calculating their bioaccessibility through *in-vitro* simulations with established methods. Finally, the implementation of a novel regulation (Directive 2020/2184/EU) PFAS in drinking water necessitates the development of methodologies for their quantification and the development of novel removal technologies, as e.g. using anodic electrochemical oxidation, that can safeguard human and environmental health.

Thus, in detail, this thesis presents a compilation of 6 smaller and interconnected research projects which are summarised below:

- Screening of organic chemicals associated to virgin low-density polyethylene MP pellets exposed to the Mediterranean Sea environment by combining GC and LC coupled to quadrupole-time-of-flight mass spectrometry (**Results and discussion section 4.1**).

This study investigated the presence of organic chemicals associated with MPs exposed to a human-influenced coastal environment for a duration of up to eight weeks. The aim was to understand the dynamics of (de)sorption of chemicals in/from the marine ecosystem. Primary

low-density polyethylene (LDPE) pellets produced by the plastic industry were investigated, as they represent a significant contribution of MPs to the oceans. To enhance the scope of detectable chemicals, both LC and GC coupled to quadrupole-time-of-flight (QTOF)-MS were employed. In LC-HRMS, an electrospray ionization source and both a suspect and non-target screening workflows were used. On the other hand, GC-HRMS was equipped with an electron ionization source, and compounds were screened in both raw and derivatized (silylated) extracts through deconvolution and comparison to high- and low-resolution MS libraries. Finally, the compounds that could be confirmed with standards were quantified to better understand their dynamics along the 8-week exposure period.

- Combination of a novel cost-effective glass density separator followed by quantitative ^{1}H-NMR spectroscopy for the determination of MPs in marine sediments (**Results and discussion section 4.2**).

This work introduces an innovative, portable, and cost-effective glass-made separator, for the separation of MPs, specifically polyethylene terephthalate (PET), polyvinyl chloride (PVC), and LDPE, utilizing the density flotation principle, from marine sediments. The separation process employed a unique homemade 3-part glass setup and a separation solution comprising 1.5 L of zinc chloride with a density of 1.6 g/cm^3. Following a Fenton oxidation clean-up, the proposed analytical method involves quantitative ^{1}H-NMR spectroscopy after solubilizing the microplastics in suitable deuterated solvents. As a proof-of-principle application, sediment samples from three distinct locations along the Galician coast (Northwest Spain) were analysed using the developed methodology, were PET and LDPE MPs could be quantified.

- Mimicking human ingestion of MPs: oral bioaccessibility tests of BPA and PAEs under fed and fasted states (**Results and discussion section 4.3**).

Despite the identification of MP fragments in human stool, limited attention has been directed toward understanding the impact of chemical additives on human health. This study employed standardized *in-vitro* bioaccessibility tests under both fasting and fed conditions to investigate the oral bioaccessibility of plastic additives and monomers (specifically, eight PAEs and BPA) in certified reference MP materials made of LDPE and PVC. The study also evaluated the generation of phthalate monoesters throughout the bioaccessibility tests. The proposed method allows for the accurate assessment of oral bioaccessible pools of moderately to non-polar PAEs for risk-assessment explorations.

- *In-vitro* leaching and physiologically relevant extraction tests for PAEs and BPA from MPs - Assessing the contribution of MPs to the exposure of marine vertebrates towards plastic-related chemicals (**Results and discussion section 4.4**).

Marine vertebrates are recognized for consuming significant quantities of MPs. Once ingested, MPs have the potential to induce gastrointestinal injuries and act as a conduit for the transmission of harmful plastic components, such as PAEs and BPA, within the food chain. However, a deficiency exists in standardized *in-vitro* methods capable of simulating the uptake of chemicals from MPs by fish. Thus, this study addressed this gap by conducting leaching and bioaccessibility tests on PAEs and BPA from MPs using artificial seawater and gut fluids that replicate the gastric, intestinal, and gastrointestinal compartments of marine vertebrates. The tests were performed on certified reference materials of LDPE and PVC containing eight PAEs of varying hydrophobicity and BPA (only in LDPE) as MP surrogates, maintaining realistic analyte concentrations The bioaccessibility results were further utilized for estimating fish daily intake from MPs and compare them with seawater ingestion, under various scenarios.

- Determination of regulated PFAS in drinking water according to Directive 2020/2184/EU (**Results and discussion section 4.5**).

PFAS are chemical compounds extensively utilized in industrial processes and manufacturing. The widespread occurrence, persistence, and recent toxicological findings have led to the regulation of 20 PFAS (carboxylic and sulfonic acids) in drinking water under Directive 2020/2184/EU. This directive encompasses PFAS with varying carbon chain lengths (C4-C13) and imposes a maximum total PFAS concentration (sum) of 0.1 µg/L, necessitating law-compliant analytical methods. In this study, three distinct methodologies were developed and assessed for their efficacy in determining these 20 PFAS in tap and bottled water. These methodologies involve on-line and off-line solid-phase extraction (SPE) as well as direct injection on ultra-high-pressure liquid chromatography-tandem mass spectrometry (UHPLC-MS/MS) was consistently employed as the determination technique. The optimal methodology (off-line SPE followed by UHPLC-MS/MS analysis) was then applied to analyse different Spanish and international mineral water brands and tap water samples to assess compliance with the new regulations.

- Insights into the application of the anodic oxidation process for the removal of PFAS in water matrices (**Results and discussion section 4.6**).

The current study addressed significant knowledge gaps related to the application of the anodic oxidation process utilizing boron-doped diamond (BDD) anodes for remediating water matrices contaminated with PFAS. This investigation encompassed several key aspects: (i) the degradation assessment of ultrashort-chain (C1-C3), short- and medium-chain (C4-C8) and long-chain (C9-C13) PFAS; (ii) exploring multi-solute systems featuring different PFAS concentrations (0.2 to 2.0 µg/L) and variations (24 C1-C13 *versus* 8 C1-C8 mixtures), in addition to single-solute systems; (iii) investigating the utilization of real water matrices alongside pure water; and (iv) evaluating the impact of elevated current densities (*j*) up to 250 mA/cm^2, in contrast to the usual j ($\leq$20 mA/cm^2).

RESUMO

RESUMO

No contexto actual, dado a extensa produción e uso xeneralizado de plásticos na nosa sociedade, é esencial comprender os posibles riscos que representan tanto para a saúde humana como para o medio ambiente. Neste senso, os microplásticos (MPs), definidos como partículas plásticas inferiores a 5 mm, considéranse unha nova clase de contaminantes ambientais persistentes de preocupación global. Poden chegar ao medio ambiente directamente a partir de produtos manufacturados que conteñen MPs (por exemplo, algúns produtos de coidado persoal), é dicir, MP primarios, ou formarse no medio ambiente debido á degradación, transformación e deterioración dos (micro)plásticos orixinais provocados, por exemplo, pola fotooxidación ou procesos físicos, é dicir, os coñecidos como MPs secundarios. Por iso, a detección de MPs e dos contaminantes asociados cobra un papel fundamental para revelar os seus posibles efectos. Os MPs teñen a capacidade de ad/absorber e transportar substancias químicas perigosas, moitas das cales son aditivos plásticos engadidos intencionadamente e outras substancias químicas relacionadas co plástico. Isto suscita a preocupación pola posible introdución na nosa cadea alimentaria e no noso subministro de auga, constituíndo así unha ameaza directa tanto para a saúde humana como para os organismos acuáticos. A detección destas partículas microscópicas e dos seus aditivos asociados é imprescindible para mitigar as repercusións ecolóxicas da súa presenza en ambientes de auga doce e mariña. En consecuencia, urxe contar con metodoloxías fiables para identificar e cuantificar MPs e as substancias químicas asociadas.

Neste senso, os avances na preparación de mostra, como a separación por densidade para illar MPs de matrices ambientais, a purificación dos MPs para a eliminación de interferentes do medio no que se atopan, e por último nas técnicas analíticas de análise, como son a resonancia magnética nuclear (NMR), cromatografía líquida acoplada á espectrometría de masas de alta resolución (LC-HRMS) e cromatografía de gases (GC)-HRMS, permitiron a cuantificación de diferentes tipos de MPs e a detección dunha multitude de compostos asociados aos MPs, xa sexan aditivos plásticos como sustancias adsorbidas do ambiente no que se atopan inmersos.

Ademais dos propios MPs e das moitas familias de substancias químicas relacionadas cos plásticos, esta tese tamén considera as sustancias per- e polifluoroalquiladas (PFAS), non só porque poden estar asociadas a polímeros plásticos (por exemplo, politetrafluoroetileno ou ad/absorbidas do ambiente polos MPs), senón tamén pola súa persistencia ambiental e as normativas recentes que fan que sexan compostos relevantes para o seu estudo. O desenvolvemento de técnicas de preparación de mostra como a extracción en fase sólida (SPE) ou a inxección directa son esenciais para a posterior determinación e o emprego de procesos electroquímicos avanzados para a eliminación do medio mariño.

Esta tese aborda varios aspectos sobre a determinación de MPs, PFAS e substancias químicas relacionadas cos plásticos no medio ambiente. Isto inclúe o desenvolvemento dun novo método de separación por densidade e cuantificación por NMR. Ademais, a investigación busca identificar aditivos plásticos e outras substancias quimicamente asociadas a MPs expostos ao medio mariño. Na seguinte fase, o estudo profundiza na avaliación dos ésteres dos ácidos ftálicos (PAEs) e do bisfenol A (BPA) asociados a MPs. Esta avaliación serve como base para calcular a súa bioaccesibilidade tanto en humanos como en organismos mariños mediante modelos de simulación *in-vitro* con métodos estandarizados. Finalmente, debido á recente implementación dunha nova normativa (Directiva 2020/2184/EU) sobre PFAS na auga de bebida, requírese dun desenvolvemento metodolóxico para a cuantificación e a tamén a

creación de novas tecnoloxías de eliminación do medio mediante procesos electroquímicos avanzados, como pode ser o emprego da oxidación anódica.

Así, en detalle, esta tese presenta unha recompilación de 6 proxectos de investigación agrupados por capítulos e interconectados, que se resumen a continuación:

- A detección de produtos químicos orgánicos asociados a MPs granulares de polietileno de baixa densidade (LDPE) virxes expostos no medio mariño do Mar Mediterráneo mediante a combinación de GC e LC acoplados á espectrometría de masas de quadrupolo-tempo de voo (**Capítulos 3.1 e 4.1**).

Neste estudo, investigouse a presenza de produtos químicos orgánicos asociados a MPs expostos a un ambiente costeiro influenciado polo ser humano durante un período de até oito semanas nun porto da illa de Mallorca. O obxectivo era comprender a dinámica da (des)sorción de produtos químicos no/dende o ecosistema mariño. Os gránulos de polietileno de baixa densidade (LDPE), que son MPs primarios producidos para o seu posterior uso pola industria do plástico representan unha contribución significativa da presenza de MPs nos océanos. Para ampliar o alcance dos produtos químicos detectables, empregáronse tanto LC como GC acoplados a quadrupolo-tempo de voo (QTOF). No LC-HRMS utilizouse unha fonte de ionización por electrospray e aplicáronse fluxos de traballo de detección de sospeitosos (*Suspect screening*) e descoñecidos (*Non-target screening*). O GC-HRMS, equipado cunha fonte de ionización de impacto electrónico, analizáronse extractos sen derivatizar e derivatizados (sililados) despois da extracción mediante ultrasóns, a través do emprego dun algoritmo de deconvolución cromatográfica e comparación con bibliotecas de espectros de alta e baixa resolución (elaboradas no laboratorio ou comerciais).

Identificáronse un total de 50 compostos de diversas familias, do que preto do 50% foron confirmados con estándares e os restantes foron identificados tentativamente mediante correspondencia coas bibliotecas e interpretación espectral. Despois, clasificáronse por tipo de uso, onde o 60% corresponden a aditivos plásticos (principalmente plastificantes e filtros UV), aproximadamente o 20% procede de compostos adsorbidos aos MPs (por exemplo, produtos de coidado persoal), e o 20% restante a compostos naturais. Resaltar, a melamina e o salicilato de 2-etilhexilo (EHS) foron inicialmente atopados nos MPs virxes pero tiveron unha rápida desorción cando se sumerxiron no medio mariño. A melamina foi liberada por completo na primeira semana de exposición, mentres que o EHS foi desorbido paulatinamente, cunha porción que quedou nos MPs despois das 8 semanas. Polo contrario, outros produtos químicos de orixe antropoxénica (por exemplo, fenantreno ou benzofenona) e de orixe natural (por exemplo, betaína e varios ácidos graxos), acumuláronse nos MPs ao longo do tempo de exposición. Tamén se fixo unha cuantificación de 12 compostos químicos confirmados e que revelou unha concentración total nos MPs de 810 µg/kg despois de oito semanas de exposición.

- Combinación dun novidoso separador de densidade de vidro rendible, seguido da espectroscopía cuantitativa de ^{1}H-NMR para a determinación de MPs en sedimentos mariños (**Capítulos 3.2 e 4.2**).

Unha vez que os MPs chegan ao medio mariño, poden ser perigosos para os organismos mariños, incluíndo fitoplancto, zooplancto, bivalvos (por exemplo, mexillóns), mamíferos mariños, aves mariñas e peixes. Non só poden causar danos físicos aos organismos mariños debido ao contacto, a absorción ou a inxestión, senón que tamén poden converterse nunha vía potencial de exposición a contaminantes orgánicos para os organismos mariños. Ademais,

poden entrar na cadea alimentaria humana eventualmente ameazando a saúde humana, por exemplo a través da inxestión de produtos do mar.

As técnicas que existen para a determinación de MPs no medio mariño, especialmente en sedimentos e area de praia, son, polo xeral, moi laboriosas. Ademais, a separación de MPs xeralmente realízase en separadores de densidade de gran tamaño. Polo tanto, é necesario desenvolver métodos analíticos fiables, máis sinxelos e económicos para avaliar mellor a súa distribución no medio mariño. Por isto, este traballo presenta unha configuración innovadora, portátil e económica para a separación de MPs, en particular tereftalato de polietileno (PET), cloruro de polivinilo (PVC) e LDPE, utilizando o principio de flotación por densidade. No proceso de separación empregou un separador de vidro deseñado no laboratorio formado por tres partes separables, e que contén 1,5 L dunha disolución salina de cloruro de zinc cunha densidade de 1,6 g/cm^3. Despois do illamento dos MPs faise unha limpeza mediante oxidación Fenton e, posteriormente, a análise realizase mediante a espectroscopía cuantitativa de ^{1}H-RMN despois da disolución dos MPs nos disolventes deuterados adecuados.

A validez da metodoloxía desenvolta confirmouse mediante a análise de mostras de sedimentos fortificados con MPs dun tamaño aproximado de 300 µm a dúas concentracións, logrando recuperacións que van do 71% ao 107%, cunha desviación estándar relativa (RSD) inferior ao 22%. Ademais, o método presenta uns límites de cuantificación (LOQs) que varían de 15 a 245 ng/g. Este procedemento aplicouse en mostras de area de praia de tres lugares distintos ao longo da costa galega empregando a metodoloxía desenvolvida. As concentracións de MPs oscilaron entre 62 e 186 ng/g de PET e entre 91 e 114 ng/g de LDPE, cunha RSD ≤26%. Este protocolo é rápido, preciso e económico para obter avaliacións precisas da distribución e abundancia de polímeros plásticos de tamaño microscópico en sedimentos mariños.

- Simulación da inxestión humana de MPs: probas de bioaccesibilidade oral de BPA e PAEs en estados alimentados e en xaxún (**Capítulos 3.3 e 4.3**).

A pesar da recente identificación de fragmentos de MPs nas feces humanas e outras probas que demostran a exposición humana aos MPs, non se ten prestado a conveniente atención a entender adecuadamente o impacto dos aditivos químicos relacionados cos (micro)plásticos na saúde humana. Así, neste estudo utilizáronse protocolos estandarizados *in-vitro* de bioaccesibilidade oral baixo condicións de xaxún (*Unified Fasted BARGE Method*, UBM) e de alimentación (*Relative in-vitro Model*, RIVM) para investigar a bioaccesibilidade oral de aditivos plásticos e monómeros (en particular, oito PAEs e BPA) nun material de referencia certificado como MPs feitos de LDPE e PVC, cun tamaño promedio de partícula inferior a 150 µm. A análise da fase bioaccessible realizouse mediante a dilución e filtrado dos dixeridos e posterior análise por cromatografía líquida de ultra-alto rendemento acoplada a espectrometría de masas en tándem (UHPLC-MS/MS) no caso dos PAEs, e extracción líquido-líquido (LLE) seguida de derivatización (sililación) e GC-MS para o BPA. As fraccións non bioaccesibles determináronse mediante extracción por ultrasóns con disolvente seguidas de UHPLC-MS/MS ou GC-MS. O estudo tamén avalía a xeración produtos de transformación (metabolitos) dos PAEs durante os ensaios de bioaccesibilidade, tales como os monoésteres dos ftalatos, mediante UHPLC-MS/MS.

Observáronse bioaccesibilidades nas fraccións gástrica e gastrointestinal para o ftalato de dimetilo (DMP), ftalato de dietilo (DEP) e BPA, que van do 55% ao 83%, do 40% ao 68% e do 37% ao 67%, respectivamente. Ao considerar os seus produtos de hidrólise, estas fraccións aumentan ao 56-92% e 41-70% para DMP e DEP, respectivamente. A bioaccesibilidade destes

PAEs máis polares está influenciada polas características físico-químicas dos MPs, cunha maior bioaccesibilidade observada para o polímero máis elástico (LDPE).

O método proposto permite a avaliación precisa da bioaccesibilidade oral dos PAEs de polaridades moderada a baixa, os cales amosan valores que oscilan entre o 1,8% e o 32,2%, con porcentaxes de desorción significativamente maiores para o LDPE. Os resultados indican que a maior bioaccesibilidade gástrica/gastrointestinal dos oito PAEs e BPA obtense baixo condicións de extracción gastrointestinal en estado alimentado debido ás maiores cantidades de biomoléculas activas na superficie. Por outra banda, ao incorporar o factor de bioaccesibilidade en estudos de avaliación de riscos humanos destes contaminantes desde MPs, concentracións superiores ao 0,3% (p/p) para DMP, ftalato de di-n-butilo (DnBP) e BPA poden representar riscos severos debido á absorción oral, en contraste cos conxéneres máis hidrófobos para os que se tolerarían concentracións superiores ao 3% (p/p), excepto para o ftalato de dietilhexilo (DEHP).

- Lixiviación *in-vitro* e probas de extracción fisioloxicamente relevantes para PAEs e BPA dende MPs - Avaliando a contribución dos MPs á exposición de vertebrados mariños aos produtos químicos relacionados co plástico (**Capítulos 3.4 e 4.4**).

Os vertebrados mariños son recoñecidos por consumir cantidades significativas de MPs que acaban nos medios mariños como produtos de refugallo primarios ou secundarios, por degradacións dos plásticos. Unha vez inxeridos, os MPs teñen o potencial de inducir lesións gastrointestinais e actuar como vehículos para a transmisión de compoñentes nocivos do plástico, como PAEs e BPA, dentro da cadea alimentaria. Porén, existe unha carencia de métodos de dixestión *in-vitro* estandarizados que sexan capaces de simular a absorción de produtos químicos asociados aos MPs polos peixes e outros vertebrados mariños. Así, este estudo aborda esta fenda no coñecemento, realizando probas de extracción e bioaccesibilidade de PAEs e BPA dende MPs, usando auga do mar artificial e fluídos que replican os compartimentos gástrico, intestinal e gastrointestinal de vertebrados mariños. As probas realizáronse en materiais de referencia certificados de LDPE e PVC (coma os que se empregaron no estudo de bioaccesibilidade humana) que conteñen oito PAEs de diferente hidrofobicidade e BPA, que conteñen concentracións realistas destes compostos químicos.

A análise dos lixiviados/extractos de fluídos gástricos realizouse mediante unha dilución e inxección nun equipo de UHPLC-MS/MS, de maneira semellante ao caso da bioaccesibilidade humana. Só os compoñentes máis hidrófilos, como o DMP, DEP e BPA, mostraron valores de lixiviación significativos baixo condicións de extracción ambiental (acuosa), mostrando tamén os valores máis altos de bioaccesibilidade baixo extraccións *in-vitro* fisioloxicamente relevantes (34-83%).

Calculouse o aporte diario de DMP, DEP e BPA para diversas especies de peixes a partir de MPs e a través da inxestión de auga do mar en varios escenarios. En ambientes mariños realistas (1 µg MP/L auga do mar; 10 µg PAE ou BPA/g MP; 100 mL de auga do mar consumida/kg de peso ao día e 0,05 µg PAE ou BPA/L auga do mar), a inxestión diaria de DMP, DEP e BPA a partir de MPs constituiría só o 0,016% do que representa a contribución da inxesta acuosa. Por conseguinte, a inxestión de MPs non debe considerarse a ruta principal de exposición dos peixes a BPA e aos PAEs máis polares en ambientes mariños. Con todo, hai unha incerteza substancial nesta estimación debido a datos contraditorios na literatura recente.

- Determinación de PFAS regulados en auga potable segundo a Directiva 2020/2184/EU (**Capítulos 3.5 e 4.5**).

Os PFAS son compoñentes químicos amplamente utilizados en procesos industriais e de fabricación durante máis de 80 anos debido ao seu carácter anfifílico e persistencia que os fan moi atractivos para moitas aplicacións. Como resultado, están moi estendidos no medio ambiente, o que fai que sexan moi complicados de eliminar e pode constituír nun problema para a saúde humana pola súa chegada á auga de bebida. Varios estudos concluíron que os PFAS afectan o sistema inmunitario dos humanos, aumentan as concentracións de colesterol sérico, inducen a perda de peso nos neonatos, ou mesmo afectan a resposta ás vacinas. Por todo isto, a Unión Europea recentemente tomou medidas que levaron á regulación de 20 PFAS (ácidos carboxilos e sulfónicos) en auga potable a través da Directiva 2020/2184/EU. Esta directiva inclúe PFAS con diferentes lonxitudes de cadea carbonada (C4-C13) e impón unha concentración total máxima de PFAS (suma) de 0,1 µg/L, polo que se requiren métodos analíticos capaces de determinar estes 20 compostos de maneira sensible. Por tanto, neste estudo, desenvolvéronse e avaliáronse tres metodoloxías distintas para determinar estes 20 PFAS en auga da billa e embotellada. Estas metodoloxías implican extracción mediante SPE en liña (acoplamento a un LC) e fora de liña, así como inxección directa, empregando (UHP)LC-MS/MS como técnica de determinación.

Entre as metodoloxías avaliadas, a SPE fora de liña usando cartuchos Oasis® *Weak Anion Exchange* (WAX) mostrou unha maior sensibilidade, logrando LOQs ≤0,3 ng/L, cunhas recuperacións superiores ao 70% e unha RSD inferior ao 19% en mostras de auga potable a tres niveis de concentración diferentes. A SPE en liña e a inxección directa enfrontáronse a problemas de contaminación de fondo e menor precisión, especialmente para os PFAS más hidrófobos.

Finalmente, a metodoloxía de SPE fora de liña combinada con UHPLC-MS/MS aplicouse para á análise de 46 mostras de auga potable, incluíndo 11 mostras comerciais embotelladas e 23 mostras de auga da billa españolas e 12 internacionais (Europa e Norte América). Nestas mostras foi posible cuantificar un total de 10 PFAS, oscilando as súas concentracións entre 0,1 e 20,1 ng/L, cunhas frecuencias de detección que ían do 2 ao 91%. Con todo, a concentración total de PFAS non superou o límite establecido pola directiva en ningunha das 46 mostras.

- Aplicación dun proceso de oxidación anódica para a eliminación de PFAS de matrices acuosas (**Capítulos 3.6 e 4.6**).

A problemática presentada anteriormente respecto da presenza e efectos dos PFAS implica a necesidade da súa eliminación do medio acuoso, para salvagardar a saúde humana e ambiental. Debido á súa elevada persistencia, os PFAS resisten a hidrólise e fotólise e non son facilmente biodegradados, polo que é difícil eliminalos do medio (acuático). Os tratamentos convencionais das estacións depuradoras e potabilizadoras non son, por tanto, eficaces para a súa correcta eliminación do medio, polo que se están a desenvolver novas tecnoloxías para facer fronte a esta ameaza global e que permita a protección dos recursos hídricos e seguridade da auga de bebida.

Por tanto, o presente traballo ten como obxectivo avaliar o rendemento do proceso de oxidación electroquímica, utilizando un ánodo de diamante dopado con boro (BDD) para a eliminación de PFAS de matrices acuosas. Esta investigación abrangueu varios aspectos chave, como son: (i) a avaliación da degradación de PFAS de longa (C9-C13) e curta-media (C4-C8), o que abranguería ao actualmente grupo regulado de PFAS pola Directiva 2020/2184/UE (C4-C13), ademais de PFAS de interese emerxente de cadea ultracurta (C1-C3); (ii) a exploración de sistemas multisoluto con diferentes concentracións de PFAS (0,2 a 2,0 µg/L) e número e tipo

de compostos (24 PFAS C1-C13 *versus* 8 PFAS C1-C8), ademais de sistemas de soluto único; (iii) a investigación da utilización de matrices reais de auga xunto con auga ultrapura; e (iv) a avaliación do impacto de densidades de corrente elevadas (*j*) ata 250 mA/cm^2, en contraste coa xeralmente utilizada *j* (≤20 mA/cm^2). Os ensaios da oxidación electroquímica avanzada na celda electrolítica foron cuantificados mediante UHPLC-MS/MS.

O estudo revelou que os PFAS con grupos sulfonato, especialmente C1-C4, mostraron maior resistencia á degradación. Polo contrario, os PFAS ≥C9 con grupo sulfonato e os PFAS ≥C12 con grupo carboxilo mostraron potencial para unha rápida degradación. As cinéticas de degradación de PFEtS (C2), PFPrA (C3) e PFBA (C4) víronse notablemente influenciadas polo contido e diversidade de PFAS. A investigación abarcou catro matrices reais de auga: auga potable da billa, auga residual urbana despois do tratamento secundario, concentrado de nanofiltración e concentrado de osmose inversa procedente da auga residual urbana. A degradación de PFAS mellorou xeralmente nas matrices reais, principalmente pola presenza de ións de cloruro e a xeración posterior de especies activas de cloro por electrólise. Pola contra, en augas con alto contido orgánico, como cunha demanda química de oxíxeno de 319 mg O_2/L, a degradación de PFAS viuse diminuída. Ademais, a eficacia de eliminación da maioría dos PFAS mellorou coa aplicación de *j* >20 mA/cm^2, e para PFAS específicos, foi necesario *j* ≥250 mA/cm^2 para acadar taxas de eliminación máximas. Os PFAS con grupos carboxilo demostraron ser máis facilmente degradables cós que teñen os grupos sulfónico. Por outra banda, mentres que os PFAS máis hidrófobos foron (case) eliminados por completo, a eliminación dos hidrófilos variou moito coa lonxitude da cadea fluorocarbonada, dende menos do 10% para C1 ata a eliminación completa para PFAS C8.

INTRODUCTION

1. INTRODUCTION

1.1. (MICRO)PLASTICS: DEFINITION AND CLASSIFICATION

Plastic has become an increasingly common and indispensable material in recent times, to the point of becoming one of the most commonly used man-made materials. However, the overuse of plastic has led to significant threats to public health and the environment (Geyer et al., 2017). The first plastic to be chemically synthesized was Bakelite in 1907 (Baekeland, 1909), but the first patented plastic polymer was nylon in 1938 (Weissermel, 1981). Since then, derivatives of petrochemical products, such as plastics, have been introduced on a large scale in world production, giving rise to what is known as 'The Age of Plastic' (*The age of plastic: from Parkesine to pollution*, 2019) in the mid-twentieth century. Over the years, the variety of plastic materials with different characteristics and physical properties has continued to increase, as shown in Table 1.1. Plastics are typically categorized into three groups based on their structure: (i) Thermoplastics, which soften when heated and harden when cooled, such as PE, PP, PTFE, PET, PA, PVC, and PS (see full names in Table 1.1); (ii) Thermosets, which never soften once they have been moulded, such as epoxy resins, PU and polyester resins; and (iii) Elastomers, which can return to their original shape after being stretched, such as rubber and neoprene.

Table 1.1. Chronology of the invention of polymeric materials.

Polymer	Acronym	Source	Main application	Year
Rubber	-	Natural	Automotive industry	1839
Parkesine	-	Semi-synthetic	Arts industry	1862
Celluloid	-	Semi-synthetic	Film industry	1863
Rayon	-	Semi-synthetic	Textile industry	1894
Bakelite	BK	Synthetic	Automotive industry	1907
Polyvinyl chloride	PVC	Synthetic	Construction industry	1926
Low-density polyethylene	LDPE	Synthetic	Packaging industry	1935
Polyurethane	PU	Synthetic	Automotive industry	1937
Polytetrafluoroethylene	PTFE	Synthetic	Aerospace industry	1938
Polystyrene	PS	Synthetic	Packaging industry	1938
Nylon	PA	Synthetic	Packaging industry	1939
Polyethylene terephthalate	PET	Synthetic	Packaging industry	1941
Unsaturated polyester	UP	Synthetic	Composite materials	1942
Polypropylene	PP	Synthetic	Packaging industry	1951
High-density polyethylene	HDPE	Synthetic	Packaging industry	1951
Extruded polystyrene	XPS	Synthetic	Packaging industry	1954
Thermoplastic polyesters	-	Synthetic	Packaging industry	1970
Liquid crystal polymers	LCP	Synthetic	Optic industry	1985

Own elaboration based on Dodiuk (2021)

Due to the high demand for plastics, their production has dramatically increased over the last 70 years (Ritchie, 2018). In 1950, approximately 2 million tonnes of plastics were produced

worldwide, but by 2021, production had surged to over 461 million tonnes, an increase of nearly 230-fold (OECD, 2022). Of the total amount, 50% of plastics are disposable or single-use, with special mention to the COVID-19 pandemic resulting in a rapid increase in demand for personal protective equipment, including facemasks, which increased single-use plastic waste by 2.2% compared to 2019 levels (OECD, 2022). This exponential growth in plastic waste has become a significant environmental concern (Ritchie, 2018), as plastics are a durable synthetic material that resists chemical and physical degradation. Currently, plastic waste is accumulating indiscriminately in terrestrial and aquatic habitats and ecosystems around the globe, as its fragments into progressively smaller pieces known as microplastics (MPs), as shown in Figure 1.1. Despite this mounting concern, production shows no signs of slowing down, as plastics remain in high demand due to their low production cost. Of the plastics produced, 66% are used for packaging, building materials, and textiles, while the remaining 34% are used for electronics, furniture, transport, agriculture, toys, medicine, and others (Geyer et al., 2017).

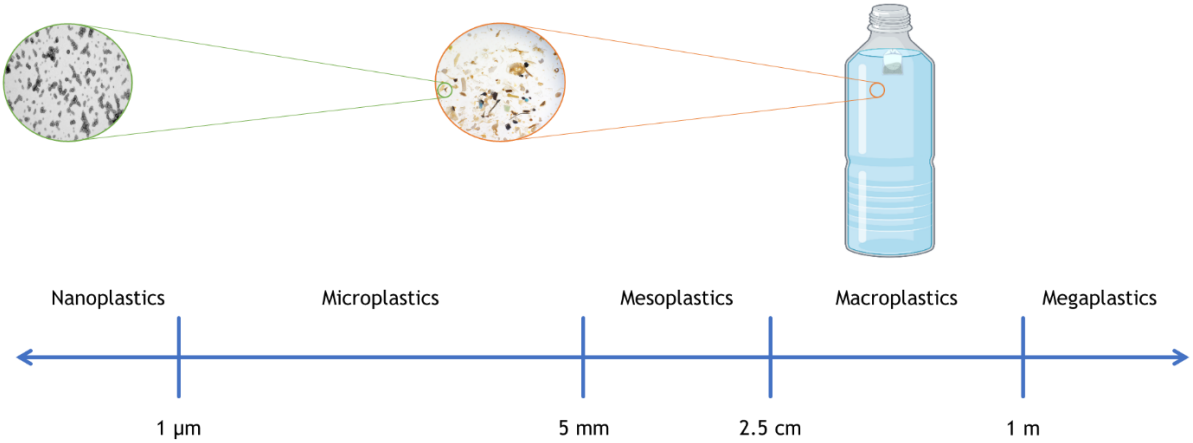

Figure 1.1. Currently accepted size scale for plastics and their physical degradation products.

Own elaboration

In 2004, Richard Thompson discovered micrometric particles of plastic debris for the first time in beach sediment samples from the coast of England (Thompson et al., 2004). However, the current definition of MPs is given by the National Oceanic and Atmospheric Administration (NOAA) and is usually defined as plastic pieces ranging between 1 µm and 5 mm that originate from household waste (Andrady, 2011; Arthur et al., 2009). MPs have become a significant challenge for environmental science, analytical chemistry, and environmental toxicology in recent years. Depending on their origin, they can be classified into two groups: primary and secondary MPs.

Primary MPs have been intentionally manufactured for specific applications to be of microscopic dimensions in industrial pellets that serve as precursors for manufactured plastic products. They can also be present in personal care products (such as facial creams, make-up, and shampoos), medicines, or cleaning products. These products are used because of their versatility and low cost as a substitute for expensive natural ingredients. On the other hand, secondary MPs are generated through fragmentation and/or (selective) degradation of larger plastic material exposed to external factors, such as combined chemical and physical phenomena (such as photodegradation, hydrolysis, and thermooxidative degradation), and can even be susceptible to biological fragmentation (such as biodegradation and ingestion) by bacteria and fungi. However, the degradation processes of plastics are extremely slow, and thus

MPs potentially persist for very long time periods in the (marine) environment (Hidalgo-Ruz et al., 2012).

Moreover, there is a wide array of MPs with varying types and densities, ranging from 0.9 to 2.3 g/cm^3. These MPs can be categorized based on their density, classifying them as either light or heavy, or according to their flexibility, labelling them as hard or soft, depending on their distinct physical attributes. Since the sources of plastics are diverse, the physiochemical characteristics of MPs also exhibit significant variations. For instance, (1) the coloration of MPs differs; (2) MPs display a plethora of shapes, including fibrous, pellet-like, film-like, scrubbing particles, twine-like, foamy, sheet-like, filamentous, nurdle-shaped, beady, flaky, angular, round, spherical, and fragmentary structures (Aragaw, 2021); (3) the chemical composition of MPs is intricate and encompasses materials such as polyethylene (PE), polypropylene (PP), polystyrene (PS), polyamide (PA), polyethylene terephthalate (PET) and polyvinyl chloride (PVC), among others.

1.2. MICROPLASTICS IN THE MARINE ENVIRONMENT

According to the OECD's 2019 estimates, of the total amount of plastic waste generated (ca. 353 million tons) only 9% was recycled, 19% was incinerated, and nearly 50% ended up in landfills or the environment. The remaining 22% was disposed of in uncontrolled dumpsites, burned in open pits or leaked into the environment (OECD, 2022). Furthermore, the occurrence of MPs in the aquatic environment has become a major concern globally and is closely related to plastic production. A fraction between 1.5 and 4.5% of the global production is released directly into the environment during usage and waste. However, no current figures of MPs emissions during production exist.

Personal care products such as toothpaste, facial cleansers, facial scrubs, and bath foam contain MPs, which can collectively discharge significant amounts of MPs into sewer systems during use, along with synthetic clothing washing . The latter can produce more than 1,900 fibres (100 particles/L) in one wash cycle (Andrady, 2011). Additionally, waterborne paints, electronics, coatings, medical applications, and adhesives can also produce high amounts of MPs through friction and decomposition. These MPs may end up in sewage systems, and subsequently in wastewater treatment plants (WWTPs), where they undergo a series of physical, chemical, and biological processes along the different treatment stages.

During the preliminary and primary treatment stage in WWTPs, large plastic debris are removed through filtration using screen meshes sized 6 mm or larger. Low-density MPs are collected with the suspended and floating solids present in the grease layer. On average, 65% of the influent MPs are removed during this stage (Habib et al., 2020). In the secondary treatment stage, suspended and dissolved organic material is removed through the action of microorganisms in large aeration tanks. Sewage sludge is separated from the post-processing effluent through flocculation processes and settling tanks. Secondary treatment removes additional MPs through entrapment in solid flocs, sedimentation in secondary clarifiers, or even by action of microorganisms. Overall, WWTPs equipped with primary and secondary wastewater treatment can remove between 88-94% of MPs (Iyare et al., 2020). However, the majority of MPs removed during the sewage treatment process remain in the resulting sewage sludge This is followed by disinfection processes, polishing, or advanced (tertiary) treatment, such as filtration through sand and/or activated carbon columns, before the treated water is

discharged into a neighbouring waterbody. WWTPs equipped with a tertiary treatment can remove between 90-99.9% (Habib et al., 2020). Thus, it is important to note that even the inclusion of a tertiary treatment is not always effective in completely removing MPs from the final effluent.

WWTP technologies are not specifically designed to remove or degrade MPs during any of the three stages of the treatment process. Therefore, MPs can be discharged into the ocean directly or indirectly through river systems (Figure 1.2). In Europe, about 520,000 tons of plastic waste is estimated to be discharged through WWTPs annually (Horton et al., 2017).

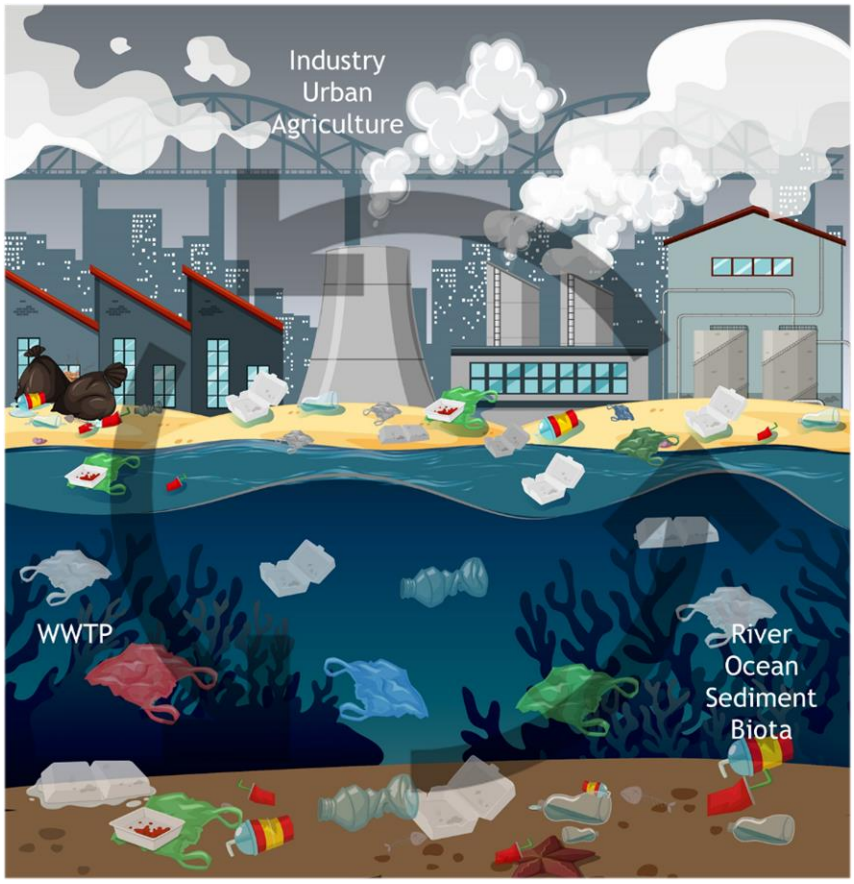

Figure 1.2. The cycle of MPs in the marine environment.

Own elaboration

Rivers play a crucial role in the transportation of MPs to oceans and coasts. According to recent modelling studies, it is estimated that worldwide, rivers discharge approximately 1.2-2.4 million tons of floating plastic particles annually from WWTPs into oceans, lakes, and reservoirs (Lebreton et al., 2017). The variability in this estimation is dependent on factors such as discharges, turbulence, and weather events, which are also believed to cause variations in the abundance of MPs in rivers. Furthermore, Lechner et al. (2014) reported that the Danube River in Austria discharged an estimated 4.2 tons of MPs into the Black Sea per day, based on stationary driftnets over a two-year period (2010-2012). In addition, other sources of MPs in the coastal zone include shipyards, harbours, and other industries, as well as urban run-off, which creates significant environmental reservoirs in the oceans (Kane & Clare, 2019). MPs

not only float in water and are transported by water flows from rivers to oceans, but also sink and accumulate in the riverbed. This river sediments were studied by different authors (Ding et al., 2019; Eo et al., 2019; Haave et al., 2019; L. Lin et al., 2018; Mani et al., 2019; Simon-Sánchez et al., 2019) who found between 80-200,000 items/kg of sediments all over the world. Depending on the variable river flow regimes and the interaction with sediment clays, such settled plastic debris can be either remobilized or remain settled. Furthermore, MPs can also accumulate in lakes. For instance, in Asian countries MPs range from 90-34,000 items/m^3 (Bharath K et al., 2021; Yuan et al., 2019), in Europe from 1-23 items/m^3 (Bordós et al., 2019; Tamminga et al., 2019) and in America from 12-180 items/m^3 (Alfonso et al., 2020; Bertoldi et al., 2021; Dekiff et al., 2014).

The presence of MPs has been also documented in almost all types of marine environments and beaches, and the most studied aquatic ecosystem for their presence is the oceans. Plastic debris was first reported on the surface of the Atlantic and Pacific oceans in the early 1970s (Choy et al., 2019). MPs remain in the oceans for many years, and their abundance has recently been estimated to be 24.4 trillion pieces, weighing between 82,000 to 578,000 tons or the equivalent of roughly 30 billion 500-mL plastic water bottles (Isobe et al., 2021). The largest accumulation of ocean plastic is the Great Pacific Garbage Patch, with at least 79 thousand tonnes of ocean plastic (~8% of total are MPs) floating inside an area of 1.6 million km^2 (Lebreton et al., 2018). Recent studies suggest that the highest concentrations of MPs may be found between 200 to 600 m of depth in the seafloor (Choy et al., 2019) and the largest deposits of marine MPs may be in deep-sea water bodies and animal communities (Thompson et al., 2004). Researchers have also conducted studies on the seabed and have found that it is predominantly composed of microfibres from fishing gear and synthetic textiles from washing machines.

It is noteworthy that beach sediments are also an important reservoir of MPs. Hence MPs concentration in Asia ranged from 15-12,852 items/kg dw (Li, Zhang, Zhang, et al., 2018), in Europe from 2-170 items/kg dw (Laglbauer et al., 2014; Van Cauwenberghe et al., 2013) and in America from 30-261 items/kg dw (Bosker et al., 2018; Mazariegos-Ortíz et al., 2020) The zone sampled, however, differs amongst studies: while some cover entire beach transects (perpendicular to the shoreline), others studied specific littoral zones. As was already remarked by Hidalgo-Ruz et al. (2012), this lack in uniformity between studies explains why the distribution of MPs on beaches is still little understood, and that there is a need to systematically examine potential accumulation zones. These results suggest that local development levels and economic structures in different countries and regions are closely related to regional differences in MPs abundance.

Once MPs enter the marine environment, they pose a serious threat to various marine organisms, including phytoplankton, zooplankton, bivalves (such as mussels), marine mammals, seabirds, and fish. It is well known that large plastic objects can cause entanglement after ingestion by vertebrates, with more than 250 marine species believed to be affected by plastic ingestion (Laist, 1997). The death of higher organisms, especially vertebrates, often receives extensive academic research and media coverage due to the emotional impact it has on the population. However, the biological impact of MPs on marine life, from a broader perspective, has received less attention and is only just beginning to be studied. According to a technical report on the impact of marine litter on biodiversity, over 80% of reported incidents between organisms and marine litter involved plastics, and 11% of these incidents involved MPs (GEF, 2012).

Since MPs are similar in size to sediments and some plankton, they are potentially bioavailable to a wide range of organisms, including low-nutrient suspensions, filter-feeders, sediment feeders, scavengers, and herbivores (Graham & Thompson, 2009). As a result, MPs can accumulate in the organism and cause physical damage, such as internal abrasions and blockages. In addition to physical effects, leaching of constituent impurities, such as monomers and plastic additives, can also be toxic and lead to carcinogenesis and endocrine disruption (Talsness et al., 2009). MPs also tend to concentrate hydrophobic persistent organic pollutants (POPs), which have a greater affinity for the hydrophobic surface of plastics than seawater. Due to their large surface-to-volume ratio, MPs can be highly contaminated with water-based POPs, up to six orders of magnitude more than the surrounding seawater. This presents a possible route of exposure to marine organisms, whereby bioaccumulation and biomagnification could occur through the food chain. Therefore, it is important to determine the additives and other chemicals contained in these MPs, as the pathways and uptake of MPs particles are of relevance to both chemical transfer and physical harm.

1.3. PLASTIC ADDITIVES

Plastics are composed not only of polymeric hydrocarbon chains but also of additives that enhance their physical and chemical properties. Thus, additives are intentionally added chemicals during plastic production to improve their properties and can include light stabilizers, heat stabilizers, antioxidants, nucleating agents, pigment agents, plasticizers, flame-retardants, lubricants, and emulsifiers. Residual monomers can also be retained inside MPs (ECHA, 2021b). The type of additive used depends on the plastic polymer and the requirements of the final product (see Table 1.2). These plastic additives can be found in trace amounts (<1% w/w) or as major components (>50% w/w) of plastic materials.

Due to their weak binding to plastic, these additives have the potential to leach out during use or disposal. Additionally, they can remain in the plastic product and potentially form toxic compounds after leaching, which can accumulate in the environment and affect organisms. The risks associated with these additives are present throughout the entire life cycle of plastics. Moreover, they are difficult to remove, meaning they can be incorporated into newly manufactured products during the recycling process (Wagner & Schlummer, 2020). However, due to a lack of transparency from industrial manufacturers regarding the additives used and their concentrations, there is no detailed overview of the chemical characteristics of the final product or associated health risks available (Mafuta et al., 2021).

When plastic waste is incinerated, the health risks associated with plastic additives are not reduced and can be particularly problematic when incinerators are low-tech or used in uncontrolled conditions. Incomplete combustion can lead to the release of harmful compounds, such as POPs, including dioxins, acid gas, and contaminated ash (Da Costa et al., 2020). As a result, the risks to the ecosystem and biota associated with the presence of additives in MPs are related to their inherent hazards and exposure to ecosystems. Additives that are determined to be harmful to humans, the environment, and living organisms are regulated internationally through initiatives like the Stockholm Convention, which was adopted in 2001 and entered into force in 2004. This global agreement requires parties to take active steps to reduce or eliminate the release of POPs into the environment (Da Costa et al., 2020). However, the Convention only regulates a small subset of hazardous compounds found in plastics and plastic waste, and

some of these compounds are still in use due to current exceptions (Mafuta et al., 2021). Furthermore, existing regulations do not cover a growing list of additives.

Table 1.2. List of the most relevant polymers and their associated plastic additives based on ECHA (2022).

Polymer	Additives type	Amount in polymers (% w/w)	Hazardous substances according to the ECHA (2022)
PP	Antioxidant	0.05-3	Bisphenol A; Octylphenol; Nonylphenol
	Flame retardant	5-10	Tetrabromobisphenol A
HDPE	Antioxidant	0.05-3	Bisphenol A; Octylphenol; Nonylphenol
	Flame retardant	5-10	Tetrabromobisphenol A
LDPE	Antioxidant	0.05-3	Bisphenol A; Octylphenol; Nonylphenol
	Flame retardant	5-10	Tetrabromobisphenol A
PET	Light stabilizers	0.2-6	Phenol derivatives; Zinc oxide
PS	Light stabilizers	0.2-5	Octabenzone; Zinc oxide
	Plasticizers	2-35	Phthalates
PVC	Plasticizers	10-35	Phthalates
	Heat stabilizers	2-3	Phosphite and sulphate derivatives
	Light stabilizers	0.2-6	Octabenzone; phenol derivatives; Zinc oxide
PU	Flame retardant	10-25	Melamine; Triethyl phosphate
	Phthalic acid esters	10-35	Phthalates
	Light stabilizers	0.2-5	Octabenzone; phenol derivates; Zinc oxide

Own elaboration

The most relevant families of plastic additives, in the context of this thesis, are listed below.

1.3.1. Phthalates

Phthalic acid esters (PAEs), also named phthalates, are a family of plastic additives used as plasticizers. They are colourless, odourless, flavourless, liquids at a large temperature range (80-140ºC) and chemically stable. PAEs can be classified in two types (i) low-molecular weight PAEs, such as dimethyl phthalate (DMP), diethyl phthalate (DEP), di-n-butyl phthalate (DnBP) and benzylbutyl phthalate (BzBP), which are frequently found as constituents of sunscreens, car care products, cosmetics and plastic film (Saeidnia, 2014); and (ii) high-molecular weight PAEs, such as di(2-ethylhexyl) phthalate (DEHP), di-n-octyl phthalate (DnOP), diisononyl phthalate (DiNP), diisodecyl phthalate (DiDP) (Saeidnia, 2014) and are mainly added to PVC production synthesized by reaction of phthalic anhydride and alcohols (see structures in Figure 1.3). For example, PVC used in clothes, food packaging and toys for infants can contain between 10 to 60% of phthalates by weight (Net et al., 2015).

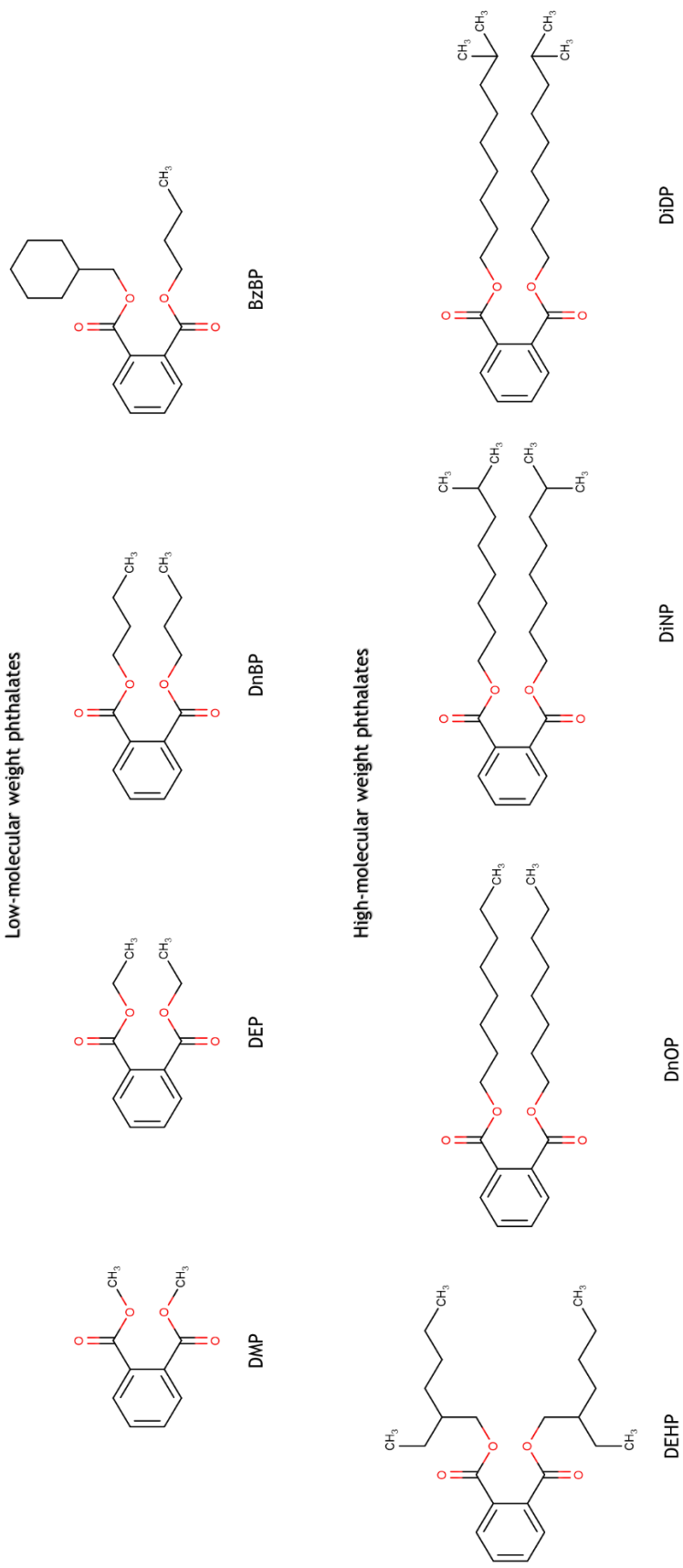

Figure 1.3. Structure of the main phthalates according to their molecular weight.

Own elaboration

According to the OECD (2018), PAEs were widely used globally up to approximately 5.5 million metric tons per year in 2018, through various sources, including household stuffs (furnishings, clothing, cosmetics, children's toys, food packaging, etc.). Among them, DEHP was the most commonly used plasticizer to improve flexibility and elasticity, representing 40% of the global plasticizer market (ECPI, 2022). Europe accounted for 1.35 million tons of the global plasticizer market in 2020 (ECPI, 2022), but DEHP was not the most commonly used plasticizer in Europe, as suggested by its 20% decrease in consumption between 1999 and 2004. DEHP has gradually been replaced by high-molecular weight phthalates such as DiNP, DiDP and di(2-propylheptyl) phthalate (DPHP), which represented 54% of plasticizer consumption in Europe in 2020 (ECPI, 2022).

PAEs are considered endocrine disruptors that affect foetal development in addition to primarily target the male reproductive system (Oehlmann et al., 2009). Since PAEs are not chemically bound to the polymer matrix, they can easily leach into the environment during manufacturing, use and disposal (Net et al., 2015). The European Parliament Directive 2005/84/EC banned DEHP, DnBP, and BzBP at concentration levels above 0.1% by mass in toys and child-care articles (EC, 2014b). For higher-molecular mass PAEs, namely, DiNP, DiDP, and DnOP, the Directive ban only applies to toys that can be put into children's mouths (EC, 2014a).

1.3.2. Bisphenol A

Bisphenol A (BPA) is a crystalline colourless solid that was firstly reported in 1891 and then synthesized from phenol and acetone (Zincke, 1905). BPA can be used as an antioxidant or as a plasticizer in other polymers (PP, PE and PVC), even as a monomer intermediate in the production of polycarbonate (PC) plastics (65% of volume used) and epoxy resins (30% of volume used) (Goodman & Peterson, 2014). This compound is the most commonly produced chemicals worldwide, with over three million tons produced annually (Goodman & Peterson, 2014). It is mainly used for the lining layer of aluminium cans and another different products of daily life, including digital media (typically CDs and DVDs), electronic equipment, automobiles and medical devices. It may also be present as an additive in other forms of plastic, as is the case with some children's toys (Staples et al., 1998).

The high production volume of BPA is increasing due to the increasing demand for PC, and epoxy resins. The global demand for BPA have grown from 6.5 million tonnes (in 2012) to more than 10 million tonnes in 2022 (Gonkowski & Makowska, 2022). The US market is projected to experience a 5.3% annual growth in the demand for PC and epoxy resins from 2021 to 2028. In Europe, the demand is expected to remain stable, while the most significant growth is anticipated in Asia, particularly in China. Initially, the growth was primarily driven by the demand for epoxy resin. However, with the establishment of PC production capacity in China by Teijin and Bayer, along with several planned projects, the future demand for BPA in China will be fuelled by PC (ICB, 2008).

BPA can leach from plastic containers into foods and beverages, leading to the release of this additive from food and drink packaging, which is considered as a source of exposure for human beings especially when they are heated, or used for long periods of time. Despite its potential to leach from food packaging and the fact that is known as oestrogen agonist and androgen antagonist with a broad range of effects on the human reproductive system such as

hormonal system damage and leading to decreased fertility rates (Oehlmann et al., 2009) only it have been banned in PC drinking containers for infants and toddlers and recently, in 2020 limited to 0.02% (w/w) in thermal paper under EU regulation, but is still allowed in the EU for use in food contact material (EC, 2016). Other bisphenol analogues, such as bisphenol B, bisphenol F and bisphenol S are used for replacing BPA in plastics and may represent a threat to the environment even though their toxicity is still unknown (Yichang Chen et al., 2016).

1.3.3. Organophosphate flame retardants

Organophosphate flame retardants (OPFRs) are organic esters of phosphoric acid-containing either alkyl chains or aryl groups, and they may be halogenated or nonhalogenated. They are commonly used in a variety of industries, including plastics, foams, textiles and other materials due to their physicochemical characteristics as stabilizers for antifoaming and lubricants (Du et al., 2019). Flame retardants are added to reduce the flammability or delay the ignition and spread of flames in plastic materials. The most used OPFRs are tris(2-chloroethyl) phosphate (TCEP), tris(1,3-dichloro-2-propyl) phosphate (TDCPP) and tris(1-chloro-2-propyl) phosphate (TCPP). The total annual global consumption of OPFRs was 759,000 tons in 2017 (Dou et al., 2022) and the total annual global consumption of OPFRs has continued increasing in recent years. OPFRs can be released into the environment through various processes, such as production, use, and improper disposal. In addition, OPFRs are found in marine environments and freshwater biota (Sundkvist et al., 2010). The widespread existence of OPFRs has led to concerns regarding the biological potential for toxicity and risks to human health and some studies have suggested that these chemicals may have adverse effects on human health due to these compounds are endocrine disruptors with high persistence and bioaccumulation in the environment (Du et al., 2019).

Due to these concerns, there have been efforts to regulate or phase out the use of certain OPFRs and other flame retardants that have raised environmental and health concerns. The USA has included TDCPP, TCEP and TCPP in the list of chemicals of concern under United States Environmental Protection Agency (USEPA) and the EU has classified TCEP as a Substance of Very High Concern under Registration, Evaluation, Authorisation, and Restriction of Chemicals (REACH) regulation.

1.3.4. Brominated flame retardants

Brominated flame retardants (BFRs) are additives used in a variety of plastic products (e.g. electronic devices) as flame retardants. The most frequently BFRs used are polybrominated diphenyl ethers (PBDEs), hexabromocyclododecane (HBCD) and tetrabromobisphenol A (TBBPA). These compounds are not chemically bound to the polymer matrix (except TBBPA) and hence, they can leach into the surrounding environment.

PBDEs are hydrophobic BFRs used in many plastic formulations. In fact, there are three main commercial formulations known as penta-, octa- and deca-BDEs, comprising different mixtures of isomers with different degrees of bromination. These additives are ubiquitous, toxic, persistent and bioaccumulative in the environment and are a major concern for human health. As a result, penta- and octa-BDEs have been banned in the EU since 2004 (EC, 2003),

while deca-BDE was only banned in the EU in 2009 for electronic and electrical applications (EC, 2009). These preparations shall no longer be used in mixtures or products in concentrations exceeding 0.1% by mass. In addition, tetra- to hepta- and deca-BDEs are listed in Annex A of the Stockholm Convention on POPs as substances to be eliminated (Convention, 2016). Since 2006, penta- to octa-BDEs must be notified 90 days prior to import or production in the USA. Since 2013, the import and production of deca-BDE has been completely stopped (USEPA, 2012).

HBCD has three main stereoisomers: α-, β- and γ-HBCD. All of them are listed as POPs requiring authorization in the EU because is limited to the uses within the scope (EC, 2006). HBCD is present in expanded and extruded PS up to 4-7% by weight (Al-Odaini et al., 2015). In addition, HBCD was listed for elimination in Annex A of the Stockholm Convention in 2013, with specific exemptions for its use and manufacture in expanded and extruded PS (Convention, 2016). USEPA (2010) conducted a risk assessment of HBCD under the "Toxic Substances Control Act" of 2010 action plan.

TBBPA is the most widely produced BFR representing a 60% of the market, being synthesized by brominating BPA. This BFR is used in ABS and in other plastic such as high impact PS and phenolic resins (Cruz et al., 2015). Until now, no legislation concerning TBBPA has been applied in the EU.

1.3.5. Light and heat stabilizers

Stabilizers are additives used to prevent the ageing of plastics due to UV light (photostabilizers) and temperature (heat stabilizers). Currently, long-term type of thermal and light stabilizers are the hindered amines, which act by trapping free radicals and limiting the degradation process. Instead, the most common stabilizers are Tinuvins® and Chimassorb®, which are mainly added in PE, PU and PP for the automotive industry to protect pigmented systems from fading and colour changes (Ambrogi et al., 2017). These compounds have a very low solubility in water and hence, the migration process from plastic material can be very low (Silva et al., 2006). The regulation of EU (EC, 2011) about the quality of food packaging materials established an overall migration limit of 10 mg/dm^2 for these additives.

1.3.6. Antioxidants

Antioxidants are additives used to prevent the ageing of plastics and to delay oxidation, which can occur due to exposure to atmospheric oxygen, heat, or light, including sunlight. The most common antioxidants are the commercial Irganox® and Irgafos® brands, including Octadecyl 3-(3,5-di-tert-butyl-4-hydroxyphenyl)propionate (Irganox® 1076), Pentaerythrityl-tetrakis-3-(3,5-di-tert-butyl-4-hydroxyphenyl)propionate (Irganox® 1010) and 2,4-di-tert-butylphenol (Irgafos® 168). These compounds represent around 60% of global demand in PE and PP of the total oxidants. However, these substances can leach out of the plastic and may migrate to food from plastic packaging and pose a health risk. No legislation for antioxidants has been applied in the EU, but must comply the migration legislation (EC, 2011) of the previous section 1.3.5.

1.3.7. Nonylphenols

Nonylphenols are derived from phenol that belong to the group of alkylphenols. They have been used as antioxidants and plasticizers to produce plastics and being valued for their detergent and emulsifying properties. These organic chemicals have many applications such as paints, pesticides, detergents and personal care products. Instead, they are strongly bounded to plastic material due not been found to leach from plastic bottles to their water content (Loyo-Rosales et al., 2004). Nonylphenols are considered as endocrine disruptors and their use is prohibited in the EU due to their effects on the environment and human health (Rani et al., 2015).

1.4. MICROPLASTICS AS VECTORS OF POLLUTANTS

MPs interaction with environmental contaminants before, during, and after entering ecosystems has been the subject of experimental studies and review papers (Rios et al., 2007; Rochman, 2015). Some studies suggest that chemical pollutants such as hydrophobic organic compounds, including POPs, heavy metals, endocrine-disrupting chemicals and microbial contaminants, can absorb on plastics due to both the large specific surface area and strong hydrophobic allowing to increase the overall bioavailability of these chemical compounds to aquatic organisms and humans (Vethaak & Leslie, 2016). However, this assumption has been challenged by the fact that plastics are less common in the environment than natural particles such as organic matter and grit, and therefore would play a smaller role as pollutant carriers (Koelmans et al., 2016). To assess the overall relative importance of MPs as pollution vectors compared to other naturally occurring sorbents, calculations were performed based on data from published studies (Koelmans et al., 2016). Sophisticated models have been developed to simulate partition ratios between solid phases, including plastics, and water, MP age distributions, relative abundance and uptake of MPs, and the effects of surfactants, pH, and temperature during adsorption of chemical compounds (Koelmans et al., 2016), concluding that it depends on the affinity of polarities between the compounds dissolved in the marine environment under specific conditions (temperature and pH) and the surface of the MP being different depending on the type of plastic material and its surface area. With increasing plastic production and use, the environmental occurrence of MPs will certainly increase in the future. Therefore, it is crucial to expand our fundamental understanding of the processes by which MPs facilitate pollutant transport to develop more accurate models and to assess the role of MPs as pollutant transporters in different and specific contexts (see Figure 1.4).

When reviewing the potential transfer of chemical pollutants between aquatic environments such as water, sediment, MPs, and organisms, it is crucial to consider the specific conditions under which measurements or predictions were made. It is important to note that the net direction of compound transfer between interacting compartments depends on the differences in chemical activity, which describes the potential for movement among compartments, rather than the concentrations of the compounds present. Net transfer among compartments only happens until the chemical activities in the interacting phases reach equilibrium (Caruso, 2019).

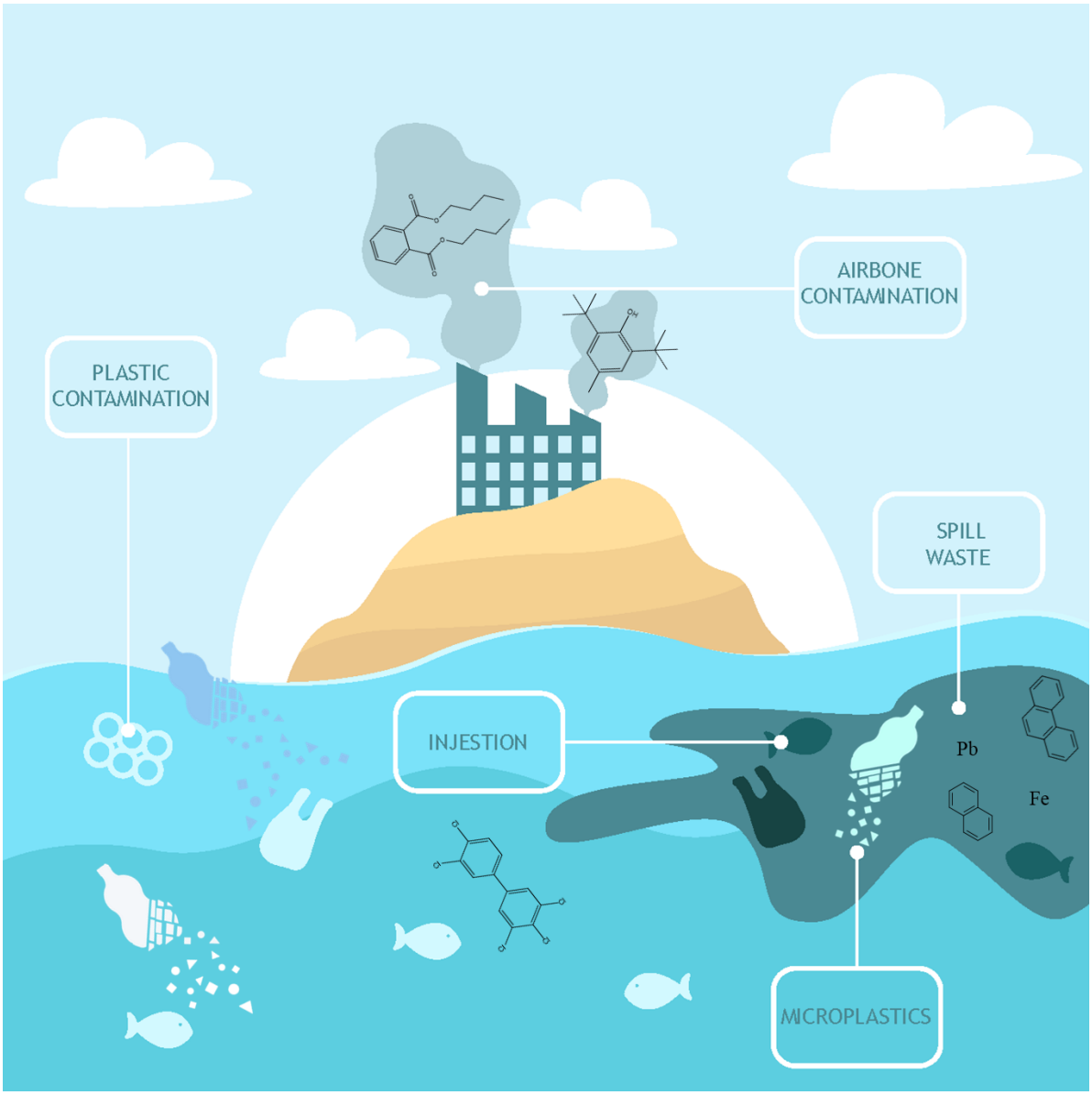

Figure 1.4. MPs act as vectors of pollutants in the marine environment.

Own elaboration

The partitioning of POPs to plastics has been extensively studied, and polymer-water partitioning coefficients for various plastic and chemical combinations (as shown in Table 1.3) are correlated with octanol-water partition coefficients (Ghosh et al., 2014; Lee et al., 2014). Due to their high sorptive capacity, plastics have been used as passive samplers of POPs in water and sediment. There is also sufficient evidence to demonstrate that MPs can absorb a wide range of organic chemicals, including polychlorinated biphenyls (PCBs), polycyclic aromatic hydrocarbons (PAHs), and organochlorine pesticides (OCPs).

Table 1.3. Partitioning of POPs to various types of plastic in seawater.

Plastic	POP	log partition coefficient*	log partition coefficient value	Source
PE	PCB	K_f	4.93-10.43	(Velzeboer et al., 2014)
		K_{PE-W}	4.19-6.88	(Gouin et al., 2011)
	Acenaphthene	K_{PE-W}	3.62	(Gouin et al., 2011)
	Naphthalene	K_{PE-W}	2.81	(Gouin et al., 2011)
	Fluorene	K_{PE-W}	3.77	(Gouin et al., 2011)
	Fluoranthene	K_{PEsw}	5.52 (5.41-5.62)	(Lee et al., 2014)
		K_{PE-W}	4.93	(Gouin et al., 2011)
	Anthracene	K_{PEsw}	4.77 (4.67-4.87)	(Lee et al., 2014)
		K_{PE-W}	4.33	(Gouin et al., 2011)
	Pyrene	K_{PEsw}	5.57 (5.45-5.67)	(Lee et al., 2014)
		K_{PE-W}	5.1	(Gouin et al., 2011)
	Chrysene	K_{PEsw}	6.39 (6.27-6.50)	(Lee et al., 2014)
		K_{PE-W}	5.78	(Gouin et al., 2011)
	Benzo[a]pyrene	K_{PEsw}	7.17 (7.03-7.30)	(Lee et al., 2014)
		K_{PE-W}	6.75	(Gouin et al., 2011)
	Benz[a]anthracene	K_{PE-W}	5.73	(Gouin et al., 2011)
	Dibenz[a,h]anthracene	K_{PEsw}	7.87 (7.72-8.00)	(Lee et al., 2014)
	Benz[k]fluoranthene	K_{PE-W}	6.66	(Gouin et al., 2011)
	Benzo[ghi]perylene	K_{PEsw}	7.61 (7.46-7.75)	(Lee et al., 2014)
		K_{PE-W}	7.27	(Gouin et al., 2011)
	α-Hexachlorohexane	K_{PEsw}	2.41 (2.36-2.46)	(Lee et al., 2014)
		K_{PE-W}	2.8	(Gouin et al., 2011)
	ß-Hexachlorohexane	K_{PEsw}	2.04 (1.99-2.09)	(Lee et al., 2014)
	γ-Hexachlorohexane	K_{PE-W}	2.33 (2.28-2.38)	(Lee et al., 2014)
		K_{PE-W}	2.2	(Gouin et al., 2011)
	δ-Hexachlorohexane	K_{PE-W}	2.08 (2.03-2.12)	(Lee et al., 2014)
	Pentachlorobenzene	K_{PE-W}	4.63 (4.49-4.75)	(Lee et al., 2014)
	Hexachlorobenzene	K_{PE-W}	5.22 (5.08-5.34)	(Lee et al., 2014)
		K_{PE-W}	5.43	(Gouin et al., 2011)
	Phenanthrene	K_f	4.6 ± 0.12	(Teuten et al., 2007)
		K_f	4.9	(Bakir et al., 2014a)
		K_{PE-W}	4.00 (4.33-4.54)	(Lee et al., 2014)
		K_{PE-W}	4.22	(Gouin et al., 2011)
	Dichloro-diphenyl-trichloroethane	K_f	5.9	(Bakir et al., 2014a)
		K_{PE-W}	5.59	(Gouin et al., 2011)
	Dichloro-diphenyl-dichloroethylene	K_{PE-W}	5.77	(Gouin et al., 2011)
	Methoxychlor	K_{PE-W}	4.39	(Gouin et al., 2011)
	Heptachlor	K_{PE-W}	5.22	(Gouin et al., 2011)
	Aldrin	K_{PE-W}	4.71	(Gouin et al., 2011)
	Dieldrin	K_{PE-W}	4.75	(Gouin et al., 2011)
	Perfluorooctanoic acid	K_f	3.0	(Bakir et al., 2014a)
	DEHP	K_f	2.4	(Bakir et al., 2014a)
	Perfluorooctanesulfonic acid	K_d	1.52	(Wang et al., 2015)
	Perfluorooctanesulfonamide	K_d	2.47	(Wang et al., 2015)

Plastic	POP	log partition coefficient*	log partition coefficient value	Source
PP	PCB	K_d	4.98-5.45	(Mato et al., 2001)
	Dichloro-diphenyl-dichloroethylene	K_d	5.44	(Mato et al., 2001)
	Nonylphenol	K_d	4.92	(Mato et al., 2001)
	Phenanthrene	K_{PPSsw}	4.00 (3.88-4.11)	(Lee et al., 2014)
	Fluoranthene	K_{PPSsw}	4.79 (4.67-4.90)	(Lee et al., 2014)
	Anthracene	K_{PPSsw}	4.29 (4.18-4.38)	(Lee et al., 2014)
	Pyrene	K_{PPSsw}	4.80 (4.68-4.90)	(Lee et al., 2014)
	Chrysene	K_{PPSsw}	5.51 (5.40-5.61)	(Lee et al., 2014)
	Benzo[a]pyrene	K_{PPSsw}	6.10 (5.97-6.20)	(Lee et al., 2014)
	Dibenz[a,h]anthracene	K_{PPSsw}	7.00 (6.89-7.10)	(Lee et al., 2014)
	Benzo[ghi]perylene	K_{PPSsw}	6.69 (6.56-6.81)	(Lee et al., 2014)
	α-Hexachlorohexane	K_{PPSsw}	2.69 (2.64-2.75)	(Lee et al., 2014)
	β-Hexachlorohexane	K_{PPSsw}	2.18 (2.08-2.28)	(Lee et al., 2014)
	γ-Hexachlorohexane	K_{PPSsw}	2.58 (2.52-2.64)	(Lee et al., 2014)
	δ-Hexachlorohexane	K_{PPSsw}	2.23 (2.13-2.34)	(Lee et al., 2014)
	Pentachlorobenzene	K_{PPSsw}	4.50 (4.39-4.59)	(Lee et al., 2014)
	Hexachlorobenzene	K_{PPSsw}	5.01 (4.89-5.10)	(Lee et al., 2014)
	Phenanthrene	K_f	3.33 ± 0.01	(Teuten et al., 2007)
PS	Phenanthrene	K_{PSsw}	5.39 (5.27-5.49)	(Lee et al., 2014)
	Fluoranthene	K_{PSsw}	5.91 (5.79-6.01)	(Lee et al., 2014)
	Anthracene	K_{PSsw}	5.61 (5.51-5.70)	(Lee et al., 2014)
	Pyrene	K_{PSsw}	5.84 (5.71-5.96)	(Lee et al., 2014)
	Chrysene	K_{PSsw}	6.63 (6.52-6.72)	(Lee et al., 2014)
	Benzo[a]pyrene	K_{PSsw}	6.92 (6.80-7.02)	(Lee et al., 2014)
	Dibenz[a,h]anthracene	K_{PSsw}	7.52 (7.41-7.61)	(Lee et al., 2014)
	Benzo[ghi]perylene	K_{PSsw}	7.15 (7.03-7.24)	(Lee et al., 2014)
	α-Hexachlorohexane	K_{PSsw}	3.19 (3.15-3.23)	(Lee et al., 2014)
	β-Hexachlorohexane	K_{PSsw}	2.63 (2.59-2.67)	(Lee et al., 2014)
	γ-Hexachlorohexane	K_{PSsw}	3.01 (2.97-3.05)	(Lee et al., 2014)
	δ-Hexachlorohexane	K_{PSsw}	2.80 (2.75-2.85)	(Lee et al., 2014)
	Pentachlorobenzene	K_{PSsw}	5.10 (4.99-5.20)	(Lee et al., 2014)
	Hexachlorobenzene	K_{PSsw}	5.28 (5.17-5.38)	(Lee et al., 2014)
	Perfluorooctanesulfonamide	K_d	1.93	(Wang et al., 2015)
PVC	Phenanthrene	K_f	3.3	(Bakir et al., 2014a)
	Dichloro-diphenyl-trichloroethane	K_f	5.4	(Bakir et al., 2014a)
	Perfluorooctanoic acid	K_f	2.2	(Bakir et al., 2014a)
	DEHP	K_f	4.5	(Bakir et al., 2014a)
	Perfluorooctanesulfonic acid	K_d	2.00	(Wang et al., 2015)
	Perfluorooctanesulfonamide	K_d	2.06	(Wang et al., 2015)
PVC	Phenanthrene	K_f	3.12 (3.00-3.24)	(Teuten et al., 2007)

*K_d = linear equilibrium sorption model; K_f = Freundlich isotherm model; K_{PEsw} = equilibrium partitioning coefficient between PE and seawater; K_{PE-W} = equilibrium partitioning coefficient between PE and water; K_{PPsw} = equilibrium partitioning coefficient between PP and seawater and K_{PSsw} = equilibrium partitioning coefficient between PS and seawater.

Various physicochemical factors influence the sorption and desorption of POPs onto MPs, including the type of polymer, synthesis method, crystallinity, size, polarity, and degree of

weathering (Amelia et al., 2021; Bakir et al., 2014b). Thus, e.g. a chemical structure with a large surface area or porosity can lead to a higher sorption capacity. The affinity between MPs and pollutants varies depending on chemical interactions such as hydrophobic, π-π, van der Waals, and hydrogen bonding interactions. Hydrophobic organic chemicals, mostly POPs are the most frequently investigated substances due to their high affinity and hydrophobicity-driven sorption to MPs. For example, Tan et al. (2019) reported strong interaction of PAHs on MPs in marine environments.

However, POPs are not the sole group of contaminants that can undergo adsorption onto MPs. Other substances, including pharmaceuticals, heavy metals, and hydrophobic organic compounds, are also present in the marine environment and have the potential to be adsorbed onto the surface of MPs (see Table 1.4).

Table 1.4. Concentration of chemical contaminants on MPs in different types in marine environment.

MP type	Chemical group	Contaminant type	Sample matrix	Concentrations reported on MPs	Reference
PE, PS	POPs	PAHs	Water	3,400-119,000 ng/g	(Mai et al., 2018)
HDPE PP	POPs	PCBs, PBDEs, Dichloro-diphenyl-trichloroethane	Water	PBDEs 10-133 ng/g PCBs 3-60 ng/g Dichloro-diphenyl-trichloroethane 0.1-7 ng/g	(Pozo et al., 2020)
-	POPs	PAH, PCBs	Water	PAH 1,454-6,000 ng/g PCBs 0.8-104.6 ng/g	(Gorman et al., 2019)
PE, PS, PP, PE, PVC	Pharmaceuticals	Antibiotics	Water		(Li, Zhang, & Zhang, 2018)
-	POPs	PBDE	Fish	9.72 ng/g	(Gorman et al., 2019)
PS, PE,	POPs		Fish		(Ašmonaitė et al., 2020)
Beached MPs, Virgin MPs	Heavy metals	Al, Fe	Sediment	Fe 22.78 mg/kg Al 45.27 mg/kg	(Vedolin et al., 2018)
Virgin PS, aged PVC	Heavy metals	Cu, Zn	Water	Cu on PS 1,101 ± 273 mg/kg Cu on PVC 1,321 ± 269 mg/kg Zn on PS 160 ± 97 mg/kg Zn on PVC 102 ± 21 mg/kg	(Brennecke et al., 2016)

It is worth noting that environmental conditions and water properties affect to sorption process on MPs, such as pH, salinity, dissolved organic matter, and even the aging level can

affect the pollutant sorption capacity of MPs. For example, Guo et al. (2018) studied the sorption capacity of the antibiotic tyrosine on PS, PP, PE and PVC. The sorption capacity of tyrosine on MPs followed the of PVC > PC > PP > PE but was found that the sorption of the antibiotic on MPs decreased with the increasing the pH because the electronegativity of the surface increased. Similarity reported Wang et al. (2015) for perfluorooctanesulfonic acid (PFOS) adsorption on PE and PS. The results indicated that the sorption of PFOS on PE and PS increased with the decreased of solution pH. Similarly, Velzeboer et al. (2014) and Wang et al. (2015) assessed the effect of salinity on PCBs sorption to MPs, finding that an increase in salinity led to higher sorption capacity on PE and PS, while the opposite effect was observed for dichlorodiphenyltrichloroethane (Bakir et al., 2014b; G. Liu et al., 2019).

Dissolved and particulate organic matter can also affect the sorption of pollutants to MPs, through mechanisms such as hydrophobic interactions, complexation, and competition. Wu et al. (2016) studied the effect of organic matter on the sorption of three pharmaceuticals and personal care products to PE, finding that high levels of dissolved organic matter reduced the sorption of triclosan, 17α-ethinyl oestradiol, and 4-methylbenzylidene, but not carbamazepine.

Finally, weathering can also impact the sorption behaviour of MPs, as photo-oxidation and other reactions with oxygen can modify plastic surfaces. For example, Teuten et al. (2007) observed an increase in the distribution coefficient of phenanthrene to PE by increasing the duration of artificial photo-weathering, likely due to the development of cracks and increased surface area. However, other studies on the effects of photo-weathering on other plastics have been variable, potentially due to competing effects of photo-oxidation and changes in surface polarity (Ziccardi et al., 2016).

Therefore, these pollutants (i.e. PAHs, PCBs and pesticides) can be concentrated on the surface of MPs with a concentration factor of up to 10^6 times compared to surrounding seawater (Mato et al., 2001). Finally, these MPs transport over long distances these pollutants and make highly bioavailable to organisms when consumed as feed. Rochman et al. (2013) reported the transfer of PCBs and PBDEs found in fish fed with the marine plastic than those fed with the virgin plastic, indicating that plastic debris serves as a vector for the sorbed pollutants to wildlife.

Moreover, ingested MPs can accumulate in the tissues of organisms, leading to the bioaccumulation of toxic substances that can ultimately make their way up the food web, even affecting human health (Carbery et al., 2018). This has raised increasing concerns about the threats to aquatic biota.

1.5. DETERMINATION OF MICROPLASTICS IN SEDIMENT AND SAND SAMPLES

Many analytical methods have been developed to measure MPs in water systems, sediments, and soils. These procedures typically involve separation, identification, and quantification. Parameters such as the shape, size, and colour of MPs are relevant for determining their origin and residence time, as well as the source of their entry into the aquatic environment and the pathway from their manufacture through degradation processes to their deposition in the marine environment. Another important parameter is plastic ageing, but measuring this parameter is more complicated due to the lack of libraries in the detection methods. Typically, the results

are expressed as the total number of MPs per sample unit, with some studies providing a detailed classification of size, colour, and shape (e.g., fibre, pellet, fragment).

The determination of MPs in sediment samples can be a challenging task due to the small size and low concentration of MPs present in sediments and risk of environmental contamination or plastic contact. To date there is a wide range of sampling, extraction, purification, and final analysis methods in the literature, as discussed below.

During the entire analytical process, it is essential to take measures to avoid contamination from the environment, such as keeping the windows closed, using non-plastic tools, wearing cotton lab coats and gloves, and rinsing tools with ultrapure water (UPW). Procedural blanks should be established to verify the background contamination of laboratory sources during the entire recovery experiment (B. Zhang et al., 2019).

1.5.1. Collection of sediment and sand samples

The first step in studying MPs involves choosing a sampling methodology. The collection method and amount of sample material can impact the representativeness of the results.

It is important to keep in mind that the distribution of MPs in sediments is uneven and largely influenced by environmental factors such as winds and currents. The results will be highly dependent on the sampling area (e.g., high-tide line, intertidal areas, transects) and depth since some areas may contain higher concentrations of MPs. For example, collecting sediments from the tide line, the highest accumulation area, may lead to overestimation. Collection of plastic particles on beaches involves direct sampling with forceps, sieving, and collection of sediment samples, which are easy to implement, rapid, and allow for the collection of large volumes of samples or replicates. However, the variability of the sampled area and depth can be a drawback. Collection of samples from the seabed requires a vessel and the use of specialized equipment that is lowered to the seabed to collect the samples (e.g., grab sampler, box corer, or gravity core), which is also easy to use and allows for replicates, but the equipment is expensive and may disturb the sediment surface, affecting the results.

To accurately estimate MP concentrations in sediment samples, it may be necessary to define the sampling site by e.g. using a wooden ruler to mark the sampling area (typically of 40 x 40 cm^2), sampling depth (frequently ranged from 1 to 5 cm), and the number of replicates. The sample weight (25-3,000 g) or volume (0.05-1.2 L) varies widely between studies and may affect representativeness. NOAA recommends collecting 400 g per replicate, followed by drying and weighing to adjust the results (Masura et al., 2015), while the Marine Strategy Framework Directive (MSFD) technical subgroup recommends using at least five replicates of the top 5 cm of sediment (Hanke et al., 2013).

1.5.2. Separation of microplastics from sediment samples

The MP particles must be extracted from sediment samples in order to be quantified and characterized. For that purpose, the samples need to be submitted to three steps: (i) a step of sample pretreatment, for instance, through the use of sieves during the sample collection, (ii) a

separation step, usually through density separation and/or filtration and (iii) a purification step (if necessary) using different type of oxidants to degrade the organic matter.

1.5.2.1. Sample pretreatment

After collecting the sediment sample, it should be filtrated or sieved with pore or mesh sizes varying from 0.45 to 5,000 μm and then, homogenize to create a uniform sample. Finally, the sample should then be weighed and dried at a temperature higher than 50ºC overnight or for several days, depending on the sample's moisture content. The dried sediments should be weighed again to determine the weight loss due to evaporation and stored at -20ºC until extraction. Therefore, a standardized pore or mesh size should be defined to enable comparison between studies, even though this may be dependent on protocol constraints that could be overcome by creating a universal sampling protocol. This information should always be clearly stated.

1.5.2.2. Separation of microplastics

The most common method for extracting MPs from sediment samples is through density separation using saturated salty solutions due to the different density of plastic particles (ρ = 0.89-2.30 g/cm^3) (Table 1.5) from sediment particles (ρ~2.7 g/cm^3). The supernatant containing MPs is then collected for further filtration and removal of the solution. It is generally accepted that solutions with densities greater than 1.4 g/cm^3 are required to separate MPs from sediments (Quinn et al., 2017).

A simple density separation using water can recover some types of plastics, such as PS, PE, and PP from soil samples or fibres from sediments, due to their shape and large surface area (Prata et al., 2019). However, NaCl is one of the most commonly used salt for density separation due to its availability, low cost, and eco-friendliness which led to its recommendation by both the MSFD technical subgroup (Hanke et al., 2013) and NOAA (Masura et al., 2015). Unfortunately, it cannot achieve good recoveries for heavier density polymers, such as PVC, PET, and polyoxymethylene (POM). Quinn et al. (2017) found that NaCl (1.2 g/cm^3) had low recovery rates (<90%) and worse precision for lighter polymers. NaBr (1.4 g/cm^3) produced similar results, while both NaI (1.6 g/cm^3) and $ZnBr_2$ (1.7 g/cm^3) were able to separate heavier polymers with good recovery rates (99%) and better precision. Many authors resort to denser salts like $ZnCl_2$, which is cheaper, allows for reuse, and has a higher density. However, its high toxicity in the environment requires recycling for each extraction (Stock et al., 2019). Furthermore, separation using high denser salts solution may only require a single separation step, while NaCl typically requires three.

Table 1.5. Separation of polymer types by solutions used in density separation based on Hidalgo-Ruz et al. (2012).

Polymer	MPs density (g/cm^3)	Water	NaCl	NaI	$ZnBr_2$	NaI	$ZnCl_2$
		-	10-23% (w/w)	15-100% (w/w)	10-55% (w/w)	15-100% (w/w)	10-100% (w/w)
		1 g/cm^3	1.1-1.2 g/cm^3	1.1-1.8 g/cm^3	1.1-1.7 g/cm^3	1.1-1.8 g/cm^3	1.1-1.8 g/cm^3
PP	0.89-0.92	Yes	Yes	Yes	Yes	Yes	Yes
LDPE	0.89-0.93	Yes	Yes	Yes	Yes	Yes	Yes
EVA	0.94-0.95	Yes	Yes	Yes	Yes	Yes	Yes
HDPE	0.94-0.97	Yes	Yes	Yes	Yes	Yes	Yes
PS	0.96-1.06	Yes	Yes	Yes	Yes	Yes	Yes
Acrylic	1.09-1.20	No	Yes	Yes	Yes	Yes	Yes
PA	1.13-1.15	No	Yes	Yes	Yes	Yes	Yes
PMMA	1.17-1.20	No	Yes	Yes	Yes	Yes	Yes
PC	1.20-1.22	No	Y/N	Yes	Yes	Yes	Yes
PU	1.20-1.26	No	Y/N	Yes	Yes	Yes	Yes
PVA	1.19-1.31	No	Y/N	Yes	Yes	Yes	Yes
Alkyd	1.24-2.10	No	No	Y/N	Y/N	Y/N	Y/N
Polyester	1.24-2.30	No	No	Y/N	Y/N	Y/N	Y/N
PVC	1.38-1.41	No	No	Yes	Yes	Yes	Yes
PET	1.38-1.41	No	No	Yes	Yes	Yes	Yes
POM	1.41-1.61	No	No	Y/N	Yes	Y/N	Yes
PTFE	2.10-2.30	No	No	No	No	No	No

EVA: Ethylene-vinyl acetate, PMMA: poly methyl methacrylate and PVA: polyvinyl alcohol

Elutriation is another method that uses a column filled with a saturated salt solution to separate MPs from sediment. In this process, samples are placed at the top of the column, and as water enters from the bottom, the water level and buoyant sample portions move upward. The exiting suspension passes through a fixed sieve before draining. Afterward, the water is drained from the column through a bottom outlet, and the sample residues, mainly sandy sediment, are disposed of by releasing the flange. This method allows for cheap and efficient separation of MPs from large volumes of sediments, reducing sample volume undergoing density separation. However, it takes at least 1 hour per sample and requires previous sieving by size range (Prata et al., 2019).

When transferring the supernatant containing the PMs to the filter, one problem that often arises is how to do so without passing the sediment. Different devices have been developed to solve this problem. One example is the Sediment-Microplastic Isolation (SMI), an apparatus comprised of two PVC tubes connected by a valve that allows separation of the supernatant and sediment, which has been used with $ZnCl_2$ and achieved an efficiency of 95.8% (Coppock et

al., 2017), however the use of PVC for MPs analysis may be a significant long term disadvantage if degradation occurs. Another separator is the Munich Plastic Sediment Separator (MPSS), which uses a large volume (40 L) of dense solution of $ZnCl_2$ injected at the bottom of the column, allowing MPs from many amount of sediment (6 kg) to ascend and be collected in the supernatant or by direct vacuum filtration, but at greater time expense (e.g. settling phase may take 1-2h) and expensive to produce and limiting its portability and feasibility when processing numerous replicates of small samples. Finally design is Bauta MP-sediment separator, based on the MPSS separator, composed by a sediment chamber with rotation, a glass column to separate the MP from sediment rinsed with $ZnCl_2$:$CaCl_2$ and a separation chamber with a valve to collect the supernatant and allowed for the filtration of both lighter and heavier MPs, providing an average recovery rate of 94% (Mahat, 2017).

Other alternatives to the density separation have been employed. For example, Fuller and Gautam (2016) developed a procedure using accelerated solvent extraction (ASE) to extract MPs with recoveries ranging from 85-94%. Additionally, Felsing et al. (2018) used a Korona-Walzen-Scheider electrostatic bell separator to separate MPs (63-5,000 μm), reducing the sample volume by 99% with recoveries around 100% for each type of material. Shimizu et al. (2017) proposed an *in-situ* method that utilizes the frequency of impact of MPs in solution with an electrode, caused by Brownian motion, to infer concentration. Flow cytometry with visual stochastic network embedding (viSNE) also allows for the quantification of small MPs (1-20 μm) in water samples (Sgier et al., 2016). However, these methods have limitations such as the requirement for specialized equipment, long processing times, inability to characterize polymer types, potential saturation of measuring equipment, and changes in surface charge of plastics due to weathering and biofouling.

1.5.2.3. Purification treatments

Environmental samples may contain organic matter, which may interfere in the determinations. This can lead to an overestimation of environmental concentrations and an increase in the number of particles subjected to further analysis. When identification is primarily based on visual inspection, a digestion step is strongly recommended. However, most studies did not remove organic matter from their samples, probably because the authors thought their organic matter content was low. Therefore, it is important to include a digestion method that can reduce it without affecting the structural or chemical integrity of polymers (Prata et al., 2019). However, the need for digestion varies depending on the quantity of organic matter in each sample.

The types of purification treatments can be classified into acid, basic and enzymatic digestion and oxidizing agents (see Table 1.6). The most commonly used digestion methods for sediment samples are H_2O_2 (30%), Fenton's reagent (H_2O_2 with ferrous iron catalyst), enzymatic digestion, and HCl (5-10%). The NOAA also recommends purify using Fenton's reaction with H_2O_2 (30%) and 0.05M of Fe (II) sulphate solution heated at 75ºC in a glass beaker containing the MPs fraction for both water and sediment samples. The different oxidative treatments will be discussed in detail below.

Table 1.6. Digestion methods for the removal of organic matter to improve the identification of MPs, their efficiency and effects on synthetic polymers.

Digestion	Treatment	Recovery MPs	Polymer degradation	Organic matter degradation	Reference
Acid	HNO_3 (35%), 60ºC 1h	n.a.	Fusion of PET and HDPE; destruction of PA	100%	(Catarino et al., 2017)
	HNO_3 (65%), RT overnight, 60ºC 2h, dilution 80ºC distilled water	n.a.	PA degradation; yellowing	n.a.	(Dehaut et al., 2016)
	HNO_3 (65%) and $HClO_4$ (65%) 4:1 overnight, boiled 10 min, dilution 80ºC distilled water	n.a.	PA degradation; yellowing	n.a.	(Dehaut et al., 2016)
	HNO_3 (5-69%), RT 96h	<95%	Melted LDPE and PP; color change in PP, PVC, PET; decrease Raman peaks	n.a.	(Karami et al., 2017)
	HNO_3 (55%), RT 1 month	n.a.	Whitening of PVC, degradation of PA	n.a.	(Naidoo et al., 2017)
	HCl (5-37%), 25-60ºC 96h	n.a.	Changes in PET and PVC	>95%	(Karami et al., 2017)
Alkaline	NaOH, 60ºC 1h	94%	No	100%	(Catarino et al., 2017)
	NaOH (10M), 60ºC 24h	n.a.	CA degradation	n.a.	(Dehaut et al., 2016)
	$K_2S_2O_8$ (0.27M) and NaOH (0.24M), 65ºC 24h	n.a.	CA degradation; unpredictable weight increase	n.a.	(Dehaut et al., 2016)
	KOH (10%), RT 3 weeks	n.a.	No	n.a.	(Dehaut et al., 2016)
	KOH (10%), 60ºC 24h	n.a.	CA degradation	n.a.	(Dehaut et al., 2016)
	KOH (10%), 50ºC 96h	n.a.	Loss of PET and PVC	n.a.	(Karami et al., 2017)
	KOH (10%), 40ºC 96h	n.a.	Loss of PET; yellowing of PA	n.a.	(Karami et al., 2017)
	KOH (1M), RT 2 days	n.a.	Degradation of LDPE, CA, Cradonyl and PA	n.a.	(Kühn et al., 2017)
Acid and alkaline	NaOH (1M), 17.5 mL of 65% HNO_3 and 2.5 mL of water and drying	95%	Degradation of PA, PET, LDPE, PVC; colour change in PVC and PET	n.a.	(Roch & Brinker, 2017)

Digestion	Treatment	Recovery MPs	Polymer degradation	Organic matter degradation	Reference
Oxidative	H_2O_2 (30%), 60ºC 1h and 100ºC 7h	91%	n.a.	n.a.	(Erni-Cassola et al., 2017)
	H_2O_2 (35%), RT, 40ºC 96h	n.a.	Decrease in Raman peaks of PVC and PA	n.a.	(Karami et al., 2017)
	H_2O_2 (35%), RT, 50ºC 96h	n.a.	Degradation of PA; colour change of PET; foam and oxidization	n.a.	(Karami et al., 2017)
	H_2O_2 (6%), 70ºC 24h	78% (PE)	n.a.	n.a.	(Sujathan et al., 2017)
	H_2O_2 (30%), 60ºC until evaporation	<99% (PS)	n.a.	>10%	(Ziajahromi et al., 2017)
	Fenton's reaction (3:1) with H_2O_2 (30%) and 0.05M ferrous sulphate, RT 2h	97%	n.a.	>85%	(Lin et al., 2021)
	Fenton's reaction (3:1) with H_2O_2 (30%) and 0.05M ferrous sulphate, 40ºC 1h	n.a.	No	>99%	(Möller et al., 2022)
Enzymatic	Corolase 7086, 60ºC 1h	93%	n.a.	n.a.	(Catarino et al., 2017)
	Trypsin, 38-42ºC 30 min	n.a.	No	88%	(Courtene-Jones et al., 2017)
	Collagenase, 38-42ºC 30 min	n.a.	No	76%	(Courtene-Jones et al., 2017)
	Papain, 38-42ºC 30 min	n.a.	No	72%	(Courtene-Jones et al., 2017)
	Pepsin (0.5%) and HCl (0.063M)	n.a.	No	n.a.	(Dehaut et al., 2016)
	15 mL Tris-HCl 60ºC 60 min, proteinase K (500 µg/mL) and $CaCl_2$ 50ºC 2h, shaken 20 min, incubated 60ºC 2h, 30 mL H_2O_2 (30%) overnight	97%	No	n.a.	(Karlsson et al., 2017)

n.a. - not available; RT: room temperature; CA: Cellulose acetate.

1.5.2.3.1. Acid digestion

HNO_3 is the most commonly used acid for digestion to degrade organic matter in environmental samples, but it can also degrade certain types of polymers, such as nylon and PET. The resistance of polymers to acid digestion is dependent on various factors, such as the presence of organic matter in the sample, the particle size of MPs, the concentration and temperature of

the solution. Caution is advised when heating digestion solutions above 60ºC, as this can destroy MPs and cause loss of nylon, and melting of PS, LDPE, PET, and HDPE, or yellowing of polymers such as PP, PVC, and PET, but a digestion efficiency of over 95% (Catarino et al., 2017; Dehaut et al., 2016; Karami et al., 2017; Naidoo et al., 2017). Acid digestion must be used judiciously, as it may lead to underestimation of MPs in environmental samples.

1.5.2.3.2. Alkaline digestion

Alkaline digestion is a promising alternative to acid digestion, but it can also cause damage or discoloration of plastics, as well as leave oily residues, complicating characterization by vibrational spectroscopy (Prata et al., 2019). The most commonly used alkaline protocol involves using KOH (10%) to remove organic matter at 60ºC overnight or for 24 hours (Dehaut et al., 2016), and has shown to be one of the most effective digestion treatments with good recovery of MPs. However, KOH may cause discoloration and degradation of nylon, polyester, CA, LDPE, PC, PET, and PVC (Karami et al., 2017; Kühn et al., 2017). NaOH can be used as an alternative, but it may also cause degradation and colour changes in CA, PA, PET, and PVC (Dehaut et al., 2016). Instead, in several beaches samples was revealed that fish otoliths, squid beaks, paraffin, and palm fat survived the digestion process with KOH (1M) for 2 days at RT, although it can be complemented by acid digestion sequentially, with good digestion of biologic material and recovery rates (Roch & Brinker, 2017).

1.5.2.3.3. Oxidizing agents

An alternative to acid and alkaline digestion is the use of oxidizing agents such as H_2O_2 (30-35%), which can degrade organic matter more efficiently than NaOH and HCl, with little to no degradation of polymers (with only some discolouration) (Karami et al., 2017; Nuelle et al., 2014). Instead, the temperature of incubation seems to be a determinant factor in the degradation of polymers and the efficiency of removing organic matter using H_2O_2. The effect of the temperature in the removal efficiency was reported at RT for 7 days with a 25% of organic matter degraded and at 50ºC overnight to completely remove organic matter (Avio et al., 2015; Cole et al., 2014).

Moreover, another alternative more efficient of oxidizing agents is the Fenton's reaction using H_2O_2 (30%) accompanied by ferric ion (Fe^{2+}) usually 0.05M of ferrous sulphate in a 3:1 proportion. Furthermore, the pH of the reagent must be adjusted (to 3-5) to encourage the dissolution of the ferrous sulphate granules and optimize the degradation of organic material. This reaction allows the quick decomposition of biogenic matter to carboxylic acids, aldehydes, carbon dioxide, and water under relatively mild conditions. The studies reported that Fenton's reaction using H_2O_2 (30%) and 0.05M of ferrous sulphate (3:1) at 70ºC or RT with a efficiency of organic matter removal >90%, but with a 6% of loss in size of PE and PP particles and a colour change of PET due to high temperature (Tagg et al., 2017; Zobkov et al., 2020).

1.5.2.3.4. Enzymatic digestion

Enzymatic digestion is a purification method that is less hazardous and less likely to cause damage to MPs. However, the efficiency of the enzymes is influenced by the type of organic material present in the sample, and therefore, other techniques mentioned above may be needed to improve their removal efficiency (Courtene-Jones et al., 2017). Crichton et al. (2017) reported an enzymatic protocol that includes pre-digestion of sediments with an industrial enzyme blend (2.5%) at 45ºC for 60 min, followed by H_2O_2 (30%) removal of organic matter. Courtene-Jones et al. (2017) tested trypsin, collagenase, and papain enzymes with digestion efficiencies ranging from 72% to 88%, and no effect on polymer degradation was observed. Löder et al. (2017) proposed a basic enzymatic purification protocol with a 98.3% removal efficiency, based on the addition of detergent (5% w/w sodium dodecyl sulphate) in the solution, and the use of enzymes such as protease, cellulase, and chitinase and sequentially two H_2O_2 treatments (one between enzyme treatments and one at the end), totalling 13 days of sample processing. In summary, enzymatic digestion protocols can be used as a complementary technique to others and are usually followed by treatment with H_2O_2 to remove undigested debris, due to low removal efficiency, and are still used on a small scale due to their high cost.

1.5.3. Identification, chemical characterization and quantification

After extraction, the MPs are identified and quantified based on two types of methods: (i) counting the number of MPs using a variety of analytical techniques the almost recommended is the chemical characterization mainly using Fourier-transform infrared spectroscopy (FTIR) or Raman amongst other methods, even the visual identification is widely used due to easy application and inexpensive but lead the overestimation in the analysis. (ii) Mass-based methods using pyrolysis (Pyr), thermal extraction desorption (TED), thermogravimetric analyser (TGA) coupled to chromatography separation and detector, amongst others reporting MP/mass of sediment in terms of concentration.

1.5.3.1. Visual inspection

Visual inspection is a direct observation method used to classify plastic particles based on their physical characteristics using a microscope or stereoscope. This technique is widely available and is used for identification, classification, and quantification of plastic particles. It is often used as a pre-selection method before performing chemical characterization. Qualitatively, visual inspection allows classification based on colour, size, and shape, and can even provide information on their origin. It also allows for quantitative counting of particles. However, this method is subjective, and the results may vary between observers, leading to overestimation or underestimation of certain types and colours of MPs. For example, a study on multiple observers' visual detection of MPs in beach sediments had detections varying from 60% to 100%, depending on the individual, experience, and fatigue, leading to misclassification of biologic material as black fragments and underestimation of white fragments (Lavers et al., 2016).

To improve visual inspection, researchers have tried various methods such as prodding particles with needles, testing plastics with a heated needle tip, and even melting plastics to make detection easier. However, using dyes is an inexpensive way to aid in visual recognition. Although several dyes have been tested, such as Oil red EGN, Eosin B, Hostasol Yellow 3G, and Rose Bengal, their results have been unsatisfactory due to the affinity of dye for plastics and the confounding effect of staining biological material in the sample, requiring an exhaustive digestion step. For instance, although Rose-Bengal allowed for 92% coloration of 25 µm MPs and characterization by FTIR, only 22-99% of all stained particles were actual plastic (Ziajahromi et al., 2017). However, Nile Red appears to be the most promising solution for staining MPs, as it requires short incubation times (10-30 min), provides a good identification (91% of total particles), and allows vibrational spectroscopy with or without a brief bleach clean-up step (Erni-Cassola et al., 2017). Results can be seen under orange, red, or green filters on a fluorescence microscope. Although Nile Red staining does not affect biological materials such as algae, seaweed, wood, feathers, and mussel shells, certain types of plastics such as PC, PU, PET, and PVC with weak signals and fibres are difficult to stain (Erni-Cassola et al., 2017). Nile Red is a solvatochromic dye, and the fluorescence emission depends on the polarity of the solvent, which may allow the classification of MPs into a wide range of chemical groups based on fluorescence shifts, especially through image analysis with appropriate software (Prata et al., 2019). Thus, validation of staining protocols can provide researchers with a simple and time-saving tool to visually identify plastics and improve preselection methods for chemical characterization of particles.

1.5.3.2. Chemical characterization

Chemical characterization of MPs using FTIR and Raman spectroscopy is highly recommended to count particles. The MSFD technical subgroup (Hanke et al., 2013) suggests subjecting 10% of MPs ranging from 100-5,000 µm and all suspected particles in the range of 20-100 µm to these methods, but a higher percentage may be required for larger sizes due to varying accuracy in visual identification. Both vibrational spectroscopy methods are non-destructive, highly accurate and complementary, producing a spectrum based on the interaction of light with molecules: FTIR produces an infrared spectrum resulting from the change in dipole moment, whereas Raman provides a molecular fingerprint spectrum based on the polarizability of chemical bonds.

Various FTIR techniques have been used in the characterization of MPs, including attenuated total reflectance (ATR)-FTIR, which improves information on irregular MPs. Unlike transmission FTIR, ATR-FTIR is also applicable to thick or opaque samples (Courtene-Jones et al., 2017). Micro-FTIR produces a high-resolution map of the sample (down to 20 µm) without a pre-selection step (Harrison et al., 2012). On the other hand, Raman microscopy allows the characterization of MPs <20 µm but may be limited by weak signals, which can be overcome by increasing the measurement duration, and fluorescence interference, which depends on material characteristics such as colour, biofouling, and degradation (Araujo et al., 2018).

Stimulated Raman scattering (SRS) has been used to identify MPs on low Raman background filter membranes without pre-selection. Scanning at six wavenumber settings and characterizing 1 cm^2 under 4.5 h is possible, compared to the 24 h needed in Raman mapping

(Zada et al., 2018). However, the low Raman background filters used are highly expensive (about 6-7 times the price of the cellulose filters commonly used), limiting the wide application of this technique. Vibrational spectroscopy is limited by the high cost, availability of equipment, time, and effort required in analysing and processing samples, complex data treatment, the need for skilled personnel, and limited detection, especially in weathered or contaminated MPs (Prata et al., 2019).

Finally, other less commonly used alternatives to count MPs have been reported by Turner (2017). One of these involves using a portable X-ray fluorescence spectrometer to characterize the elemental composition of polymers through the diffraction and reflection of radiation, with potential use in the detection of some additives or adsorbed metals. Scanning electron microscope with an energy-dispersive X-ray microanalyzer has also been used to collect information on the morphology and chemical composition of MPs, but it requires a previous pre-selection and mounting of the particles analysed (Fries et al., 2013).

Regarding to the mass-based methods, gas chromatography coupled to mass spectrometry (GC-MS) is the main methodology used. The main challenge is the introduction of the sample in the system. Different alternatives have been applied: Pyr, TED, TGA and polymer dissolution. In the pyrolysis, MPs are thermally decomposed (pyrolyzed) under inert conditions, and the gas formed is cryo-trapped and separated on a chromatographic column, where the compounds produced are then identified by MS (Dümichen et al., 2017; Prata et al., 2019). While this method can provide chemical characterization of a single MPs or a bulk sample, it is destructive and provides no information regarding the number, size, or shape of MPs. TED-GC-MS is a two-step analytical method to quantify MPs concentration which consists of a thermogravimetric and a GC-MS system. The environmental sample is heated up to 600°C in a nitrogen atmosphere. During pyrolysis, between 300 and 600ºC polymer-specific decomposition products are produced and collected on a solid phase. On the other hand, TGA heat in a nitrogen atmosphere up to 1,000ºC with solid phase sorbent to capture the components of plastic degradation products. Afterwards the substances are desorbed, separated and analysed using the GC-MS (~3h) (Dümichen et al., 2017). This method allows for the use of relatively higher sample amounts (as compared to pyrolysis) and enables the measurement of complex, heterogeneous matrices, allowing identification and quantification of polymers in environmental samples without pre-selection. Finally, for polymer dissolution , Fuller and Gautam (2016) used pressurized fluid extraction with solvents (methanol, hexane, and dichloromethane), temperature, and pressure conditions to separate the bulk MPs fraction from soil samples and analysed the extracts under GC-MS.

Similarly to GC methods, liquid chromatography (LC) uses an appropriate solvent for the dissolution of the polymer and size exclusion chromatography for characterization, but it requires large amounts of sample (Prata et al., 2019). These methods present the advantage of analysing relatively high masses, improving representativeness. However, they are also destructive, and the information provided is limited to chemical composition.

Another method which requires the polymer dissolution is quantitative-NMR, proposed by Peez et al. (2019), a novel alternative for determining PE granules, PET fibres, and PS beads with a sized distribution ranging from <0.3 to 1 mm and resulting in an limit of quantification (LOQ) in the range of 74 to 85 mg/mL.

1.6. BIOACCESSIBILITY TESTING

To evaluate the risks of chemical compounds on human and fish health, it is important to understand the impact of exposure through ingestion, inhalation, and dermal contact. Bioaccessibility, defined as the fraction of a chemical compound solubilized from a sample that becomes available for absorption and potentially bioavailable to cross cellular barriers into the bloodstream (Kelley et al., 2002), is a key parameter to reach such goals. In particular, oral bioaccessibility can be represented as described by equation 1:

$$Bioaccessibility\ (\%) = \frac{M_E}{M_S}\ x\ 100 \quad \text{(Equation 1)}$$

where: M_E represents the amount of a chemical released into the digestive fluid (or the amount extracted in an absorption sink), and M_S is the total amount of the chemical in the original ingested material or food. The oral bioaccessibility of a substance is influenced by several factors, including the matrix, the physicochemical properties of the contaminants, and the digestive processes that occur in the gastrointestinal tract (GIT).

The value of the bioaccessibility can have important implications for the nutritional or toxicological effects of a substance. For instance, a contaminant that is highly bioaccessible may pose a greater health risk than a less bioaccessible one. Thus, it is important to be able to calculate this parameter, particularly by *in-vitro* methods that do not require animal testing, as discussed in the following subsections.

1.6.1. Human oral bioaccessibility

Understanding the stages that have to be considered in the development of an *in-vitro* oral bioaccessibility testing method requires an understanding of human physiology (Figure 1.5).

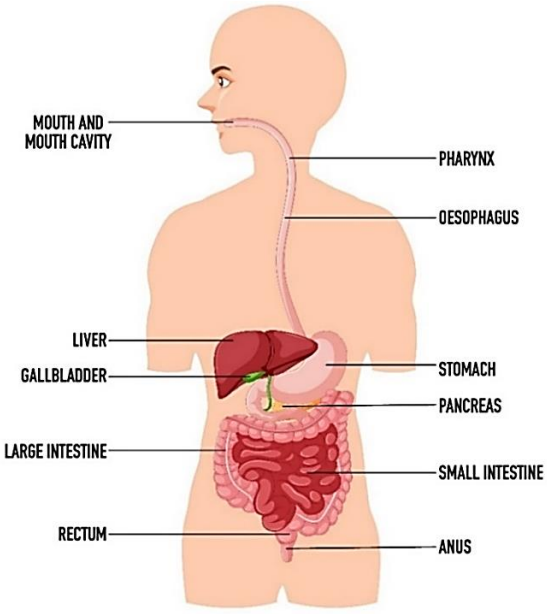

Figure 1.5. The human digestive system including the GIT and associated organs.

Own elaboration

The process of human digestion begins when the material is ingested into the mouth, where it undergoes initial breakdown in the presence of saliva with a pH of ca. 6.5. The material is then masticated, which breaks down larger components into smaller fragments, increasing their surface area for further digestion in the stomach. This entire process is relatively short and lasts from a few seconds to a few minutes. The material is then swallowed and transported via the pharynx and oesophagus into the stomach in just a few seconds. Swallowed material is transferred from the mouth to the stomach by wavelike muscular contractions, called peristalsis.

The stomach stores the material, initiates the digestion of proteins, and transports it into the small intestine. This gastric digestion can take between 1 or 2 hours. Cells within the stomach wall secrete the inactive enzyme pepsinogen and HCl (with a pH of less than 2). The presence of HCl serves three functions: (1) proteins become denatured, (2) the enzyme pepsin is formed from pepsinogen, and (3) pepsin is more active at a pH of 2. Pepsin is important in the stomach because it can partially digest proteins.

The small intestine is composed of the duodenum, jejunum, and ileum, which are approximately 3 meters long in the human body with an intestinal digestion time ranged from the shortest of 1 hour to 4 hours depending on the method. It contains various enzymes, including enterokinase, which activates the protein-digesting enzyme trypsin that is secreted by the pancreas. The small intestines are the main site within the GIT where materials are absorbed, including fats, carbohydrates, proteins, vitamins, water, and pollutants present in the materials. Furthermore, the liver produces and secretes bile, which is initially stored in the gallbladder prior to its release into the small intestine. Bile is composed of bile salts (mainly cholic acid and chenodeoxycholic acid), bile pigments (bilirubin), phospholipids (lecithin), cholesterol, and inorganic ions (sodium, potassium, chloride, and bicarbonate). The pancreas secretes pancreatic juice into the duodenum. Pancreatic juice contains water, bicarbonate, as well as a range of digestive enzymes, including amylase (which digests starch), trypsin (which digests protein), and lipase (which digests triglycerides).

Finally, water and electrolytes are absorbed from the food material in the large intestine or colon, and after absorption, the waste material that is left passes to the rectum. At this point, the waste products pass through the anal canal and exit the anus (Dean & Ma, 2007).

To assess the oral bioaccessibility of chemical compounds, *in-vitro* test models are recommended over *in-vivo* models as they are less time-consuming and expensive (Lu et al., 2021), besides also minimizing animal testing. These methods were originally developed for food nutrition and pharmacological research on drug absorption efficiency and later applied to the environmental field to estimate human exposure to chemical contaminants. These models aim to simulate the major processes that occur in the human GIT in order to assess oral bioaccessibility. The three distinct areas of the human digestive system that are important in designing the extraction process are the mouth, stomach and small intestine. Although the mouth is an essential part of the entire human process of digestion, it is often not included in simulated gastrointestinal extraction methods as food remains in this compartment for a relatively short period of time. In practice, *in-vitro* gastrointestinal extraction approaches aim to mimic the stomach where material is subject to pepsin at pH = 2 for a few minutes or hours. Then, intestine where nutrient absorption occurs in presence of pancreatic juice and bile salts at pH ranged from 6 to 7.5 for a couple of hours to days. Lastly, the undigested food and water can reabsorb in the colon in presence of microbiota at similar pH than intestine for a half day to several days (Guerra et al., 2012).

Several factors can influence the bioaccessibility of compounds in body fluids, including the composition of body fluids with enzymes and/or bile salts that can form micelles to enhance the bioaccessibility of POPs (Tao et al., 2011). The pH of body fluids can also impact bioaccessibility, with bile salts precipitating at acid medium and decreasing bioaccessibility. Digestion time can also play a role in facilitating organic chemicals release from the matrix until equilibrium is reached with an extended time. Finally, the organic matter content of the matrix (i.e., proteins, carbohydrates and lipids) may influence the bioaccessibility of organic compounds too.

The methods using *in-vitro* models can be classified in two types: static and dynamic. The most relevant *in-vitro* human bioaccessibility testing methods are described below.

1.6.1.1. Static *in-vitro* methods

In static *in-vitro* bioaccessibility testing methods the material is mixed with simulated saliva, gastric and intestinal fluids (body fluids) and allowed to incubate in physiological conditions of temperature, pH and specified period of time. The advantages of these methods are their simplicity, low cost and ease of use. However, they have some limitations due to not consider the dynamic nature of the human digestive system, including the movement of food and digestive juices through the system and may not accurately reflect the complex interactions that occur between food components and the digestive system. Within methods the most widely used are the physiologically based extraction test (PBET) based on Ruby et al. (1996), simulation of the human intestinal microbial ecosystem (SHIME), fed organic estimation human simulation test (FOREhST) and unified Bioaccessibility Research Group of Europe (BARGE) method (UBM) methods summarised in the Table 1.7.

Table 1.7. Oral *In-vitro* gastrointestinal methods for organic pollutants.

	Specific	PBET	Colon extend-PBET	FOREhST	UBM	SHIME
Reference		Ruby et al. (1996)	Tilston et al. (2011)	Cave et al. (2010)	BARGE (2011)	Molly et al. (1993)
Main contaminants		Pb/As	PAHs	PAHs	As, Cd and Pb	Fatty acids
Matrix		0.4 g soil	1.2 g soil	0.3 g soil	0.6 g soil	20 g food
Organs mimicked	Oral cavity	X	X	✓	✓	X
	Stomach	✓	✓	✓	✓	X
	Small intestine	✓	✓	✓	✓	✓
	Large intestine	X	Colon	X	X	Colon
Oral cavity	Volume	-	-	7 mL	9 mL	-
	Components	-	-	-	Inorganic salts, urea, α-amylase,	-

	Specific	PBET	Colon extend-PBET	FOREhST	UBM	SHIME
					mucin and uric acid	
	pH	-	-	6.8 ± 0.5	6.5 ± 0.5	-
	Digestion time	-	-	5 min	0.5 min	-
Stomach phase	Volume	40 mL	-	9 mL	13.5 mL	-
	Components	Pepsin, citrate, maleate, lactic and acetic acid	Pepsin, mucin, HCl and NaCl	-	Inorganic and organic salts, pepsin, mucin and bovine serum albumin (BSA)	-
	pH	1.3-4.0	2.5	1.3 ± 0.5	1.2 ± 0.05	-
	Digestion time	1h	1h	2h	1h	-
Intestinal phase	Volume	40 mL	-	9 mL of duodenal + 4.5 mL of bile	27 mL of duodenal + 9 mL of bile	80 mL
	Components	$NaHCO_3$, Porcine, pancreatin and bile salts	Pepsin, pancreatin, mucin and bile salts	-	Inorganic and organic salts, pancreatin, lipase, BSA and bile	Inorganic and organic salts with extracts
	pH	7.0	7.0	6.2 ± 0.5	6.3 ± 0.5	7.0 ± 0.5
			6.5			
	Digestion time	3h	4h	2h	4h	1h
			8h			
Operating condition	Temperature	37ºC	37ºC	37ºC	37ºC	37ºC
	Food components	X	X	Organic creamy porridge with sunflower oil	X	Human food
	Mechanic treatments	Argon gas mixing at 1 L/min	-	Magnetic stirring 30 rpm	End-over-end mixing at 30 rpm	Magnetic stirring at 150 rpm
	Centrifugation filtration	2100 g for 25 min	3,000 g for 10 min	3,000 g for 5 min	4,500 g for 15 min	-

The first method called PBET was reported by Ruby et al. (1996), focused on determining the bioaccessibility of Pb and As in soil samples. It was later modified in 2002 to analyse

organic pollutants like dioxins and furans (Ruby et al., 2002). This method divides the human body into two compartments: a gastric phase and an intestinal phase, each with specific parameters and dissolved salts, these details are summarized in Table 1.7. Numerous improvements have been made to this method, allowing for the study of bioaccessibility of organic compounds such as PAHs, PCBs, PAEs, PBDEs, OPFRs, perfluorooctanoic acid (PFOA), dichloro-diphenyl-trichloroethane, and its metabolites in various matrices like soil, indoor dust, and food. Comparisons between *in-vitro* and *in-vivo* methods involving animals have also been conducted (Juhasz et al., 2016; Pan et al., 2016).

To address the limitations of the initial PBET method in testing the bioaccessibility of hydrophobic POPs, a modified approach called colon extend-PBET was developed. Tilston et al. (2011) introduced a colon phase to facilitate the release of POPs from matrices. This method, consisting of three phases (gastric, intestinal, and colon), has been used to investigate the bioaccessibility of BFRs and dichloro-diphenyl-trichloroethane in soil, dust, and food samples. The colon extend-PBET method has shown varying degrees of bioaccessibility for different compounds, such as TBBPA, HBCD, and PBDEs in house dust samples, with recoveries ranging from 32% to 94% (Abdallah et al., 2012).

The SHIME method, proposed by Molly et al. (1993), provides a more accurate simulation of the human gastrointestinal microbial ecosystem. It incorporates a colon phase that includes both organic and inorganic components as well as colon microbiota. This method has been widely used to evaluate the release of hydrophobic POPs from food and soil/dust matrices. Studies using the SHIME method have reported bioaccessibility ranges for PAHs and pesticides in animal-based foods. Yu et al. (2012) reported the SHIME model without faecal microbiota to research PAH bioaccessibility in animal-based foods and found that the mean bioaccessibility ranged from 29-61%.

The FOREhST method, developed by Cave et al. (2010), includes three digestion phases: oral cavity, gastric, and intestinal. It incorporates specific food contents, such as infant formula. The FOREhST method has been utilized to assess PAH bioaccessibility in soil polluted by creosote (Juhasz et al., 2014) with low bioaccessibility lower than 4%, conversely were also studied chlorinated organophosphate esters in indoor dust samples (Quintana et al., 2017) with bioaccessibility range from 11-103% depending on the $\log K_{ow}$ of each compound.

The UBM method, developed by BARGE (2011), is another three-phase method similar to the FOREhST approach. However, the UBM method involves comparatively less digestion time in the oral cavity and the gastric phase than the FOREhST method. It has been used to study the bioaccessibility of trace elements in soil and the bioavailability of PFOA in foods. The UBM method has shown promise in simulating human digestion and predicting the relative bioavailability of chemicals. Smith et al. (2012) used the UBM method to study dichloro-diphenyl-trichloroethane in soil with a bioaccessibility lower than 4% and relative bioavailability ranging from 2% to 25%. However, it has limitations when it comes to highly lipophilic substances and low bile concentrations.

In summary, these different *in-vitro* oral bioaccessibility methods offer various approaches to studying the release and bioaccessibility of organic compounds in different matrices. Each method has its advantages and limitations, and the choice of method depends on the specific compounds and matrices under investigation.

1.6.1.2. Dynamic *in-vitro* methods

Dynamic models have been developed to more accurately simulate the release and absorption of pollutants in the GIT, where these processes occur simultaneously in a batch format by adding a sorptive-based material retaining pollutants from simulated gastric and intestinal fluids extracted from the sample, which is agitated at each step.

Most recently developed dynamic models are modified static methods. The first dynamic methods were modified from a static method introduced Caco-2 cells and EVA thin film by Vasiluk et al. (2007). However, these methods are not truly dynamic because Caco-2 cells or EVA thin film is added as a lipid sink to the digestion solution containing released substances after the digestion process has finished. This poses a problem as the release and absorption of pollutants from the matrix do not happen at the same time. To overcome this shortcoming, Hurdzan et al. (2008) and James et al. (2011) have used an absorptive sink, such as a C18 membrane, during incubation to ensure that the release and absorption processes occur simultaneously. Later, the porous polymer resin Tenax-TA was introduced in a study on PBDE bioaccessibility by Yu et al. (2013), which had a bioaccessibility range of 20-51% for tri-to hepta-BDEs, and 5-14% for decabromodiphenyl ether in dust fractions of varied particle size. The ideal absorption sink material should have a high capability of maintaining the concentration gradient between the matrix and the digestion solution, facilitate chemicals release, trap the released compounds quickly, and behave well in back-extraction with solvent for bioaccessibility calculation (Gouliarmou et al., 2013).

Before adding the absorption material to the simulated digestion fluid, researchers should determine its sorption kinetics and capacity (Gouliarmou et al., 2013). The final bioaccessibility is the fraction of extractable compound found in the digestive fluid and absorptive sink. Li et al. (2016) found a 3-22 times bioaccessibility improvement (27-56% against 1-15%) for dichloro-diphenyl-trichloroethane in soil using the PBET method with Tenax addition. If the bioaccessibility data is comparable to the bioavailability from animals, the method is considered meaningful. In recent years, many studies have used absorptive sinks, including Tenax, silicone rods/sheets, and C18 membranes (Gouliarmou et al., 2013; Juhasz et al., 2016; Pan et al., 2016; Yu et al., 2013).

Other studies preferred automatic online dynamic flow systems with the aid of robotic systems and/or flow injection approaches that resemble physiological conditions in the small intestine compartment by continuous extraction and removal of bioaccessible species. The flow through dynamic procedures have been only applied once to investigate the bioaccessibility of pharmaceutical and personal care compounds from mussels preconcentrated onto a SPE microcolumn and injected into LC-MS with an gastrointestinal bioaccessibility ranged from 17 to 55% (Rosende et al., 2019). The same methodology was applied to plastic additives such as PAEs and BPA sorbed on MPs under fasted (UBM) and fed conditions (Versantvoort et al., 2005) with a bioaccessibility ranged from 48 to 87% (Sixto et al., 2021).

1.6.2. Aquatic organisms bioaccessibility

The bioaccessibility of chemicals from aquatic particulate matter, including MPs, to aquatic organism, particularly fish, is of relevance because this sheds light over the real risk of such

bound pollutants to such organisms, and ultimately how they are incorporated into fish tissues and can then reach the food market. Numerous studies have focused on salmonids, primarily rainbow trout, and to a lesser extent, other species such as gilthead seabream (*Sparus aurata*), bluefin tuna (*Tunnus thynnus*), common carp (*Cyprimus carpio*), and turbot (*Psetta maxima*). Figure 1.6 presents the physiology of a fish.

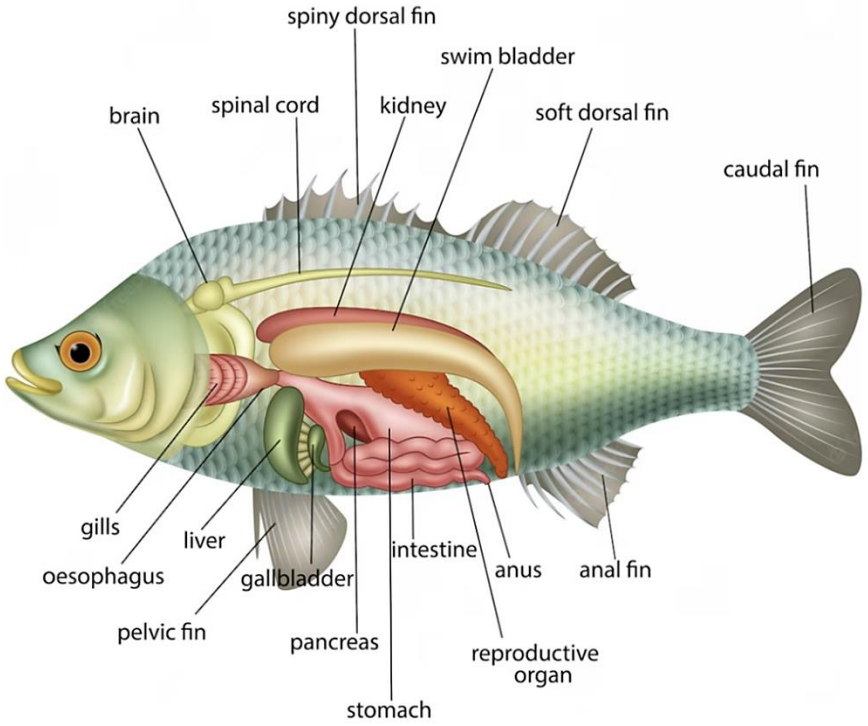

Figure 1.6. The digestive system of fish including the GIT and associated organs.

Own elaboration

Fish digestion is simpler than in humans. The material is ingested into the mouth, transported via the oesophagus due to wavelike peristalsis, and reaches the stomach in a matter of minutes. In the stomach, material is stored, proteins are digested, and the material is transported to the intestine through the pyloric caeca. Cells in the stomach wall secrete inactive pepsinogen, which is converted to pepsin and HCl to break down materials in the pH range of 1-3 depending on the species and type of material. The spiral intestine, which connects the stomach to the rectum, secretes trypsin, α-chymotrypsin, and protease. The intestine itself is relatively straight but has a long fold running along the inner surface in a spiral fashion. This fold varies in length, structure and composition of enzymes depending on the fish's feeding habits and type of food. The pyloric caeca valve increases the surface area and effective length of the intestine, allowing for absorption of water, fats, carbohydrates, proteins, vitamins, and pollutants present in the material, while passing waste material out of the body through the cloacae.

Given the difficulty and high cost of accessing the relevance and effect of each factor using *in-vivo* experiments, an alternative approach is to simplify the digestion process through *in-vitro* assays. However, a lack of standardized protocols for fish *in-vitro* digestion tests is a major problem, and most literature uses fish stomach and intestinal extracts, which have the disadvantage of harming the animal. Therefore, two distinct but linked areas of the fish

digestive system - the stomach and intestine - are crucial to consider when designing the extraction process.

Table 1.8. Vertebrate and invertebrate organisms *in-vitro* methods for assess the bioaccessibility of organic pollutants.

	Reference	Morales and Moyano (2010)	Hamdan et al. (2009)	Cabañero et al. (2004)	Coffin, Lee, et al. (2019)	Mohamed Nor and Koelmans (2019)
Fish		*Oncorrhynchus mykiss* (vertebrate)	*Argyrosomus regius* (vertebrate)	*Aphanopus carbo*, *Sardina pilchardus* and *Thunnus spp.* (vertebrate)	*Mugil cephalus* (vertebrate)	*Gammarus* (organism invertebrate)
Main pollutants		Nitrogen and phosphorous	Total amino acids	Se and Hg	DEHP	PCBs
Matrix		Fish meal and soybean meal	0.1-0.2 g commercial food	25 g fish	180 mg PS	227-236 g LDPE and PVC
Organs mimicked	Stomach	✓	✓	✓	✓	X
	Intestine	✓	✓	✓	X	✓
Stomach phase	Volume	-	-	75 mL	-	-
	Components	Stomach extracts	Stomach extracts	Pepsin	Pepsin	-
	pH	2.0	2.0	1.8	2.0	-
	Digestion time	1h	0.25h	4h	24h	-
Intestinal phase	Volume	-	-	50 mL	-	70 mL
	Components	Pyloric caeca extract	Pyloric caeca extract and bile salts (Taurocholate and chenodeoxyc.)	Pancreatin, sodium chloride, α-amylase and bile salts	-	*Gammarus* gut extracts with BSA and bile salts
	pH	9.0	8.0	7.0	-	4.0
	Digestion time	2h	2h	4h	-	28 days
Operating condition	Temperature	37ºC	37ºC	37ºC	24ºC	27ºC
	Mechanic treatments	Semi-permeable membrane reactor	Semi-permeable membrane reactor	Thermostatic water bath	Rotatory incubator	Horizontal shaker 100 rpm
	Centrifug. filtration	4,000 g for 15 min	4,000 g for 15 min	3,500 g for 60 min	SPE	-

Unlike in humans, in fishes, the mouth is not technically part of the digestive tract and is only the point of entry for the material is what happens for invertebrate organisms and fishes. Vertebrate fish contain teeth that help break down and prepare food for digestion. In the last 20 years, many *in-vitro* methods have been developed, primarily used in food nutrition to determine the bioaccessibility of omega-3 fatty acids (Moyano et al., 2015), and later extended to pollutants such as heavy metals and PCBs found in the digestive tract of fish (Cabañero et al., 2004).

Table 1.8 provides a summary of some of the diverse procedures employed to date, which distinguishes between vertebrate and invertebrate organisms. While most vertebrate models include both gastric and intestinal phases, the invertebrate ones only have an intestinal phase. Compared to oral bioaccessibility in humans, the temperature is typically lower than 37ºC, the digestion time in the gastric phase is shorter (≤1 hour), and longer in the intestinal phase (ranging from 2-4 hours depending on the protocol). Nonetheless, there is significant variability in temperature, digestion times, pH, and composition across these studies. This variability is even greater than that observed in oral bioaccessibility studies in humans, as the only commonality between these studies is that extracts of fish grindings are used to simulate gastric and intestinal juices mixed with enzymes and salts.

Numerous studies have examined the bioaccessibility of nutrients in food to assess dietary recommendations. In terms of contaminants, studies have focused on heavy metals such as Hg and Se. For example, Cabañero et al. (2007) investigated the bioaccessibility of these metals dissolved in aqueous matrix exposed for three fish samples (swordfish, sardine, and tuna) using simulated gastric and intestinal digestion. The results showed that less than 20% of Hg in the fish was bioaccessible, whereas 50-83% of Se was bioaccessible. Interestingly, sardine had a very low bioaccessible Hg content (10%) and a high bioaccessible Se content (83%), making it a more beneficial option compared to the other fish studied.

In contrast, there is less research on POPs. For example, Masset et al. (2022) studied the bioaccessibility of organic chemical compounds associated to tire and road wear particles into fish digestive fluids using an *in-vitro* digestion model based on *Oncorhynchus mykiss*. Overall, for the more polar compounds, such as aniline, benzothiazoles, and 1,3-diphenylguanidine, the bioaccessible fraction (BF) was higher than for more hydrophobic PAHs due to the solubilization of PAHs may be strongly affected by the nature of the digestion fluids.

1.6.3. *In-vitro* bioaccessibility in organisms from microplastics

In-vitro bioaccessibility tests are also used to evaluate contaminants adsorbed on MPs. The main studies are based on evaluating contaminants by simulating human digestion in the most common MPs found in the marine environment, such as LDPE and PVC. The previously commented dynamic *in-vitro* method Sixto et al. (2021) studied the bioaccessibility of PAEs and BPA sorbed on LDPE and PVC MPs using fasted (UBM) and fed (Versantvoort et al., 2005) methods with an average results ranged from 51-84% and 48-87%, respectively while the bioaccessibility was inversely proportional to $\log K_{ow}$. Moreover, Bao et al. (2023) reported bioaccessibility of PAHs such as naphthalene and 2-hydroxynaphthalente from PVC with values ranged from 5.5 to 5.7% and 49 to 52%, respectively. Instead, Chen et al. (2022) studied the bioaccessibility of heavy metals such as Pb (II), Cr (VI), Cd (II) and As (V) from PVC using

an *in-vitro* Soluble Bioavailability Research Consortium digestion method using a extractor device consisting in a bath heater and gear motor, but the same conditions than other fasted PBET models and obtained the highest bioaccessibility for Pb(II) in the gastric phase, while As (V), Cr (VI), and Cd (II) bioaccessibilities showed the opposite trend.

In contrast, a few studies were reported using vertebrate and invertebrate organisms. For example, Coffin, Lee, et al. (2019) tested the bioaccessibility in vertebrate (*Mugil cephalus*) and invertebrate (*Arenicola marina*) organisms in the gastric phase, and performed a leaching study in seawater to evaluate DEHP, bisphenol S, and 4-tert-octylphenol sorbed on PS. They found that the concentration of DEHP increased 6.3 ± 2.0-fold in extracts from invertebrate gut conditions. In another study, Coffin, Huang, et al. (2019) tested the bioaccessibility of *Mugil cephalus* and seabird in the gastric phase, and performed a leaching study in seawater to evaluate 12 plastic additives. They found that BPA, DEHP, and BzBP sorbed on 16 common plastic items (LDPE, PP, and PS) had significantly increased concentrations in seabird gut conditions relative to control. Similarly, BzBP was significantly increased in fish gut conditions relative to control. Mohamed Nor and Koelmans (2019) conducted a study on the bioaccessibility of 14 PCBs sorbed in LDPE and PVC MPs, using *Gammarus* as an invertebrate organism model. The results show that the leaching ranged from 53-82% for LDPE and 73-89% for PVC.

1.7. PER-/POLY-FLUOROALKYLATED SUBSTANCES

Per-/poly-fluoroalkyl substances (PFAS) is a term used to refer to highly fluorinated aliphatic substances that have at least one fully fluorinated carbon atom (-CF2-) in their structure. These substances typically contain a terminal functional group such as perfluoroalkyl carboxylic acid (PFCA) or perfluorosulfonic acid (PFSA), in addition to the fully or partially fluorinated alkyl chain. PFAS can be classified as short chain (C <8) or long chain (C ≥8), based on the number of fluorinated carbon atoms present in their backbone.

The strong C-F bond strength (485 kJ/mol) in PFAS makes them thermodynamically stable and highly resistant to heat, water, and other environmental factors. Their ability to repel water, oil, and stains makes them useful in products such as non-stick cookware, food packaging, carpets, and outdoor gear (Al Amin et al., 2020). PFAS have been widely used for over 70 years in various applications, especially in manufacturing, aerospace, firefighting, and plastic materials. However, their widespread use has led to their presence in the environment as emerging contaminants, known as "forever chemicals," that do not easily break down in the environment or in the human body.

PFAS can also form in the environment from polyfluorinated precursors such as acrylates, fluorotelomer alcohols, per-fluoroalkyl sulphonamides, and sulphonamido ethanols. Moreover, PFAS have been found to have long-term negative health effects on humans and wildlife because of their persistence and bioaccumulation (in the case of long chain PFAS) in the environment and the fact of being endocrine disruptors. Their effects include foetal and children developmental alterations, liver and immune system toxicity, and even some studies have suggested a possible link between PFAS exposure and increased risk of certain types of cancer such as kidney and testicular cancer (Steenland & Winquist, 2021). Due to concerns about the health effects of PFAS, many countries have implemented regulations to limit their use and disposal. For these reasons, the USEPA has set a lifetime health advisory level for PFOA and

PFOS of 70 ng/L in drinking water (USEPA, 2016a, 2016b). Recently, in March of 2023 USEPA proposed a National Primary Drinking Water Regulation for six PFAS: PFOA and PFOS as individual contaminants, and perfluorononanoic acid (PFNA), GenX, perfluorohexanesulfonic acid (PFHxS) and perfluorobutanesulfonic acid (PFBS) as a mixture of contaminants to establish a concentration level less than 4 ng/L in drinking water (USEPA, 2023). In addition, in surface and groundwater, several US States regulate the discharge of pollutants and implement their own regulations. For example, in 2019, the state of Vermont became the first in the USA to regulate PFAS in surface water, setting a limit of 20 ng/L for five different PFAS compounds.

Instead, the European regulated the presence of PFOS in surface water, by including this substance it in the priority substances list in 2013 under the Water Framework Directive by the Directive 2013/39/EU (EC, 2013), and recently, in 2020, the EU Directive 2020/2184/EU limited the presence of 20 PFAS (C4-C13) as a sum of concentrations to ≤0.1 µg/L in drinking water (EC, 2020). In 2020, the Spanish Ministry of Ecological Transition and Demographic Challenge published a draft regulation proposing limits for several PFAS compounds in surface water, including rivers, lakes, and reservoirs. The proposed limits are 0.3 ng/L for PFOA, 0.4 ng/L for PFOS, and 6 ng/L for the sum of six other PFAS. The regulation is currently under review and has not yet been implemented ("Real Decreto 1/2016, de 8 de enero, por el que se aprueba la revisión de los Planes Hidrológicos de las demarcaciones hidrográficas del Cantábrico Occidental, Guadalquivir, Ceuta, Melilla, Segura y Júcar, y de la parte española de las demarcaciones hidrográficas del Cantábrico Oriental, Miño-Sil, Duero, Tajo, Guadiana y Ebro.,"). Currently, in January of 2023, the European Economic and Social Committee proposed to add 24 PFAS to the lists of priority substances for surface and groundwater, which will be used to assess chemical status under the Water Framework Directive (EESC, 2023).

Moreover, the main sources of PFAS in surface water are the WWTPs. The discharge of PFAS from industrial wastes or biosolids has been widely reported to pollute surface water and groundwater (Rahman et al., 2014). Rahman et al. (2014) stated that the hydrophobic/hydrophilic properties, high water solubility, and low volatility of most PFAS play a role in their occurrence in all aquatic environments, including rainwater. Table 1.9 summarizes the concentrations of PFAS in aquatic environments worldwide. The reported studies concentrations of PFAS in drinking water range from less than 0.2 ng/L in Ireland to 644.6 ng/L in South Korea, and in river water from less than 0.1 ng/L in Australia to 16,000 ng/L in the Samondogawa River in Japan. Groundwater samples showed PFAS concentrations between 0.03 ng/L in Melbourne, Australia, and 51,000 ng/L in Sweden. Surface water samples exhibited PFAS concentrations from 1.0 ng/L in Lake Victoria in Kampala, Uganda, to 13,000 ng/L across Sweden.

Table 1.9. Occurrence of PFAS in water bodies.

Water sources	PFAS	Concentrations in ng/L (ranges or mean)	Locations	References
Drinking water	ΣPFAS	502.9 332.6 122.4 119.4	Zigong, China Lianyungang, China Changshu, China Chengdu, China	(Liu et al., 2021)
	ΣPFAS	80.0-119.8	Beidagang Reservoir, China	(Li et al., 2023)
	ΣPFAS	4.40-184	Several villages in China	(Yin et al., 2023)
	PFOA PFOS	20.2 16.7	Taiwan	(Jiang et al., 2021)
	PFOA PFBS PFOS ΣPFAS	1.9-65.2 ND - 10.7 0.5-4.6 8.9-644.6	South Korea	(Kim et al., 2020)
	PFBS	ND - 10.2	Near Ganges River basin, India	(Sharma et al., 2016)
	PFOA PFOS PFBS	0.04-1.7 <0.1-0.7 <0.2-15.0	Irish Drinking water, Ireland	(Harrad et al., 2019)
	PFCA	10.4-42.9	Northern France	(Boiteux et al., 2017)
	PFOA	519	Ruhr and Moehne area, Germany (maximum concentrations)	(Domingo & Nadal, 2019)
	PFOS PFOA PFBS ΣPFAS	ND - 120 ND - 3.1 ND - 3.1 ND - 120	Residences and public spaces in Alaska, USA	(Babayev et al., 2022)
	PFOA	213	Brookings, South Dakota residential tap water, USA	(Skaggs & Logue, 2021)
	PFOS PFOA	16.0 9.7	34 locations around Australia	(Thompson et al., 2011)
	ΣPFAS	ND - 5.3	Kampala, Uganda	(Arinaitwe et al., 2021)
Groundwater	ΣPFAS	0.1-13.4	Groundwater in the Alluvial-Pluvial Plain of Hutuo River, China	(Pan et al., 2014)
	ΣPFAS	20-4,773	North Carolina, USA	(Pétré et al., 2021)
	PFOA PFOS PFBS	109 830 9,250	Hurlburt Field AFB, Florida, USA	(Cui et al., 2020)
	26ΣPFAS	6,400	Across Sweden	(Gobelius et al., 2018)
	PFOS PFBS PFOA 20ΣPFAS	<0.03-34 4.4 2.2 <0.03-74	Melbourne, Australia	(Szabo et al., 2018)

Water sources	PFAS	Concentrations in ng/L (ranges or mean)	Locations	References
River	PFBS PFHxS PFOS	0.5-2.6 2.9-15 6.5-45	Australia	(Allinson et al., 2019)
	PFCA	17.0	Northern France	(Boiteux et al., 2017)
	GenX	3830	Shandong, China	(Hopkins et al., 2018)
	ΣPFAS	2,300-16,000	Samondogawa River, Japan	(Takemine et al., 2014)
	PFOA PFBS PFOS ΣPFAS	1.6-19.2 2.3-11.4 ND - 17.4 441.7	Truckee River, USA	(Bai & Son, 2021)
	PFHxS PFOS	12-37 0.01-128	Jucar River, Spain	(Campo et al., 2016)
	PFOS PFOA	390 47	Salt River, South Africa	(Mudumbi et al., 2013)
	PFOA	1,613	Bormida river, Italy	(Valsecchi et al., 2015)
Lake	PFOS	1.7-16.2	Multiple rivers, Nigeria	(Ololade, 2014)
	PFOS PFOA	17-54 <25	Tennessee river, USA	(Hansen et al., 2002)
	PFOA PFOS	3.4 11.1	Albufera Natural Park, Spain (estuary)	(Lorenzo et al., 2019)
	26ΣPFAS	13,000	Sweden	(Gobelius et al., 2018)
	26ΣPFAS	1.0-2.4	Lake Victoria in Kampala, Uganda	(Dalahmeh et al., 2018)
	ΣPFAS	82.3	Pyramid Lake, Nevada	(Bai & Son, 2021)

Given the concern about PFAS contamination, it is crucial to determine using an appropriate analytical methodology and also to remove these substances from both drinking water treatment plants (DWTPs) and WWTPs. However, classical methods for removing PFAS in water have proven ineffective, necessitating the development of physico-chemical processes such as advanced oxidation process (AOPs) to prevent these substances from reaching drinking water.

1.7.1. Removal of PFAS by AOPs

Biological methods such as the activated sludge process and certain physicochemical techniques like adsorption and membrane treatment have significant limitations to remove and break down toxic and persistent organic contaminants. These limitations include low efficiency and the potential for causing secondary pollution. Consequently, alternative methods known as

AOPs have emerged as an effective solution for eliminating non-biodegradable organic pollutants. AOPs operate by utilizing highly reactive free radicals, particularly hydroxyl radicals (•OH), but also hydrogen peroxide (H_2O_2) and superoxide ions (O_2^-), which are produced through chemical and photochemical reactions. The •OH oxidants generated by AOPs are reactive, non-toxic, non-corrosive, and have a short lifespan. These radicals can be easily generated within an electrochemical system (Isaev & Magomedova, 2022; Manna & Sen, 2023). These radicals facilitate the oxidation of organic pollutants, converting them into water (H_2O), carbon dioxide (CO_2), and inorganic compounds, as described by equation (2) proposed by Poyatos et al. (2010).

$$\text{AOPs} \rightarrow {}^{\bullet}\text{OH} + \text{Pollutants} \rightarrow CO_2 + H_2O + \text{Inorganic ions (Equation 2)}$$

The primary advantage of AOPs lies in the considerable potential of the oxidizing agents, particularly hydroxyl radicals (•OH), for effectively reducing organic compounds, phenolic compounds, and stubborn organic chemicals. However, the principal drawback of AOPs is the substantial operational cost associated with the use of chemicals and energy consumption (Dang et al., 2020). AOPs can be categorized into two main groups: chemical AOPs, including ozone, hydrogen peroxide, Fenton, electrochemical oxidation, and catalytic methods, and non-conventional AOPs, such as ultrasound, microwaves, and photocatalytic approaches (Manna & Sen, 2023). Defluorination, which involves breaking the carbon-fluorine (C-F) bond and removing one or more fluorine (F) atoms, is one of the crucial processes in PFAS removal using AOPs. Through this mechanism, PFAS compounds are converted into shorter-chain precursors, leading to enhanced removal and degradation. It should be noted that during the AOPs process, the original PFAS compounds (e.g., PFOA) undergo gradual degradation, while shorter-chain intermediates (e.g., PFHxS) are continually formed, indicating a stepwise defluorination process (Li et al., 2020). The mechanisms of PFAS removal using each AOP method are discussed in the following sections.

1.7.1.1. Electrochemical oxidation

Most studies investigating free radicals for PFAS oxidation have focused on electrochemical advanced oxidation process (EAOPs). These methods have gained increasing interest in recent years for water treatment due to their ability to degrade a wide range of recalcitrant organic compounds, including PFAS. In an EAOP, an electric current is applied to a specially designed electrode, which generates reactive oxidants such as hydroxyl radicals (•OH) or ozone from water or oxidants added to the medium, such as H_2O_2. These reactive species can oxidize the target contaminants into simpler and less harmful compounds such as, ideally, carbon dioxide and water, or mineralize them into inorganic ions such as chloride, sulphate, and nitrate. Electrochemical oxidation proceeds via direct and indirect anodic oxidation (Radjenovic & Sedlak, 2015).

Electrochemical oxidation proceeds via direct and indirect anodic oxidation (Radjenovic & Sedlak, 2015). In direct electrolysis, contaminants are adsorbed onto an electrode and degraded directly on its surface, while in indirect electrolysis, contaminants are degraded in the bulk liquid in reactions with oxidizing agents formed at the electrode (Radjenovic & Sedlak, 2015).

Operating conditions and parameters such as pH, current density, electrolyte type, electrode gap, initial PFAS concentration and temperature are also important factors affecting the electrochemical oxidation of PFAS (Nzeribe et al., 2019). Numerous materials have been used as electrodes, but most research on PFAS removal has been conducted using a boron-doped diamond (BDD) electrode due to its mechanical, chemical, and thermal stability. Other electrodes such as lead dioxide, titanium oxide, and tin oxide have also shown the ability to treat PFAS-contaminated water when compared with other inactive electrode materials such as iridium oxide and platinum (Nzeribe et al., 2019). The superiority of high-electron transfer capability materials may be due to the ability of their atoms to maintain the same oxidation state during the reaction, while atoms in the active anode continuously cycle during oxidation process (Zhuo et al., 2012).

The defluorination of PFOA increased with higher current density. Acidic pH promoted PFOA degradation compared to alkaline solutions, which may be related to the pH-dependent adsorption properties of PFAS. In a low-pH environment, the concentration of hydrogen ion adsorbed to the anode surface increases, and PFAS, which are anions, are easily adsorbed to the active sites on the anode surface through electrostatic attractions (Duinslaeger & Radjenovic, 2022; Schaefer et al., 2015; Zhuo et al., 2012).

Kinetic studies of PFAS show that the rate constant increases with chain length. It is well known the hydrophobicity of PFAS increases with chain length. Therefore, the increased rate constant may be the result of their easier adsorption onto the anode surface. Instead, pentafluorobenzoic acid (PFBA) was completely degraded and PFBS was not, which this fact may be PFSAs with the same carbon number as PFCAs were more difficult to degrade due to the electrophilic nature of their functional group. The rate constant also increased with an increase in the initial concentration of PFAS, suggesting that higher concentrations of PFAS molecules can reach the electrode surface, resulting in higher removal rates using BDD thin film electrodes (Zhuo et al., 2012). The electrochemical degradation of PFAS under high dissolved organic carbon (DOC) concentrations showed a defluorination higher of long-chain PFSAs than shorter. The concentration of PFCAs was increasing during the treatment reaction, while the degradability of PFSAs was higher in PFOS > PFHxS > PFBS > 6:2 FTSA (6:2 fluorotelomer sulfonate), indicating a gradual degradation mechanism of PFSAs (formation of shorter chain length) following the proposed pathway degradation of PFAS in Figure 1.7.

Electrochemical oxidation has several advantages over other oxidation processes, including the ability to work at RT, no chemical requirements, and no waste generation (Radjenovic & Sedlak, 2015). However, the disadvantage of electrochemical oxidation is its high energy consumption (Equation 3). For instance, the formation of toxic by-products such as bromate, hydrogen fluoride, lead, and perchlorate has been reported in the literature (Radjenovic & Sedlak, 2015).

$$Specific\ energy\ consumption = \frac{E\ I\ t}{V\ (C_0 - C_t)} \quad \text{(Equation 3)}$$

where I, t, E, and V represent current (A), time (h), average voltage (V), and volume (L), respectively. C_0 and C_t are the initial concentration and the concentration in time (t) of PFAS, respectively.

The degradation pathway involves several steps following the Figure 1.7. Firstly, there is the transfer of electrons, followed by the breaking of carbon-carbon (C-C) bonds between PFCAs and the carboxyl (COOH) group or carbon-sulphur (C-S) bonds between PFSAs and

the sulfonate (SO_3^-) group. These bond cleavages result in the formation of unstable perfluoroalkyl radicals (C_nF_{2n+1}) (Hori et al., 2004; Lee et al., 2012).

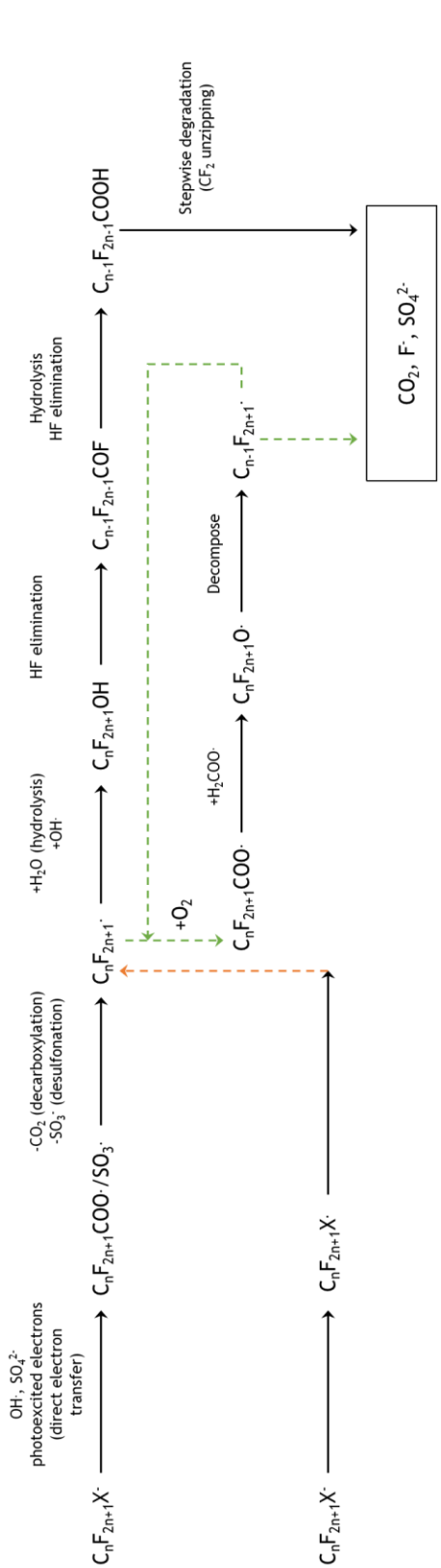

Figure 1.7. Proposed degradation pathway of PFAS by chemical oxidative processes as adapted from references cited herein (Hori et al., 2007; Jin et al., 2014; Lee et al., 2012; Niu et al., 2013; Wang et al., 2008).

Own elaboration

In the case of electrochemical oxidation, PFAS degradation occurs through direct electron transfer from the carboxyl (COO^-) or sulfonate (SO_3^-) group to the anode surface (Zhuo et al., 2012). The resulting unstable perfluoroalkyl radicals then react with water to form hydroxyl radicals, leading to the formation of thermally unstable alcohols ($C_nF_{2n+1}OH$). Subsequently, the alcohol undergoes hydrogen fluoride elimination (HF) to form $C_{n-1}F_{2n-1}COF$, which further undergoes hydrolysis, resulting in the formation of shorter-chain PFAS ($C_{n-1}F_{2n-1}COOH$). This series of reactions continues, with the shorter-chain PFAS undergoing stepwise degradation through the loss of CF_2 units, until complete mineralization into CO_2, F^-, and SO_4^{2-} (Jin et al., 2014; Schaefer et al., 2015), even a similar stepwise degradation for PFOS using sulphate radicals was reported (Yang et al., 2013).

However, some researchers have proposed alternative oxidative pathways for the degradation of PFAS using activated persulfate oxidation (Lee et al., 2012), electrochemical oxidation (Niu et al., 2013), and photochemical oxidation (Jin et al., 2014). According to these studies, the perfluoroalkyl radicals formed during the degradation process may undergo reactions with molecular oxygen generated through water electrolysis, resulting in the formation of perfluoroperoxy radicals. These perfluoroperoxy radicals can then combine with other perfluoroperoxy radicals to produce perfluoroalkoxy radicals. Subsequently, the perfluoroalkoxy radicals react with other radicals to form perfluorinated alcohols. These perfluorinated alcohols then undergo a series of reactions, including stepwise degradation, as mentioned earlier. In the case of the UV-Fenton system, it is also possible for a complex to form between PFAS and iron before desulfonation or decarboxylation occurs, leading to the generation of a perfluoroalkyl radical (Hori et al., 2007; Jin et al., 2014; Wang et al., 2008).

1.7.1.2. Microwave radiation and ultrasound

Microwave (MW) is an electromagnetic spectrum that spans in the frequency range of 0.3 to 300 GHz (Vialkova et al., 2021) and has primarily thermal and non-thermal impacts. Special devices, such as semiconductors and vacuum devices, are used to generate MWs. MWs exhibit wave-particle duality and display absorption, penetration, and reflection characteristics when interacting with substances. MW-induced oxidation, known for its fast and effective performance, absence of secondary contamination, and low energy consumption, has gained traction in chemistry, environmental protection, material science, and catalysis fields (Remya & Lin, 2011).

MWs serve as potent tools for the degradation of specific organic compounds like pesticides and organic dyes. MWs induce a process known as dielectric heating. Molecules with high dielectric constants, such as water and certain organic compounds, align and rotate under MW irradiation. The resulting heat facilitates molecular motion and collisions between molecules, thereby enhancing degradation. Moreover, MW energy can induce non-thermal effects by causing dipole rotation and ion migration, leading to increased degradation of refractory compounds. MW energy interacts with the polar portion of a substance and is absorbed, rapidly heating the surface sites to create “hot spots”. This process weakens the chemical bonds of organic molecules and stimulates oxidative degradation of organic pollutants. The transformed energy leads to the weakening of chemical bonds and the induction of oxidative degradation reactions (Remya & Lin, 2011). This treatment was used for PFOA

resulting in its completely removal to form shorter-chain PFCAs and fluoride ions, with 22.5% defluorination efficiency (Lee et al., 2010).

Ultrasound has been also applied as an AOP in the treatment of water and wastewater due to the production of •OH radicals in water and the oxidation of contaminants (Mahamuni & Adewuyi, 2010). Ultrasound creates alternating regions of positive and negative pressures in the sample, causing compression and expansion cycles of the liquid molecules. This process leads to the formation of cavitational bubbles during the rarefaction of ultrasonic waves, where the pressure exceeds the liquid's tensile strength. The collapse of these bubbles during the compression cycle generates localized hotspots with pressures of approximately 500 atm and temperatures of 5,000 K. This phenomenon, known as sonochemical oxidation, results in the dissociation of water molecules within the cavities, leading to the formation of reactive hydroxyl radicals and other reactive species. These radicals can oxidize organic contaminants in water (Chen et al., 2011). In addition, studies have demonstrated the effectiveness of ultrasonic waves to break down a substance through high-frequency ultrasound (>100 kHz) for mineralization of long-chain PFAS (Lei et al., 2020; Uriakhil et al., 2021; Zhang et al., 2022).

1.7.1.3. Photocatalysis process and UV

Photocatalysis involves reactions between excited electrons and contaminants on the surface of photocatalysts (Rafieenia et al., 2022). It offers several advantages, including stability, nontoxicity, the potential use of solar light as a light source, and operation at ambient temperature. However, there are limitations such as catalyst fouling and recovery. Photocatalytic reactions generally involve three steps: photoexcitation leading to the generation of electrons and holes, transfer of electrons and holes to the photocatalyst surface, and their subsequent reactions with adsorbed electron acceptors and donors. An effective photocatalyst requires a semiconductor with an appropriate band gap for light absorption, efficient charge carrier separation and transportation, and suitable valence and conduction band potentials for redox reactions.

Photocatalysts can be activated by visible or UV light depending on their bandgap energy. While only a small fraction of solar light (<5%) can be absorbed by photocatalysts with a large band gap, UV-based AOPs have been found to be highly effective in removing trace organic contaminants from various water sources (Rafieenia et al., 2022). Heterogeneous photocatalysis employs semiconductor slurries (e.g., ZnO/UV and TiO_2/UV), while homogeneous photochemistry (e.g., O_3/UV, Fe^{3+}/UV, and H_2O_2/UV) is used in single-phase systems (Agustina et al., 2005). Studies have shown that TiO_2-photocatalysis can remove 85% of PFCA after 420 minutes (Panchangam et al., 2009).

1.7.1.4. Ozonation

Ozonation is a promising method for treating water and wastewater as it can effectively remove organic contaminants, oxidize both inorganic and organic compounds, and disinfect pathogens. The degradation of organic contaminants by ozone involves both direct and indirect oxidation processes. Direct oxidation occurs through the reaction of ozone molecules with the contaminants, while indirect oxidation involves the formation of free radicals such as hydroxyl

radicals ($^{\bullet}OH$) and superoxide radicals ($^{\bullet}O_2^-$), which then react with the contaminants (Wang et al., 2022). The rate of hydroxyl radical formation depends on factors such as the chemical composition of the contaminants, water pH, the presence of natural organic matter, and alkalinity (von Gunten, 2003). At low pH, the main reaction mechanism is the direct electrophilic attack of ozone, while under alkaline conditions, the non-selective and rapid indirect ozone oxidation becomes the predominant mechanism (Derco et al., 2015).

The primary drawbacks of ozonation are its high production cost and short half-life. Additionally, there are other notable limitations such as the restricted concentrations of ozone in air or oxygen (approximately 4% to 8%), low energy efficiency in ozone production (around 5% to 10%), and the requirement for dry air or oxygen (Derco et al., 2015). Studies have shown that ozone alone is ineffective in removing PFAS from water, even with extended contact times and high doses (Lashuk, 2021).

1.7.1.5. Hydrogen peroxide, Fenton and sulphate radical-based system

H_2O_2 is a powerful oxidant commonly used for treating organic and inorganic contaminants. It serves as a source of $^{\bullet}OH$, making it suitable for *in situ* chemical oxidation. H_2O_2 can be used alone or in combination with catalytic agents like UV, iron, or ozone. However, the efficiency of H_2O_2 alone is limited for high concentrations of aromatic compounds (Zaharia et al., 2009).

In addition, previous studies (Shen & Wang, 2002) have explored the combination of H_2O_2 with UV radiation. UV/H_2O_2 has been found to be highly efficient in degrading different organic contaminants. This process offers several advantages, including the absence of sludge production, high removal rates of chemical oxygen demand (COD), and the formation of low molecular weight oxygenated compounds that are easily biodegradable. In some cases, the organic compounds can be completely reduced to water and carbon dioxide.

Moreover, H_2O_2 is frequently combined with ferrous ions generating the Fenton's reaction. Fenton is a highly effective technique for degrading organic contaminants due to its efficient generation of reactive oxygen species such as H_2O_2, $^{\bullet}OH$, and $^{\bullet}O_2^-$. The conventional homogeneous Fenton process produces $^{\bullet}OH$ through the reactions of hydrogen peroxide with soluble Fe(III) or Fe(II) salts in acid conditions (Bolobajev et al., 2015). However, conventional homogeneous Fenton has limitations, including the formation of iron sludge and a narrow pH range of 2-3.5. To overcome these limitations, the heterogeneous Fenton process has been developed, allowing for a broader pH range of 3-9 and easy separation of Fenton reagents (Hou et al., 2016). This protocol was used with UV and catalysed by Fe_3O_4 nanoparticles showed greater than 90% rates of short-chain PFAS destruction (Schlesinger et al., 2022).

Sulphate radical ($SO4^{\bullet-}$) based methods have become a focus of research due to their comparable or higher redox potential (2.5-3.1 V) compared to hydroxyl radicals. These methods offer advantages such as higher selectivity and longer half-life than $^{\bullet}OH$ under various conditions. As a result, sulphate radical-based systems, generated using persulfate ($S_2O_8^{2-}$) and peroxymonosulfate (HSO_5^-), have shown similar or superior capabilities in degrading emerging pollutants when compared to H_2O_2 (Wang & Wang, 2018). The sulphate radicals were used to completely removal of PFOA in resins (Gao et al., 2021).

1.7.2. Determination of PFAS in water

Aqueous samples, including surface water, groundwater, drinking water, lake and coastal or sea waters, usually contain a PFAS at low levels (see Table 1.9). Therefore, low LOQs are required, thereby pre-concentration and clean-up become critical steps for their preconcentration. Several extraction techniques, such as solid-phase extraction (SPE), liquid-liquid extraction (LLE), solid-phase micro extraction (SPME) and dispersive liquid-liquid microextraction (DLLME) have been investigated. Determination is normally performed by liquid chromatography coupled to mass spectrometry (LC-MS) and, less frequently and only for some particular PFAS by GC-MS. Table 1.10 summarises some of the methods published in the literature for the determination of PFAS in chronological order according to technological developments.

Multiple methods have been developed to determine PFASs in aqueous matrices, and as a result, many PFAS compounds with different chain lengths and functional groups (i.e., anionic, cationic, zwitterionic, short and ultra-short chain) have been detected (Kaboré et al., 2018). Commercial SPE columns, cartridges, and disks are commonly used, including materials such as weak anion exchange (WAX) sorbents, polymeric sorbents like N-vinyl pyrrolidone and divinylbenzene polymer (HLB), and less common options like bamboo charcoal-packed cartridges. Traditional SPE involves using large sample volumes (e.g. 100-2,000 mL) and extended extraction times, which can introduce contamination risks. For example, short-chain PFCAs (C4-C8) were identified in ground, surface and tap waters using SPE with OASIS® WAX and Strata® X-AW, and a recovery of 83-107% was achieved at different pH levels (Janda et al., 2019). Recently, Montes et al. (2020) also used an OASIS® WAX SPE cartridge to analyse PFAS from ultra-short to large (C1-C18) with recoveries of ≥81% (RSD ≤15%) in river water.

Table 1.10. Selection of methods employed in the literature for the determination of PFAS in chronological order.

Identified PFAS	Analysis approaches	Extraction methods (sorbent)	LOQs (ng/L)	Sources	Reference
PFOA, PFHxA, PFDoA	GC-EI-MS	SPE (SAX)	36,000	Ground water	Moody and Field (1999)
PFOA, PFOS	LC-ESI-MS/MS	SPE (C18)	10-50	River water	Hansen et al. (2002)
PFOA, PFOS, PFOSAA, N-Et-FOSAA, FOSA, N-Et-FOSA, N-Et-FOSE	LC-ESI-MS	SPE (C18)	0.2-13	Surface water	Boulanger et al. (2004)
PFOS, PFOA, PFNA, PFDA, PFUdA, PFDoA, 6:2, 8:2, 10:2 FTCA, 6:2, 8:2, 10:2 FTUCA,	LC-ESI-MS/MS	SPE (C18)	0.04-7.2	Rain water	Loewen et al. (2005)
PFOS, PFOA, PFNA, PFDA, PFUdA, PFHxA, PFHpA	LC-ESI-MS	SPE (C18)	0.28-0.58	Surface water	Simcik and Dorweiler (2005)
PFOS, PFDS, PFHxA, PFHpA, PFOA, PFNA, PFDA, PFUdA, PFDoA	LC-ESI-MS/MS	Automated SPE, LLE (C18)	0.2-6.4	DWTP effluent	González-Barreiro et al. (2006)
PFOA, PFOS	LC-nano ESI-MS	Online-SPE (C18)	0.5-1	River water	Wilson et al. (2007)

Identified PFAS	Analysis approaches	Extraction methods (sorbent)	LOQs (ng/L)	Sources	Reference
C4-C10 PFCA	GC-EI-MS	LLE (HLB)	0.5	DWTP effluent, surface and rainwater	Scott et al. (2006)
PFOS, PFOA	LC-ESI-MS/MS	SPE (SDB)	2.3-84 and 5.2-92	Tap and fresh water	Takagi et al. (2008)
C5-C17 PFAS	LC-ESI-HRMS	Online SPE (C18)	5-90,000	Wastewater	Liu et al. (2015)
PFBS, PFHxA, PFHpA, PFOA, PFNA, PFOS	LC-ESI-MS/MS	Automated SPE (HLB)	0.2-100	River water	Loos et al. (2017)
C4-C8 PFCA, 4:2 FTSA, 6:2 FTSA	LC-ESI/GC-EI-MS/MS	SPME (PDMS)	13-131.9	Surface, drinking and river water	Boiteux et al. (2017)
PFOS, PFOA, PFHxA, PFHpA, PFHxS, PFPeA, PFBA, PFNA, PFDA, PFBS	LC-ESI-MS/MS	Automated SPE (WAX)	Max. 76	Fresh and treated water	Boiteux et al. (2012)
PFHxS, PFHpA, PFOA, PFOS, PFNA, PFDA	LC-ESI-MS/MS	SPE (Bamboo-charcoal)	0.01-1.15	Drinking, tap, lake and pond water	Deng et al. (2018)
C4-C14 PFCA, PFBS, PFHxS, PFOS, PFDS, FOSA, 6:2FTSA, 5:3FTCA, PFOAB	LC-ESI-HRMS	Automated off line SPE (WAX)	>39	Drinking water	Kaboré et al. (2018)
C2-C8 PFCA	LC-ESI-MS/MS	SPE (WAX)	0.1-3.3	Surface, ground and drinking water	Janda et al. (2019)
C2-C18 PFCA and C1-C10 PFSA	LC-ESI-MS/MS	SPE (WAX)	10-560	River and drinking water	Montes et al. (2020)

LC-ESI-MS/MS: Liquid Chromatography electrospray ionization coupled to mass spectrometry in tandem; SAX: Strong anion exchange; HLB: Hydrophilic-Lipophilic Balance; SDB: Styrene-divinylbenzene; PDMS: Polydimethylsiloxane; WAX: Weak anion exchange; PFPeA: Perfluoropentanoic acid; PFHxA: Perfluorohexanoic acid; PFHpA: Perfluoroheptanoic acid; PFDA: Perfluorodecanoic acid; PFUdA: Perfluoroundecanoic acid; PFDoA: Perfluorododecanoic acid; PFDS: Perfluorodecane sulfonic acid; PFOSAA: Perfluorooctane sulfonamidoacetate; PFOAB: Perfluorooctane amido betaine; FOSAA: Fluoro-1-octanesulfonamidoacetic acid; FOSA: Fluorooctane sulfonamide; FOSE: Fluorooctane sulfonamidoethanol; FTCA: Fluorotelomer carboxylic acid; FTUCA: Fluorotelomer unsaturated carboxylic acid; FTSA: Fluorotelomer sulfonate

Moreover, online SPE coupled with liquid chromatography-tandem mass spectrometry (LC-MS/MS) offers a solution by reducing sample volume and pre-treatment duration. Liu et al. (2015) described the use of LC with an orbitrap mass analyser for PFAS monitoring from wastewater via on-line SPE using C18 sorbent, and detection limits were estimated between 0.005 ng/mL to 0.2 ng/mL. Instead, the main issue of PFAS is the background contamination of short-chain PFAS reported in the literature (González-Barreiro et al., 2006) introduced from the solvent, tubing, and the degasser from the desired analytes of the equipment.

Another alternative is the LC direct injection analysis, which eliminates sample pre-treatment, requires extended chromatographic analysis to separate analytes from matrix components. It requires a highly sensitive instrument for adequate detection levels and need for individual internal standard (IS) due to due to high signal suppression from the aqueous matrix. Ciofi et al. (2018) reported the successful use of direct injection analysis for 3 short and 4 long-chain PFAS (C4-C10) in water samples, achieving low detection limits (0.014-0.44 ng/L) with minimal sample volumes.

Additionally, SPME is an alternative method for PFAS analysis. It combines sampling, sorbent extraction, preconcentration, and injection into a single step, streamlining the analysis process and improving its environmental impact, conversely it has low sensitivity for short-chain PFAS due to weaker interactions with the adsorbent. Huang et al. (2018) proposed a new, multiply monolithic fibre-SPME connected with the monolithic adsorbent combining fluorophilic and anion-exchange interactions to be analysed by LC requiring only 20 mL of the water sample with recoveries >87% for C4-C10 PFAS and LOQs ranged from 1.65-14.5 ng/L.

Finally, the conventional DLLME was reported to extract different types of PFAS from tap, river water, and urine samples by LC (Wang et al., 2018). The method is simple, cost-effective, less time-consuming, and achieves sufficient recoveries (81-121%) for medium and long-chain PFAS with LOQs ≤10 ng/L. However, it is not suitable for short-chain PFAS due to low recovery rates (17-57%).

1.8. SCREENING WITH HIGH-RESOLUTION MASS SPECTROMETRY SYSTEMS

Recent advances in high-resolution mass spectrometry (HRMS) instrumentation, such as time-of-flight (TOF), orbitrap, and ion mobility mass spectrometers, have enabled the development of powerful screening strategies for environmental analysis. This data can then be processed using specialized software to detect and identify a wide range of compounds with different physio-chemical properties. HRMS instruments provide high-mass accuracy and resolution in full-scan mode, which allows for the recording of virtually unlimited numbers of compounds. Additionally, HRMS full-scan data enables retrospective analysis of the data to identify previously unconsidered compounds, thereby opening up the possibility of performing retrospective screening using older HRMS data. Screening approaches based on HRMS have proven effective in detecting and identifying a wide range of compounds in complex samples (Chiaia-Hernández et al., 2020; Choi et al., 2021; Salihovic et al., 2012).

LC-HRMS screening is typically based on soft ionization techniques (normally electrospray ionization), while most GC-(HR)MS approaches are based on hard ionization (electron ionization). Thus, screening methods differ significantly among the two chromatographic techniques, as discussed below.

1.8.1. Screening by LC-HRMS

1.8.1.1. Data acquisition modes

LC-HRMS instruments utilize three different acquisition modes: Full-scan, data-dependent acquisition (DDA), data-independent acquisition (DIA) and target MS/MS (Geer Wallace & McCord, 2020). The choice of acquisition mode will depend on the specific goals of the analysis, such as targeted *versus* non-targeted screening, quantitative *versus* qualitative analysis, sensitivity requirements, and the complexity of the sample matrix.

- Full-scan: In full-scan mode, the mass spectrometer continuously scans the entire mass range throughout the entire LC run. This mode allows for the detection of all ions within the specified mass range, providing comprehensive information on the mass spectrum of all analytes present in the sample, generating information of their molecular ion. Full-scan mode is typically used in non-targeted screening and discovery applications where the goal is to identify unknown or unexpected compounds in the sample. However, this approach has limitations, such as the number of compounds that can be targeted in a single chromatographic run without sacrificing sensitivity. Therefore, it is common to combine full-scan MS data with targeted MS/MS experiments.
- Data-dependent acquisition (DDA): In DDA mode, the mass spectrometer conducts full-scan and targeted MS/MS or MS^n (n = 2, 3, etc.) scans concurrently. The instrument dynamically chooses precursor ions from the full scan based on their intensity, abundance, or other criteria, and then fragments them to produce MS/MS or MS^n spectra for the identification of precursor ions. DDA mode is frequently utilized in non-targeted or suspect screening applications where broad coverage and targeted identification are both required. However, low-abundance unselected ions can result in information loss for MS/MS.
- Data-independent acquisition (DIA): DIA mode is a non-targeted acquisition mode that acquires high-resolution mass spectra across a wide mass range without selecting specific ions beforehand. In this mode, the mass spectrometer fragments all precursor ions in the sample, generating comprehensive product ions that can be retrospectively analysed using advanced data analysis techniques to identify unknown or unexpected compounds. DIA mode is commonly used in non-targeted screening and discovery applications. However, the large amount of data generated in DIA mode can make the assignment of precursor and product ions challenging and not always unequivocal.
- Target MS/MS: In this acquisition mode, a roster of desired parent ions, complete with their respective m/z values and retention times (t_R), is established. Consequently, the instrument continuously captures full-scan MS spectra during the entire chromatographic analysis. Additionally, within specified t_R windows, MS/MS spectra for predetermined compounds are documented. This approach allows for the retrieval of data pertaining to the group of signals associated with the molecular ion (in the MS function) and the precise scan spectra of product ions, employing one or multiple collision energies, all within a single LC run.

1.8.1.2. Data treatment approaches

The main workflows used in LC-HRMS screening include target, suspect and non-target screening. The selection of a strategy depends on the specific goals, requirements, characteristics of the samples or compounds being screened, and the desired outcomes of the screening process. Figure 1.8 summarise the main characteristics of wide-scope target, suspect, and non-target screening methodologies.

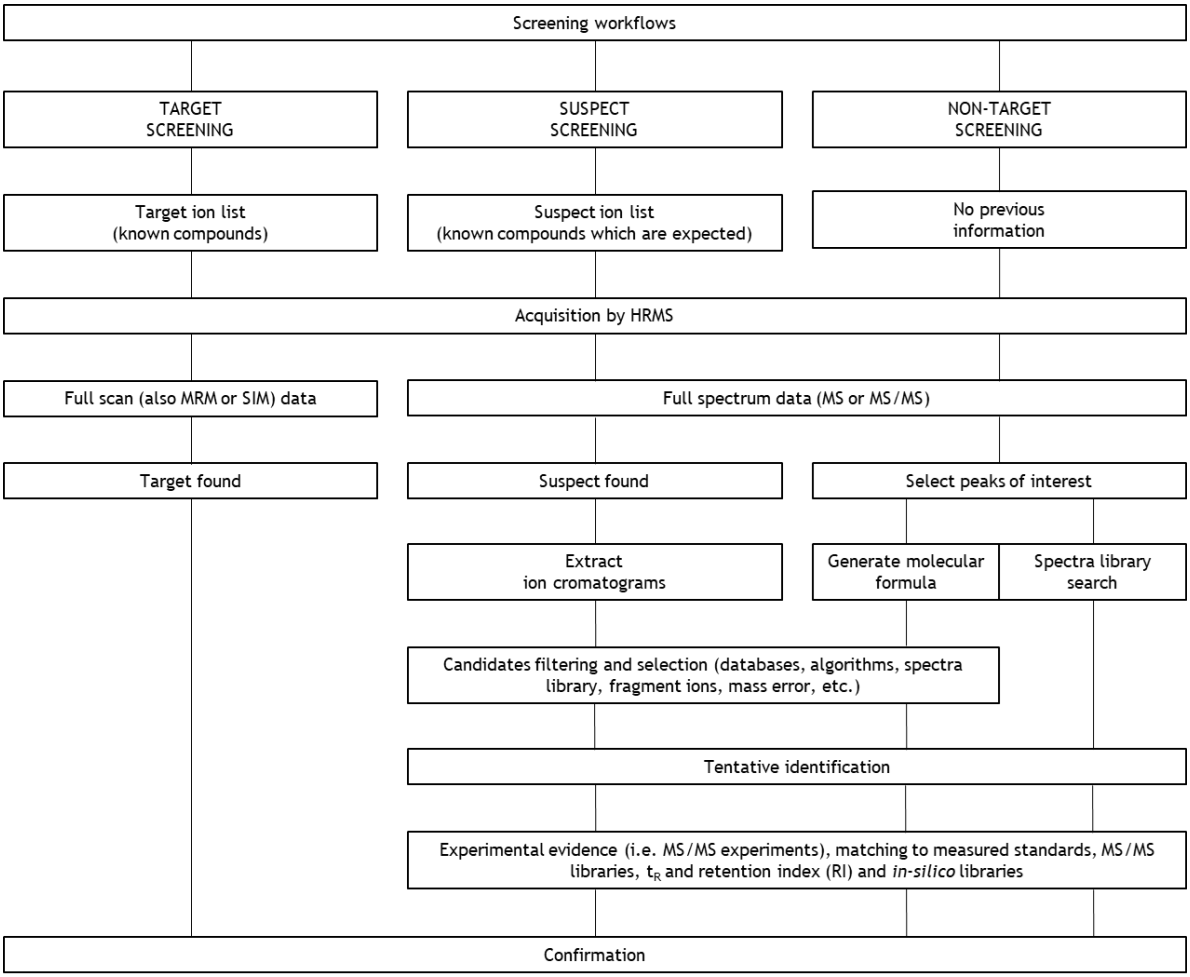

Figure 1.8. Comparison of systematic workflows for target, suspect and non-target screening based on Guo et al. (2020).

- Target screening: The analytes of interest are known or suspected to be present in the sample. Target screening typically involves the use of specific analytical standards or reference materials for calibration and quantification, and the chromatographic and mass spectrometric conditions are optimized for the targeted analytes. Therefore, this method can provide the higher degree of confidence in the identification of the compounds. In LC-HRMS, target screening can also be performed in Target MS/MS mode, allowing for the extraction of ion chromatograms for targeted compounds and subsequent comparison (e.g., t_R, difference in mass accuracy, and isotope pattern) with injected reference standards or with stored MS/MS spectra (self-created libraries).
- Suspect screening: This process begins by defining and creating a suspect list containing compounds of particular interest, but unlike target screening, standards are not available in the laboratory (at least not for most compounds), but only their formula and sometimes their MS/MS spectra. In this approach, the data obtained in HRMS analysis is compared to a library or database containing information on the name, empirical formula, and exact mass of the protonated ($[M+H]^+$), deprotonated ($[M-H]^-$), and other characteristic adducts of expected compounds. Once a suspect compound meets the requirements specified in the data processing method to appear in the hit list, further evidences are used for identification, including comparison of MS/MS spectra or

product ion obtained by DIA or DDA or further additional MS/MS experiments, prediction of t_R, ion mobilities, etc.

- Non-target screening: The most complex screening strategy since, in this mode of operation, no defined list of analytes is used, and there is no prior information about the compounds that may be present in the sample. The data analysis workflow consists in detecting all (or at least the most intense) chromatographic peaks (features) using DDA or DIA modes and then trying to identify all features or those which are prioritized (by intensity, statistical comparison, etc.). For feature identification, the main strategy involves generating molecular formulas using accurate mass and isotope patterns, searching possible candidate structures in spectral libraries with experimental MS/MS data, or predicting MS/MS fragmentation models. Advanced software is used to carry out the analysis of different substances and obtain as much information as possible, but when no information is available, the identification process becomes a laborious and costly process, taking up a lot of time. Recently, the identification of unknown and suspect compounds has become easier due to significantly enhanced access to commercial libraries, openly accessible databases (e.g. PubChem, ChemSpider, and Chemaxon), online experimental mass spectral libraries (e.g. MassBank, mzCloud, and METLIN), and online *in-silico* or predicted mass spectral libraries (e.g. Metfrag). However, despite these advances, the identification of unknown compounds remains a significant challenge.

1.8.1.3. Tentative identification thresholds

The analysis of different environmental matrices using LC-HRMS is a complex and laborious process and requires the establishment of some thresholds for identification.

Generally, the following identification criteria are used for HRMS data evaluation in target screening: peak height ≥1,000 counts, accuracy mass error ≤5 ppm, t_R tolerance of ± 0.2 min (when available), and a certain degree of correlation between the measured and reference isotopic profile. These parameters are used to avoid false positives (Chindarkar et al., 2014; Odoardi et al., 2017; Telving et al., 2016). Other criteria such as blank subtraction, and minimum score associated with the degree of coincidence of the candidate with the mass spectrum (e.g. isotopic profile) are also used for tentative identification. The minimum score is usually set at 70%, and it is essential to search for corresponding protonated or deprotonated molecular ions, or other characteristic adducts of suspect compounds in the full-scan MS data of injected samples.

It should be noted that screening workflows require an algorithm for data processing that depends on the type of instrument (e.g. ion mobility spectrometry (IMS), Orbitrap, QTOF) and even the suppliers (e.g. Waters, Agilent, Thermo, Shimadzu, Bruker) with specific software packages used to evaluate data information. Each software uses a particular algorithm to extract individual ion chromatograms from full-scan data and subsequently search and compare them with a predefined database or library.

Tentative identification of compounds in full-scan MS data poses a high risk of false positive hits, lacking sufficient analytical evidence to support any potential identification. To confirm suspect hits, MS/MS data are typically acquired at different collision energies (e.g. 10, 20 and 40 V) and matched against MS/MS spectra from commercial, in-house or open libraries.

Unambiguous identification is achieved when the experimental MS/MS spectra and t_R match with reference standards that were injected under the same instrumental conditions. The most commonly used criteria for positive identification as regards MS/MS comparisons include at least two fragment ions that match with the mass spectral library in two replicates and maximum mass error of experimental MS/MS data ≤5 ppm.

If no reference standards or mass spectral databases are available, the identification of suspect compounds can still be attempted by diagnostic evidences and comparison with various sources, such as literature search, *in-silico* fragmentation platforms (e.g. MetFrag and Molecular Structure Correlator), or interpretation of the spectra. Similar criteria can be used in non-target screening workflows, where usually the similar compounds of different samples are aligned according to retention time (typically a ± 0.2 min threshold is used) with peak alignment tools (e.g. Profinder) and then compared statistically for more confidence using statistical tools (e.g. Mass Profiler Pro).

In contrast to conventional methods used for the determination of targeted compounds, in screening approaches there are currently no official guidelines that establish or explain specific criteria to ensure the quality of results. Yet, Schymanski et al. (2015) proposed a criteria for communicating confidence on tentative identifications by HRMS that has been widely adopted by the scientific community. This proposal considers five levels of identification confidence with sublevels, that are described below (see also Figure 1.9):

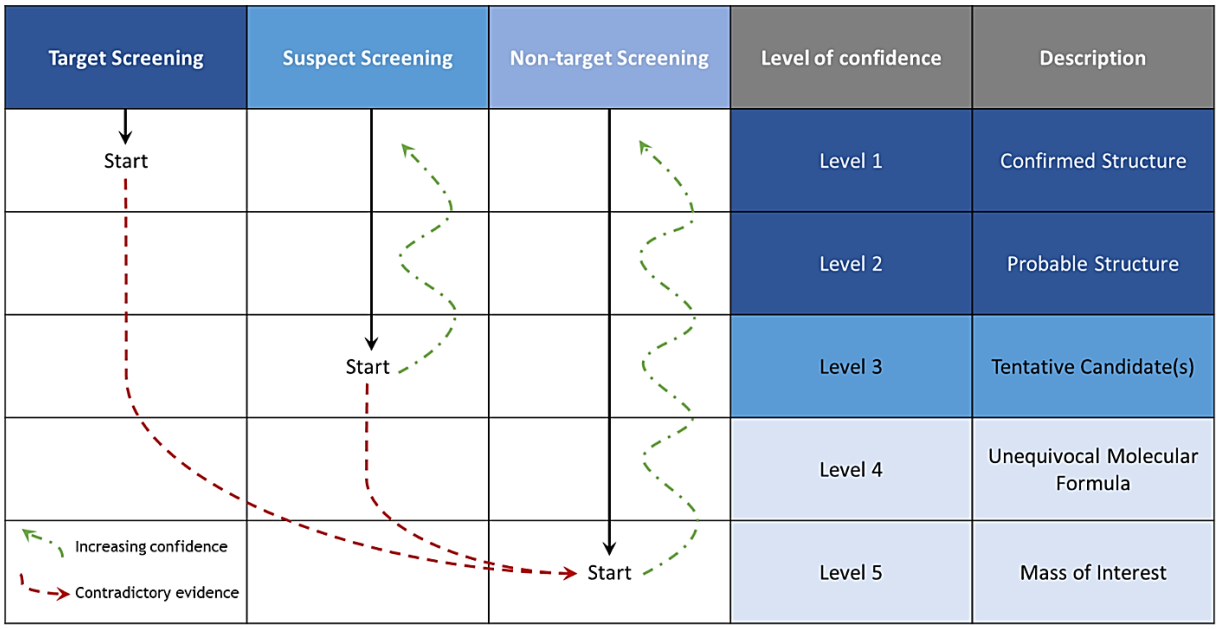

Figure 1.9. Matrix of identification approach *versus* identification confidence based on Cuñat et al. (2022).

Own elaboration

- Level 1: The most confidence level with a confirmed structure corroborated against a standard through MS, MS/MS and t_R matching.
- Level 2: Probable structure subdivided into two different subcategories:
  - Sublevel 2a: A candidate proposed structure matches with the library or literature spectrum, and the spectrum-structure match is unambiguous.

  - Sublevel 2b: The diagnostic evidence can be based on distinctive MS/MS fragments and isotope patterns, presence of additional adducts and via comparison from compounds with similar spectra.
- Level 3: Tentative candidates. The candidates are assigned a possible structure, but information is insufficient for proposing only one exact structure.
- Level 4: Unequivocal molecular formula is presented, but insufficient evidences exist to propose a structure.
- Level 5: The lowest level of confidence, where only the exact mass is presented due to an insufficient information to propose a molecular formula.

1.8.2. Screening by GC-HRMS

Most GC-HRMS screening methods involve acquiring accurate mass data, deconvoluting mass spectra, and comparing obtained data with mass spectral libraries (or reference standards in target screening methods). Among the various ionization methods available, electron ionization (EI) is the most widely used, reliable, and efficient for GC-HRMS screening analysis. This is due to the reproducible fragmentation patterns and well-understood rules of fragmentation of organic molecules at standard conditions, allowing for efficient use of both commercial and user-created mass spectral libraries for known compound identification, as well as identification of unknowns (Mazur et al., 2021). In this context, the most commonly employed methodologies for screening using GC-EI-HRMS systems are described below.

Whether the aim is to perform a target, suspect, or non-target analysis, but software controlling the GC-HRMS does not offer the possibility to operate in the above described DDA, DIA and Target MS/MS. So, in most cases, data are just acquired in the scan MS mode and product ion scan spectra are limited to a pre-selection of target compounds. Therefore, the first step usually involves acquiring samples in full-scan MS mode. The selection of acquisition parameters, such as the mass range, number of data points per m/z value, and acquisition rate, can significantly impact data quality and the final results. MS data can be acquired in profile, centroid mode, or both, depending on the instrument's specifications. The mode of data acquisition used is closely linked to the data processing software requirements. For example, the Unknowns Analysis software from Agilent Technologies (Santa Clara, CA, USA), which has been applied in suspect and non-target screening workflows, requires data files to be acquired in profile to use its Suremass deconvolution algorithm used for HRMS data.

Spectral deconvolution is the most commonly used strategy for data analysis in screening approaches when the source is EI. It extracts the true mass spectra of individual compounds from complex mixtures where peaks may overlap or be distorted due to chromatographic or instrumental factors. This process enhances the accuracy and reliability of compound identification and quantification, even at trace levels. However, data processing is a critical and time-consuming step due to the co-elution of the interest compounds, which can generate thousands of detected peaks. Therefore, it is important to establish a set of parameters in the deconvolution method to search for peaks matching certain criteria, such as intensity thresholds. This reduces the complexity of the candidate list and data processing. Default method parameters may not always be the best parameters for data processing, and selecting one value or another may positively or negatively affect compound identification. Users can determine and optimize parameter types in the development method depending on any software. However,

very few studies have optimized these parameters to achieve greater effectiveness in data processing as in the elaboration of HRMS library by Castro et al. (2022).

Once the list of possible candidates is available, it is compared with libraries of spectra, generating a score or match factor according to the degree of similarity between the experimental spectrum and that of the library. This is the case due to the fragmentation pattern in EI because it is highly consistent across instruments, reliable unit mass library spectra have been established for more than 15,000 compounds at low-resolution databases (NIST). Unfortunately, as of now, there are no precise EI-MS spectra libraries available, with the exception of small collections of accurate spectra for relatively limited compound families (e.g. pesticides). Furthermore, commercial HRMS databases for derivatized compounds are not yet available. Thus, in most cases, the spectral search relies on the low-resolution NIST EI-MS database. Additionally, comparing experimental m/z values with calculated ratios for fragment ions of known composition in the NIST database is sometimes helpful in distinguishing candidates with varying empirical formulas.

Creating a large HRMS database is a challenging task that requires a significant many reference standards to obtain high-quality mass spectra for screening, being a time and cost intensive task because it is necessary to inject individual standards in full scan mode and extract their EI-HRMS spectrum, and then incorporate into an in-house HRMS database with other parameters such as t_R or retention index (RI), which are used for further confirmation. Thus, lab-constructed libraries typically contain a limited number of entries, usually a few hundred compounds (Castro et al., 2022), due to the availability of reference standards and the economic resources of each laboratory. Because of that, some researchers have combined the use of GC-HRMS systems with low-resolution libraries such as NIST, especially in non-target screening studies, as a first approach for compound prioritization and subsequent identification.

The global report contains all spectral matches with their scores, compound name, accurate mass difference among reference and experimental spectrum, among other information. As a final step, the user manually reviews the report to evaluate the tentative identification results and check if there are any false positive or false negative compounds. Tentative identification for the analysis of target and suspect compounds using GC-EI-HRMS systems is relatively easier since there is available information a priori. Instead, in non-target screening studies, this process is complicated and tedious, requiring many working hours for interpretation of spectra, intensive search in openly online databases, additional experiments, and the use of complementary soft ionization techniques. Yet, a drawback of EI is excessive or very little fragmentation of some compounds that can compromise identification and particularly differentiation of isomers.

This drawback of EI could be circumvented by using retention indexes (see next section) or atmospheric pressure chemical ionization (APCI) as ionization method. APCI is a soft ionization method with minimal molecule fragmentation, similarly to APCI (and electrospray) in LC-MS. APCI has the ability to ionize a wide range of compounds, but the choice of reagent gas and other operating parameters can affect the ionization efficiency and selectivity of APCI, requiring optimization for different analytes and applications. The identification workflows using GC-APCI-HRMS systems are similar to those used in LC-HRMS. This approach can provide complementary information to well-established GC-EI-HRMS screening methods but has so far received limited attention in the literature.

1.8.2.1. Retention indexes

RI was a concept proposed by Kováts (1958), as a numeric value that represents the t_R of a compound normalized to the t_R of adjacently eluting reference standards, using a homologous series of n-alkanes and run under the same chromatographic conditions. It can be calculated by the Van Den Dool and Kratz (1963) equation (Equation 4), which is one of the most thoroughly studied and accepted RI calculation methods.

$$RI = 100 \left[\frac{t_R(x) - t_R(z)}{t_R(z+1) - t_R(z)} + z\right] \text{ (Equation 4)}$$

where x is the symbol of the substance investigated and z and z+1 are the carbon atoms of the n-alkane eluted pre and post of the target compound.

This value only depends on the chemical nature of the compound, the stationary phase, and carrier gas used. Therefore, it offers the possibility of comparing retention data regardless of instrumental variations, column length, and type of chromatographic system.

As mentioned earlier, a sample chromatogram may contain several deconvoluted peaks, and calculating the RI from t_R can be a laborious and time-consuming process. However, deconvolution software, such as the previously mentioned Unknowns Analysis, can automatically calculate the RI of chromatographic peaks, creating a RI calibration data file that can be compared with library entries. The RI calibration data file is a simple text file that contains the number of carbon atoms, t_R, and RI of all eluting n-alkanes under the same chromatographic conditions as the samples. For each different sample analysis, the RI calibration data file must be adjusted with the corresponding n-alkane value to avoid instrument deviation that may affect data processing.

Tentative identification is extremely rare for two substances to have both identical (or very similar) RI and mass spectra. Thus, combining RI and mass spectral data has significantly improved confidence of identifications, allowing the distinguishing of substances that cannot be unequivocally differentiated based on mass spectra alone.

OBJECTIVES

2. OBJECTIVES

Undoubtedly, the majority of the items we use in our daily lives are made of plastic. This prevalence can be attributed to its cost-effectiveness and numerous advantages over alternative materials, such as affordability, cleanliness, and durability. Plastic finds applications in various sectors, including packaging, healthcare, transportation, construction, electronics, and more. Nevertheless, while plastic benefits these sectors and enhances our daily lives, it is impossible to ignore its role in generating significant pollution. Rather than being an ally, plastic often appears as an adversary due to its persistence in the environment and their tendency to release or sorb pollutants in/from the environment and its potential to degrade into MPs with a much larger surface area.

Currently, plastic manufacturers only disclose information regarding the types of plastics they produce, omitting any comprehensive list of additives or other plastic-related chemicals used. This information gap results in a limited understanding of the potential adverse impacts on the environment and human health. Numerous substances have been reported by researchers for their toxicity, forming a foundation for potential regulations and monitoring efforts. Nonetheless, ongoing research remains essential due to the emergence of new regulations governing the use of these additives and the discovery of novel substances capable of enhancing plastic properties. This continuous process underscores the dynamic nature of this field of study. Similarly, per-/poly-fluoroalkylated substances (PFAS), also associated to some type of plastics, but with a far wider range of applications, are highly persistent chemicals of current concern.

Thus, the primary aim of this thesis is to advance our understanding of MPs, their presence, and the presence of associated chemicals, including PFAS, in the aquatic environment. This research also involves assessing potential risks to both human health and marine organisms. Additionally, an enhanced methodology for the removal of PFAS will be developed. To achieve these objectives, we predominantly utilized LC-HRMS and GC-HRMS systems, chosen for their screening and confirmatory capabilities. Furthermore, LC-MS/MS and GC-MS systems were employed when enhanced sensitivity was necessary.

To this end, the work was divided into three stages:

1. Development and application of analytical procedures for the determination of MPs and screening characterization of associated leachable additives and contaminants sorbed to MPs in the marine environment. **This sub-objective is presented in Chapters 4.1 & 4.2**.
2. Assessment of the impact of plastic-related chemicals to aquatic organisms and humans, primarily considering their bioaccessibility, but also toxicity and ecological effects. **This sub-objective is presented in Chapters 4.3 & 4.4**.

3. Development an analytical determination and effective removal methods of a wide range of PFAS in water from a human and environmental safety perspectives. **This sub-objective is presented in Chapters 4.5 & 4.6**.

MATERIALS AND METHODS

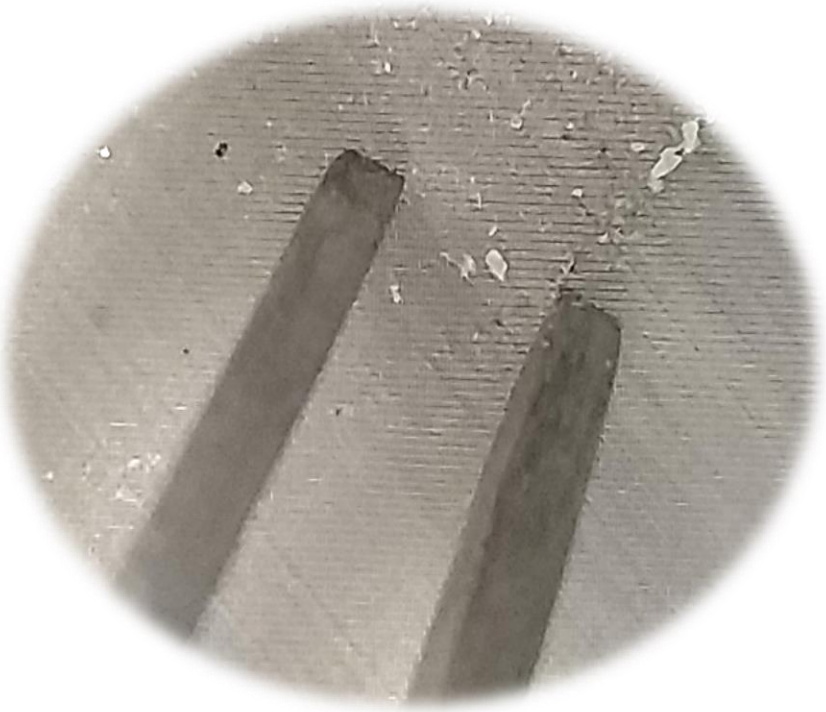

3. MATERIALS AND METHODS

3.1. SCREENING OF ORGANIC CHEMICALS ASSOCIATED TO VIRGIN LOW-DENSITY POLYETHYLENE MICROPLASTIC PELLETS EXPOSED TO THE MEDITERRANEAN SEA ENVIRONMENT BY COMBINING GAS CHROMATOGRAPHY AND LIQUID CHROMATOGRAPHY COUPLED TO QUADRUPOLE-TIME-OF-FLIGHT MASS SPECTROMETRY

3.1.1. Reagents and materials

All solvents used for screening organic pollutants associated to MPs pellets were of analytical quality. GC-MS grade ethyl acetate (AcOEt) was purchased from Panreac (Barcelona, Catalonia, Spain) and LC-MS grade methanol (MeOH) was purchased from Fisher Scientific (Hampton, Nova Hampshire, USA). Alumina (Al_2O_3) and N-methyl-N-(trimethylsilyl) trifluoroacetamide (MSTFA) were purchased from Merck (Darmstadt, Germany).

The gases feeding the instrumentation had a minimum purity of 99.999% and were purchased from Nippon Gases (Tokyo, Japan).

3.1.2. Samples

LDPE pellets (3 mm particle size) were provided by Repsol (Madrid, Spain). No information about pellet additives was supplied for confidentiality reasons, although they are supposed to be relatively free of additives as they are typically mixed with such chemicals during further plastic manufacturing.

In order to assess the sorption of organic pollutants, LDPE pellets were stored in nylon nets which were immersed at ca. 0.8 m deep (selected because of LDPE density and representing a typical exposure habitat for mussels and other aquatic organisms) for 8 weeks in aquaculture cages from the Marine Research and Aquaculture Laboratory (LIMIA) located in Andratx's Portuary area southwest of the island of Mallorca, Spain (39°34′15″N, 2°25′17″E) in August 2018. This facility is located in a bay with several recreative boats and ships in a highly touristic area, further impacted by a WWTP effluent. Nylon bags were previously cleaned by sonication in AcOEt, MeOH and water and then conditioned in the same area, by exposing them to the marine environment for 2 weeks.

Pellets (200 g) were introduced into eight separate bags and the nets were manually shaken every week to remove any large biofouled organisms. One bag was collected every week and the MPs were introduced into glass bottles and left dry in a desiccator for 24h. Once the pellets were dried, they were transferred to topaz glass bottles (previously washed with acetone and dried in the hood) and stored in a freezer at -20ºC. Finally, 60 g of MPs from the eight different

exposure times were shipped frozen to Santiago de Compostela, where they were analysed to screen for associated pollutants. Once received, they were stored at -20ºC and analyses were performed in the period September 2018 - June 2019, as described below.

3.1.3. Sample treatment

All glassware was previously baked at 300ºC for 12h before use. AcOEt was cleaned with 3% (w/w) baked alumina (González-Mariño et al., 2019).

Ten LDPE pellets (ca. 0.2 g) corresponding to each exposure time were weighed in 4 mL glass vials (n=3). Then, 2 mL of solvent (AcOEt or MeOH, for GC-QTOF or LC-QTOF analysis, respectively) were added, and the vials were covered with aluminium foil. The vials were sonicated in an ultrasonic bath at RT for 30 min, whereupon the solvent was transferred with a Pasteur pipette to a clean vial. The extraction was repeated with a 2 mL fresh aliquot of solvent. The combined extracts were dried under a gentle stream of nitrogen and reconstituted with 200 µL AcOEt or MeOH, for GC-QTOF or LC-QTOF analysis, respectively. In the case of GC-QTOF analysis, in addition, a 30 µL aliquot of the extracts was derivatized by adding 20 µL MSTFA and heating at 60ºC for 1h.

The whole time series (0-8 weeks) was investigated by GC-QTOF, whereas only samples from 0, 4, and 8 weeks were investigated by LC-QTOF because of the more laborious data treatment in this case. Field blank samples (n=3) were processed with each batch. Blanks, a solvent, and a standard (500 ng/mL) were analysed within each batch of samples every six injections, in order to check for response stability and potential cross-contamination. Whenever the signal varied over ±30% the whole batch was prepared again (which included new extractions and chromatographic analysis). Some compounds (mostly phthalates, organophosphorus flame retardants and fatty acids) were detected in field blanks. Therefore, their intensities were considered for the positive identification of any given substance, as detailed in sections 3.3.4-3.3.5.

3.1.4. LC-QTOF analysis and data processing

LC separation was carried out using a 1200 Infinity II series LC coupled to a 6520 iFunnel Q-TOF system, both supplied by Agilent Technologies. The QTOF was furnished with a Dual Agilent Jet Stream ESI ion source.

Chromatographic separation was carried out on a Synergi 4u Fusion-RP 80 Å column (100 mm × 2.0 mm × 4.0 µm) from Phenomenex (Torrance, California, USA), thermostated at 40ºC. The mobile phases were in Milli-Q® water (MQ) in A and MeOH in B, both containing 0.1% formic acid. The gradient elution program was as follows: initially 5% B, linear gradient to 100% B in 10 min (hold for 5 min), then returned to initial conditions (5% B), and held again for 5 min for column back-conditioning. The flow rate was 0.4 mL/min and the injection volume was 10 µL.

The ESI was operated in either positive or negative mode (separate injections) in the high-sensitivity mode (2 GHz). The needle voltage was set to 3500 V, which provides a resolution

of ca. 11,000 full width half maximum (FWHM) at 118.0863 m/z and 19,000 FWHM at 922.0099 m/z in positive mode, and ca. 16,000 FWHM at 112.9856 m/z and 21,000 FWHM at 601.9789 m/z in negative mode. Mass spectral data were stored in centroid mode. A reference calibration solution (PN G1969-85001) consisting of purine and the chemical HP-921, supplied by Agilent, was continuously sprayed in the source during the chromatographic run, in order to grant mass spectral accuracy. Nitrogen was used as nebulizing (30 psi), desolvation (300ºC) and drying gas (200ºC, 12 L/min) in the ESI source, as well as collision gas in MS/MS experiments.

Instrument control was performed using Agilent Mass Hunter Workstation software B.10.00 (Agilent). Data acquisition was performed in auto MS/MS (DDA) and whenever required by target MS/MS. In the auto MS/MS mode, three collision energies (10, 20 and 40 V) were collected for each precursor ion, with a maximum of three precursor ions per cycle, as detailed in (Castro, Quintana, Carpinteiro, et al., 2021). The mass range were 40-1,200 m/z for single-MS and 30-1,050 m/z for MS/MS. Three collision energies (10, 20, and 40 V) were also used in target MS/MS mode whenever required. The acquisition frequency for MS/MS was 6 spectra per second. The software used for data treatment were MassHunter Qualitative Analysis Workflow v.B.08.00 (Agilent), MassHunter Profinder v.10.0 and Mass Profiler Pro v.15.0 (Agilent).

The suspect screening workflow has been described in detail elsewhere (Castro, Quintana, Carpinteiro, et al., 2021; Wilson et al., 2021). The libraries/databases used for data processing were as follows: (1) the Agilent Extractables and Leachables Personal Compound Database and Library (PCDL) and the Agilent Extractables and Leachables Dyes PCDL (both without MS/MS spectra), and (2) a high-resolution MS/MS spectral library of 3,210 compounds, including pharmaceuticals, pesticides, drugs of abuse, human metabolites, and industrial chemicals, as detailed in (Castro, Quintana, Carpinteiro, et al., 2021; Wilson et al., 2021).

For non-target screening, samples were processed with the MassHunter Profinder v.10.0 software by applying the algorithm called “Batch recursive feature extraction”, which detects and further aligns the chromatographic peaks and MS spectra of each sample. The detected components (features) were exported as CEF format to the Mass Profiler Professional v.15.0 software (Agilent). Features at different exposure times were required to be present in at least two injection replicates. Those were subjected to an analysis of variance (ANOVA), from which features with a significant difference ($\alpha = 0.001$) and a fold-change ≥ 10 (relative to time 0 days) were retained for principal component analysis (PCA). Furthermore, only the 10% most abundant features in each condition in ESI+ were prioritized for structural elucidation. For the selected candidate compounds, MS/MS spectra were obtained by injection in target MS/MS mode (when not recorded in the Auto MS/MS injections), and the compounds were tentatively identified using different strategies: (1) search in the libraries described for suspect screening, (2) search in the Metlin, MassBank, and mzCloud online libraries; and (3) generation of precursor and product ions formulas using MassHunter Qualitative Analysis B.08.00 and interpretation of MS/MS spectra, aided by the tools Molecular Structure Correlator B.07.00 (Agilent) and MetFrag (Wolf et al., 2010) *in-silico* MS/MS fragmentation tools, using Chemspider as a source of structures.

All potentially detected chemicals were further extracted and integrated into all samples and blanks. Only those compounds that were present in all three injection replicates of any exposure time, but not in blanks, or with a signal higher than that of the blank + 10 times the standard deviation of the blank, were considered. The tentatively identified compounds were

classified according to the confirmation levels scale proposed by Schymanski et al. (2014). Only those compounds at identification levels 1-2b are herein reported, for reliable identification.

3.1.5. GC-QTOF analysis and data processing

Chromatographic analysis was carried out using a 7890A gas chromatograph interfaced to a 7200 QTOF mass spectrometer (Agilent). Separation was performed on a 30 m × 0.25 mm (i.d.) × 0.25 μm film thickness HP-5MS capillary column (Agilent). The GC oven temperature was programmed as follows: 50°C for 1 min, ramped to 290°C at 10°C/min and finally held for 15 min. One microliter of each extract was injected in splitless mode using an Agilent 7693B series autosampler. The injection port, transfer line, quadrupole, and source temperatures were set to 280ºC, 280ºC, 150ºC and 230ºC, respectively. Helium (99.9999%, Nippon Gases) was used as carrier gas at a flow rate of 1 mL/min. The solvent delay was set at 3.5 min for the non-derivatized samples and 5 min for the derivatized ones.

Acquisition was performed in EI mode at 70 eV with the emission current filament set at 5 μA, acquired in profile and centroid data formats. The MS was operated at 5 spectra/s in the mass range of 40 to 1,000 Da in the 2 GHz mode, which provides a spectral resolution of ca. 4,500 FWHM at 68.9947 m/z and 9,000 FWHM at 501.9708 m/z. Mass calibration was performed after three sample analyses, in accordance with the manufacturer's recommendations, using perfluorotributylamine (PF-43).

The instrument was controlled by MassHunter Acquisition B.07.06 (Agilent). Unknown Analysis v.10.00 software (Agilent) and MassHunter Qualitative Analysis v.B.08.00 software (Agilent) were used for data treatment. GC-QTOF-MS screening was performed using the SureMass deconvolution algorithm of Unknown Analysis v.10.0, as described in (Castro et al., 2022). The libraries used for data processing were (1) an in-house empirical high-resolution library with 356 mass spectra and Kovats RI available in (Castro, Quintana, López-Vázquez, et al., 2021; Castro et al., 2022); (2) a commercial high-resolution library of pesticides and related chemicals, containing 844 compounds supplied by Agilent, but modified to include RI as detailed in (Castro et al., 2022); (3) a low-resolution plastic additives library developed in the lab as a subset from NIST.17 library containing 210 compounds identified as plastic additives (Bolgar et al., 2007; ECHA, 2021a) (Table 3.1.1) and (4) the whole NIST.17 library (306,622 compounds). In the last case, only those compounds with a match factor higher than 90% (instead of 70%) were reviewed and Si-containing chemicals were prioritized in the derivatized fraction, since the derivatizing reagent (MSTFA) introduces Si atoms in the derivatized compounds.

Table 3.1.1. Compound list of plastic additives subset from NIST.17 for GC-QTOF screening.

Chemical name	Formula	CAS No.
Resorcinol	C6H6O2	108-46-3
Octabenzone	C21H26O3	1843-05-6
Ethanediamide, N-(2-ethoxyphenyl)-N'-(2-ethylphenyl)-	C18H20N2O3	23949-66-8
Drometrizole	C13H11N3O	2440-22-4

Chemical name	Formula	CAS No.
2-((2H-benzotriazo)-2-yl)-4-(1,1,3,3-tetramethylbutyl)phenol	C20H25N3O	3147-75-9
Bumetrizole	C17H18ClN3O	3896-11-5
Phenol, 2-(2H-benzotriazol-2-yl)-4,6-bis(1,1-dimethylpropyl)-	C22H29N3O	25973-55-1
Tinuvin® 1577	C27H27N3O2	147315-50-2
Dibutyltin dilaurate	C32H64O4Sn	77-58-7
1,3-Propanediol, 2-ethyl-2-(hydroxymethyl)-	C6H14O3	77-99-6
Phosphorous acid, triphenyl ester	C18H15O3P	101-02-0
Dipentaerythritol	C10H22O7	126-58-9
Bis(2-ethylhexyl) hydrogen phosphite	C16H35O3P	3658-48-8
Triethanolamine	C6H15NO3	102-71-6
Octadecanamide, N,N'-1,2-ethanediylbis-	C38H76N2O2	110-30-5
Diisopropanolamine	C6H15NO2	110-97-4
Dibenzoylmethane	C15H12O2	120-46-7
1-Hexadecanol	C16H34O	36653-82-4
Decanedioic acid, bis(2,2,6,6-tetramethyl-4-piperidinyl) ester	C28H52N2O4	52829-07-9
Phenol, 4,4'-butylidenebis[2-(1,1-dimethylethyl)-5-methyl-	C26H38O2	85-60-9
2,6-di-tert-Butyl-4-(dimethylaminomethyl)phenol	C17H29NO	88-27-7
Santonox®	C22H30O2S	96-69-5
Phenol, 4,4'-methylenebis[2,6-bis(1,1-dimethylethyl)-	C29H44O2	118-82-1
Phenol, 2,2'-methylenebis[6-(1,1-dimethylethyl)-4-methyl-	C23H32O2	119-47-1
Butylated Hydroxytoluene	C15H24O	128-37-0
Distearyl thiodipropionate	C42H82O4S	693-36-7
1,3,5-Trimethyl-2,4,6-tris(3,5-di-tert-butyl-4-hydroxybenzyl)-benzene	C54H78O3	1709-70-2
Phenol, 4,4',4"-(1-methyl-1-propanyl-3-ylidene)tris[2-(1,1-dimethylethyl)-5-methyl-	C37H52O3	1843-03-4
Benzenepropanoic acid, 3,5-bis(1,1-dimethylethyl)-4-hydroxy-, octadecyl ester	C35H62O3	2082-79-3
Dioctadecyl disulfide	C36H74S2	2500-88-1
Pentaerythritol tetrakis[3-(3',5'-di-tert-butyl-4'-hydroxyphenyl)propionate]	C73H108O12	6683-19-8
Benzenamine, 4-(1,1,3,3-tetramethylbutyl)-N-[4-(1,1,3,3-tetramethylbutyl)phenyl]-	C28H43N	15721-78-5
Phenol, 2,4-bis(1,1-dimethylethyl)-, phosphite (3:1)	C42H63O3P	31570-04-4
Benzenepropanoic acid, 3,5-bis(1,1-dimethylethyl)-4-hydroxy-, 2-[3-[3,5-bis(1,1-dimethylethyl)-4-hydroxyphenyl]-1-oxopropyl]hydrazide	C34H52N2O4	32687-78-8
Benzenepropanoic acid, 3-(1,1-dimethylethyl)-4-hydroxy-5-methyl-, 1,2-ethanediylbis(oxy-2,1-ethanediyl) ester	C34H50O8	36443-68-2
Anthra[2,1,9-def:6,5,10-d'E'f']diisoquinoline-1,3,8,10-tetraone	C24H10N2O4	106342-00-1
5,9,14,18-anthrazinetetrone, 6,15-dihydro-	C28H14N2O4	81-77-6
Triethylene glycol	C6H14O4	112-27-6
Phthalocyanine	C32H18N8	574-93-6
Quino[2,3-b]acridine-7,14-dione, 5,12-dihydro-	C20H12N2O2	1047-16-1

Chemical name	Formula	CAS No.
4-Amino-benzoic acid N'-[1-(4-nitro-phenyl)-3-oxo-but-1-enyl]-hydrazide	C17H16N4O4	53442-56-1
2-Naphthalenecarboxamide, 4-[(2,5-dichlorophenyl)azo]-3-hydroxy-N-phenyl-	C23H15Cl2N3O2	6041-94-7
Butanamide, 2-[(2-methoxy-4-nitrophenyl)azo]-N-(2-methoxyphenyl)-3-oxo-	C18H18N4O6	6358-31-2
Dodecanamide, N,N-bis(2-hydroxyethyl)-	C16H33NO3	120-40-1
Octadecanoic acid, 2-hydroxy-1-(hydroxymethyl)ethyl ester	C21H42O4	621-61-4
Triethyl phosphate	C6H15O4P	78-40-0
Phenol, 4,4'-(1-methylethylidene)bis[2,6-dibromo-	C15H12Br4O2	79-94-7
1,3,5-Triazine-2,4,6-triamine (Melamine)	C3H6N6	108-78-1
Cyanuric acid	C3H3N3O3	108-80-5
Azodicarbonamide	C2H4N4O2	123-77-3
Pentabromophenyl ether	C12Br10O	1163-19-5
1,3-Propanediol, 2,2-bis(bromomethyl)-	C5H10Br2O2	3296-90-0
Tris(1,3-dichloroisopropyl)phosphate	C9H15Cl6O4P	13674-87-8
Dimethyl-n-propylphosphonate	C5H13O3P	18755-43-6
1,2,5,6,9,10-Hexabromocyclododecane	C12H18Br6	3194-55-6
9,10-Dihydro-9-oxa-10-phosphaphenanthrene-10-oxide	C12H9O2P	35948-25-5
Glycerin	C3H8O3	56-81-5
n-Hexadecanoic acid	C16H32O2	57-10-3
Octadecanoic acid	C18H36O2	57-11-4
13-Docosenamide, (Z)-	C22H43NO	112-84-5
2-Propanol, 1,1',1"-nitrilotris-	C9H21NO3	122-20-3
Octadecanamide	C18H37NO	124-26-5
Dodecanoic acid	C12H24O2	143-07-7
Tristearin	C57H110O6	555-43-1
Hexadecanoic acid, 1,2-ethanediyl ester	C34H66O4	624-03-3
Decyl oleate	C28H54O2	3687-46-5
Tributyl acetylcitrate	C20H34O8	77-90-7
Triethyl citrate	C12H20O7	77-93-0
Butyl citrate	C18H32O7	77-94-1
Di-n-butyl phthalate	C16H22O4	84-74-2
Triethylene glycol di(2-ethylhexoate)	C22H42O6	94-28-0
Triacetin	C9H14O6	102-76-1
Hexanedioic acid, bis(2-ethylhexyl) ester	C22H42O4	103-23-1
Dibutyl adipate	C14H26O4	105-99-7
Decanedioic acid, dimethyl ester	C12H22O4	106-79-6
Decanedioic acid, dibutyl ester	C18H34O4	109-43-3
Hexanedioic acid, dihexyl ester	C18H34O4	110-33-8
Triphenyl phosphate	C18H15O4P	115-86-6
Bis(2-ethylhexyl) phthalate	C24H38O4	117-81-7
Diethylene glycol dibenzoate	C18H18O5	120-55-8
Decanedioic acid, bis(2-ethylhexyl) ester	C26H50O4	122-62-3
Diallyl phthalate	C14H14O4	131-17-9

Chemical name	Formula	CAS No.
Hexanedioic acid, bis[2-(2-butoxyethoxy)ethyl] ester	C22H42O8	141-17-3
tri(2-Ethylhexyl) trimellitate	C33H54O6	3319-31-1
Benzenesulfonamide, N-butyl-	C10H15NO2S	3622-84-2
1,4-Benzenedicarboxylic acid, bis(2-ethylhexyl) ester	C24H38O4	6422-86-2
1,3-Pentanediol, 2,2,4-trimethyl-	C8H18O2	144-19-4
Di-isononyl phthalate	C26H42O4	20548-62-3
Phosphoric acid, isodecyl diphenyl ester	C22H31O4P	29761-21-5
2-Benzothiazolesulfenamide, N-(1,1-dimethylethyl)-	C11H14N2S2	95-31-8
2-Mercaptobenzothiazole	C7H5NS2	149-30-4
Disulfide, bis(diisobutylthiocarbamoyl)	C18H36N2S4	3064-73-1
2-Benzothiazolesulfenamide, N-cyclohexyl-	C13H16N2S2	95-33-0
Urea	CH4N2O	57-13-6
2-Imidazolidinethione	C3H6N2S	96-45-7
Thiourea, N,N'-diphenyl-	C13H12N2S	102-08-9
Guanidine, N,N'-bis(2-methylphenyl)-	C15H17N3	97-39-2
1,4-Benzenediamine, N-(1-methylethyl)-N'-phenyl-	C15H18N2	101-72-4
1,4-Benzenediamine, N,N'-bis(1,4-dimethylpentyl)-	C20H36N2	3081-14-9
1,4-Benzenediamine, N-(1,3-dimethylbutyl)-N'-phenyl-	C18H24N2	793-24-8
Decanedioic acid, bis(1,2,2,6,6-pentamethyl-4-piperidinyl) ester	C30H56N2O4	41556-26-7
Phenol, 2,2'-methylenebis[6-(1,1-dimethylethyl)-4-ethyl-	C25H36O2	88-24-4
Propanoic acid, 3,3'-thiobis-, didodecyl ester	C30H58O4S	123-28-4
Phosphonic acid, [[3,5-bis(1,1-dimethylethyl)-4-hydroxyphenyl]methyl]-, diethyl ester	C19H33O4P	976-56-7
Thiourea, N,N'-diethyl-	C5H12N2S	105-55-5
Phenol, 2,6-bis(1,1-dimethylethyl)-4-ethyl-	C16H26O	4130-42-1
Phenol, 2,6-bis(1,1-dimethylethyl)-	C14H22O	128-39-2
2,2'-Ethylidenebis(4,6-di-tert-butylphenol)	C30H46O2	35958-30-6
Benzenepropanoic acid, 3,5-bis(1,1-dimethylethyl)-4-hydroxy-, thiodi-2,1-ethanediyl ester	C38H58O6S	41484-35-9
2,2'-Thiobis(4-methyl-6-tert-butylphenol)	C22H30O2S	90-66-4
dl-α-Tocopherol	C29H50O2	10191-41-0
1,4-Benzenediol, 2,5-bis(1,1-dimethylpropyl)-	C16H26O2	79-74-3
Phenol, 2,6-bis(1,1-dimethylethyl)-4-(1-methylpropyl)-	C18H30O	17540-75-9
Benzenamine, 4-(1-methyl-1-phenylethyl)-N-[4-(1-methyl-1-phenylethyl)phenyl]-	C30H31N	10081-67-1
1,4-Benzenediamine, N,N'-diphenyl-	C18H16N2	74-31-7
1-Naphthalenamine, N-phenyl-	C16H13N	90-30-2
Propyl gallate	C10H12O5	121-79-9
2,5-Bis(5-tert-butyl-2-benzoxazolyl)thiophene	C26H26N2O2S	7128-64-5
Silane, trimethoxy[3-(oxiranylmethoxy)propyl]-	C9H20O5Si	2530-83-8
1-Propanamine, 3-(triethoxysilyl)-	C9H23NO3Si	919-30-2
n-Octyltriethoxysilane	C14H32O3Si	2943-75-1
Silane, ethenyldimethoxymethyl-	C5H12O2Si	16753-62-1
Benzothiazole, 2,2'-dithiobis-	C14H8N2S4	120-78-5
Guanidine, N,N'-diphenyl-	C13H13N3	102-06-7

Chemical name	Formula	CAS No.
2,2',3,4,4',5',6-Heptabromodiphenyl ether	C12H3Br7O	207122-16-5
2,2',4,4',5,6'-Hexabromodiphenyl ether	C12H4Br6O	207122-15-4
Dibromophenyl ether	C12H6Br4O	5436-43-1
2,2',4,4',5,-Penabromodiphenyl ether	C12H5Br5O	60348-60-9
2,2',4,4',5,5'-Hexabromodiphenyl ether	C12H4Br6O	68631-49-2
m-Terphenyl	C18H14	92-06-8
Naphthalene, octachloro-	C10Cl8	2234-13-1
o-Terphenyl	C18H14	84-15-1
p-Terphenyl	C18H14	92-94-4
Phenol, 4,4'-(1-methylethylidene)bis-	C15H16O2	80-05-7
n-Butyl ricinoleate	C22H42O3	151-13-3
O-Acetylcitric acid triethyl ester	C14H22O8	77-89-4
Octadecanoic acid, butyl ester	C22H44O2	123-95-5
2-Butenedioic acid (E)-, dibutyl ester	C12H20O4	105-75-9
Diethyl adipate	C10H18O4	141-28-6
Nonanedioic acid, bis(2-ethylhexyl) ester	C25H48O4	103-24-2
Bis(2-ethylhexyl) maleate	C20H36O4	142-16-5
Butanedioic acid, diethyl ester	C8H14O4	123-25-1
Diisodecyl adipate	C26H50O4	27178-16-1
Nonanedioic acid, dihexyl ester	C21H40O4	109-31-9
Hexanedioic acid, bis(2-methylpropyl) ester	C14H26O4	141-04-8
Hexanedioic acid, dimethyl ester	C8H14O4	627-93-0
Octadecanoic acid, 2-hydroxyethyl ester	C20H40O3	111-60-4
Nonanedioic acid, dimethyl ester	C11H20O4	1732-10-1
Isopropyl myristate	C17H34O2	110-27-0
Isopropyl palmitate	C19H38O2	142-91-6
1,2-Benzenedicarboxylic acid, diundecyl ester	C30H50O4	3648-20-2
9-Octadecenoic acid, 12-(acetyloxy)-, methyl ester, [R-(Z)]-	C21H38O4	140-03-4
9-Octadecenoic acid (Z)-, methyl ester	C19H36O2	112-62-9
Dicyclohexyl phthalate	C20H26O4	84-61-7
Phthalic acid, butyl ester, ester with butyl glycolate	C18H24O6	85-70-1
1,2,4-Benzenetricarboxylic acid, trihexyl ester	C27H42O6	1528-49-0
Bis(tridecyl) phthalate	C34H58O4	119-06-2
Oleic acid, butyl ester	C22H42O2	142-77-8
Octicizer	C20H27O4P	1241-94-7
Benzyl butyl phthalate	C19H20O4	85-68-7
Ethanol, 2-butoxy-, phosphate (3:1)	C18H39O7P	78-51-3
Tributyl phosphate	C12H27O4P	126-73-8
2,2,4-Trimethyl-1,3-pentanediol diisobutyrate	C16H30O4	6846-50-0
Benzoic acid	C7H6O2	65-85-0
Phthalic anhydride	C8H4O3	85-44-9
Phenol, 2-(5-chloro-2H-benzotriazol-2-yl)-4,6-bis(1,1-dimethylethyl)-	C20H24ClN3O	3864-99-1
Methanone, bis(2-hydroxy-4-methoxyphenyl)-	C15H14O5	131-54-4
Methanone, (2,4-dihydroxyphenyl)phenyl-	C13H10O3	131-56-6

Chemical name	Formula	CAS No.
Oxybenzone	C14H12O3	131-57-7
Oxirane, 2,2'-[(1-methylethylidene)bis(4,1-phenyleneoxymethylene)]bis-	C21H24O4	1675-54-3
4,4'-(α-Methylbenzylidene)diphenol	C20H18O2	1571-75-1
2,2-Bis-(4-hyxroxyphenyl)-butane	C16H18O2	77-40-7
Bisphenol C	C17H20O2	79-97-0
4,4'-(Hexafluoroisopropylidene)diphenol	C15H10F6O2	1478-61-1
Phenol, 4,4'-(dichloroethenylidene)bis-	C14H10Cl2O2	14868-03-2
4,4'-Dihydroxydiphenylsulphone	C12H10O4S	80-09-1
4,4'-((p-Phenylene)diisopropylidene)diphenol	C24H26O2	2167-51-3
Bisphenol TMC	C21H26O2	129188-99-4
Phenol, 4,4'-methylenebis-	C13H12O2	620-92-8
Phenol, 4,4'-cyclohexylidenebis-	C18H20O2	843-55-0
Bisphenol G	C21H28O2	127-54-8
Bis(2-methoxyethyl) phthalate	C14H18O6	117-82-8
Diamyl phthalate	C18H26O4	131-18-0
Bis(2-butoxyethyl) phthalate	C20H30O6	117-83-9
Dibenzyl phthalate	C22H18O4	523-31-9
1,2-Benzenedicarboxylic acid, bis(2-ethoxyethyl) ester	C16H22O6	605-54-9
Didodecyl phthalate	C32H54O4	2432-90-8
1,2-Benzenedicarboxylic acid, bis(2-methylpropyl) ester (di-iso-butyl phthalate)	C16H22O4	84-69-5
Di-n-octyl phthalate	C24H38O4	117-84-0
Diethyl phthalate	C12H14O4	84-66-2
1,2-Benzenedicarboxylic acid, bis(3-methylbutyl) ester	C18H26O4	605-50-5
1,2-Benzenedicarboxylic acid, diphenyl ester	C20H14O4	84-62-8
1,2-Benzenedicarboxylic acid, bis(1-methylethyl) ester	C14H18O4	605-45-8
1,2-Benzenedicarboxylic acid, dihexyl ester	C20H30O4	84-75-3
Dimethyl phthalate	C10H10O4	131-11-3
1,3-Benzenedicarboxylic acid, dimethyl ester	C10H10O4	1459-93-4
Diphenyl isophthalate	C20H14O4	744-45-6
1,4-Benzenedicarboxylic acid, diethyl ester	C12H14O4	636-09-9
1,4-Benzenedicarboxylic acid, dimethyl ester	C10H10O4	120-61-6
1,2-Benzenedicarboxylic acid, mono(phenylmethyl) ester	C15H12O4	2528-16-7
1,2-Benzenedicarboxylic acid, monobutyl ester	C12H14O4	131-70-4
Phthalic acid, monocyclohexyl ester	C14H16O4	7517-36-4
Phthalic acid, monoethyl ester	C10H10O4	2306-33-4
2-(Isobutoxycarbonyl)benzoic acid	C12H14O4	30833-53-5
Phthalic acid, monooctyl ester	C16H22O4	5393-19-1
Mono(2-ethylhexyl) phthalate	C16H22O4	4376-20-9
2-(Pentyloxycarbonyl)benzoic acid	C13H16O4	24539-56-8
1,2-Benzenedicarboxylic acid, mono(1-methylethyl) ester	C11H12O4	35118-50-4
Phthalic acid, monohexyl ester	C14H18O4	24539-57-9
Methyl hydrogen phthalate	C9H8O4	4376-18-5

A comparison with blanks was performed akin to LC-QTOF. The confirmation level scale proposed by Schymanski et al. (2014) was again used and compounds at identification levels 1-2b are reported.

3.1.6. Trend analysis

Those chemicals detected by GC-QTOF were integrated at all exposure times (n=3) and the peak areas were investigated for the potential monotonic relationship with exposure time by Spearman's rank correlation test ($\alpha = 0.05$) with the software Statgraphics® 18 (Statpoint Technologies Inc., Dallas, TX, USA). This was not performed with LC-QTOF data because only three exposure times were considered in that case.

3.1.7. Quantitative assessment of selected chemicals

For the compounds detected by GC-QTOF, with standards were readily available, relative recoveries (RR), as well as the linearity and limits of detection (LOD) and LOQ were calculated. To this end, ten LDPE pellets (ca. 0.2 g) were poured into 4 mL vials and spiked with 200 ng of each analyte (n=5). These samples together with unspiked samples (n=3) were analysed as described above. Calibration curves spanned from 20 to 2,000 ng/mL (10 different levels). LODs and LOQs were obtained for a signal-to-noise ratio of 3 and 10 respectively, whenever not detected in the blank, or for a standard deviation of the blank of 3 and 10, respectively, if detected in the blank. Samples were analysed against external calibration in solvent (corrected by RR) to estimate the concentration of the MP-borne chemicals over time.

3.2. COMBINATION OF A NOVEL COST-EFFECTIVE GLASS DENSITY SEPARATOR FOLLOWED BY QUANTITATIVE 1H-NUCLEAR MAGNETIC RESONANCE SPECTROSCOPY FOR THE DETERMINATION OF MICROPLASTICS IN MARINE SEDIMENTS

3.2.1. Chemicals

Ultrapure deionized water (UPW, 18.2 MΩ/cm) was supplied by a Rephile water purification system (Shanghai, China). Dioxane, dimethyl sulfoxide (DMSO), toluene (Tol), trifluoroacetic acid (TFA) and iron (II) sulphate hepta-hydrate with a purity of ≥99%, gradient grade ethanol (EtOH), chloroform, bencene, carbon tetrachloride, chlorobencene, cyclohexanone, diethyl ether, hexane, isooctane, pyridine, 2-propanol, trichloroethylene and 30% (w/w) hydrogen peroxide solution were purchased from Merck. Tetrahydrofuran (THF) and 0.1M hydrochloric acid were purchased from Panreac. Formic acid and diethylamine were purchased from Scharlab (Barcelona, Spain). Dichlorobencene (DCM) and acetone were purchased from VWR (Radnor, PA, USA). Carbon disulfide and trichlorobencene were acquired from Honeywell (Morristown, NY, USA). O- and p-xylene were acquired from Acros Organics (Antwerp, Belgium). MeOH purchased from Fisher Scientific. The ^{1}H-NMR deuterated solvents used were deuterated trifluoroacetic acid (TFA-d), tetrahydrofuran-d8 (THF-d_8) and toluene-d_8 (Tol-d_8), all ≥99.5% deuteration degree. These solvents were obtained from Cambridge Isotopes Laboratories (Tewksbury, MA, USA).

Several types of commercial MP particles were used to validate the methodology, including PET, PVC and LDPE powders with a nominal distribution size of ≤300 µm. All MP particles were obtained from Goodfellow (Cambridge, UK).

Zinc chloride anhydrous ≥97% was acquired from VWR (Radnor, PA, USA) and potassium iodide and sodium bromide ≥99% were acquired from Merck. These salts were dissolved in UPW to produce solutions with densities in the range 1.28-1.60 g/cm^3. The solutions were filtered with 0.7 µm glass fibre filter.

3.2.2. Sampling

Three marine sediments samples were collected between February and April 2022 from different Galician beaches in Northwestern Spain (42º45'25.222"N 8º57'2.873"W (M1), 42º38'20.749"N 8º52'59.974"W (M2) and 42º31'45.43"N 9º0'7.229"W (M3)) selected based on their fishing and tourism impacts. The sampling locations were between the high-water mark (HWM) and low-water mark (LWM). A wooden scale was employed to measure an area of 40 x 40 cm. The material that was up to 5 cm deep was scooped out using a stainless-steel spoon with an in-situ sieved using 5 mm sieves from Filtra Vibración (Badalona, Spain). Samples were then collected into PP buckets and particles larger than 5 mm discarded. In the laboratory, the samples were transferred into pre-weighted aluminium trays. The trays were placed inside an oven overnight at 60ºC to dry. In addition, for method validation, a commercial sand sample purchased to Torneiro (Lugo, Spain) was sieved and dried.

3.2.3. Density separator setup

A novel density separator setup, as illustrated in Figure 3.2.1, was used for separating different types of MPs, made of glass to avoid plastic contamination.

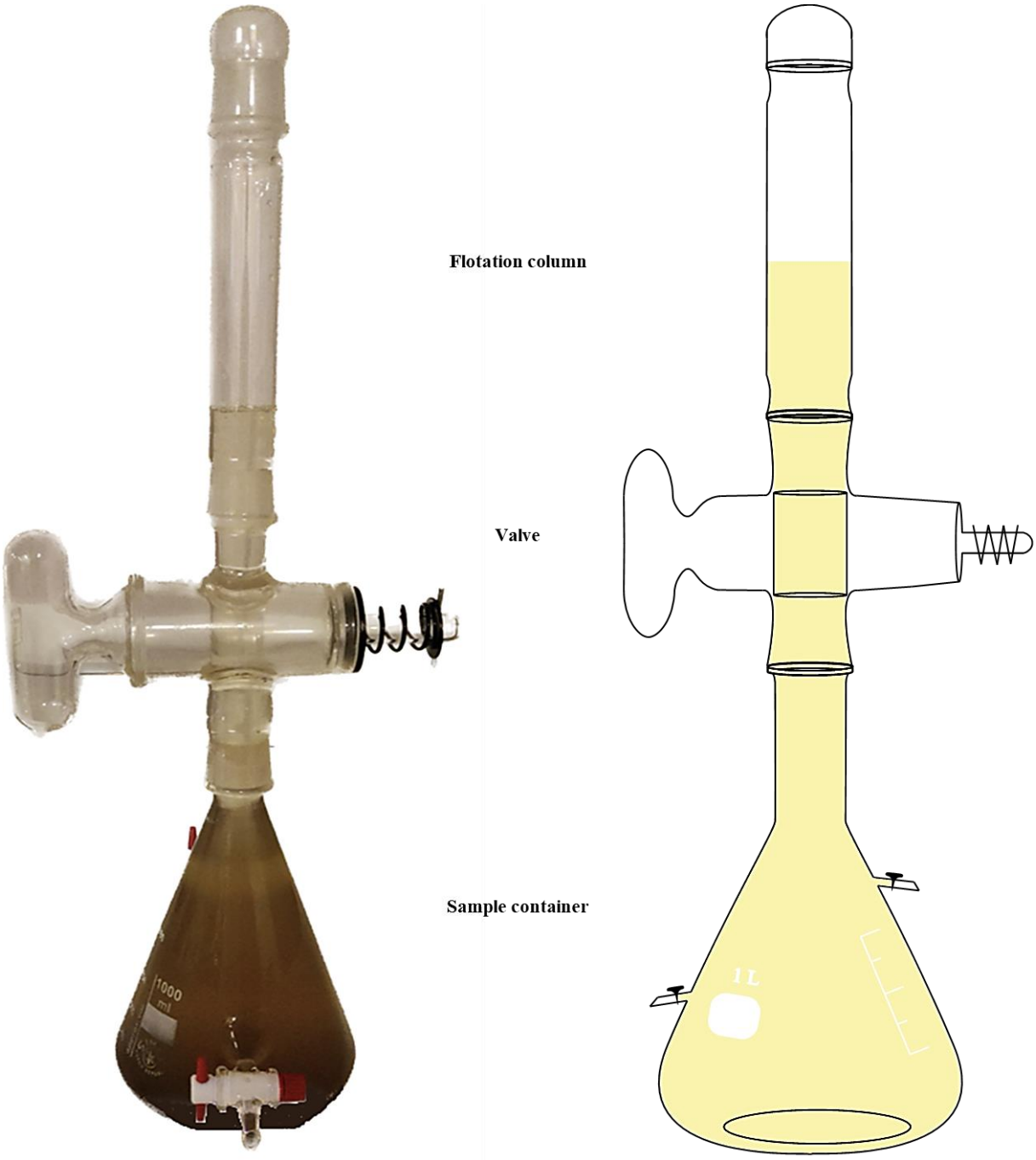

Figure 3.2.1. Density separator setup used for the extraction of microplastics in samples.

The separator was consisted of three parts:

- A 1 L Erlenmeyer flask with a 29/32 ground joint and a glass stopper obtained from SIMAX (Choratice, Czech Republic). The flask was modified with two side arms fitted with PTFE stopcocks by workshop of the university.

- A glass stopcock with a 29/32 ground joint with a hole diameter of 25 mm (Goel Scientific Glass Works Ltd., Gujarat, India).
- A glass column with a 29/32 ground joint with glass stopper (Goel Scientific Glass Works Ltd.).

The advantages of this setup included its resistance to corrosion, durability, and portability. In addition, the cost of each unit is ca. 500 EUR.

3.2.4. Microplastic extraction from sediment

In a stainless-steel vessel of a shaker (Jiecheng, Shanghai, China) with a capacity of approximately 500 mL, 100 g of marine sediment were weighed. Next, 100 mL of $ZnCl_2$ (with a density of 1.60 g/cm^3) were added, mixed with the sediment and the mixture transferred into the modified Erlenmeyer flask (Figure 3.2.1) of the density separator, dragging all particles with up to 600 mL of $ZnCl_2$. Subsequently, the Erlenmeyer flask was shaken with a SBS orbital shaker MOS-30 (Instrumentación Científica Técnica, Logroño, Spain) for 30 min at 250 opm. After this time, flask's content was left to stand for 15 min. Following that, the density separation setup was assembled, keeping the glass stopcock open, and filled with $ZnCl_2$ to a volume of 1.5 L and left to stand for 1h. After this time, the glass stopcock was closed. The supernatant in the flotation column was then vacuum-filtered through a stainless-steel filter of 20 µm (5 x 5 cm) (Filtra Vibración). The density separation was repeated with fresh $ZnCl_2$ which was allowed to settle for 15 min. The resulting supernatant was then filtered through the same stainless-steel filter. Lastly, the $ZnCl_2$ used in the process was reclaimed by filtration with a 0.7 µm glass fibre filter (Merck) and reserved for future extractions.

A Fenton's reaction was used in order to clean-up the filter from organic matter, as described by Hurley et al. (2018). Briefly, 2 mL of H_2O_2 (30%, v/v) and 1 mL of 20 g/L $FeSO_4$ (pH <3) were added to the filter and allowed it to react for 15 min. Subsequently, the filter was connected to the vacuum system to eliminate the Fenton's reagent. The Fe^{3+} precipitated during the oxidation on the filter was dissolved with 5 mL of HCl (0.1M). The particulate material is then dragged towards the filter using 5 mL of EtOH.

For ^{1}H-NMR analysis, the contents of the filters were transferred into a vial with 4 mL of fresh EtOH and left overnight in an oven at 60ºC. This was done to ensure complete evaporation of the solvent. Once this evaporation was achieved, MPs were dissolved in deuterated solvents. PVC MPs were dissolved in 600 µL of THF-d_8 by sonication at RT for 1h. LDPE MPs were dissolved in 1.5 mL Tol-d_8 by heating to 80ºC with magnetic stirring for 1h. For PET, MPs were dissolved in a mixture containing 600 µL of TFA-d and 30 µL of dioxane as IS by sonication at RT for 1h. Subsequently, 600 µL of these solutions were transferred into 5 mm screw-cap NMR tubes from Wilmad (Warminster, PA, USA) and analysed by NMR as described below.

3.2.5. NMR equipment and quantification conditions

^{1}H-NMR experiments were recorded on a NEO-750 spectrometer from Bruker (Billerica, MA, USA), operating at 750 MHz proton frequency. Typical ^{1}H-NMR spectra were acquired with the zg30 pulse program from the Bruker standard library, 128 transients per spectrum, 1.50 s inter scan delay and 32 K points per FID, with a spectral width of 11904.8 Hz (LDPE) or 15625.0 Hz (PVC), corresponding to an acquisition time of 2.75 s (LDPE) or 2.10 s (PVC), respectively. Spectra were recorded at different temperatures depending on the polymer analysed: 25ºC for PET, 0ºC for PVC and 80ºC for LDPE. The recorded FID data were processed with MestreNova version 14.2.2 (Mestrelab Research, S.L., Santiago de Compostela, Spain) as follows. The first point of each FID was multiplied by 0.5, data were zero filled to 128 K points, apodization was applied only to PET samples (exponential multiplication with LB = 3 Hz), phase correction was done manually and a final multipoint baseline correction was done with a Smooth of 8 and Segments algorithm of MestreNova. The same integration limits were set for all spectra of the same polymer.

3.2.6. Method validation

The NMR method was assessed in terms of instrumental limits of quantification (iLOQ), repeatability and linearity. Quantification of MP particles was achieved through internal calibration using as IS the residual signal of the deuterated solvent (PVC and LDPE samples) or the signal of added dioxane (PET samples). Calibration curves for linearity were done for PET, PVC and LDPE in deuterated solvents. The concentration of dioxane as IS was 1.63 mg/L, in PET samples. The minimum concentration of a standard that produced a signal-to-noise ratio (S/N) of 10 was determined as the iLOQ. The S/N ratio was estimated as described Saadati et al. (2013). The MP concentration ranges used were from iLOQ to 36.70, 38.46 or 1.05 mg/mL, for PET, PVC or LDPE MP, respectively. Instrumental repeatability was assessed by determining the relative standard deviation (%RSD) of five samples at concentrations of 8.33 mg/mL for PVC, 7.93 mg/mL for PET and 0.75 mg/mL for LDPE.

The accuracy and precision of the method were assessed by quintuplicated recovery experiments. A commercial sediment sample weighing 100 g was spiked with two levels of PET and PVC (20 µg/g and 200 µg/g) and one level of LDPE (10 µg/g) because of the low solubility of the latter in Tol-d_8 even at 80°C.

3.2.7. Quality control

All the equipment (including the density separator setup, glassware and metallic material) used for sample preparation was rinsed with UPW, MeOH and acetone and covered afterwards with clean aluminium foil prior their use. The density separator setup was dismantled in three constituent parts to ensure that a thorough cleaning was achieved between every sample.

MPs extraction was carried out in a clean room equipped with continuous air filtration. A cotton laboratory coat was worn throughout to minimise the risk of MP contamination. Procedural blanks were carried out using the density solution and the density separator following the recommendations reported by Dioses-Salinas et al. (2020).

Quality control samples (QCs) were prepared using sediment samples containing MP particles at the same concentrations used in the accuracy evaluation (10-20 μg/g). Recoveries of QCs were considered satisfactory between 70% and 120%, with %RSD below 20%.

3.3. MIMICKING HUMAN INGESTION OF MICROPLASTICS: ORAL BIOACCESSIBILITY TESTS OF BISPHENOL A AND PHTHALATE ESTERS UNDER FED AND FASTED STATES

3.3.1. Reagents and materials

AcOEt GC-MS grade was purchased from Panreac and MeOH LC-MS grade from Fisher Scientific. DCM Pestinorm grade was obtained from VWR. MQ water was obtained through a Millipore® water purification system (Burlington, MA, USA). Acetic acid and formic acid LC-MS grade were purchased from Scharlab. Alumina (Al_2O_3), hydrochloric acid 37% and MSTFA were purchased from Merck.

Analytical standards of BPA, DMP, DEP, DnBP, BzBP, DEHP, DnOP, DiNP, DiDP and deuterated standards used as IS (i.e., DMP-d_4, DnBP-d_4, BPA-d_{16} and DEHP-d_4) were purchased from Merck. Analytical standards of phthalate monoesters, namely, monomethyl phthalate (MMP), monoethyl phthalate (MEP), monobutyl phthalate (MBP), monobenzyl phthalate (MBzP), mono-(2-ethylhexyl) phthalate (MEHHP), mono-(2-ethyl-5-carboxylpentyl) phthalate (MECPP), mono-(2-ethyl-5-oxohexyl) phthalate (MEOHP) and mono-(hydroxyisononyl) phthalate (MHINP) were purchased from AccuStandard (New Haven, CT, USA) and potassium hydrogen phthalate was purchased from Merck. MMP-d_4, MBP-d_4 and MEHHP-d_4, used as IS, were purchased from Toronto Research Chemicals (Toronto, ON, Canada). All standards were of a purity ≥97%. Individual stock standard solutions of ca. 1,000 mg/L were prepared in AcOEt and MeOH for further separation and detection by GC-MS and ultra-high performance liquid chromatography coupled to mass spectrometry in tandem (UHPLC-MS/MS), respectively. All standard solutions were stored at -20°C pending use.

Four distinct GIT fluids mimicking saliva, gastric, duodenal and bile phases were prepared according to Versantvoort et al. (2005) and UBM (BARGE, 2011) *in-vitro* digestion models. Those complex human body fluid surrogates were composed of inorganic salts, organic compounds and a variety of enzymes, all of analytical grade purchased from Merck with a purity ≥97%. Each individual extractant (saliva, gastric, duodenal and bile fluids) was a composite reagent of 100 mL (50 mL for bile) obtained by mixing the so-called 'inorganic solution' and 'organic solution' (see chemical composition in Table 3.3.1), to which a given number of solid enzymes (see Table 3.3.1) were added prior to orbital mixing using amber glass bottles. The mock-digestive fluids were prepared the day before performing the tests to ensure the dissolution and activation of all the enzyme components. Prior to undertaking the *in-vitro* bioaccessibility testing, the pH of each surrogate body fluid was adjusted by dropwise addition of NaOH (1 M) or HCl (37%) to ensure the pH in the tolerance range specified by Versantvoort and UBM (Table 3.3.1). The fluids were kept overnight at RT and heated to 37 ± 2°C one hour prior to carrying out the bioaccessibility tests.

Table 3.3.1. Constituents and concentrations of the various synthetic fluids of the *in-vitro* digestion model mimicking fasted (UBM) conditions and modifications thereof for fed conditions (Versantvoort) in brackets.

		Saliva	Gastric	Duodenal	Bile
Inorganic solution	Total volume (mL)	50	50	50	25
Species	Concentration	Volume (mL)			
KCl	1.2M	1.00	0.92	0.63	0.21
KSCN	0.2M	1.00	-	-	-
NaH_2PO_4	0.6M	1.00	0.30	-	-
Na_2SO_4	0.4M	1.00	-	-	-
NaCl	3.0M	0.17	1.57	4.00	1.50
$CaCl_2$	0.2M	-	1.80	-	-
NH_4Cl	0.6M	-	1.00	-	-
$NaHCO_3$	1.0M	- (2.00)	-	6.62 (4.00)	3.40
KH_2PO_4	0.06M	-	-	1.00	-
$MgCl_2$	0.03M	-	-	1.00	-
NaOH	1.0M	0.18 (-)	-	-	-
HCl	37%	-	0.82 (0.65)	$18\ 10^{-3}$	$4\ 10^{-3}$ ($7.5\ 10^{-3}$)
Organic solution	Total volume (mL)	50	50	50	25
Species	Concentration	Volume (mL)			
Urea	0.4M	0.8	0.34	0.4	0.5
D+ Glucose	0.4M	-	1.00	-	-
D-Glucuronic acid	0.01M	-	1.00	-	-
D- Glucosamine hydrocloride	0.15M	-	1.00	-	-
Enzymes		Amount (mg)			
α-Amylase		14.5 (29)	-	-	-
Uric acid		1.5	-	-	-
Mucin		5.0 (2.5)	300	-	-
BSA		-	100	100	90
Pepsin		-	100 (250)	-	-
$CaCl_2$		-	-	20	11.1
Pancreatin		-	-	300 (900)	-
Lipase		-	-	50 (150)	-
Bile		-	-	-	300 (1,500)
pH		6.8 ± 0.2	1.30 ± 0.02	8.1 ± 0.2	8.2 ± 0.2

Two certified reference materials (CRM) of LDPE (CRM-PE002) and PVC (CRM-PVC001) MPs (Spex CertiPrep, Stanmore, UK), with average particle sizes of 110 µm and 140 µm (see SEM images in the Figures. 3.3.1 and 3.3.2), respectively, with certified concentrations of DiDP and DiNP at ca. 30,000 µg/g level, and DMP, DEP, DnBP, BzBP, BPA (only in LDPE), DEHP and DnOP at ca. 3,000 µg/g level were used in this study (see actual certified concentrations in Table 3.3.2).

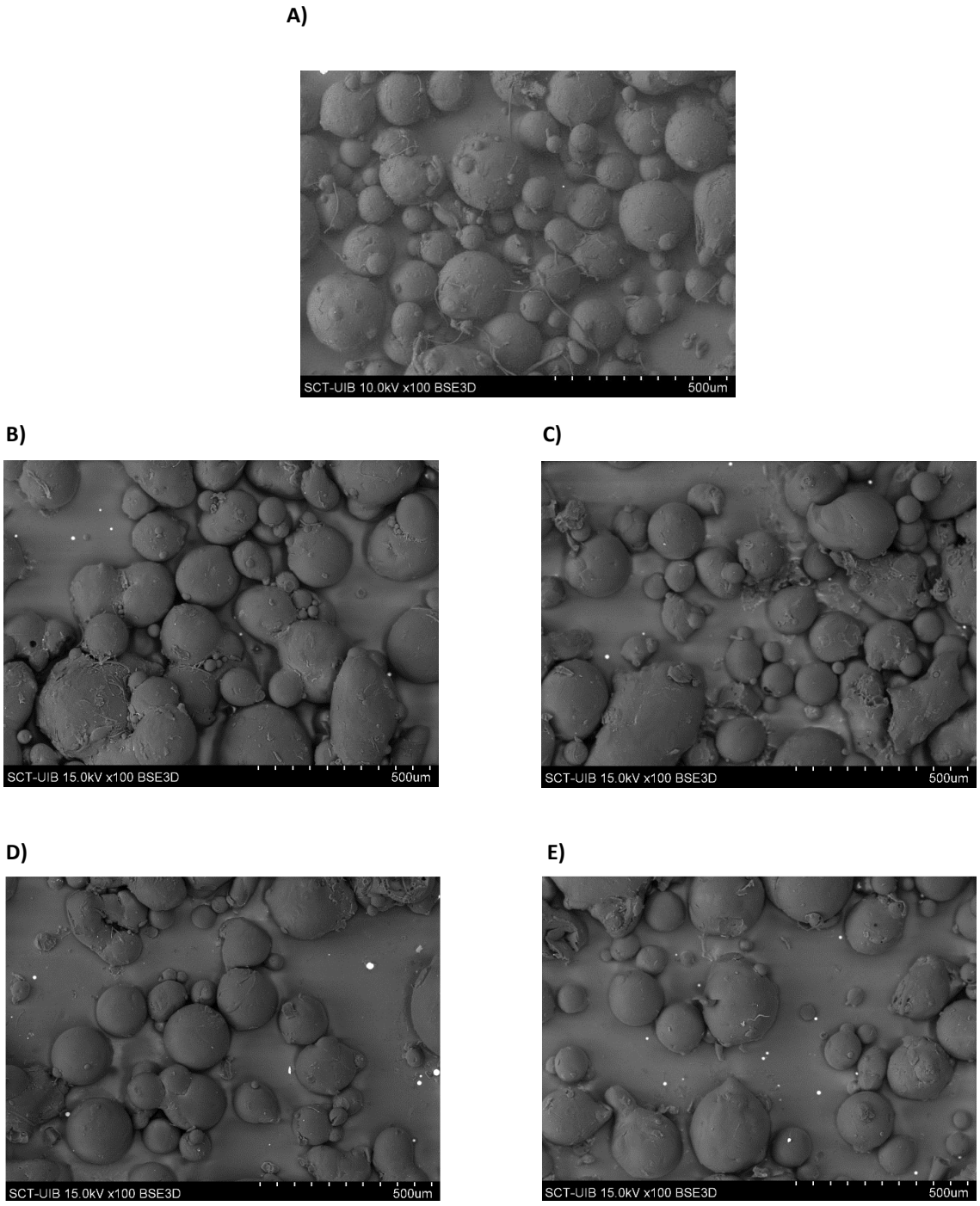

Figure 3.3.1. Scanning electron micrographs of LDPE MPs containing PAEs and BPA at 100-fold magnification for (A) pristine MPs, (B) MPs after gastric fed extraction, (C) MPs after gastric fasted extraction, (D) MPs after gastrointestinal fed extraction and (E) MPs after gastrointestinal fasted extraction.

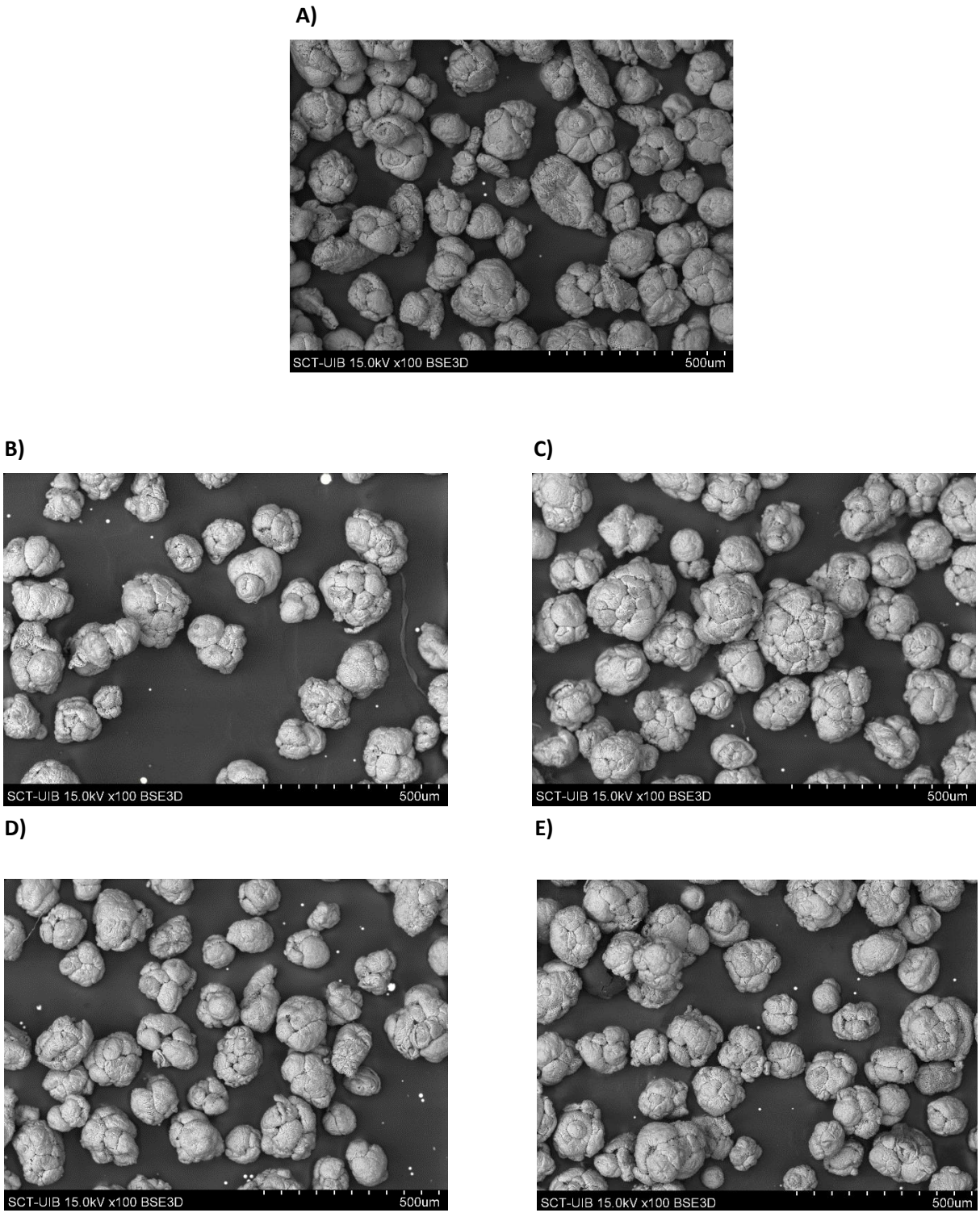

Figure 3.3.2. Scanning electron micrographs of PVC MPs containing phthalate esters at 100-fold magnification for (A) pristine MPs, (B) MPs after gastric fed extraction, (C) MPs after gastric fasted extraction, (D) MPs after gastrointestinal fed extraction and (E) MPs after gastrointestinal fasted extraction.

Table 3.3.2. Certified concentrations of PAEs and BPA in LDPE and PVC reference materials.

Compounds	CAS number	Concentration ± U* (µg/g)	
		LDPE	PVC
DMP	131-11-3	3,002 ± 360	3,021 ± 361
DEP	84-66-2	3,002 ± 360	3,023 ± 360
BPA	80-05-7	2,995 ± 359	-
DnBP	84-74-2	2,994 ± 359	3,029 ± 362
BzBP	85-68-7	2,991 ± 359	3,005 ± 360
DEHP	117-81-7	2,998 ± 360	3,004 ± 361
DnOP	117-84-0	2,996 ± 360	3,019 ± 360
DiNP	28553-12-0	29,944 ± 3593	30,025 ± 3606
DiDP	26761-40-0	30,005 ± 3601	30,038 ± 3602

*Expanded uncertainty with a coverage factor at the 95% confidence level k=2

To minimize contamination, all glassware were baked at 300°C for 12h before use, and alumina (3% (w/w)) was added to AcOEt (González-Mariño et al., 2019).

3.3.2. *In-vitro* fed and fasted human bioaccessibility models

The digestion process in the GIT of humans is herein simulated by applying physiologically relevant extraction conditions, i.e. the complex chemical composition of the digestive fluids, pH, and residence periods expected in every GIT compartment. Fed (Versantvoort) (Versantvoort et al., 2005) and fasted (UBM) (BARGE, 2011) models encompass a three-step additive procedure mimicking the GIT transit of the chyme, and the sequential extraction processes of ingested material in mouth, stomach, and small intestine, as these compartments are accounting for the largest percentage of bioaccessible pools, which can ultimately reach the systemic circulation.

A diagram of the workflow of both fed and fasted state tests is illustrated in Figure 3.3.3. In brief, the oral bioaccessibility tests were performed by accurately weighing 0.1 g of LDPE or PVC MPs into glass test tubes by triplicate. Then, 1.2 mL or 1.5 mL (fed/fasted) of saliva fluid was added and mixed manually for 10 s. Thereafter, 2.3 mL of gastric fluid was added, and the pH adjusted by the addition of 1M NaOH or 37% HCl within the pH interval between 2 and 3 for the fed state and pH = 1.20 ± 0.05 for the fasted state. Then, the samples were incubated at 37 ± 2 °C for 2h (fed state) or 1h (fasted state) under agitation using an end-over shaker at 37 rpm. For estimation of the gastric BF, the gastric extracts were retrieved by sample centrifugation at 1500 rcf for 30 min, whereupon an aliquot of supernatant was collected in a glass vial.

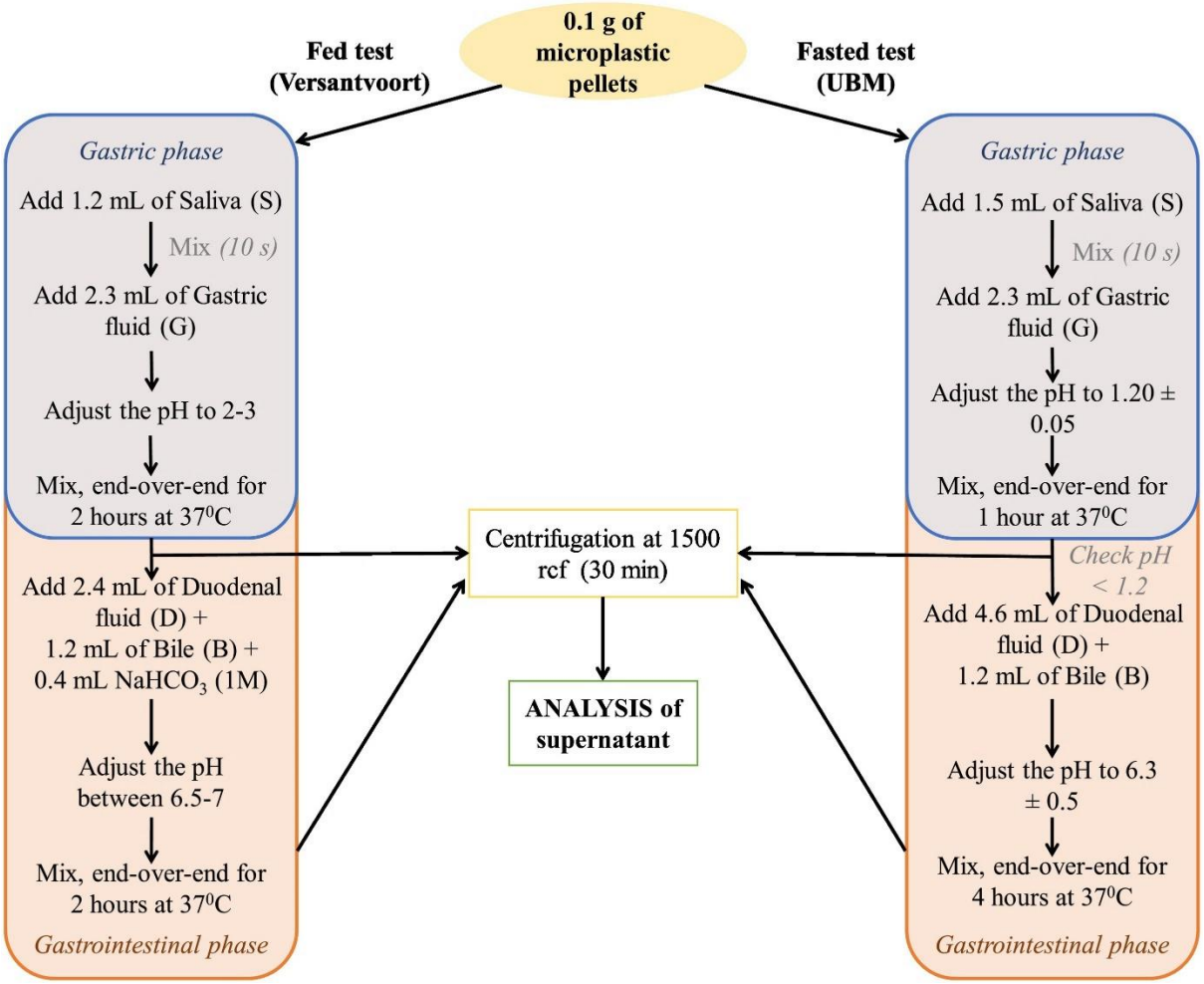

Figure 3.3.3. Schematic diagram of the fed and fasted *in-vitro* digestion models.

For assessment of the gastrointestinal BFs, 2.4 mL or 4.6 mL (fed/fasted) of duodenal fluid and 1.2 mL bile and, only under fed conditions 0.4 mL of 1M $NaHCO_3$, were added to the gastric phase. The pH was adjusted to the interval of 6.5-7 in the fed state or to 6.3 ± 0.5 in the fasted state. The gastrointestinal extraction lasted 2h (fed state) or 4h (fasted state) under physiological temperature and identical shaking conditions as those of the gastric phase. Finally, the MP suspension was centrifuged at 1500 rcf for 30 min and an aliquot of supernatant was collected in a glass vial.

SEM images of LDPE and PVC after gastric and gastrointestinal extractions for both PBETs (Figures 3.3.1 and 3.3.2) revealed that there are no appreciable changes on neither the average particle size nor the characteristic spherical-shaped and brain-shaped particles for the analysed LDPE and PVC MPs, respectively.

3.3.3. Determination of the bioaccessible fraction of PAEs and BPA in microplastics

The determination of the BF of PAEs was performed by dilute and shoot with a 1:100 (v/v) dilution of the gastric extracts and 1:40 (v/v) of the gastrointestinal extracts taking into account the larger volume of gastrointestinal phase, with the subsequent potential dilution of the

extracted species. In both cases UPW/MeOH (80:20, v/v) was used as diluent. The percentage of MeOH was selected to minimize the sorption of PAEs onto the surface of the borosilicate glass and tubing of the analytical detection instruments. ISs were added to the final extract at a concentration level of 700 µg/L. 1 mL-aliquots of the extracts were filtered through hydrophilic PTFE filters (Ø 13 mm, 0.22 µm) from Phenomenex followed by percolating 250 µL MeOH through the filters to prevent losses of the target species. The extracts of the PBETs (including the filtered MeOH) were further analysed by UHPLC-MS/MS.

For determination of the oral bioaccessible BPA, a prior LLE was performed. To this end, 100 µL of the gastric or gastrointestinal extracts containing 700 µg/L IS was extracted with 2 mL of AcOEt. A volume of 20 µL of the extracts was derivatized with 30 µL of MSTFA at 60°C for 1h and further analysed by GC-MS.

Detection and quantification of potential degradation/hydrolysed products (viz., phthalate monoesters) of the bioaccessible PAEs were performed by dilute and shoot with a dilution 1:7.5 of the gastric extract or 1:3 of the gastrointestinal extract using UPW/MeOH (80:20) with a final concentration of 200 µg/L of IS-metabolites. Aliquots of 500 µL of the extracts were filtered through hydrophilic PTFE filters (Ø 13 mm, 0.22 µm) and after that 125 µL MeOH was percolated through the filter. The IS containing extracts and washing MeOH were analysed by UHPLC-MS/MS.

3.3.4. Determination of the non-bioaccessible fraction of PAEs and BPA in microplastics

The residual MPs after the PBETs were transferred to a 20 µm-steel mesh (3 × 3 cm) (Filtra Vibración), washed with 4 mL of UPW and dried at 40°C overnight. Then, the MPs were transferred to a glass vial and extracted with 2 mL of DCM by ultrasonic solvent extraction (USE) during 30 min at RT. The supernatant (1 mL) was filtered through hydrophobic PTFE filters (Ø 13 mm, 0.22 µm).

An aliquot of 10 µL of the DCM extract was diluted with AcOEt (1:200, v/v) and ISs were added at a final concentration of 700 µg/L prior to determination of PAEs by GC-MS. The determination of non-bioaccessible BPA in LDPE was undertaken following a derivatization reaction at 60°C for 1h with the addition of 30 µL MSTFA to 20 µL extract.

Another 10 µL aliquot of the DCM extract was diluted 1:2,000 (v/v) with MeOH and ISs were added at a final concentration of 700 µg/L for further determination of non-bioaccessible DiNP and DiDP by UHPLC-MS/MS.

3.3.5. GC-MS analysis

GC-MS determination of oral bioaccessible BPA and non-bioaccessible BPA and PAEs, excepting DiNP and DiDP, was carried out by a 7890A gas chromatograph interfaced with a triple-axis detector mass spectrometer (MSD 5975C, Agilent Technologies). Separation was performed onto a HP-5MS capillary column (30 m × 0.25 mm × 0.25 µm) supplied by Agilent.

Table 3.3.3. GC-MS analytical method for determination of PAEs and BPA.

Compounds	RT (min)	Quantification ion (m/z)	Qualification ions (m/z)	IS	Linear range (mg/L)	Determination coefficient (R^2)	RSD (%)[a]	LOQ (µg/L)[b]
DMP	8.30	163	133, 77	DMP-d4	0.001-10	0.9997	11	0.35
DMP-d4	8.30	167						
DEP	9.30	149	177, 121	DMP-d4	0.001-10	0.9996	7	0.40
BPA 2TMS	13.60	357	358, 372	BPA-d16 2TMS	0.001-5	0.9997	5	0.01
BPA-d16 2TMS	13.60	372						
DnBP	12.05	149	223, 104	DnBP-d4	0.001-10	0.9994	11	0.30
DnBP-d4	12.05	153						
BzBP	14.40	149	91, 104	DnBP-d4	0.005-10	0.9992	11	1.15
DEHP	16.10	149	167, 279	DEHP-d4	0.001-10	0.9990	13	0.10
DEHP-d4	16.10	153						
DnOP	18.20	149	327, 279	DEHP-d4	0.005-10	0.9999	9	1.35
DiNP	18.80	149	293, 193	DEHP-d4	0.5-40	0.9990	15	500
DiDP	19.25	149	307, 167	DEHP-d4	0.5-40	0.9992	19	300

[a]Repeatability at 50 µg/L, but 1 mg/L for DiNP and DiDP; n=5 and [b]LOQ determined for a peak-to-peak S/N of 10

The GC oven temperature was programmed as follows: 60°C for 1 min, then ramped to 250°C at 15°C/min and held for 10 min, and finally increased to 280°C at 5°C/min and held for 10 min. Two microliters of the extract were injected in splitless mode using an Agilent 7693 series autosampler. Injection port, transfer line, MS and source temperatures were set at 280°C, 280°C, 150°C and 230°C, respectively. Helium 99.9999% (Nippon Gases) at a flow rate of 1 mL/min was used as a carrier gas with a solvent delay set at 7.5 min.

Acquisition was performed with an EI source at 70 eV and operated under selected-ion monitoring mode (SIM) (see Table 3.3.3). The instrument was controlled by Agilent Chemstation E.02, and MassHunter Quantitative Analysis MS software v.10.1 (Agilent) was used for MS data treatment.

3.3.6. UHPLC-MS/MS analysis

UHPLC-MS/MS analyses were performed in a Waters Acquity UPLC H class system (Milford, MA, USA), equipped with a sample manager, a quaternary solvent pump, and a column oven thermostated at 40°C, coupled to a QqQ mass spectrometer Xevo-TQD (Waters) with an ESI source. Nitrogen, used as desolvation and cone gas, was provided by a nitrogen generator (Peak Scientific, Barcelona, Spain), and argon, used for the collision induced dissociation, was purchased from Nippon Gases. Ionization was performed in positive mode using the following parameters: 4 kV (capillary voltage), 150°C (source temperature), 500°C (desolvation temperature), 1,000 L/h (desolvation gas flow, N_2) and 50 L/h (cone gas flow, N_2). Collision energy (CE) and cone voltage (CV) values were adjusted individually for every compound. Analyses were done in selected reaction monitoring (SRM) mode recording one (IS) or two (analytes) precursor/product ion transitions per compound. Selected transitions, together with their corresponding CE and CV values, RT and labelled compounds used as IS are listed in the Supplementary Material, Tables 3.3.4 and 3.3.5.

Separation of PAEs and BPA (in preliminary tests) was carried out on a Synergi 4u Fusion-RP 80 Å C18 column (100 mm × 2.0 mm × 4.0 µm) from Phenomenex with a dual eluent system consisting of (A) UPW containing 0.1% of formic acid and (B) MeOH containing 0.1% of formic acid at a flow rate of 0.4 mL/min. The gradient elution started with 5% B, increased linearly to 100% B in 10 min, and held at 100% B for 4 min. Returning to initial conditions (5% B) was performed in 0.1 min and held for 6 min for column reconditioning. Injection volume was set to 1 µL.

Separation of phthalate monoesters was carried out on a Raptor Biphenyl 90 Å C18 column (150 × 2.1 mm × 1.8 µm) from Restek (Bellefonte, PA, USA) as described elsewhere (Estévez-Danta et al., 2021). Briefly, a dual eluent system consisting of (A) UPW containing 0.1% of acetic acid and (B) MeOH containing 0.1% of acetic acid at a flow rate of 0.3 mL/min was used. The linear gradient elution started with 50% B, increased to 100% B in 17 min, held at 100% B for 5 min, and finally returned to initial conditions (50% B) in 0.05 min and held for 5 min for column reconditioning. Injection volume was set to 2 µL.

The software MassLynx v4.1 and TargetLynx v4.1 (Waters) were used for control of the UHPLC-MS/MS system and data treatment, respectively.

Table 3.3.4. UHPLC-MS/MS analytical method for determination of PAEs and BPA.

Compounds	RT (min)	1st MRM transition[a]	2nd MRM transition[a]	IS	Linear range (mg/L)	Determination coefficient (R^2)	RSD (%)[b]	LOQ (µg/L)[c]
DMP	4.80	195 (15) → 163 (8)	195 (15) → 133 (23)	DMP-d4	0.001-5	0.9998	16	0.10
DMP-d4	4.80	199 (15) → 167 (8)						
DEP	6.40	223 (12) → 149 (15)	223 (12) → 177 (7)	DMP-d4	0.001-5	0.9993	12	0.15
BPA	6.30	227 (51) → 212 (17)	227 (51) → 133 (28)	BPA-d16	0.5-10	0.9990	19	500
BPA-d16	6.30	241 (51) → 223 (17)						
DnBP	8.60	279 (15) → 121 (34)	279 (15) → 149 (12)	DnBP-d4	0.001-5	0.9995	16	0.15
DnBP-d4	8.60	283 (15) → 153 (12)						
BzBP	8.60	313 (19) → 239 (5)	313 (19) → 91 (14)	DnBP-d4	0.001-5	0.9997	6	0.35
DEHP	10.90	391 (32) → 279 (9)	391 (32) → 149 (22)	DEHP-d4	0.001-5	0.9996	18	0.10
DEHP-d4	10.90	395 (32) → 153 (22)						
DnOP	10.95	391 (29) → 261 (6)	391 (29) → 149 (24)	DEHP-d4	0.1-10	0.9999	4	67
DiNP	11.30	419 (38) → 127 (10)	419 (38) → 149 (27)	DEHP-d4	0.001-10	0.9992	16	0.70
DiDP	11.60	447 (48) → 71 (19)	447 (48) → 85 (15)	DEHP-d4	0.001-10	0.9990	15	0.40

[a]Precursor ion m/z (CV, V) → product ion m/z (CE, V); [b]Repeatability at 100 µg/L, but 1 mg/L for BPA; n=5 and [c]LOQ determined for a peak-to-peak S/N of 10

Table 3.3.5. UHPLC-MS/MS analytical method for determination of PAEs metabolites.

Compounds	RT (min)	1st MRM transition[a]	2nd MRM transition[a]	IS	Linear range (mg/L)	Determination coefficient (R^2)	RSD (%)[b]	LOQ (µg/L)
Phthalic acid	1.80	165 (36) → 121 (9)	165 (36) → 77 (14)	MMP-d4	0.1-1	0.9997	19	6
MMP	2.15	179 (27) → 107 (8)	179 (27) → 77 (17)	MMP-d4	0.001-1	0.9996	13	0.010
MEP	2.75	193 (22) → 77 (15)	193 (22) → 121 (10)	MMP-d4	0.001-1	0.9997	10	0.015
MMP-d4	2.15	183 (27) → 111 (8)						
MnBP	4.90	221 (23) → 77 (17)	221 (23) → 177 (9)	MnBP-d4	0.001-1	0.9994	14	0.50
MnBP-d4	4.90	225 (23) → 81 (17)						
MBzBP	6.15	255 (27) → 77 (20)	255 (27) → 183 (10)	MnBP-d4	0.001-1	0.9992	15	0.060
MEHHP	5.30	293 (32) → 145 (13)	293 (32) → 121 (20)	MEHHP-d4	0.001-1	0.9994	9	0.20
MEHHP-d4	5.30	297 (32) → 125 (20)						
MECPP	5.40	307 (23) → 159 (10)	307 (23) → 113 (27)	MEHHP-d4	0.001-1	0.9995	10	0.35
MEOHP	5.90	291 (27) → 121 (16)	291 (27) → 143 (12)	MEHHP-d4	0.001-1	0.9994	9	0.60
MHINP	6.40	307 (44) → 121 (14)	307 (44) → 77 (29)	MEHHP-d4	0.001-1	0.9997	8	0.60

[a]Precursor ion m/z (CV, V) → product ion m/z (CE, V) and [b]Repeatability at 10 µg/L; n=5

3.3.7. Statistical analysis

Statistical data treatment was performed using the Statgraphics® Centurion XVIII software. ANOVA was conducted to evaluate those factors that could potentially influence the oral bioaccessibility of PAEs and BPA, i.e. body fluids (gastric vs gastrointestinal compartments), MP type (LDPE vs PVC) and *in-vitro* (fed vs fasted) test model. The statistical significance boundary was set to $\alpha = 0.05$ in all cases.

3.4. *IN-VITRO* LEACHING AND PHYSIOLOGICALLY RELEVANT EXTRACTION TESTS FOR PHTHALATE CONGENERS AND BISPHENOL A FROM MICROPLASTICS - ASSESSING THE CONTRIBUTION OF MICROPLASTICS TO THE EXPOSURE OF MARINE VERTEBRATES TOWARDS PLASTIC-RELATED CHEMICALS

3.4.1. Reagents and materials

Solvents, analytical standards, LDPE and PVC CRMs used in the experimental procedure were the same as in section 3.3.1. but with the addition of tris(hydroxymethyl)aminomethane (Trizma-Base) and ammonium fluoride with purity ≥99% were purchased from Merck.

Artificial seawater was prepared by dissolving the following salts in MQ water: 3 mg/L NaF, 2.4 mg/L $SrCl_2 \cdot 2H_2O$, 47.5 mg/L $Na_2B_4O_7$, 100 mg/L KBr, 700 mg/L KCl, 147 mg/L $CaCl_2 \cdot 2H_2O$, 4 g/L Na_2SO_4, 10.78 g/L $MgCl_2 \cdot 6H_2O$, 23.5 g/L NaCl and 200 mg/L $NaHCO_3$ (Kester et al., 1967). Various simulated gastric and intestinal fluids were prepared in order to evaluate the effect of different gut constituents and compartments on oral bioaccessibility (Carter et al., 1999; Coffin, Huang, et al., 2019; Coffin, Lee, et al., 2019; Gilannejad et al., 2018; Hamdan et al., 2009). The gastric fluid contained 1 mg/L pepsin (ref: 1071850100, 0.7 FIP-U/mg protein) adjusted to pH to 2.0 ± 0.1 using HCl (37%). For the intestinal fluids, a buffer solution containing 0.05M Trizma-Base was prepared and adjusted to pH 8.0 using 1M NaOH. The intestinal enzyme solution (so-called Carter method) was composed of 3.2 g/L of pancreas trypsin (T7409, ≥1000 U/mg protein), 7.5 g/L pancreas alpha-chymotrypsin (C4129, ≥40 U/mg protein) and 2.8 g/L pancreas protease (P4630, ≥5 U/mg protein) in the Trizma buffer solution (pH 8) (Carter et al., 1999). To obtain the full intestinal fluid (enzymes + bile salts, so-called Hamdan method), 96 mg/L sodium taurocholate hydrate and 76 mg/L sodium chenodesoxycolate were added to the enzyme solution (Hamdan et al., 2009). All inorganic and organic salts as well as enzymes were purchased from Merck with a purity ≥97%.

All the glassware was baked following the protocol described in section 3.3.1 of González-Mariño et al. (2019).

3.4.2.Desorption experiments

3.4.2.1. Leaching tests using aqueous extractants

The leaching procedure was performed by accurately weighing 0.1 g of LDPE or PVC MPs into glass test tubes by triplicate. Subsequently, 4 mL of MQ water or artificial seawater were added to each tube and the samples were incubated for 16h at 25 ± 2ºC using an end-over-end shaker (Thermo Fisher Scientific) at 37 rpm. Following the incubation, the samples were centrifuged for 30 minutes at 1500 rcf, and the supernatant was collected into a glass vial.

3.4.2.2. *In-vitro* fish bioaccessibility tests

Physiological extraction conditions of fish gut were mimicked by adjusting the pH and the chemical composition of digestive fluids, and the typical residence time of the chyme in the gastric (viz., 4h) and intestinal (viz., 12h) compartments.

Bioaccessibility tests started by weighing 0.1 g of LDPE or PVC MPs into borosilicate glass test tubes in triplicate. Subsequently, 3 mL of gastric fluid was added to the samples. The tubes were then placed on an end-over-end shaker set at 37 rpm for 4h in a dark environment at 25 ± 2ºC. After the incubation period, the samples were centrifuged for 30 minutes at 1500 rcf, and the supernatant was collected for further analysis of the gastric bioaccessibility.

Two types of intestinal fluids, namely, the enzyme solution (Carter's method) and the enzyme solution + bile acids (Hamdan's method), were used as single extractants added to 0.1 g of LDPE or PVC MPs. To this end, 4 mL of either intestinal fluid was added to the MPs (in triplicate) and subjected to end-over-end agitation at 37 rpm for 12h at 25 ± 2ºC. The intestinal extracts were centrifuged alike the gastric phase and the supernatant retrieved for analysis of the intestinal bioaccessibility. For the two-compartment assay (gastrointestinal phase), 4 mL of intestinal fluid (Hamdan's method) was added to the gastric extract after incubation, followed by gastrointestinal extraction for further 12h at 25 ± 2ºC with agitation at 37 rpm (total extraction time of 16h). The gastrointestinal extracts were centrifuged at 1500 rcf for 30 min and the supernatant retrieved for further analysis of the gastrointestinal bioaccessibility.

3.4.3. Analysis of the gastric, intestinal and gastrointestinal bioaccessible and leachable fractions

The analysis of the leachable and the oral bioaccessible fractions was performed by dilute-and-shoot with a dilution of 1:125 (v/v) and 1:94 (v/v) of the gastric and gastrointestinal supernatants, respectively, for PAEs and BPA, and a dilution of 1:88 (v/v) and 1:66 (v/v) of the gastric and gastrointestinal supernatants, respectively, for metabolites in MQ/MeOH (80:20, v/v). The selection of the MeOH percentage is aimed at preventing protein precipitation (≤20% organic solvent) and losses of compounds bound to proteins while minimizing plasticizers sorption on the surface of the borosilicate glass and tubing of the analytical instrumentation. ISs were added to the final extract at a concentration level of 700 µg/L for PAEs and BPA, and 500 µg/L for metabolites analysis. Aliquots of 1 mL of the extracts were filtered through hydrophilic polytetrafluoroethylene (PTFE) filters (Ø 13 mm, 0.22 µm) from Phenomenex, followed by percolation of 250 µL of MeOH to prevent analyte losses. The extracts were analysed by LC-QqQ.

3.4.4. Analysis of non-bioaccessible and non-leachable fractions

The MP residues for the non-bioaccessible fraction were analysed following the procedure of section 3.3.4. diluted 1:214 (v/v) with MeOH and added 700 µg/L of IS to be analysed by LC-QqQ.

3.4.5. LC-MS/MS analysis

The bioaccessible and non-bioaccessible fractions of the eight PAEs and BPA and metabolites thereof was conducted by LC-QqQ that consisted of a Waters Acquity UPLC H class system coupled to a triple quadrupole mass spectrometer Xevo TQD. The MRM conditions are listed in Tables 3.4.1 and 3.3.5.

Table 3.4.1. Analytical performance of the LC-MS/MS method for determination of PAEs and BPA.

Compounds	RT (min)	1st MRM transition[a]	2nd MRM transition[a]	IS	Linear range (mg/L)	Determination coefficient (R^2)	RSD (%)[b]	LOQ (µg/L)
DMP	4.80	195 (15) → 163 (8)	195 (15) → 133 (23)	DMP-d4	0.010-5	0.9993	6	3.2
DMP-d4	4.80	199 (15) → 167 (8)						
DEP	6.40	223 (12) → 149 (15)	223 (12) → 177 (7)	DMP-d4	0.002-5	0.9995	7	0.90
BPA	6.30	227 (51) → 212 (17)	227 (51) → 133 (28)	BPA-d16	0.050-5	0.9999	9	9.2
BPA-d16	6.30	241 (51) → 223 (17)						
DnBP	8.60	279 (15) → 121 (34)	279 (15) → 149 (12)	DnBP-d4	0.002-5	0.9990	11	1.6
DnBP-d4	8.60	283 (15) → 153 (12)						
BzBP	8.60	313 (19) → 239 (5)	313 (19) → 91 (14)	DnBP-d4	0.010-5	0.9997	10	2.6
DEHP	10.90	391 (32) → 279 (9)	391 (32) → 149 (22)	DEHP-d4	0.002-5	0.9994	12	1.0
DEHP-d4	10.90	395 (32) → 153 (22)						
DnOP	10.95	391 (29) → 261 (6)	391 (29) → 149 (24)	DEHP-d4	0.010-5	0.9993	8	10
DiNP	11.30	419 (38) → 127 (10)	419 (38) → 149 (27)	DEHP-d4	0.010-5	0.9994	13	1.7
DiDP	11.60	447 (48) → 71 (19)	447 (48) → 85 (15)	DEHP-d4	0.010-5	0.9992	18	1.9

[a]Precursor ion m/z (cone voltage, V) → product ion m/z (collision energy, V) and [b]repeatability at 100 µg/L; n=5

Separation of PAEs and BPA was carried out using a Synergi 4u Fusion-RP 80 Å C18 column (100 mm × 2.0 mm × 4.0 µm) from Phenomenex with a dual eluent system consisting of (A) 1mM NH_4F in MQ water and (B) 1mM NH_4F in MeOH at a flow rate of 0.4 mL/min. The gradient elution started with 5% B, increasing to 95% B in 10 min, held for 3 min. Return to initial conditions (5% B) was performed in 0.1 min and held for 3 min further for reconditioning. The injection volume was set to 1 µL. The separation of phthalate metabolites is described in section 3.3.6.

3.4.6. Statistical analysis

Statistical data treatment was performed using the Statgraphics® Centurion XVIII software. ANOVA was conducted to compare the leaching and fish gastric, intestinal and gastrointestinal bioaccessible fractions of PAEs and BPA. The statistical significance boundary was set to $\alpha = 0.05$ in all cases.

3.5. DETERMINATION OF REGULATED PERFLUOROALKYL SUBSTANCES (PFAS) IN DRINKING WATER ACCORDING TO DIRECTIVE 2020/2184/EU

3.5.1. Reagents and materials

Analytical solution mixture containing 2 mg/L of 10 PFCAs and 10 PFSAs (reference EU-5813-NSS, see the list of compounds in the Table 3.5.1) in MeOH was purchased from Wellington Laboratories (Guelph, ON, Canada). An IS mixture of 2 mg/L of 10 and 3 isotopically labelled PFCAs and PFSAs, respectively in MeOH was also from Wellington Laboratories (ref. MPFAC-C-ES, Table 3.5.2). All analytical solutions were stored at 4ºC.

Table 3.5.1. Chemical information of PFCAs and PFSAs considered in the study.

Name	Acronym	Structure	CAS RN
Perfluorobutanoic acid	PFBA	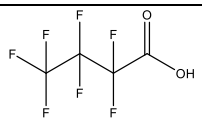	375-22-4
Perfluoropentanoic acid	PFPeA	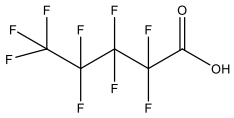	2706-90-3
Perfluorohexanoic acid	PFHxA	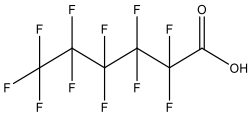	307-24-4
Perfluoroheptanoic acid	PFHpA	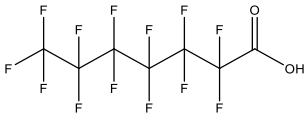	375-85-9
Perfluorooctanoic acid	PFOA	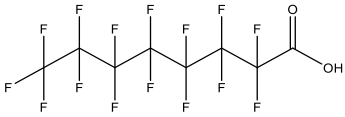	335-67-1
Perfluorononanoic acid	PFNA	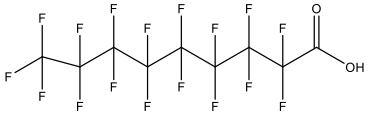	375-95-1
Perfluorodecanoic acid	PFDA	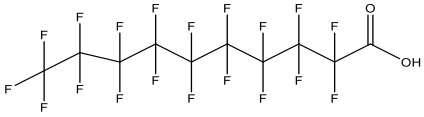	335-76-2
Perfluoroundecanoic acid	PFUdA	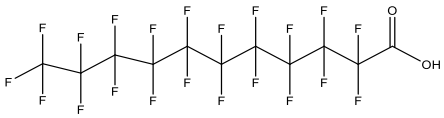	2058-94-8
Perfluorododecanoic acid	PFDoA	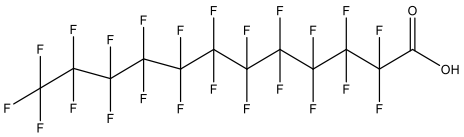	307-55-1
Perfluorotridecanoic acid	PFTrDA	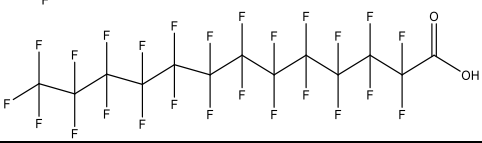	72629-94-8

Name	Acronym	Structure	CAS RN
Perfluorobutanesulfonate	PFBS	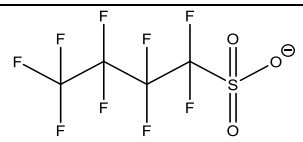	29420-49-3
Perfluoropentanesulfonate	PFPeS	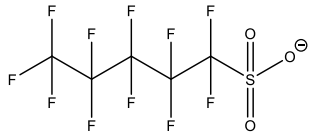	630402-22-1
Perfluorohexanesulfonate	PFHxS	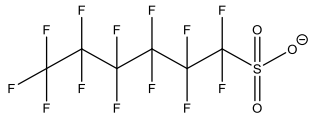	3871-99-6
Perfluoroheptanesulfonate	PFHpS	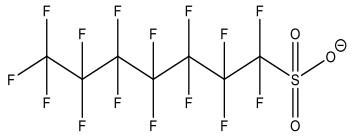	22767-50-6
Perfluorooctanesulfonate	PFOS	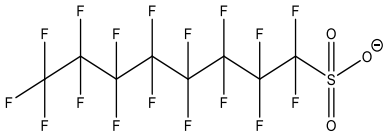	4021-47-0
Perfluorononanesulfonate	PFNS	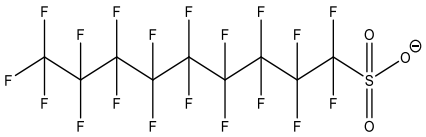	98789-57-2
Perfluorodecanesulfonate	PFDS	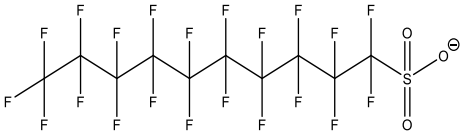	2806-15-7
Perfluoroundecanesulfonate	PFUdS	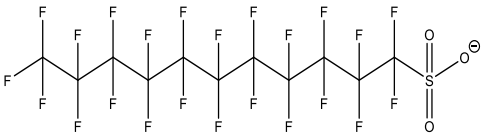	5838-34-6
Perfluorododecanesulfonate	PFDoS	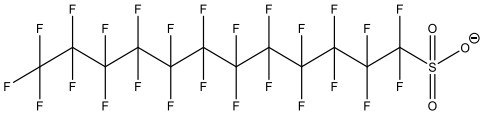	2386-53-0
Perfluorotridecanesulfonate	PFTrDS	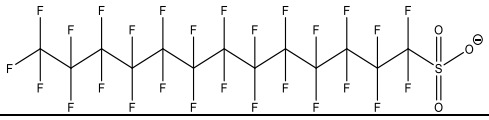	5802-89-1

Table 3.5.2. Information of the IS used in the study.

Name	Acronym
Perfluoro-n-[$^{13}C_4$]butanoic acid	$^{13}C_4$PFBA
Perfluoro-n-[$^{13}C_5$]pentanoic acid	$^{13}C_5$PFPeA
Perfluoro-n-[1,2,3,4,6-$^{13}C_5$]hexanoic acid	$^{13}C_5$PFHxA
Perfluoro-n-[1,2,3,4-$^{13}C_4$]heptanoic acid	$^{13}C_4$PFHpA
Perfluoro-n-[$^{13}C_8$]octanoic acid	$^{13}C_8$PFOA
Perfluoro-n-[$^{13}C_9$]nonanoic acid	$^{13}C_9$PFNA
Perfluoro-n-[1,2,3,4,5,6-$^{13}C_6$]decanoic acid	$^{13}C_6$PFDA
Perfluoro-n-[1,2,3,4,5,6,7-$^{13}C_7$]undecanoic acid	$^{13}C_7$PFUdA
Perfluoro-n-[1,2-$^{13}C_2$]dodecanoic acid	$^{13}C_2$PFDoA
Perfluoro-n-[1,2-$^{13}C_2$]tetradecanoic acid	$^{13}C_2$PFTeDA
Perfluoro-1-[2,3,4-$^{13}C_3$]butanesulfonate	$^{13}C_3$PFBS
Perfluoro-1-[1,2,3-$^{13}C_3$]hexanesulfonate	$^{13}C_3$PFHxS
Perfluoro-1-[$^{13}C_8$]octanesulfonate	$^{13}C_8$PFOS

UPW (18.2 MΩ/cm) was supplied by a Rephile water purification system. MeOH LC-MS grade was purchased from Fisher Scientific. Acetonitrile LC-MS grade was purchased from VWR. Ammonia 7N in MeOH was purchased from Acros Organics and 25% ammonium hydroxide (aqueous solution) LC-MS quality was purchased from Scharlab. Glacial acetic acid was obtained from Panreac and ammonium fluoride with a purity ≥99.99% from Merck.

3.5.2. Samples treatment

Bottled drinking water sold in Spanish supermarkets of variable hardness and container material (see Table 3.5.3) and tap water samples from different municipalities of Spain and other European and North American countries were analysed. Tap water was collected after letting the tap flow for 5 min with precleaned bottles by the authors or different colleagues (H. Gallard from University of Poitiers (France), T. Reemtsma from Helmholtz-Centre for Environmental Research (UFZ, Germany), S. Castiglioni and N. Salgueiro from Mario Negri Institute (Italy), A. Covaci from University of Antwerp (Netherlands), Y. Picó from Desertification Research Centre (CIDE, Spain), L. Bijlsma from University Jaume I (Spain) and M.M. Santos from Laboratory Aquatic Animal Sciences Course (CIIMAR, Portugal)). In the last case they were shipped to the University of Santiago for its analysis frozen together with empty bottles of the same materials, as to assess for background contamination. Upon receival, they were kept until their analysis at -20ºC.

Table 3.5.3. Location of commercial bottled water (A), Spanish tap water (B) and international tap water (C) samples.

A) Hardness [1]	Bottle material	Commercial Brand (code)	Spring Location
Soft	Glass	Mondariz [2] (A)	Mondariz (SP)
Soft	Glass	Cabreiroá (B)	Verín (SP)
Soft	Plastic	Sousas (C)	Verín (SP)
Soft	Plastic	Fontecelta (D)	Sarria (SP)
Soft	Plastic	Aquabona (E)	Cospeito (SP)
Soft	Plastic	Bezoya (F)	Segovia (SP)
Soft	Plastic	Aguadoy (G)	Toledo (SP)
Hard	Glass	San Benedetto (H)	San Benedetto del Tronto (IT)
Hard	Plastic	Nestlé (I)	Badajoz (SP)
Hard	Plastic	Solán de Cabras (J)	Cuenca (SP)
Hard	Plastic	Font Vella [3] (K)	Guadalajara (SP)
B) Hardness	**Bottle material**	**Location**	**Province (SP)**
Soft	Glass	Ames	A Coruña
Soft	Glass	Teo	A Coruña
Soft	Glass	Muros	A Coruña
Soft	Glass	Santiago de Compostela[1]	A Coruña
Soft	Glass	Vilagarcía de Arousa	Pontevedra
Soft	Glass	Sanxenxo	Pontevedra
Soft	Glass	Vigo	Pontevedra
Soft	Glass	Cartelle	Ourense
Soft	Glass	Outeiro de Rei	Lugo
Soft	Glass	Chantada	Lugo
Soft	Glass	Cospeito	Lugo
Soft	Glass	Lugo	Lugo
Soft	Glass	Ponferrada	León
Soft	Glass	Santander	Cantabria
Soft	Glass	Argoños	Cantabria
Soft	Glass	San Sebastián	Guipúzcoa
Soft	Glass	Hondarribia	Guipúzcoa
Soft	Glass	Madrid	Madrid
Hard	Glass	Granada	Granada
Hard	Glass	Sevilla	Sevilla
Hard	Glass	Castellón	Castellón
Hard	Plastic	Moncada	Valencia
Hard	Plastic	Valencia	Valencia
C) Hardness	**Bottle**	**Location**	**Country**
Soft	Glass	Antwerp	Belgium
Soft	Glass	Rijkevorsel	Belgium
Soft	Glass	Porto	Portugal
Soft	Glass	Vila do Conde	Portugal
Soft	Glass	Leipzig	Germany
Hard	Glass	Berlin	Germany
Hard	Plastic	Varese	Italy
Hard	Plastic	Milan	Italy
Hard	Plastic	Chatellerault	France
Hard	Plastic	Poitiers	France
Hard	Plastic	Monterrey	Mexico
Soft	Glass	Knoxville (Tennessee)	USA

[1]Evaluated according to Diggs & Parker, 2009; [2]This water was used in the validation experiments and [3]This water was used in the hardness effect evaluation. SP: Spain, IT: Italy

3.5.3. Instrumentation

The LC-MS/MS was composed by an Agilent 1290 Infinity II LC system coupled to an Agilent 6495 mass spectrometer (QqQ), through a jet stream ESI source. The system includes an autosampler, furnished with a 1.5 mL extended loop in a multidraw valve, and a temperature-controlled column compartment. In addition to the binary analytical pump, it incorporates a quaternary pump to deliver samples, conditioning or clean-up solvents through the on-line connected SPE cartridges. Both SPE cartridge and analytical column, were connected using a 10-port, 2-possition valve located in an Agilent flexible cube module. Nitrogen was employed as nebulizing (30 psi), drying (120ºC, 11 L/min) and sheath gas (350ºC, 10 L/min) in the ESI source. The ESI source was operated in negative ionization (4,000 V) and low-pressure and high-pressure radiofrequency voltages were 40 and 70 V, respectively. The fragmentor energy was set at 16 V and CE value was adjusted individually for every compound. Acquisition was performed in dynamic Multiple Reaction Monitoring (dMRM) mode recording one (IS) or two (analytes) precursor/product ion transitions per compound, whenever possible. Selected transitions, together with the CE values, RT and IS are listed in the Table 3.5.4. Chromatographic conditions and sample preparation will be explained in the following sections.

Table 3.5.4. dMRM UHPLC-MS/MS analytical method for determination of PFAS.

Compounds	RT (min)			1st MRM transition (CE)	2nd MRM transition (CE)	IS
	Off-line SPE	On-line SPE	Direct injection			
PFBA	3.18	8.68	8.89	213 → 169 (5)		$^{13}C_4$PFBA
$^{13}C_4$PFBA	3.18	8.68	8.89	217 → 172 (5)		
PFPeA	4.24	9.35	8.90	263 → 219 (4)		$^{13}C_5$PFPeA
$^{13}C_5$PFPeA	4.24	9.35	8.90	268 → 223 (4)		
PFHxA	4.97	9.79	8.91	313 → 269 (5)	313 → 119 (21)	$^{13}C_5$PFHxA
$^{13}C_5$PFHxA	4.97	9.79	8.91	318 → 273 (5)		
PFHpA	5.50	10.15	8.93	363 → 319 (8)	363 → 119 (20)	$^{13}C_4$PFHpA
$^{13}C_4$PFHpA	5.50	10.15	8.93	367 → 322 (8)		
PFOA	6.25	10.55	8.98	413 → 369 (5)	413 → 169 (17)	$^{13}C_8$PFOA
$^{13}C_8$PFOA	6.25	10.55	8.98	421 → 376 (5)		
PFNA	6.98	11.09	9.07	463 → 419 (9)	463 → 219 (17)	$^{13}C_9$PFNA
$^{13}C_9$PFNA	6.98	11.09	9.07	472 → 427 (9)		
PFDA	7.67	11.69	9.21	513 → 469 (8)	513 → 269 (20)	$^{13}C_6$PFDA
$^{13}C_6$PFDA	7.67	11.69	9.21	519 → 474 (8)		
PFUdA	8.25	12.28	9.38	563 → 519 (8)	563 → 319 (20)	$^{13}C_7$PFUdA
$^{13}C_7$PFUdA	8.25	12.28	9.38	570 → 525 (8)		

Table 3.5.4. dMRM UHPLC-MS/MS analytical method for determination of PFAS (cont.).

Compounds	RT (min)			1st MRM transition (CE)	2nd MRM transition (CE)	IS
	Off-line SPE	On-line SPE	Direct injection			
PFDoA	8.77	12.85	9.63	613 → 569 (12)	613 → 269 (20)	$^{13}C_2$PFDoA
$^{13}C_2$PFDoA	8.77	12.85	9.63	615 → 570 (12)		
PFTrDA	9.22	13.36	9.96	663 → 619 (12)	663 → 169 (36)	$^{13}C_2$PFDoA
$^{13}C_2$PFTeDA	9.71	13.84	10.40	715 → 670 (12)		
PFBS	4.45	9.48	8.90	299 → 80 (41)	299 → 99 (33)	$^{13}C_3$PFBS
$^{13}C_3$PFBS	4.45	9.48	8.90	302 → 80 (41)		
PFPeS	4.96	9.86	8.91	349 → 80 (48)	349 → 99 (36)	$^{13}C_3$PFBS
PFHxS	5.59	10.18	8.94	399 → 80 (44)	399 → 99 (40)	$^{13}C_3$PFHxS
$^{13}C_3$PFHxS	5.59	10.18	8.94	402 → 80 (44)		
PFHpS	6.27	10.61	8.98	449 → 80 (52)	449 → 99 (44)	$^{13}C_3$PFHxS
PFOS	6.98	11.13	9.06	499 → 80 (60)	499 → 99 (49)	$^{13}C_8$PFOS
$^{13}C_8$PFOS	6.98	11.13	9.06	507 → 80 (60)		
PFNS	7.61	11.71	9.19	549 → 80 (60)	549 → 99 (48)	$^{13}C_9$PFNA
PFDS	8.22	12.29	9.37	599 → 80 (56)	599 → 99 (52)	$^{13}C_6$PFDA
PFUdS	8.64	12.85	9.63	649 → 80 (60)	649 → 99 (56)	$^{13}C_7$PFUdA
PFDoS	9.21	13.36	9.89	699 → 80 (60)	699 → 99 (56)	$^{13}C_2$PFDoA
PFTrDS	9.52	13.84	10.30	749 → 80 (60)	749 → 99 (60)	$^{13}C_2$PFTeDA

3.5.4. Analytical methods

All the glassware was baked following the protocol described in section 3.3.1 of González-Mariño et al. (2019).

3.5.4.1. Off-line SPE

3.5.4.1.1. SPE protocol

Off-line SPE was carried out using Oasis® WAX-150 mg cartridges (copolymer of divinylbenzene and N-vinyl pyrrolidone, 30 µm particle size, 80 Å pore size) from Waters as validated on previous works (Montes et al., 2020). For that purpose, 200 mL of water samples were spiked with 10 ng/L of IS and prior to sample loading, the cartridges were conditioned with 5 mL of MeOH and 5 mL of UPW. Thereupon, samples were passed through the cartridges

using a vacuum pump, and after sample loading, cartridges were washed consecutively with 10 mL of UPW thereupon 10 mL of MeOH and dried under a nitrogen stream (99.999%) for 30 min. Analytes were recovered with 10 mL of 5% NH_3 in MeOH. Eluates were evaporated to dryness under a nitrogen stream, resuspended in 200 µL of MeOH and filtered by 0.22 µm PTFE hydrophobic filters (Phenomenex) prior to analysis by LC-MS/MS.

3.5.4.1.2. Chromatographic conditions

The separation of PFAS was carried out on a Zorbax Extend C18 RRHT column (50 x 2.1 mm x 1.8 µm) from Agilent thermostated at 40ºC with a dual eluent system consisting of (A) 1mM NH_4F in UPW and (B) 1mM NH_4F in MeOH at a flow rate of 0.3 mL/min. The gradient elution started with 10% B, held for 0.5 min and increasing to 100% B in 9.5 min, held for 2 min. Return to initial conditions (10% B) was performed in 0.1 min and held for 5 min for back-conditioning. The injection volume was set at 2 µL. In order to reduce the PFAS background from the system, a InfinityLab PFC delay column (4.6 x 30 mm) from Agilent was placed before the multisampler valve (USEPA, 2020).

3.5.4.2. On-line SPE

For on-line SPE concentration, water samples were also spiked with IS (50 ng/L) and 0.005% HAc. The injection volume was 1.5 mL by the LC autosampler and loaded onto Strata®-X-AW (20 x 2.0 mm, 85 Å pore size, maximum operational pressure 275 bar) 33 µm polymeric weak cartridge purchased from Phenomenex with similar functionalized polymeric sorbent than WAX cartridges. Compounds elution was carried out using 0.05% NH_3 with (A) UPW and (B) MeOH as mobile phases employed in the UHPLC separation process (see section 3.5.3).

The compounds were separated using the same analytical column than off-line SPE (Zorbax Extend C18 RRHT) thermostated at 40ºC. The mobile phases consisted in UPW (A) and MeOH (B), both containing 0.05% NH_3, at a flow rate of 0.2 mL/min. The gradient elution started with 10% B, held for 6.5 min and increasing to 100% B in 15.5 min, held for 2 min. Return to initial conditions (10% B) was performed in 0.1 min and held for 5 min for back-conditioning. The injection volume was 1.5 mL, which was loaded onto Strata®-X-AW cartridge, delivered by the quaternary pump, the SPE mobile phases were UPW (C), 0.1% HAc in UPW (D), 2.5% NH_3 in MeOH (E) and MeOH (F). The sample was loaded at 1 mL/min using a mixture C:D:F (85:5:10) for 2 min, then the cartridge was washed (the cartridge eluate sent to waste through the flexible cube 10-port valve) consecutively with C:F (90:10) held for 1 min, with C:F (25:75) held for 1 min and with C:F (90:10) held for 2.5 min. At this point (6.5 min), the flexible cube 10-port valve was switched for the elution of PFAS with the binary pump from the cartridge and the subsequent separation in the analytical column using the abovementioned gradient. Meanwhile the quaternary pump remained at 0.05 mL/min for 9 min with C:F (90:10), at 2 mL/min for 2.5 min with 100% E and finally at 1 mL/min for 2 min with C:D:F (85:5:10) for SPE cartridge back-conditioning purposes. As in the case of off-line SPE a delay column to avoid mobile phases contaminations is mandatory, however as the InfinityLab PFC delay column does not support the overly basic conditions of the SPE elution solvent (pH=12), as a replacement, another Strata®-X-AW cartridge was used.

3.5.5. Analytical methods

The methods were evaluated in terms iLOQ, repeatability and linearity. Analytes were quantified by IS calibration using the isotopic labelled IS. In those (eight) cases where no labelled analogues were available, the labelled compounds providing the best results in terms of trueness were selected (see Table 3.5.4).

The calibration curves for linearity were prepared in MeOH between iLOQ and 200 µg/L for off-line SPE and in UPW in the iLOQ-500 ng/L and iLOQ-100 ng/L ranges, for on-line SPE and direct injection, respectively. Due to the detection of PFBA in UPW, for this compound, bottled water A (see Table 3.5.3) was used in validation experiments. The IS level was 10 µg/L (off-line SPE) and 50 ng/L (on-line SPE and direct injection). iLOQs were calculated as the highest concentration from two different approaches: a) standard providing a S/N ratio of 10 for the first MRM transition and ≥3 for the confirmation transition (when available) and b) considering the PFAS background as the mean of the blanks signal plus 10 times their standard deviation (Hernández et al., 2023). Instrumental repeatability was assessed as the %RSD of six consecutive injections at two different levels of concentration (0.5 and 50 µg/L) in the case of off-line SPE method and at 10 and 50 ng/L level for on-line SPE and direct injection, respectively.

Trueness and precision of the whole methods were estimated by quintuplicated analysis from recovery experiments performed in tap and bottled water samples spiked at 100 ng/L (high-level), 10 ng/L (medium-level) and 1 ng/L (low-level) of each analyte and 10 ng/L of IS for off-line SPE and at 50 ng/L for on-line SPE and direct injection. Samples were also analysed without analyte addition in order to correct for their native content. Method limits of quantification (mLOQs) were assessed from spiked tap water samples, in analogous way to iLOQs.

Finally, QCs were prepared and analysed in each sample batch to support the quality of analysis at 10 ng/L addition level. Satisfactory recoveries of QCs were considered between 70 and 120% and reliable identification of positives needed to comply established deviations in ion intensity ratios (≤30%) and t_R (≤0.1 min) in comparison with the reference standard (Hernández et al., 2023).

3.6. INSIGHTS INTO THE APPLICATION OF THE ANODIC OXIDATION PROCESS FOR THE REMOVAL OF PER- AND POLYFLUOROALKYL SUBSTANCES (PFAS) IN WATER MATRICES

3.6.1. Chemicals

Details on the applied PFAS are given in Tables 3.6.1 (with the solution mixture EU-5813-NSS listed in Table 3.5.1) and 3.6.2. Two ISs, perfluoro-n-[$^{13}C_2$]octanoic acid ($^{13}C_2$PFOA) and perfluoro-1-[$^{13}C_8$]octanesulfonic acid ($^{13}C_8$PFOS), both from Wellington Laboratories, were spiked to the samples before analysis at a concentration of 1 µg/L. Sodium sulphate anhydrous (Na_2SO_4) ≥99% purity (w/w) provided by Merck was used as the supporting electrolyte in UPW, DW, and urban wastewater after secondary treatment (UWW) matrices. Concentrated sulfuric acid (H_2SO_4) 96% purity (w/w) and sodium hydroxide (NaOH) ≥99% purity (w/w) supplied by Pronalab and Merck, respectively, were used for pH adjustment. UPW obtained from a Millipore® Direct-Q system (18.2 MΩ cm resistivity at 25ºC) was used in some analyses and as a water matrix. Demineralized water obtained from a reverse osmosis system (Panice) was used in some analyses.

Table 3.6.1. Chemical information of PFAS used in 24 C1-C13 PFAS solutions.

Name	Acronym	Formula	CAS RN	Supplier	Purity/ Conc.
Perfluoromethanesulfonic acid	PFMS	CHF_3O_3S	1493-13-6	Carbolution	98% w/w
Perfluoroethanesulfonic acid	PFEtS	$C_2HF_5O_3S$	354-88-1	Kanto Corporation	95% w/w
Perfluoropropanoic acid	PFPrA	$C_3HF_5O_2$	422-64-0	Merck	97% w/w
Perfluoropropanesulfonic acid	PFPrS	$C_3HF_7O_3S$	423-41-6	Kanto Corporation	95% w/w

Table 3.6.2. Chemical information of PFAS used in 8 C1-C8 PFAS solutions and single-solute solutions.

Name	Acronym	Formula	CAS RN	Supplier	Purity
Perfluoromethanesulfonic acid	PFMS	CHF_3O_3S	1493-13-6	Carbolution	98% w/w
Perfluoroethanesulfonic acid	PFEtS	$C_2HF_5O_3S$	354-88-1	Kanto Corporation	95% w/w
Perfluoropropanoic acid	PFPrA	$C_3HF_5O_2$	422-64-0	Merck	97% w/w
Perfluoropropanesulfonic acid	PFPrS	$C_3HF_7O_3S$	423-41-6	Kanto Corporation	95% w/w
Perfluorobutanoic acid	PFBA	$C_4HF_7O_2$	375-22-4	Merck	98% w/w
Perfluorobutanesulfonic acid	PFBS	$C_4HF_9O_3S$	29420-49-3	Merck	96% w/w
Perfluorooctanoic acid	PFOA	$C_8HF_{15}O_2$	335-67-1	Merck	95% w/w
Perfluorooctanesulfonic acid	PFOS	$C_8HF_{17}O_3S$	4021-47-0	Merck	98% w/w

3.6.2. Water and wastewater matrices

UPW was used directly from the Millipore® Direct-Q system after adding 30mM Na_2SO_4 to provide sufficient conductivity for carrying out the electrochemical processes. DW was collected from a DWTP in Northern Portugal. The DWTP comprised the following treatment

line: (i) filtration (pre-treatment), (ii) ozonation (pre-oxidation), (iii) coagulation/flocculation, (iv) air flotation and filtration, and (v) chlorination (final disinfection).

Table 3.6.3. Physicochemical characterization of the water/wastewater matrices.

Parameter (units)	UPW	DW	UWW	NF	RO
Color	n.d.	n.d.	Light yellow	Dark yellow	Dark yellow
Odor	n.d.	n.d.	Slight	Moderate	Moderate
pH	5.3	7.8	7.9	8.1	8.3
Turbidity (NTU)	0.1	0.2	15	10	50
Total suspended solids - TSS (mg/L)	n.d.	n.d.	35.7	18.5	96.0
Volatile suspended solids - VSS (mg/L)	n.d.	n.d.	30.7	5.5	78.5
Fixed suspended solids - FSS (mg/L)	n.d.	n.d.	5.0	24.0	17.5
Total dissolved carbon - TDC (mg/L)	<0.03 [a]	21	84	227	319
Dissolved inorganic carbon - DIC (mg/L)	<0.03 [a]	19	71	176	262
Dissolved organic carbon - DOC (mg C/L)	<0.03 [a]	2.4	14	51	56
Chemical oxygen demand - COD (mg O_2/L)	n.d.	n.d.	75	135	319
Absorbance at 254 nm (a.u.)	n.d.	0.013	0.530	1.112	1.688
Specific UV absorbance at 254 nm - $SUVA_{254}$ (L/mg m)	n.d.	0.54	3.92	2.19	3.00
Conductivity (µS/cm)	n.d. / 4,150 [c]	3.3 / 4,200 [c]	1,442 / 3,800 [c]	3,130	5,850
Chloride - Cl^- (mg/L)	<0.02 [a]	17	130	322	799
Sulfate - SO_4^{2-} (mg/L)	<0.03 [a] / 2,882 [c]	41 / 2,923 [c]	54 / 1,015 [c]	219	354
Sodium - Na^+ (mg/L)	<0.1 [a] / 1,380 [c]	12 / 1,392 [c]	105 / 565 [c]	299	541
Nitrite - NO_2^- (mg/L)	0.04	1.4	7.6	39	217
Nitrate - NO_3^- (mg/L)	<0.01 [b]	4.2	1.5	3.8	32
Ammonium - NH_4^+ (mg/L)	<0.004 [a]	<0.05 [a]	63	143	287
Phosphate - PO_4^{3-} (mg/L)	<0.03 [b]	<0.03 [b]	18	57	65
Calcium - Ca^{2+} (mg/L)	<0.1 [a]	34	32	92	125
Magnesium - Mg^{2+} (mg/L)	<0.08 [a]	7.1	6.4	34	47
Potassium - K^+ (mg/L)	<0.01 [a]	2.2	26	63	191

n.d. - not detected; [a]LOQ; [b]Limit of detection and [c]After adding supporting electrolyte (Na_2SO_4) - 30mM for UPW and DW, 10mM for UWW

3.6.3. Electrochemical system and experimental procedure

Electrochemical experiments were performed in the lab-scale flow system represented in Figure 3.6.1. This system mainly included: (i) an electrochemical filter-press flow cell (MicroFlowCell® from ElectroCell, Denamark), (ii) a 1.7 L cylindrical glass vessel thermostatically controlled and magnetically stirred acting as homogenization reservoir, (iii) a gear pump (Ismatec, model BVP-Z with pump head Ismatec Z-142), and (iv) a power supply (Velleman®, model LABPS3005DN, 0-5 A, 0-30 V). All system components were connected by PTFE tubing. The electrochemical cell comprised two flat electrodes of 10 cm^2 active area. A BDD electrode consisting of a conductive niobium (Nb) plate coated with a BDD thin film of 5 μm thickness was applied as the anode. A platinum (Pt) electrode composed of a conductive titanium (Ti) plate coated with a pure Pt layer of 2.5 μm thickness was employed as the cathode. Both electrodes were supplied by ElectroCell. The electrodes were separated by a PTFE flow frame of 2 mm thickness with a trapezoid-shaped central channel for fluid circulation. The channel was filled with a PP turbulence promoter mesh with 80% porosity. Two PTFE end frames and two stainless steel frames held the cell components together by mechanical compression. Peroxide-cured ethylene propylene diene monomer (EPDM) gaskets of 1 mm thickness were placed between all the cell components to avoid leakages. The interelectrode gap was 4.0 mm. One bottom inlet (position 1) and one upper outlet (position 1) among a total of 4 inlets and outlets (frontal and rear) were used in this study.

A solution volume of 200 mL was placed in the homogenization reservoir under magnetic stirring, and the thermostatic bath was switched on and set to provide a solution temperature of 25±1ºC. The solution was composed of the water/wastewater matrix, with or without the addition of Na_2SO_4, as previously mentioned, spiked with the 24 PFAS (C1-C13) of Table 3.6.1 with an individual content of 0.2 μg/L or the 8 PFAS (C1-C8) presented in Table 3.6.2 with an individual content of 2.0 μg/L. The gear pump was switched on at a flow rate of 100 L/h (Reynolds number (Re) of ~2,300) to recirculate all the solution throughout the system (semi-continuous mode with recirculation of the total amount of solution). The pH was adjusted to 7.0±0.2 using H_2SO_4 and NaOH solutions. After pH adjustment and stabilization of solution temperature at 25±1ºC (approximately 20 min), a first control sample was taken (t = 0 min). Following, the power supply was switched on at a fixed current density from 20 to 250 mA/cm^2 (galvanostatic mode), and the reaction time started running. In the first hour, samples were taken every 15 min and then every hour until a total reaction time of 4h. The pH and the temperature were adjusted during the reaction to remain at 7.0±0.2 and 25±1ºC, respectively. The cell voltage was registered during the reaction. In each set of three trials, one was conducted in duplicate. The duplicates exhibited variations always below 12%, with an average discrepancy of 6%. This highlights the robustness and reliability of the experimental procedures.

Control tests were carried out either by recirculating PFAS-free UPW or PFAS solutions (for the various water matrices) in the system for 4h in the absence of current. The former control test demonstrated that the release of PFAS from the experimental system, specifically from the PTFE tubing, was below LOQs. The latter control tests are elaborated in Section 4.6.

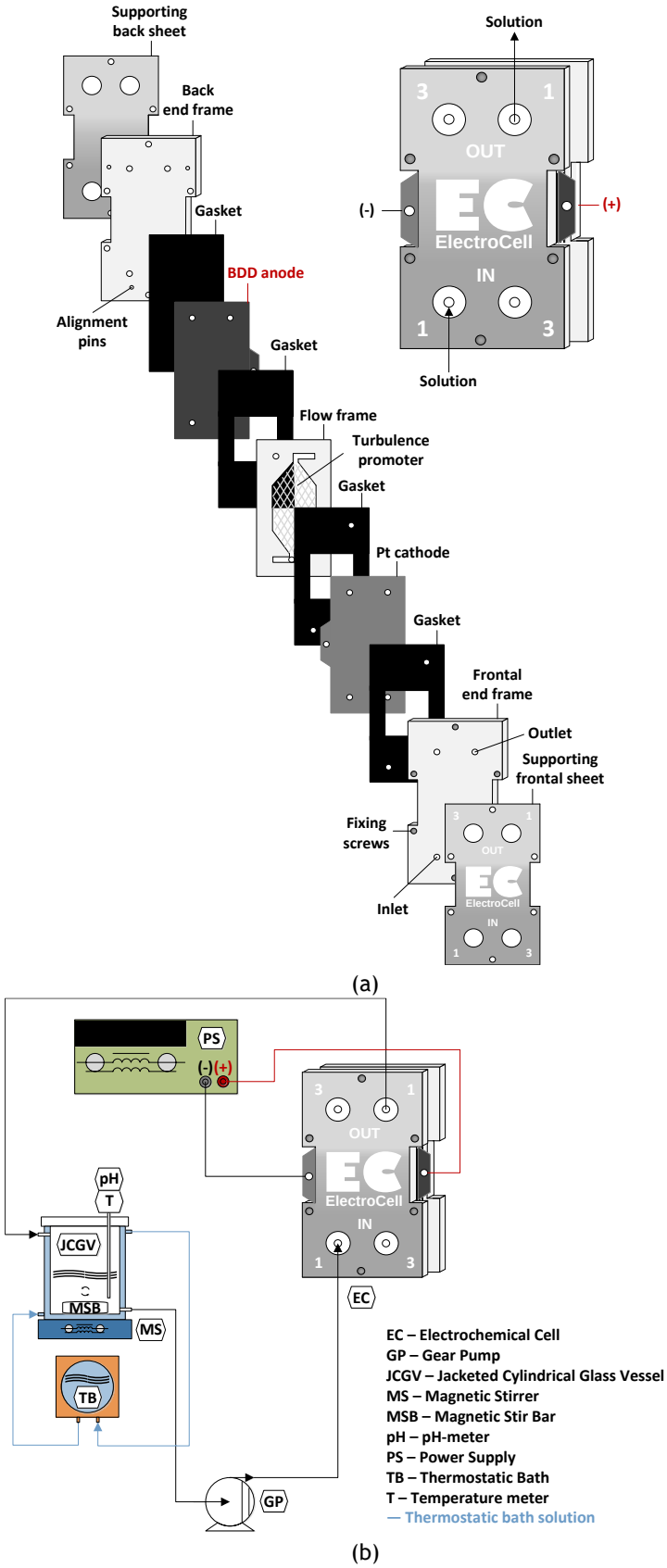

Figure 3.6.1. Sketch of the (a) electrochemical cell (MicroFlowCell®) and (b) electrochemical flow system.

3.6.4. Analytical determinations

PFAS quantification was performed in a LC-MS/MS composed by an Agilent Technologies 1290 Infinity II LC unit coupled to a 6495 triple quadrupole mass spectrometer (QqQ) from Agilent Technologies with an ESI jet stream source. The system was equipped with an Agilent InfinityLab PFC Delay Column (4.6 × 30 mm), placed between the LC pumps and the injection port, to avoid undesirable LC system peaks. The samples injection volume was 10 µL, directly injected into a Phenomenex Luna C18 100Å column (50 mm × 2 mm, 3 µm particle size) maintained at a constant temperature of 30ºC. The mobile phases consisted of (A) 1mM NH_4F in UPW and (B) 1mM NH_4F in MeOH. The gradient was as follows: 0-1 min, 0% B; 1-8 min, linear gradient to 100% B; 8-13 min, 100% B; 13-20 min, 0% B. The flow rate was 0.2 mL/min. Nitrogen was used as nebulizing, drying, sheath gas, and collision gas. N_2 acting as drying gas operated at 120ºC and a flow rate of 11 L/min, while N_2 acting as sheath gas operated at 350ºC and a flow rate of 10 L/min. The analyses were determined in the ESI negative polarity, and the acquisition mode was MRM. Two MRM transitions were used as quantifier (Q) and qualifier (q) transitions for each compound, except in the case of PFPrA (C3), PFBA (C4), and PFPeA (C5), for which only one intense MRM transition was observed. Selected transitions, together with the CE values, RT, and fragmentor of 166 V are listed in Table 3.6.4. Quantification was performed by the standard addition method. The method performance parameters are given in Table 3.6.5. Before injection, samples were filtered through hydrophilic PTFE filters (Ø 13 mm, 0.22 µm) from Phenomenex. UPW samples filtered with the same material were proven not to present PFAS above LOQs. The PFAS retention in filters was carefully assessed as well and no sorption was observed. Furthermore, the storage of PFAS standards in glass vials for up to 48h showed negligible loss of PFAS. Perfluoro-n-[$^{13}C_2$]octanoic acid ($^{13}C_2$PFOA) and perfluoro-1-[$^{13}C_8$]octanesulfonic acid ($^{13}C_8$PFOS) internal standards were spiked to the samples before analysis at a concentration of 1 µg/L.

Table 3.6.4. Instrumental LC-MS/MS parameters.

PFAS [a]	t_R (min)	1st MRM transition [b]	2nd MRM transition [b]
PFMS (C1)	1.80	149 → 80 (20)	149 → 99 (20)
PFEtS (C2)	5.16	199 → 80 (29)	199 → 99 (29)
PFPrA (C3)	6.81	163 → 119 (9)	
PFPrS (C3)	7.84	249 → 80 (33)	249 → 99 (33)
PFBA (C4)	7.51	213 → 169 (5)	
PFBS (C4)	9.02	299 → 80 (41)	299 → 99 (33)
PFPeA (C5)	8.80	263 → 219 (4)	
PFPeS (C5)	9.74	349 → 80 (48)	349 → 99 (36)
PFHxA (C6)	9.65	313 → 269 (5)	313 → 119 (21)
PFHxS (C6)	10.25	399 → 80 (44)	399 → 99 (40)
PFHpA (C7)	10.16	363 → 319 (8)	363 → 119 (20)
PFHpS (C7)	10.56	449 → 80 (52)	449 → 99 (44)
PFOA (C8)	10.58	413 → 369 (5)	413 → 169 (17)
$^{13}C_2$PFOA (C8)	10.58	415 → 370 (5)	
PFOS (C8)	10.90	499 → 80 (60)	499 → 99 (49)

PFAS [a]	t_R (min)	1st MRM transition [b]	2nd MRM transition [b]
$^{13}C_8$PFOS (C8)	10.90	507 → 80 (60)	
PFNA (C9)	11.02	463 → 419 (9)	463 → 219 (17)
PFNS (C9)	11.32	549 → 80 (60)	549 → 99 (48)
PFDA (C10)	11.20	513 → 469 (8)	513 → 269 (20)
PFDS (C10)	11.55	599 → 80 (56)	599 → 99 (52)
PFUdA (C11)	11.52	563 → 519 (8)	563 → 319 (20)
PFUdS (C11)	11.75	649 → 80 (60)	649 → 99 (56)
PFDoA (C12)	11.95	613 → 569 (12)	613 → 269 (20)
PFDoS (C12)	11.79	699 → 80 (60)	699 → 99 (56)
PFTrDA (C13)	12.11	663 → 619 (12)	663 → 169 (36)
PFTrDS (C13)	12.02	749 → 80 (60)	749 → 99 (60)

[a]Please note that the number in parenthesis refers to the total no. of C in the molecule and not the perfluorinated chain and [b]Precursor ion m/z → product ion m/z (CE, V)

Table 3.6.5. LC-MS/MS method performance.

PFAS [a]	Linearity (R^2) LOQ [b] to 5 µg/L	Precision (RSD [c] %) at 0.5 µg/L	LOQ [b] (µg/L)
PFMS (C1)	0.999	3	0.01
PFEtS (C2)	0.999	3	0.01
PFPrA (C3)	0.997	1	0.01
PFPrS (C3)	0.996	2	0.03
PFBA (C4)	0.998	1	0.01
PFBS (C4)	0.997	1	0.01
PFPeA (C5)	0.997	1	0.01
PFPeS (C5)	0.998	1	0.03
PFHxA (C6)	0.995	2	0.01
PFHxS (C6)	0.998	1	0.03
PFHpA (C7)	0.997	1	0.01
PFHpS (C7)	0.997	1	0.01
PFOA (C8)	0.997	1	0.01
PFOS (C8)	0.998	2	0.03
PFNA (C9)	0.995	2	0.01
PFNS (C9)	0.998	2	0.02
PFDA (C10)	0.999	1	0.02
PFDS (C10)	0.999	2	0.02
PFUdA (C11)	0.997	1	0.03
PFUdS (C11)	0.999	4	0.02
PFDoA (C12)	0.999	2	0.03
PFDoS (C12)	0.999	2	0.01
PFTrDA (C13)	0.999	2	0.05
PFTrDS (C13)	0.999	3	0.02

[a]Please note that the number in parenthesis refers to the total no. of C in the molecule and not the perfluorinated chain [b]LOQ defined for the lowest value obtained from a peak with a S/N = 10 or the lowest calibration level and [c]RSD- Relative standard desviation

The analytical determinations applied for the characterization of all water/wastewater matrices are provided in Table 3.6.6.

Table 3.6.6. Analytical determinations for characterization of water/wastewater matrices following the characterisation made in previous studies based on Moreira et al. (2015).

Parameter	Methodology
Absorbance at 254 nm	Absorbance at 254 nm was measured in a Merck Spectroquant® Prove 300 UV/Vis spectrophotometer.
Ammonium, calcium, magnesium, potassium, and sodium [a]	NH_4^+, Ca^{2+}, Mg^{2+}, K^+, and Na^+ inorganic cations were determined by ion chromatography injecting 25 µL of sample in a Dionex DX-120 device equipped with a IonPac® CS12A (4 × 250 mm) column at ambient temperature and a cation self-regenerating (CSRS® Ultra II, 4 mm) suppressor, under isocratic elution of 20mM methanesulphonic acid at a flow rate of 1.0 mL/min during 12 min.
COD	COD was measured according to the Standard Methods for the Examination of Water and Wastewater (SMEWW) (Eaton et al., 2005), 5220-D test, through oxidation with potassium dichromate followed by photometric measuring, using a WTW CR4200 thermoreactor and a Merck Spectroquant® Prove 300 UV/Vis spectrophotometer.
Chloride, nitrate, nitrite and, sulfate [a]	Cl^-, NO_3^-, NO_2^- and SO_4^{2-} inorganic anions were quantified by ion chromatography injecting 10 µL of sample in a Dionex ICS-2100 apparatus, equipped with a IonPac® AS11-HC (4 × 250 mm) column at 30ºC and an anion self-regenerating suppressor (ASRS® 300, 4 mm), under isocratic elution of 30mM NaOH at a flow rate of 1.5 mL/min during 12 min.
Conductivity	Conductivity was measured by a HANNA Instruments HI 9828 multiparameter analyzer.
pH and temperature	pH and temperature were measured by a pH meter VWR symphony SB90M5.
Specific ultraviolet absorbance at 254 nm [a]	$SUVA_{254}$ (L/mg m) was obtained by dividing the absorbance at 254 nm of filtered samples by DOC (mg/L).
Total dissolved carbon, dissolved inorganic carbon, and DOC [a]	TDC and DIC were separately determined by catalytic combustion at 680ºC and acidification, respectively, using a nondispersive infrared detector (NDIR) in a Shimadzu TOC-V_{CSN} analyzer. DOC was given by the difference between TDC and DIC (DOC = TDC - DIC).
Total oxidants	Total oxidants were determined by iodometric titration by adapting the procedure reported in Kolthoff and Carr (1953). In sum, (i) 10 mL of diluted sample were mixed with potassium iodide (KI) in excess and the mixture was vigorously shaken and left to stand for 15 min, (ii) a volume of 5 mL of sulfuric acid (H_2SO_4) 5% v/v was added to the mixture and the mixture was shaken, and (iii) sodium thiosulfate ($Na_2S_2O_3$) 0.01 M was used to titrate the mixture under agitation until a change in color from yellowish to transparent-white was observed. The volume of $Na_2S_2O_3$ was registered to calculate the content of oxidants.
Total suspended solids, volatile suspended solids, and fixed suspended solids	TSS were measured by gravimetry, drying the solid residue at 105ºC, according to the SMEWW (Eaton et al., 2005), 2540-D test. VSS were determined by gravimetry, after suspended solids oxidation at 550ºC, according to the SMEWW (Eaton et al., 2005), 2540-E test. FSS were given by the difference between TSS and VSS (FSS = TSS - VSS).
Turbidity	Turbidity was determined according to the SMEWW (Eaton et al., 2005), 2130 B test, using a HANNA Instruments HI 88703 turbidity meter.

[a]Samples were filtered through 0.45 µm Nylon membrane filters from Whatman (UK) before analysis

3.6.5. Modelling of PFAS decay

A pseudo-first-order kinetic model was fitted to the experimental data as a simple mathematical model from which kinetic constants were calculated to quantitatively compare the decay of PFAS under distinct conditions. This kinetic model was adjusted by a nonlinear regression

method using the Fig.P software for Windows from Biosoft. The pseudo-first-order kinetic constants (k), in 1/min, were calculated via equation 5:

$$[\text{PFAS}]_t = [\text{PFAS}]_0 \times e^{-kt} \text{ (Equation 5)}$$

where $[PFAS]_t$ is the content of a given PFAS (in µg/L) after time t and $[PFAS]_0$ is the content of a given PFAS (in µg/L) just before the start of the reaction. The goodness of the fitting was assessed by calculating the RSD, the residual variance (S^2_R), and the coefficient of determination (R^2).

The obtained k values, along with the goodness of the fitting, can be accessed in Tables 4.6.2-4.6.6. Longer-chain PFAS can originate shorter-chain PFAS, and thus the fitting was performed considering the reaction after the evident generation of PFAS. Nevertheless, the k values should be analysed cautiously since some non-evident PFAS formation may have occurred. In fact, the pseudo-first-order kinetic model was not adjusted or poorly adjusted to the degradation of various PFAS, which can be mainly attributed to the continuous formation of PFAS during the reaction, strong PFAS adsorption on the system, and/or PFAS recalcitrant character.

RESULTS AND DISCUSSION

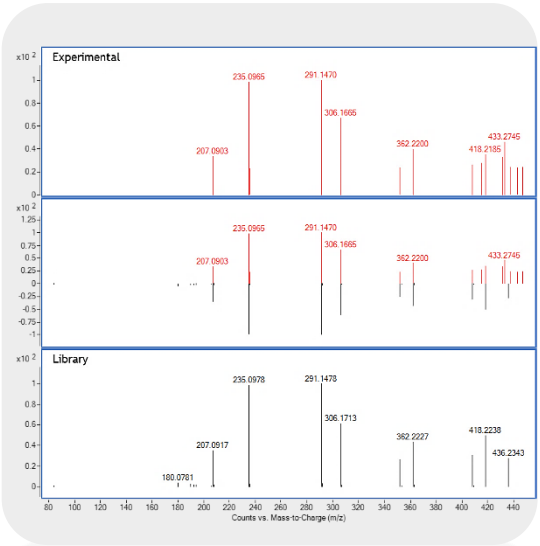

4. RESULTS AND DISCUSSION

4.1. SCREENING OF ORGANIC CHEMICALS ASSOCIATED TO VIRGIN LOW-DENSITY POLYETHYLENE MICROPLASTIC PELLETS EXPOSED TO THE MEDITERRANEAN SEA ENVIRONMENT BY COMBINING GAS CHROMATOGRAPHY AND LIQUID CHROMATOGRAPHY COUPLED TO QUADRUPOLE-TIME-OF-FLIGHT MASS SPECTROMETRY

Several workflows were combined in a holistic framework to elucidate organic compounds of varied physicochemical characteristics associated to seawater-exposed LDPE MPs. This included the use of suspect and non-target LC-HRMS screening, and a GC-HRMS spectral deconvolution-based GC-HRMS screening, based on our previous expertise (Castro, Quintana, Carpinteiro, et al., 2021; Castro et al., 2022; Wilson et al., 2021). Consequently, the compounds identified with the different approaches are first presented. Then, their temporal trends as well as the quantification of those chemicals for which standards are available are discussed.

4.1.1. LC-QTOF screening

4.1.1.1. Suspect screening

The LC-HRMS suspect screening workflow permitted the identification of six compounds (Table 4.1.1). The four chemicals detected in ESI+ mode include the very polar chemical melamine (Figure 4.1.1), which was only detected in the virgin LDPE MPs and further confirmed with pure standards, two pharmaceuticals (minoxidil and methenamine) and the plasticizer triacetin, the later three not being detected at time = 0. On the other hand, the compounds detected in ESI- are two fatty acids (erucic and behenic acid), both being detected only in the samples that had been exposed to the marine environment for 8 weeks, likely because of their natural origin or from anthropogenic sources (García-de-Vinuesa et al., 2022).

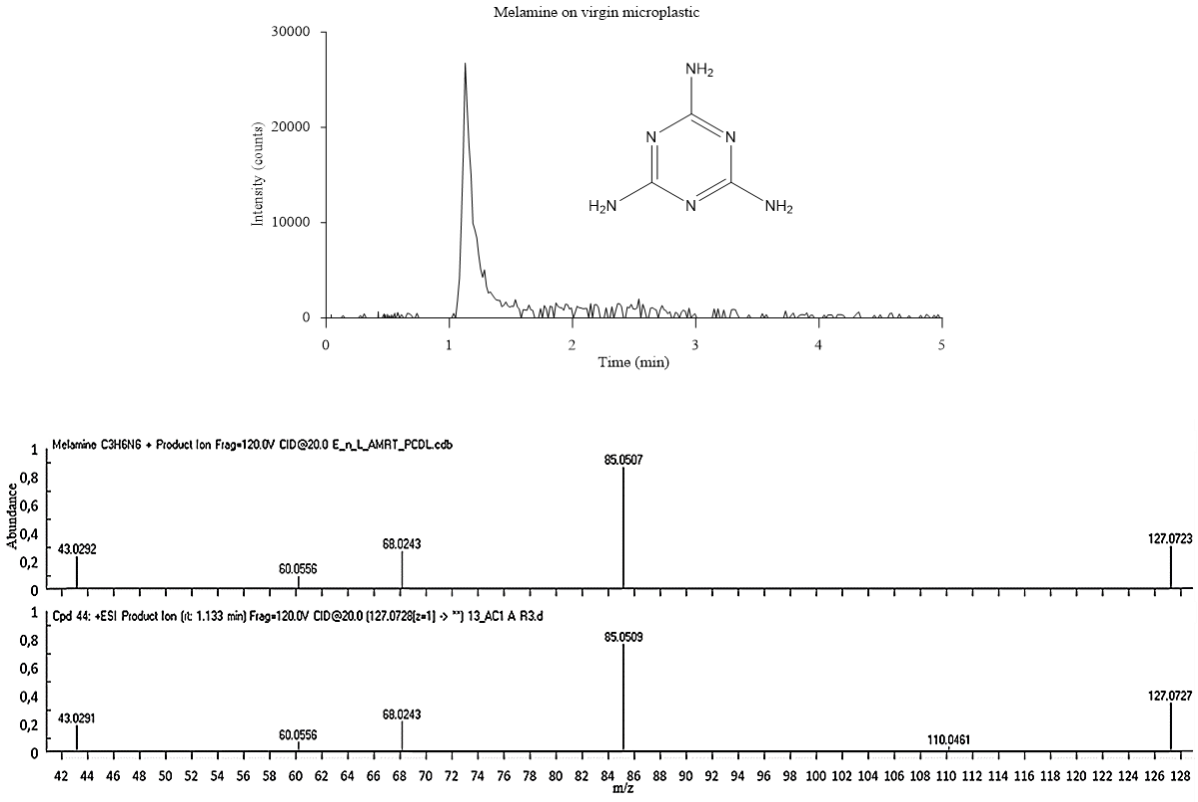

Figure 4.1.1. LC-QTOF chromatogram of the $[M+H]^+$ ion of melamine (top) and MS/MS spectra at 20 V of melamine in virgin microplastic (down bottom) against the library spectrum (down top).

Table 4.1.1. List of compounds tentatively identified by LC-QTOF screening.

t_R (min)	m/z	Species	Molecular formula	Name	CAS No. / SMILE [a]	ID method [b]	ID level [c]	Use [d]	Samples detected [e]	RSD % [f]
1.154	127.0729	$[M+H]^+$	C3 H6 N6	Melamine	108-78-1	SS	1	Resin monomer	0	25
3.515	210.1357	$[M+H]^+$	C9 H15 N5 O	Minoxidil	38304-91-5	SS	2a	Pharmaceutical	8	3
1.043	141.1124	$[M+H]^+$	C6H12N4	Methenamine	100-97-0	SS	2a	Pharmaceutical	4	11
3.421	241.0674	$[M+Na]^+$	C9H14O6	Triacetin	102-76-1	SS	2a	Plasticizer	8	12
1.053	118.0857	$[M+H]^+$	C5 H12 N O2	Betaine	107-43-7	NT-L	2a	Natural comp.	4,8	28
1.033	143.0813	$[M+H]^+$	C6 H10 N2 O2	Ectoine	96702-03-3	NT-L	2a	Natural comp	4,8	28
10.32	338.3418	$[M+H]^+$	C22 H43 N O	13-(Z)-Docosenamide	112-84-5	NT-L	2a	Slip agent	0-8	38
3.558	201.111	$[M+H]^+$	C10 H16 O4	2E-Decenedioic acid	37443-67-7	NT-IS	2b	Natural comp.	8	41
1.034	132.1015	$[M+H]^+$	C6 H13 N O2	N-Ethyl-N-methyl-ß-alanine	1095030-20-8	NT-IS	2b	Amino acid	4,8	14
11.816	871.5731	$[M+H]^+$	C55 H74 N4 O5	Pheophytin A	603-17-8	NT-IS	2b	Natural comp.	4,8	35
11.431	887.568	$[M+H]^+$	C47 H83 O13 P	PI(20:0/18:4(6Z.9Z.12Z.15Z)) / 1-eicosanoyl-2-(6Z,9Z,12Z,15Z-octadecatetraenoyl)-glycero-3-phospho-(1'-myo-inositol)	CCCCCCCCCCCCCCCCCCCC=COCC(COP(=O)(O)OC1C(C(C(C(C1O)O)O)O)O)OC(=O)CCCCC=CCC=CCC=CCC=CCC	NT-IS	2b	Natural comp.	4,8	25
6.911	274.0903	$[M+H]^+$	C12 H19 N O2 S2	2-(Methylsulfonyl)-N-[(3-methyl-2-thienyl)methyl]cyclopentanamine	CS(=O)(=O)C1CCCC1NCCC2=CC=CS2	NT-IS	2b	Natural comp.	0,8	40

[a]SMILES are provided for those chemicals lacking CAS number. [b]ID method: primary identification method employed. SS: suspect screening; NT-L: non-target screening with library matching of spectra (against lab-available libraries, otherwise the library and record is provided); NT-IS: non-target screening identification assisted by *in-silico* tools. [c]ID level: identification level as defined in Wilson et al. (2021). [d]Main application of the chemicals detected. Please note that other applications may exist. [e]Exposition time (at 0, 4 or 8 weeks) in which the chemical was detected and [f]Average RSD of the intensities across time-replicates

Table 4.1.1. List of compounds tentatively identified by LC-QTOF screening (cont.).

t_R (min)	m/z	Species	Molecular formula	Name	CAS No. / SMILE [a]	ID method [b]	ID level [c]	Use [d]	Samples detected [e]	RSD % [f]
11.457	903.5626	$[M+H]^+$	C55 H74 N4 O7	Methyl (3R.10Z.14Z.20Z.22S.23S)-12-ethyl-3-hydroxy-13.18.22.27-tetramethyl-5-oxo-23-(3-oxo-3-{[(2E.7R.11R)-3.7.11.15-tetramethyl-2-hexadecen-1-yl]oxy}propyl)-17-vinyl-4-oxa-8.24.25.26-tetraazahexacyclo[19.2.1.16.9.111.14.116.19.02.7]heptacosa-1(24).2(7).6(27).8.10.12.14.16.18.20-decaene-3-carboxylate	O=C(OC\C=C(/C)CCC[C@H](C)CCC[C@H](C)CCCC(C)C)CC[C@@H]6c2nc(cc5c(c(\C=C)c(cc1c(c(c(n1)cc\3nc\4c2[C@@](O)(OC(=O)C/4=C/3C)C(=O)OC)CC)C)n5)C)[C@H]6C	NT-IS	2b	Natural comp.	4,8	28
9.699	393.2052	$[M+H]^+$	C18 H28 N6 O2 S	N-[(2R)-3-Methyl-1-oxo-1-thiomorpholin-4-ylbutan-2-yl]-4-pyrimidin-2-ylpiperazine-1-carboxamide	CC(C)C(C(=O)N1CCSCC1)NC(=O)N2CCN(CC2)C3=NC=CC=N3	NT-IS	2b	Natural comp.	8	38
6.825	337.312	$[M-H]^-$	C22 H42 O2	Erucic acid ((Z)-Docos-13-enoic acid)	112-86-7	SS	2a	Natural comp.	8	7
6.907	339.3273	$[M-H]^-$	C22 H44 O2	Behenic acid (Docosanoic acid)	112-85-6	SS	2a	Natural comp.	8	19
4.304	143.1085	$[M-H]^-$	C8 H16 O2	Valproic Acid	99-66-1	NT-L	2a	Drug	8	33
6.298	241.145	$[M-H]^-$	C13 H22 O4	(2Z)-2-Octyl-2-pentenedioic acid	59039-06-4	NT-L (mzCloud record 7,506)	2a	Unknown	8	35
11.764	869.557	$[M-H]^-$	C55 H74 N4 O5	Pheophytin A	603-17-8	NT-IS	2b	Natural comp.	4	38
6.896	201.1497	$[M-H]^-$	C11 H22 O3	2-Hydroxyundecanoic acid	19790-86-4	NT-IS	2b	Slip agent	8	27
5.948	229.1449	$[M-H]^-$	C12 H22 O4	Dimethyl sebacate (Decanedioic acid, dimethyl ester)	106-79-6	NT-IS	2b	Fatty acid methyl ester	8	22

[a]SMILES are provided for those chemicals lacking CAS number. [b]ID method: primary identification method employed. SS: suspect screening; NT-L: non-target screening with library matching of spectra (against lab-available libraries, otherwise the library and record is provided); NT-IS: non-target screening identification assisted by *in-silico* tools. [c]ID level: identification level as defined in Wilson et al. (2021). [d]Main application of the chemicals detected. Please note that other applications may exist. [e]Exposition time (at 0, 4 or 8 weeks) in which the chemical was detected and [f]Average RSD of the intensities across time-replicates

4.1.1.2.Non-target screening

The non-target screening workflow rendered a list of 2,038 and 122 features in ESI+ and ESI-, respectively, as an output from the MassHunter Profinder software peak-picking algorithm. The statistical comparison performed by ANOVA and the fold-change of 10, respective time = 0 days samples, resulted into a total number of 691 features in ESI+ and 51 in ESI-. Afterwards, a 90th percentile (in each condition) filter was applied to ESI+ features only, so that only the 10% most abundant at each condition investigated condition (exposure time), to decrease the total number of features to be investigated for further PCA analysis and tentative identification (143 features retained).

Figure 4.1.2 shows the scores (a and c) and loadings (b and d) plots for the two first principal components obtained from the PCA in the two-ionization modes. The accumulated explained variance was 80% and 65% for ESI+ and ESI-, respectively. According to the scores plots, the first principal component (PC1) separates the features related to blank samples from those related to MPs. On the other hand, the second principal component (PC2) helps in differentiating the samples according to the exposure time. Hence, the compounds were classified in different groups (Figure 4.1.2b and d), in which group 0 was defined as those compounds which are more abundant in the blanks than in the MP samples, thereby lacking interest in this study. Regarding the remaining feature groups:

- Group A corresponds to those compounds present in MPs not exposed to seawater, whose signal intensities decrease over time, i.e. they are readily released to the marine environment.
- Group B includes those features whose intensities remain stable, i.e. they were present in the virgin MPs and are not significantly released.
- Finally, groups C-E represent those chemicals whose intensity increases over time, i.e. chemicals that are occurring in the seawater and are sorbed to LDPE MPs. The three subgroups refer to the three different behaviours observed: C-group compounds were originally in the MPs, but their intensities increase over time, D-group chemicals (only observed in ESI+) are only detected in 4- and 8-week exposed MPs, and chemicals from group E correspond to those only detected after 8 weeks.

Therefore, all substances present in groups A-E were submitted to target MS/MS experiments, unless already their spectra were obtained in Auto MS/MS injections. Then, they were tentatively identified as detailed in section 3.1.5. In this way, a total of 15 further features (14 chemicals, since pheophytin A was detected in both ionization modes) could be identified at a confirmation level 2. Four chemicals providing a match against a library were assigned level 2a and those identified by *in-silico* interpretation of MS/MS spectra were assigned level 2b (Table 4.1.1). All remaining features for which no chemical structure could be assigned were considered irrelevant, because the identification would be too ambiguous and unreliable and thus, they were discarded. It should be noted that the use of *in-silico* MS/MS interpretation tools permitted the tentative identification of up to 10 chemicals. As an example, the tentative identification of PI (20:0/18:4(6Z.9Z.12Z.15Z)) (molecular formula C47H83O13P), a glycerophospholipid, by the two *in-silico* MS/MS fragmentation tools is presented in the Figures 4.1.3 and 4.1.4.

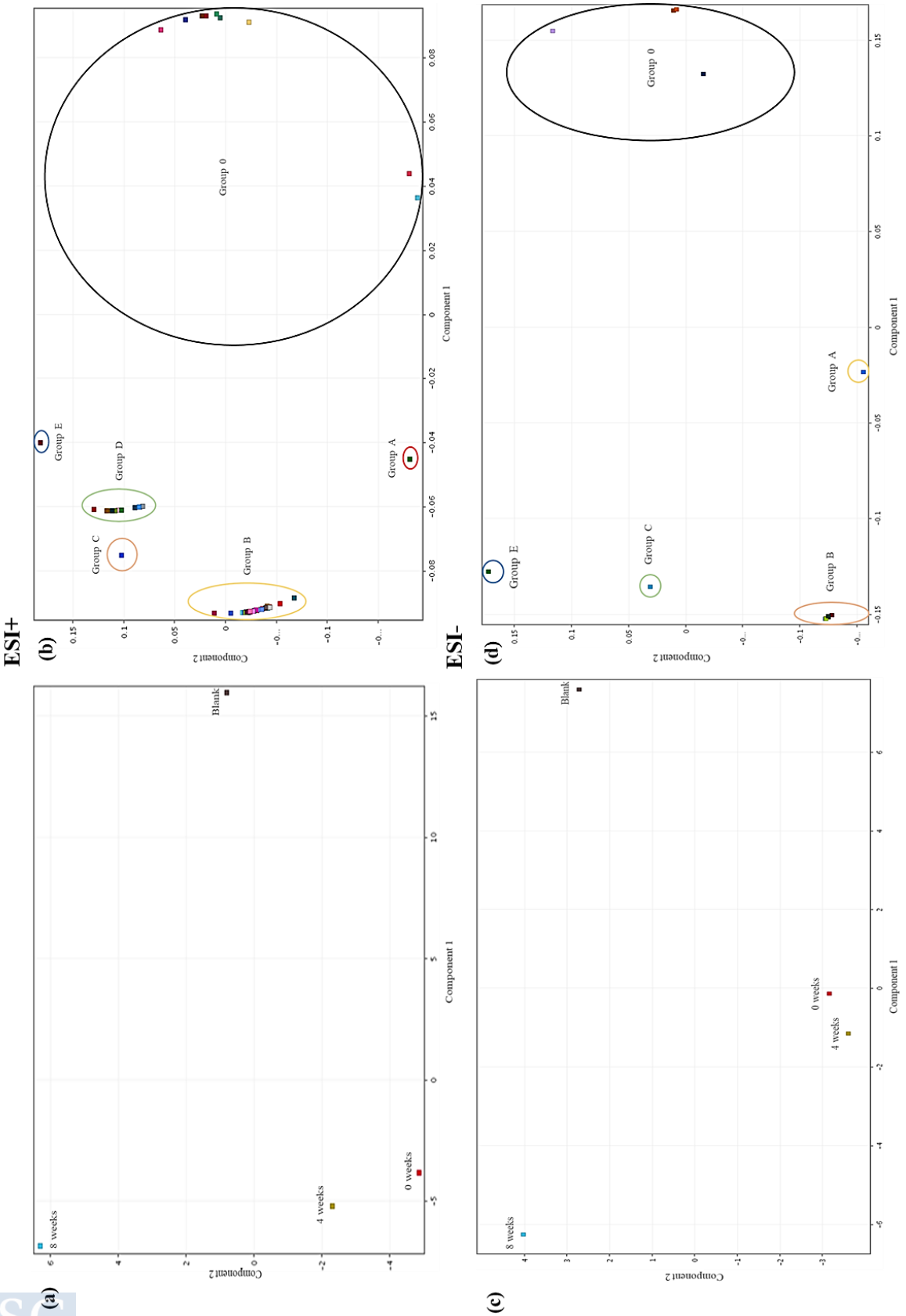

Figure 4.1.2. Scores (a and c) and loadings (b and d) plots for the two first principal components obtained after the PCA of the non-target screening LC-QTOF features in ESI+ (a and b) and ESI- (c and d). For grouping interpretation, please refer to the manuscript section 4.1.1.2.

Most of the tentatively identified chemicals were natural compounds which seem to be accumulated on the MPs over time. This may be partly related to the fouling of the nylon net containing the MPs, which would explain, for instance the build-up of the very polar compound betaine. The exception was 13-(Z)-docosenamide, a compound added to plastics as slip agent (Bolgar et al., 2007; ECHA, 2021a) that was detected at the three exposure times analysed.

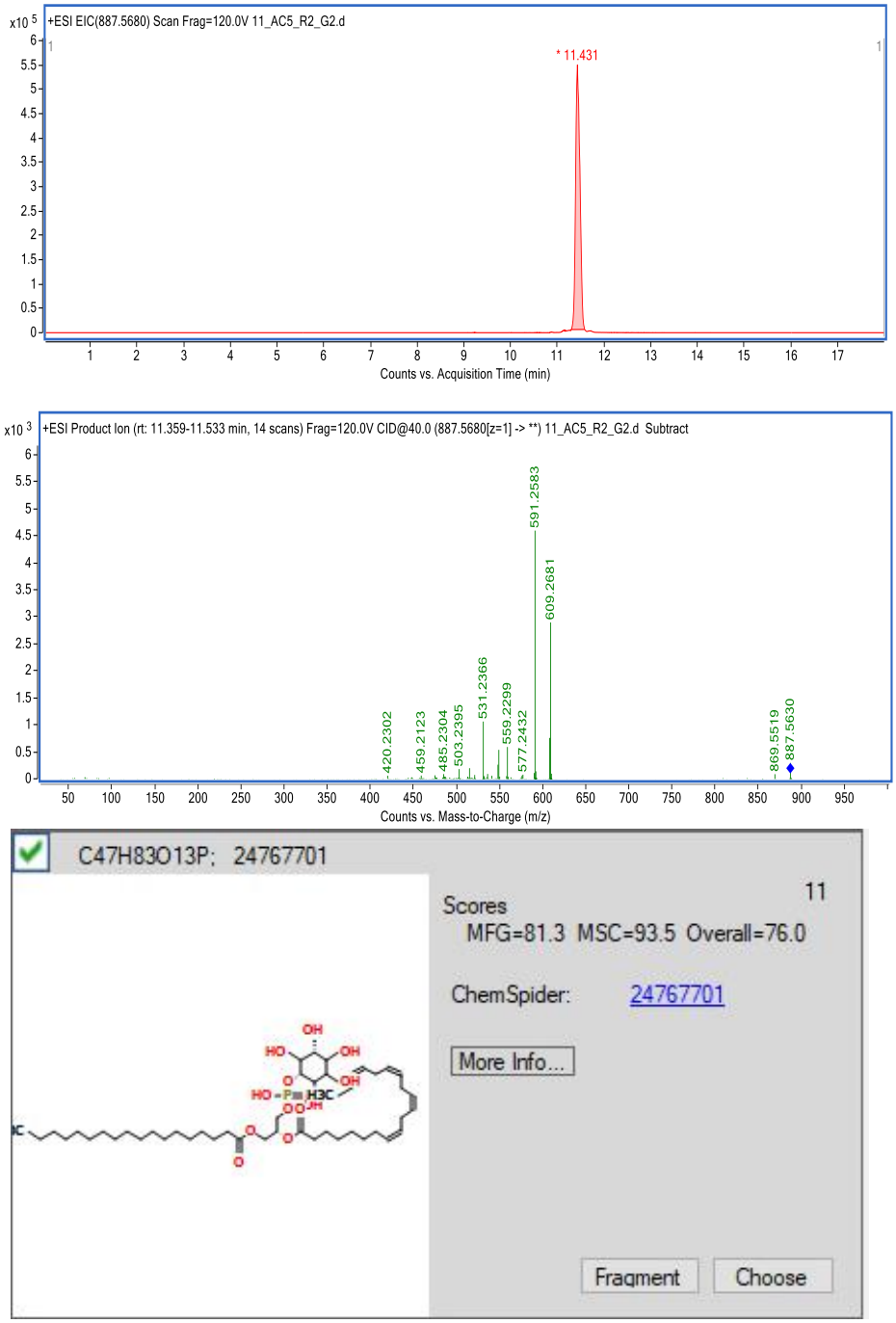

Figure 4.1.3. Tentative identification of PI (20:0/18:4(6Z.9Z.12Z.15Z)) (C47H83O13P) with the Agilent Molecular Structure Correlator. The m/z values in green in the spectrum correspond to those which could be explained by the *in-silico* fragmentation software.

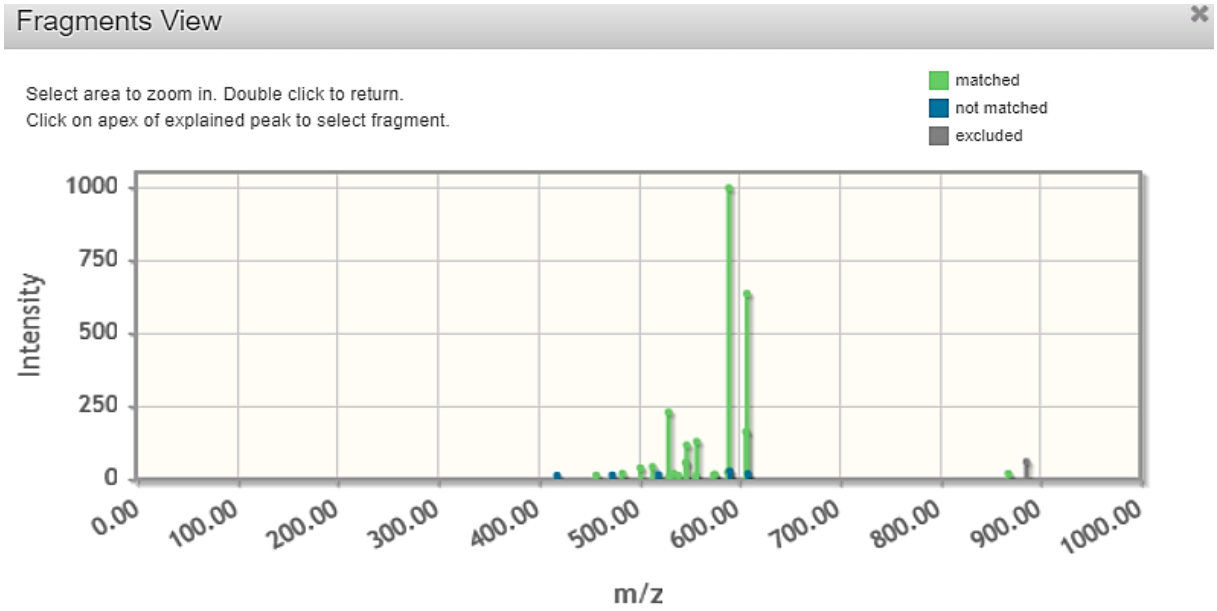

Figure 4.1.4. Tentative identification of PI (20:0/18:4(6Z.9Z.12Z.15Z)) (C47H83O13P), see chromatographic peak and structure in Figure 4.1.3, with the Metfrag open software. The m/z values in green in the spectrum correspond to those which could be explained by the *in-silico* fragmentation software.

4.1.2. GC-QTOF screening

The GC-QTOF analysis allowed the detection of a total number of 32 chemicals, of which 15 were confirmed by injecting standards (level 1), one was assigned a confirmation level 2a because of the match against the HRMS library with coincident RI, and the remaining 16 were assigned a confirmation level 2b as they were only identified against low-resolution MS spectral libraries.

Among them, triacetin and melamine (as TMS tri-derivative) were the only two compounds that had been previously detected by LC-QTOF. Again, melamine was only detected in virgin MPs, confirming that this very polar chemical is rapidly released to the environment. Regarding the remaining compounds, several plastic related chemicals, such as plasticizers (e.g., phthalates), and many fatty acids were identified (Table 4.1.2). Out of the several compounds detected (Table 4.1.2), besides melamine, only hexadecanol and octadecanol showed a significant decrease over time (ρ = -0.96). In the case of 2-ethylhexyl salicylate (EHS, see Figure 4.1.5 as identification example), although a significant monotonic trend is not observed by the Spearman's test, a visualisation of the signal intensity over time clearly indicates a high concentration in the virgin MPs, showing a rapid decrease in the first weeks followed by a steady state (see section 4.1.4). The presence of hexadecanol and octadecanol in the original LDPE pellets is likely due to their use as emulsifiers during synthesis (Bolgar et al., 2007; ECHA, 2021a), yet EHS is typically used as UV filter in cosmetics (ECHA, 2006), and thus occurrence in primary MPs is uncommon.

Table 4.1.2. List of compounds tentatively identified by GC-QTOF screening.

t_R (min)	Molecular formula	Name	CAS No.	ID Level [a]	Use [b]	Trend (ρ) [c]	RSD % [d]
17.69	C16H22O4	Di-iso-butyl phthalate (DiBP)	84-69-5	1	Plasticizer	NS	20
13.74	C15H24O	Butylated Hydroxytoluene (BHT)	128-37-0	1	Antioxidant	+0.60	42
18.63	C16H22O4	Di-n-butyl phthalate (DnBP)	84-74-2	1	Plasticizer	NS	23
14.71	C12H14O4	Diethyl phthalate (DEP)	84-66-2	1	Plasticizer	NS	24
23.68	C24H38O4	Bis(2-ethylhexyl) phthalate (DEHP)	117-81-7	1	Plasticizer	NS	43
13.00	C10H10O4	Dimethyl phthalate (DMP)	131-11-3	1	Plasticizer	NS	38
15.18	C13H10O	Benzophenone	119-61-9	1	UV filter	+0.44	38
17.63	C18H26O	Galaxolide	1222-05-5	1	Fragance	+0.57	25
12.37	C12H10O	Diphenyl Ether	101-84-8	1	Several	+0.68	34
16.93	C14H10	Phenanthrene	120-12-7	1	PAH	+0.70	27
9.95	C7H5NS	Benzothiazole	95-16-9	1	Corrosion inhibitor	+0.64	31
13.71	C12H27O4P	Tri-iso-butyl phosphate (TiBP)	126-71-6	1	Flame retardant / plasticizer	NS	31
18.49	C17H27O3Si	2-Ethylhexyl salicylate. (TMS der.)	118-60-5	1	UV filter	NS	28
21.03	C21H32O2Si2	Bisphenol A. (2xTMS der.)	80-05-7	1	Monomer	+0.51	27
9.24	C6H3Cl3	1,2,4-Trichlorobenzene	87-61-6	2a	Multiples uses	+0.84	27
17.58	C16H34O	1-Hexadecanol	36653-82-4	2b	Emulsifier	-0.96	22

[a]ID level: identification level based on Wilson et al. (2021), level 2a was assigned to those with spectral match against the HRMS libraries and 2b to matches against the low resolution MS libraries. [b]Main application of the chemicals detected. Please note that other applications may exist. [c]Relative trend identified as the ρ value of the Spearman rank correlation test. Only those values which are statistically significant (α=0.05) are provided. NS means non-statistically significant. [d]Average relative standard deviation of the intensities across time-replicates

Table 4.1.2. List of compounds tentatively identified by GC-QTOF screening (cont.).

t_R (min)	Molecular formula	Name	CAS No.	ID Level [a]	Use [b]	Trend (ρ) [c]	RSD % [d]
11.52	C9H14O6	Triacetin	102-76-1	2b	Plasticizer	NS	24
9.16	C8H14O4	Butanedioic acid diethyl ester (Diethyl succinate)	123-25-1	2b	Synthesis intermediate	+0.55	42
19.13	C19H38O2	Isopropyl palmitate	142-91-6	2b	Various	+0.78	35
19.59	C18H38O	1-Octadecanol	112-92-5	2b	Various	-0.96	21
23.99	C25H54O4Si2	1-Monopalmitin (2xTMS der.)	542-44-9	2b	Emulsifier	NS	38
10.60	C13H30OSi	2-Decanol (TMS der.)	1120-06-5	2b	Various	NS	42
12.64	C15H34OSi	2-Dodecanol (TMS der.)	10203-28-8	2b	Various	NS	28
20.88	C21H40O2Si	9,12 (Z.Z)- Octadecanoic acid (TMS der.)	506-21-8	2b	Various	+0.64	39
7.64	C9H20O2Si	Hexanoic acid (TMS der.)	142-62-1	2b	Various	0.47	29
7.51	C9H14O3Si2	Lactic acid (2xTMS der.)	50-21-5	2b	Natural comp.	NS	25
17.85	C12H30N6Si3	Melamine (3xTMS der.)	108-78-1	1	Resin monomer	-0.56	28
17.42	C17H36O2Si	Myristic acid (TMS der.)	544-63-8	2b	Natural comp.	+0.55	27
20.93	C21H42O2Si	Oleic acid (Z) (TMS der.)	112-80-1	2b	Natural comp.	NS	28
19.36	C19H40O2Si	Palmitic acid (TMS der.)	57-10-3	2b	Natural comp.	+0.62	19
7.40	C9H14OSi	Phenol (TMS der.)	108-95-2	2b	Various	NS	28
21.14	C21H44O2Si	Stearic acid (TMS der.)	57-11-4	2b	Natural comp.	+0.52	19

[a]ID level: identification level based on Wilson et al. (2021), level 2a was assigned to those with spectral match against the HRMS libraries and 2b to matches against the low resolution MS libraries. [b]Main application of the chemicals detected. Please note that other applications may exist. [c]Relative trend identified as the ρ value of the Spearman rank correlation test. Only those values which are statistically significant (α=0.05) are provided. NS means non-statistically significant. [d]Average relative standard deviation of the intensities across time-replicates

Several natural fatty acids and anthropogenic chemicals are proven to get accumulated onto the MPs over time, including butylated hydroxytoluene (BHT), galaxolide and phenanthrene, among others (Table 4.1.2), thus demonstrating the potential role of LDPE MPs as vectors of unrelated plastic components. The lack of temporal trends (increasing, then decreasing) of some other chemicals, may simply be related to the variable composition of the surrounding marine environment throughout time.

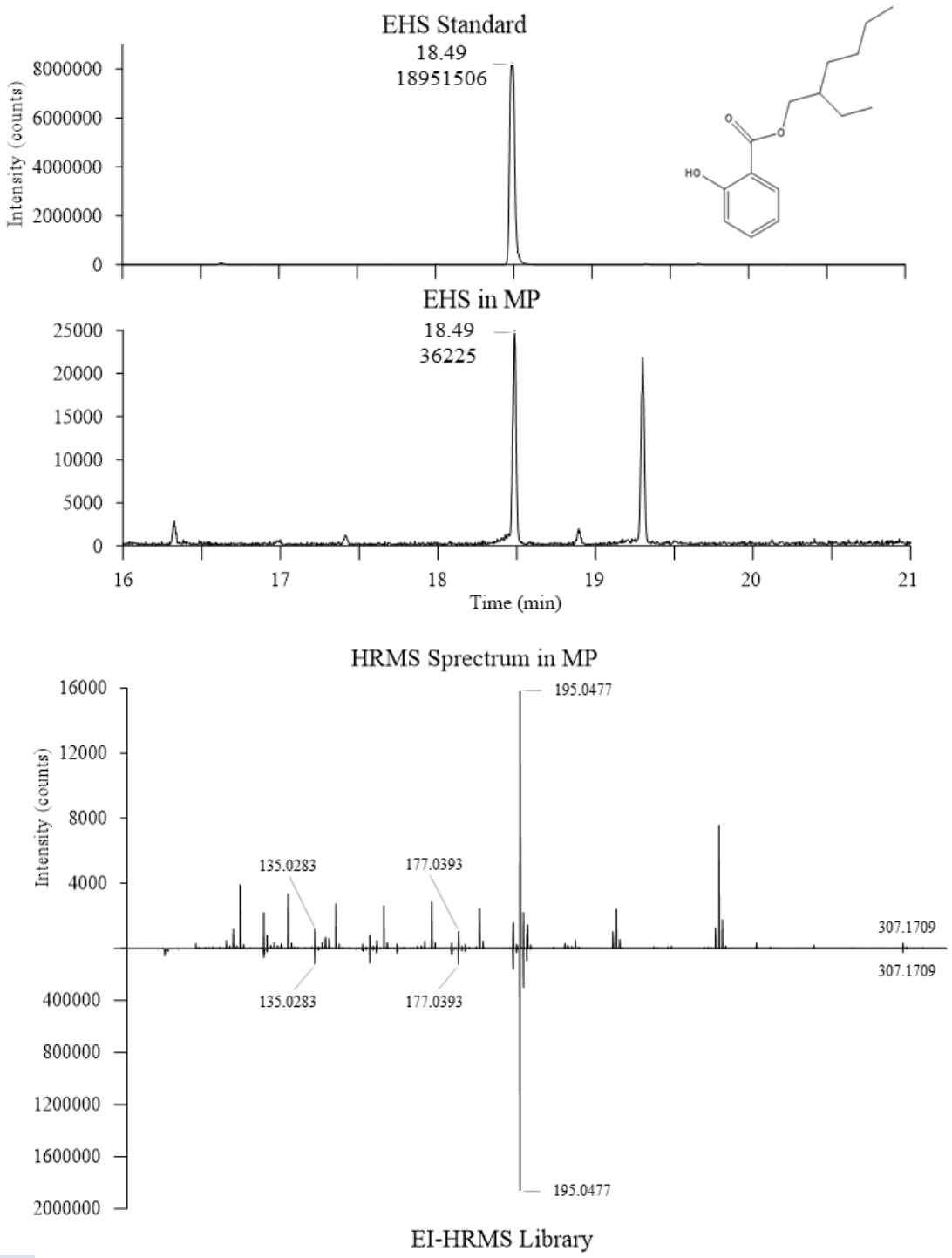

Figure 4.1.5. GC-QTOF identification of EHS as TMS derivative.

4.1.3. Comparison of the results obtained by complementary analytical approaches.

By exploiting the different analytical approaches, a total number of 50 chemicals were (tentatively) identified at level 2b or higher. As it can be observed in Figure 4.1.6, GC-HRMS and LC-HRMS enabled identifying 32 (of which 14 after derivatization with TMS) and 20 chemicals, respectively. The suspect screening LC-HRMS approach was capable of identifying only 6 compounds, from which triacetin and melamine were also detected by GC-HRMS (as TMS derivatives). The relatively less efficiency of the LC-HRMS suspect screening approach may be related to the content of the libraries used and the fact that non-polar chemicals which are expected to get strongly bound to MPs are better detected by the GC-based analytical methods.

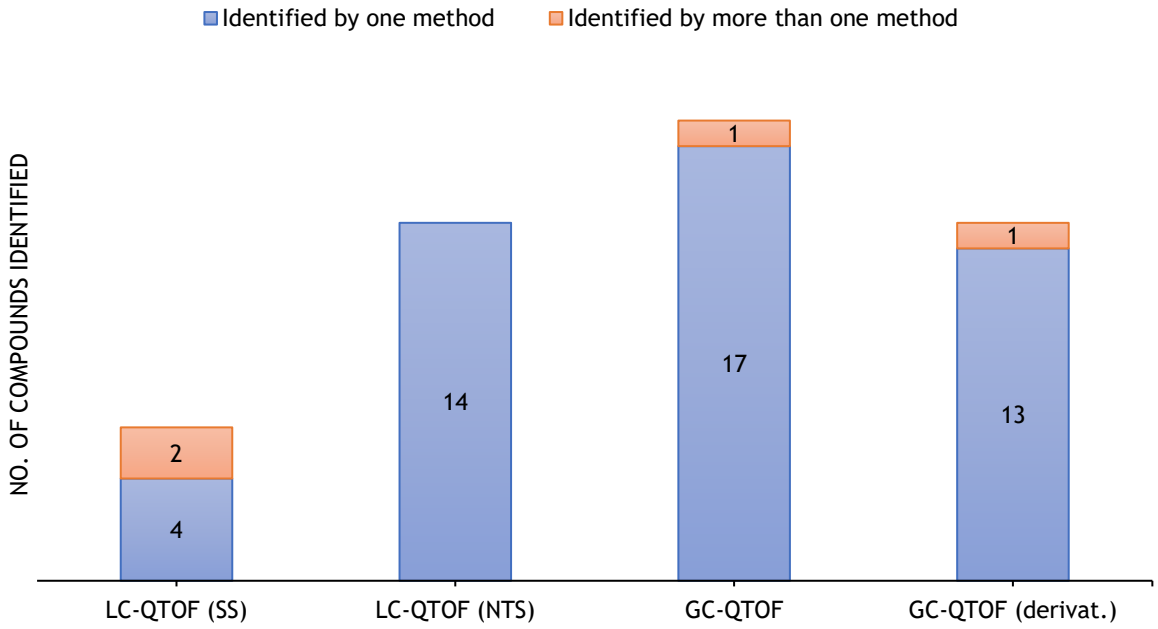

Figure 4.1.6. Number of chemicals tentatively identified by LC-QTOF by the suspect and non-target screening, respectively and by GC-QTOF without derivatization and after derivatization (marked as derivatized). The blue part of the bars represents those compounds that were only identified by a particular approach, while the orange one represents compounds detected by more than one screening approach.

In regard to the properties of the compounds detected, the GC methods permitted the determination of chemicals with a median log *D* at pH 7 (predicted with JChem® for Office®) of 4.0, whereas the LC protocols were able to detect chemicals with a median log *D* at pH 7 of 0. Besides, LC-HRMS allowed the detection of high molecular weight substances such as pheophytin A. Overall, the combination of different HRMS screening approaches increases the coverage of MP-associated compounds that can be detected in marine settings.

4.1.4. General overview of the identified chemicals associated to exposed MPs.

Our experimental results signalled that four compounds are leached out of MP over time: (i) melamine (which was only detected in the original MPs, likely because it is an additive acting

as flame retardant), (ii and iiii) 1-hexadecanol and 1-octadecanol, both used as emulsifiers in plastic manufacture, and (iv) EHS, a UV filter. The last three chemicals did not completely leach out over time, likely because they are also occurring in marine waters and a solid (MP)-liquid equilibria is established during the 8-week exposure time.

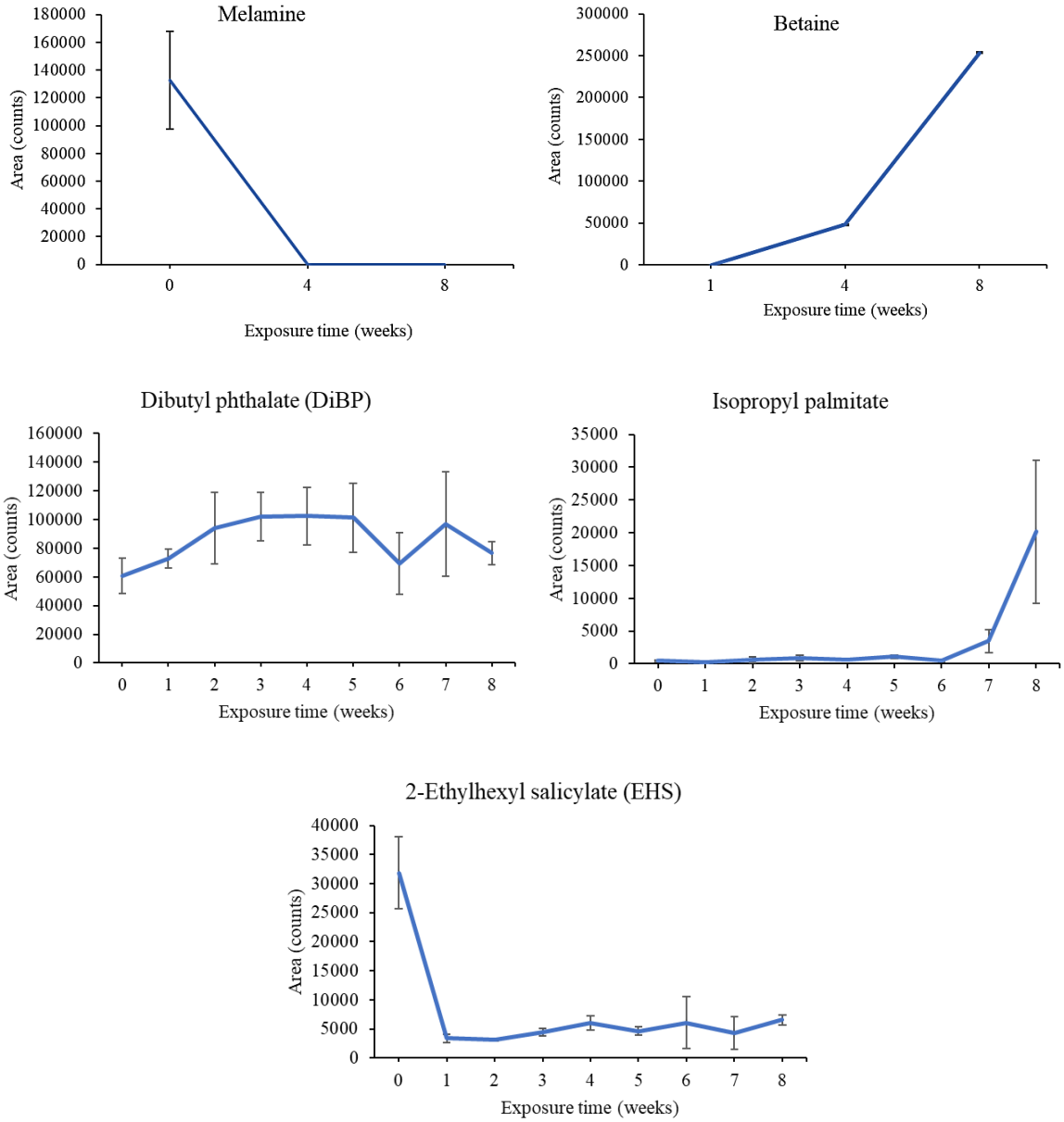

Figure 4.1.7. Example of evolution trends for 5 different compounds detected by LC-QTOF (melamine and betaine) and GC-QTOF (EHS, DiBP and isopropyl palmitate).

Besides, we have identified 26 chemicals that increasingly accumulate onto the MPs over time, while other 20 do not show clear temporal trends. Some examples are presented in Figure 4.1.7, and the overall leaching/sorption trends are summarized in Tables 4.1.1-4.1.2.

The compound classes that tend to accumulate over time are quite diverse and include both anthropogenic chemicals (e.g. galaxolide, BPA or tri-iso-butyl phosphate), which can be linked to treated wastewater or harbour activity, and natural substances (e.g. betaine). In regard to those chemicals with minute variation over time, several phthalates are worth mentioning. Phthalates are likely present in the original primary MPs in low amounts and do not desorb rapidly enough in the 8-week period and/or they achieve a rapid equilibrium with the natural seawater concentrations. This is an important finding and signals the persistence of this type of contaminants associated to plastic polymers. Since MPs are subject to long-range transport, marine organisms can be exposed to plastic additives/monomers throughout marine ecosystems and accumulated compounds (Rios-Fuster et al., 2022).

4.1.5. Quantitative assessment of selected contaminants associated to LDPE MPs

After compound screening, the quantitative performance of the MPs extraction method followed by GC-QTOF analysis was evaluated for those chemicals for which pure standards were available and provided a RR >50% in spiked samples. As shown in Table 4.1.3, the method provided recoveries >70% for ten compounds and >50% for two more. The LODs and LOQs were estimated to be in 0.1-23 µg/kg and 0.2-77 µg/kg ranges, respectively, and linear calibration graphs were obtained. The concentrations of the twelve chemicals were calculated throughout time after correction for RR if lower than 80% or higher than 120%. Indeed, these values can be regarded as semiquantitative, because method performance was not fully validated in a wide range of concentrations but provide an estimation of the environmental relevance of several organic chemicals associated to MPs. The complete results set is presented in Table 4.1.4. As it can be observed, initially EHS is by far the most abundant chemical (>1,000 µg/kg, i.e. >80%) of those quantified (total concentration of 1,311 µg/kg at time 0), but it is rapidly desorbed in the first 1-2 weeks down to a concentration of 108-115 µg/kg (26% from a total concentration of 437 µg/kg at 1 week). From that point, EHS concentration fluctuates in the 100-200 µg/kg likely because a dynamic equilibrium with the surrounding environment is reached (this explains the reason for which no monotonic trend was detected by the rank-correlation analysis).

Table 4.1.3. Analytical performance for the quantitative assessment of selected MP-associated chemicals.

Compounds	LOD (µg/kg) [a]	LOQ (µg/kg) [a]	Relative Recovery (%) [b]	RSD (%) [b]	Linearity (R^2) [c]
Di-iso-butyl phthalate (DiBP)	2.0	6.8	102	13	0.9999
Butylated Hydroxytoluene (BHT)	2.0	6.8	57	13	0.9999
Di-n-butyl phthalate (DBP)	3.4	11.2	112	14	0.9999
Diethyl phthalate (DEP)	6.3	20.8	80	14	0.9999
Bis(2-ethylhexyl) phthalate (DEHP)	10.3	34.5	149	12	0.9999
Dimethyl phthalate (DMP)	20.0	66.7	77	13	0.9999
Benzophenone	23.1	76.9	91	7	0.9999
Galaxolide	3.8	12.7	100	18	0.9999
Phenanthrene	9.4	31.3	114	7	0.9999
Triisobutyl phosphate (TiBP)	0.1	0.3	53	22	0.9999
2-Ethylhexyl salicyate (EHS, as TMS derivative)	0.1	0.2	114	15	0.9999
Bisphenol A (as 2×TMS derivative)	0.1	0.2	115	1	0.9999

[a]Defined for a S/N of 3 and 10 (LOD and LOQ, respectively) or 3 or 10 times the standard deviation of the blank signal (LOQ and LOQ, respectively), if the analyte was identified in the blank. [b]Performed with LDPE MPs spiked with 1000 µg/kg of each analyte (n=5) and [c]Calibration over the 20-2000 ng/mL level (10 different concentration levels)

Table 4.1.4. Average concentrations (µg/kg) of the identified compounds at different exposure times (n=3, RSD was typically <20%).

Compound	Exposure time (weeks)								
	0	1	2	3	4	5	6	7	8
Di-iso-butyl phthalate (DiBP)	53	63	85	91	86	78	61	80	66
Butylated Hydroxytoluene (BHT)	5.6	10	18	41	44	59	32	60	38
Dibutyl phthalate (DBP)	44	54	73	80	81	80	51	76	58
Diethyl phthalate (DEP)	28	15	31	22	24	44	18	45	43
Bis(2-ethylhexyl) phthalate (DEHP)	71	142	184	190	172	135	254	377	162
Dimethyl phthalate (DMP)	2.4	0.9	2.5	2.6	1.7	6.2	0.2	4.6	3.1
Benzophenone	8.8	7.5	13	15	16	33	7.2	30	21
Galaxolide	1.8	4.5	4.8	6.3	6.4	7.4	4.8	7.1	8.7
Phenanthrene	2.4	2.5	5.0	6.4	8.5	10.7	7.7	9.2	8.2
Triisobutyl phosphate (TiBP)	4.3	15	25	40	32	18	12	18	12
2-Ethylhexyl salicylate (as TMS derivative)	1086	115	108	152	207	159	207	144	223
Bisphenol A (as 2×TMS derivative)	5.1	6.0	65	37	18	7.1	7.7	43	160
TOTAL	1311	437	618	687	700	641	668	901	810

Of the remaining 11 compounds, five presented a statistically monotonic upward trend, viz. benzophenone, galaxolide, BPA and BHT, whose cumulative concentrations increased 1-fold in the 8-week period, from 24 to 236 µg/kg. Among them, BPA is the most concentrated substance on MPs (160 µg/kg at 8 weeks). Finally, 5 phthalates and 1 alkyl triphosphate (tris-iso-butyl phosphate) showed no monotonic trend.

In brief, we have detected a sharp monotonic decrease of the total concentration of MPs-laden compounds within the first exposure week due to the desorption of EHS, followed by an increasing trend afterwards that resulted in the change of cumulative concentrations from the initial 1,311 to the final 810 µg/kg. All together, these results show no clear association of chemical hydrophobicity with the observed monotonic trend, as e.g. the relatively polar DMP and DEP (log *D* at pH 7 = 2.0 and 2.7, respectively) would be expected to be desorbed over time. This might be explained by the initial low concentration of these polar substances in primary MPs before being exposed to the seawater, which is compensated by dissolved concentrations in the surrounding environment. Likely, if the MPs would contain higher initial amounts of these relatively polar substances, we would have observed a behaviour similar to EHS, i.e. a fast desorption followed by an equilibrium plateau at lower concentration levels.

Obviously, these concentrations represent only 12 of the 50 identified chemicals, of which about 50% are anthropogenic substances. According to results from this study, the total concentration of anthropogenic pollutants sorbed to LDPE pellets after an 8-week exposition might likely be in the 2,000 µg/kg range. These pollutants can then enter into aquatic organisms, where the impact of such chemicals may be largely linked to their oral bioaccesibility and bioavailability, a topic that still requires further research (Martín et al., 2022).

4.1.6. Limitations of this study

Although the present study aimed to an expanded coverage of chemicals by combining different analytical methodologies, it is still possible that some compounds remain undetected for several reasons, as e.g.: may not have been desorbed with the solvents employed, may be loss due to evaporation if they are very volatile or can still not be suitable for GC and/or reversed-phase chromatography. Furthermore, only a portion of the thousands of features could be identified with enough reliability and smaller fraction quantified. Yet, it is worth mentioning that the GC-HRMS and LC-HRMS raw data will be openly available (see Data Availability section), so that it could be reused, and more compounds could be eventually identified in the future. Besides, this study represents only virgin LDPE MPs on a particular coastal setting and a more diverse situation can be expected from different marine environments and MPs.

4.2. COMBINATION OF A NOVEL COST-EFFECTIVE GLASS DENSITY SEPARATOR FOLLOWED BY QUANTITATIVE ^{1}H-NUCLEAR MAGNETIC RESONANCE SPECTROSCOPY FOR THE DETERMINATION OF MICROPLASTICS IN MARINE SEDIMENTS

4.2.1. ^{1}H-NMR method optimization

Initially, different types of MPs (PET, PVC and LDPE) were exposed to different solvents and conditions to test their chemical resistance (see Table 4.2.1). None of the solvents was able to completely dissolve all MP polymer types. Therefore, a different solvent was used for each polymer. After evaluating factors such as toxicity, dissolution time and cost, TFA-d was chosen as the best option for dissolving PET. THF-d_8 was used for PVC, accompanied by sonication at RT. Finally, LDPE was dissolved in Tol-d_8 by heating at 80ºC for 1h with magnetic stirring.

Table 4.2.1. Chemical resistance chart for MP particles using different conditions for 1h.

Solvent	Processing	Temperature (ºC)	PET	PVC	LDPE
Acetone	Magnetic stirring	RT	A	A	A
Bencene	Ultrasounds	RT	A	A	A
Carbon disulfide	Ultrasounds	RT	A	A	A
Carbon tetrachloride	Ultrasounds	RT	A	A	A
Chlorobencene	Ultrasounds/Magnetic stirring	RT/80ºC	A	A	A/B
Chloroform	Magnetic stirring/Ultrasounds	RT	A	A	A
Chloroform:Formic acid (8:2)	Magnetic stirring	RT	A	A	A
Cyclohexanone	Ultrasounds	RT	A	D	A
DCM	Magnetic stirring/Ultrasounds	RT	A	A	B
DCM:Formic acid (8:2)	Magnetic stirring	RT	A	A	A
Diethyl ether	Magnetic stirring/Ultrasounds	RT	A	A	A
Diethylamine	Ultrasounds	RT	A	A	A
DMSO	Magnetic stirring	RT/80ºC	A	A	A/B
Hexane	Magnetic stirring	RT	A	A	A
Isoctane	Magnetic stirring	80^0C	A	A	B
MeOH	Magnetic stirring	RT	A	A	A
Pyridine	Ultrasounds	RT	A	D	A
2-propanol	Magnetic stirring/Ultrasounds	RT	A	A	A
THF	Magnetic stirring/Ultrasounds	RT	A	D	A
Tol	Ultrasounds/Magnetic stirring	RT/80ºC	A	A	A/D
Trichlorobencene	Ultrasounds/Magnetic stirring	RT/80ºC	D	A	A/B
Trichloroethylene	Ultrasounds	RT	A	A	A
TFA	Ultrasounds	RT	D	A	B
o-Xylene	Ultrasounds/Magnetic stirring	RT/80ºC	A	A	A/D
p-Xylene	Ultrasounds/Magnetic stirring	RT/80ºC	A	A	A/D

A = No appreciable dissolution; B = Partial dissolution, presence of particulate matter and D = Material dissolved

Once the solvents were selected, individual solutions of the polymers were prepared at a concentration of 10 mg/mL in TFA-d, THF-d_8 and Tol-d_8, respectively. These solutions were analysed by ^{1}H-NMR to identify the optimal signal for quantifying the MPs material and the appropriate solvent signal for use as IS, based on their respective spectra.

The ^{1}H-NMR spectrum of PET dissolved in TFA-d has two signals from the polymer, with chemical shifts (δ) of 8.43-8.17 ppm (the aromatic protons H^{a}),and 5.11-4.91 ppm (the ethylene protons H^{b}) (Figure 4.2.1). Each of the two signals corresponds to four equivalent protons in the repeating unit of the polymer, so their integrals should be equal. The aromatic signal was selected for quantification, due to better repeatability of the signal in terms of RSD being lower than 1.5% for 6.53 mg/mL (n=5). The residual signal of the solvent (TFA-d) was observed as a singlet between 12.75-10.52 ppm. This signal exhibited a high variability of intensity between samples (>100% of RSD), most likely due to the easy H/D exchange of the deuterium of the carboxylic acid upon exposure to environmental moisture. Several compounds were evaluated as IS: natural chloroform and dioxane. Chloroform generated multiple peaks and blurred peaks in the presence of TFA-d solution, very likely due to chemical reaction. Finally, dioxane, with signal at 4.27 ppm (-CH_2 group), was selected as IS because of its good repeatability (<2.5%) in five samples.

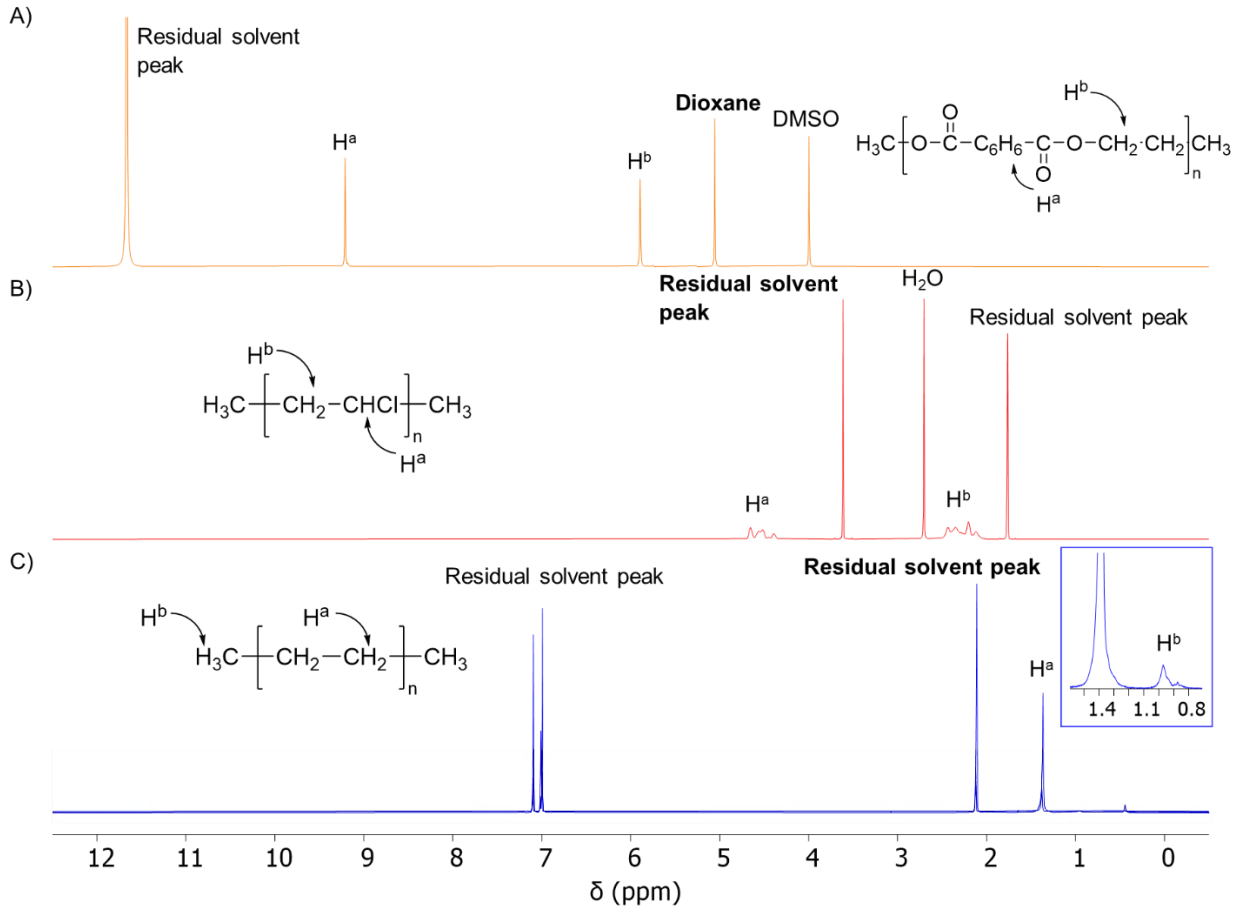

Figure 4.2.1. ^{1}H-NMR spectrum: A) 10 mg/mL PET in TFA-d with dioxane/DMSO (1/24), B) 10 mg/mL PVC in THF-d_8 and C) 1 mg/mL LDPE in Tol-d_8. The signals in bold correspond to IS used for each MP.

For the acquisition of ^{1}H-NMR spectra, the tip angle of the excitation pulse and the repolarisation time (inter scan recovery time) were optimised because the integrals of the two PET signals were different when the instrument default parameters were used. It is noted that both signals should have equal integrals, as each of them corresponds to four hydrogens in the polymer repeating unit. More precisely, the difference between the two PET signals was larger than 5% when using a 90-degree tip angle and a repolarisation time of 1.5 s. The difference in the integrals is due to incomplete relaxation of the slow-relaxing spins, that are the aromatic

ones in this molecule. Increasing the repolarisation time to 5 s decreased the integral difference to 0.4%, but the time per analysis was much longer. Therefore, the tip angle was reduced to 30º (set up with the pulse program zg30 from the Bruker standard library) and several repolarisation times were tested: 1.5, 3.0, 5.0 and 8.0 s. The differences between the integrals were small in all cases, ranging between 0.4% and 1.3%. Consequently, it was decided to perform the analyses with the shortest one, 1.5 s (Table 4.2.2), to save experimental time.

Table 4.2.2. Optimization of NMR acquisition parameters. Sample: 5 mg of PET dissolved in TFA-d. 25ºC, 750 MHz.

Tip angle [a]	Repolarisation time (s) [b]	Difference between two PET signal (%) [c]
zg	1.5	5.4
zg	5.0	0.4
zg30	1.5	1.3
zg30	3.0	0.4
zg30	5.0	1.0
zg30	8.0	1.2

[a]Tip angle of the proton excitation pulse; [b]Inter scan delay and [c]Difference of the integrals of the two signals of PET. Note that, ideally, the two signals should have equal intensities as each of them corresponds to 4 hydrogens in the polymer repeating unit

The spectrum of dissolved PVC showed two distinct signals that can be clearly assigned. Both signals span over a relative broad range of ~0.5 ppm and have several maxima The signal with a chemical shift of 4.71-4.30 ppm (H^a) corresponds to the H-(CCl) atoms, while the signal in the range of 2.50-2.04 ppm (H^b) corresponds to the CH_2 atoms (Figure 4.2.1 B). On the other hand, the solvent gives two signals at 3.69-3.53 ppm and at 1.83-1.70 ppm (α-O and β-O hydrogen atoms, respectively), with the former being selected as IS. Furthermore, there is a peak of dissolved water at 2.70-2.39 ppm, most likely due to absorption of moisture during sample manipulation. Quantification using the PVC signal H^b is difficult due to proximity to the water signal, which overlaps when working at RT (see Fig. 4.2.1). Therefore, the quantification was performed at 0ºC (Fulmer et al., 2010). Finally, the PVC signal H^a was employed for quantification as it is not affected by overlap with other signals of spectrum.

Finally, the ^{1}H-NMR spectrum of LDPE showed two clear signals from the polymer: 1.15-0.77 ppm (H^b) corresponding to the terminal CH_3 groups, and the signal at 1.58-1.16 ppm (H^a) corresponding to the CH_2 groups. H^a was used for quantification due to its higher intensity compared to the H^b signal. The deuterated solvent (Tol-d_8) gives four residual signals: one at 2.18-2.05 from the methyl group, and three at 7.17, 7.03 and 6.92 ppm from the three non-equivalent positions of the phenyl ring. The methyl signal of the solvent was used as IS.

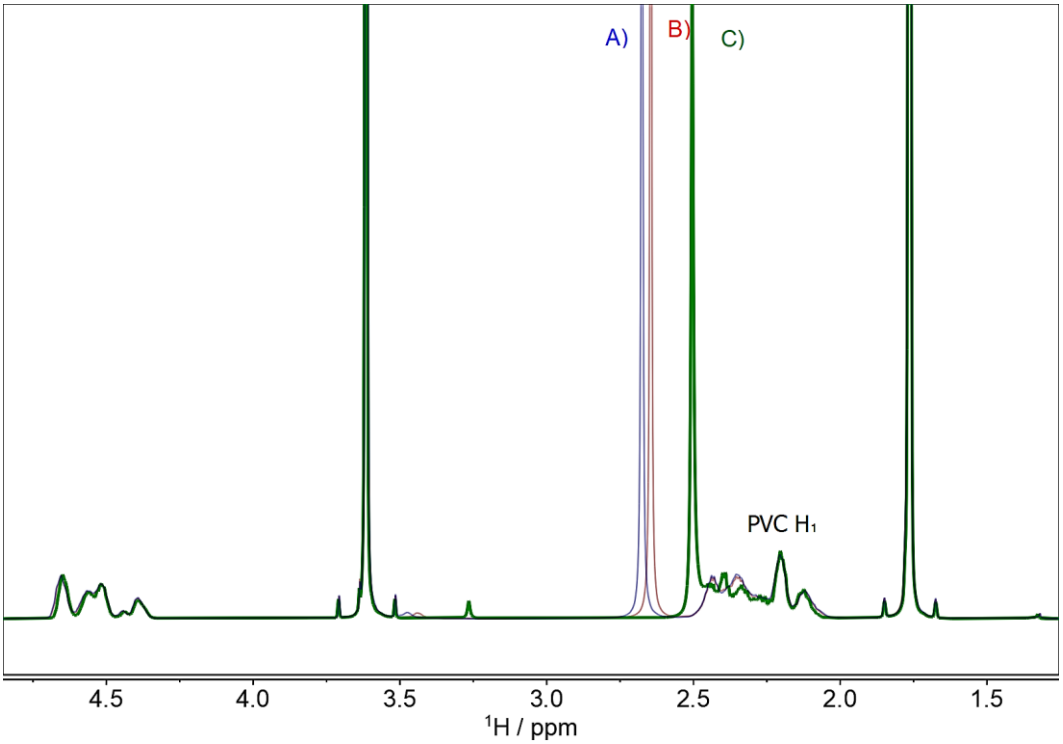

Figure 4.2.2. Overlay of the NMR spectra of PVC obtained at different temperatures: A) 0°C; B) 5°C and C) 25°C. THF-d_8, 750 MHz.

4.2.2. ^{1}H-NMR method validation

In order to verify the suitability of ^{1}H-NMR spectroscopy for the quantitative analysis of MP particles, several key parameters were assessed, including repeatability, linearity and iLOQs, as outlined in section 3.2.6. The results are summarized in Table 4.2.3. Repeatability was evaluated by quintuplicated analysis at concentration levels of 8.33 mg/mL for PVC, 7.93 mg/mL for PET and 1.67 mg/mL for LDPE, obtaining RSD values below 5%. Linearity was evaluated using a 7-point calibration curve, prepared in each deuterated solvent, ranging from iLOQ to 36.70, 38.46 and 1.05 mg/mL for PET, PVC and LDPE particles, respectively. The results were satisfactory, with coefficients of determination above 0.996. In addition, the iLOQs provided for PET, PVC and LDPE in solution were 0.001, 0.008 and 0.003 mg/mL. These values are lower than those reported using NMR, by Peez et al. (2019) for PET (0.081 mg/mL) and LDPE (0.074 mg/mL). Consequently, the LOQs for PET, PVC and LDPE in terms of mass were determined as 0.63, 4.8 and 4.5 µg, respectively. These LOQs are similar to those obtained by pyrolysis-GC-MS, which report LOQ ranges of 0.5-27.8 µg for PE, 0.5-5.3 µg for PVC, and 0.5-5 µg for PET (Gomiero et al., 2019; Gomiero et al., 2021; Peters et al., 2018; Santos et al., 2023).

Table 4.2.3. NMR method validation.

Microplastic	Repeatability (%RSD) [a]	Lineal range (mg/mL) (correlation coefficient)	iLOQs (mg/mL)
PET	1.4	iLOQ - 36.70 (0.9997)	0.001
PVC	1.3	iLOQ - 38.46 (0.9999)	0.008
LDPE	4.7	iLOQ - 1.05 (0.9963)	0.003

[a]Repeatability evaluated by quintuplicated at 8.33 mg/mL for PVC, 7.93 mg/mL for PET and 0.75 mg/mL for LDPE

4.2.3. Selection of floatation media

Sodium chloride is one of the most commonly used salt for density separation due to its availability, low cost, and eco-friendliness which led to its recommendation by both the MSFD technical subgroup (Hanke et al., 2013) and NOAA (Masura et al., 2015). Unfortunately, it cannot achieve good recoveries for heavier density polymers, such as PVC and PET (Quinn et al., 2017). Thus, zinc chloride presents a more appropriate option to allowing for the attainment of densities up to 1.6 g/cm^3. This enables effective separation of high-density MPs however its high toxicity poses a significant environmental challenge. In this study, $ZnCl_2$ was identified as the optimal salt solution for microplastics floatation using the density separator (Krasowska et al., 2022; Tang & Luo, 2023). Different $ZnCl_2$ concentrations (70% and 90%) were tested in order to determine the minimum amount of this salt achieving acceptable recoveries for high-density microplastics following SANTE guide (EC, 2021). Recoveries for PVC and LDPE were assessed at densities of 1.50 g/cm^3 (70% (w/v)) and 1.60 g/cm^3 (90 % (w/v)) as the Figure 4.2.3.

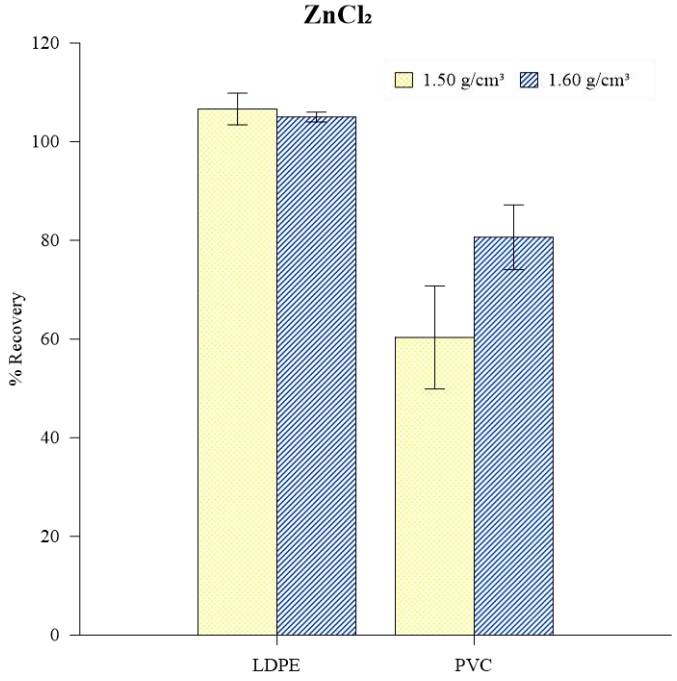

Figure 4.2.3. Comparison of recoveries obtained for PVC and LDPE using $ZnCl_2$ with different densities.

The optimal density of 1.60 g/cm^3 enabled floatation of denser plastics, including PVC. Nevertheless, $ZnCl_2$ solutions were recycled after every extraction, in order to minimize the expense of this relatively hazardous salt.

4.2.4. Validation of the method

The whole method was evaluated at two levels for PET and PVC (20 µg/g and 200 µg/g) and at one level for LDPE (10 µg/g), due to its low solubility at 80ºC in low volume (1.5 mL) of Tol-d_8 (Wong et al., 2015), as detailed in section 3.2.6. The results are summarized in Table 4.2.4. Accuracy and precision were satisfactory with recovery values between 71% and 107% and RSD values below 20%. LOQs for PET, PVC and LDPE were estimated as 15 ng/g, 245 ng/g and 90 ng/g, respectively. Although the values of the extrapolated LOQs are far below the investigated levels, it is very difficult to accurately prepare spiked samples at lower levels. This issue has also been encountered in most literature (Imhof et al., 2012; Mahat, 2017).

Table 4.2.4. Validation figures of the separation method combined with ^{1}H-NMR determination on spiked samples prepared in the laboratory.

MPs	Accuracy (%RSD)		LOQs (ng/g)
	Low level [a]	High level [b]	
PET	71% (9)	77% (12)	15
PVC	84% (9)	80% (20)	245
LDPE	107% (19)	-	90

[a]PET: 20 µg/g; PVC: 20 µg/g and LDPE: 10 µg/g. [b]PET: 200 µg/g and PVC: 200 µg/g

The recoveries obtained in our work are similar or better than those reported in the literature using several separation techniques (Table 4.2.5). MPSS, using a decanting method on a sediment sample with 12 L of $ZnCl_2$ (1.6-1.7 g/cm^3), was employed to extract PET, PVC and LDPE particles, achieving recovery rates (number) of 100% with 1-5 mm of particle size (Imhof et al., 2012). BMSS reported a recovery rate of 85% for PET MPs and quantitative recoveries for lighter PE MPs (Mahat, 2017), but several extractions were necessary to achieve these recoveries and prolonged flotation times. Similarly, the use of air bubbles in the microplastics-separator design approach (µSEP) resulted in recoveries greater than 99% for light MPs such as POM in 20 min, but for heavier MPs, such as PVC, the recoveries were lower than 30%, even with an extended extraction time of 6 hours (Renner et al., 2020). The results from the SMI for LDPE, nylon, and PVC showed values exceeding 96%, yet they do not offer exact information on the spiked MPs concentration or size, merely indicating that they are below 1 mm (Coppock et al., 2017). In contrast, the JAMSTEC microplastic-sediment separator (JAMSS) yielded recoveries higher than 92% in a single step using 40 MPs particles of different densities and particle size in 30 g of sediment, but its volume capacity was limited (Nakajima et al., 2019). Our device facilitates working with reduced sediment samples (100 g) and salt solution volume (1.5 L), producing good recoveries between 71 and 107% for a wide range of

MPs densities (PET, PVC and LDPE). Moreover, it is completely made of glass to avoid contamination by degradation of the plastic material and is cost-effective.

Table 4.2.5. Comparison of the published methodologies for extraction MPs from sediment samples.

Extractor	Sample weight	Saline solution	Extraction time	MPs test		Recovery ratios	Reference
MPSS	400 g	12 L of $ZnCl_2$ (1.6-1.7 g/cm^3)	≈2-14 h	100 mg (1-5 mm)	PET PVC LDPE	≈100 %	(Imhof et al., 2012)
BMSS	500 g	600 mL $ZnCl_2$:$CaCl_2$ (1.6 g/cm^3)	≈24 h and 12 h	100 mg (>75 µm)	PET LDPE	85 % ≈100 %	(Mahat, 2017)
µSEP	200 g	-	20-30 min	5 mg	PVC POM	<30 % 99%	(Renner, 2020)
SMI	30-50 g	700 mL of $ZnCl_2$ (1.5 g/cm^3)	≈20 min	50 MPs (<1 mm)	PVC LDPE	96 % 98 %	(Coppock, 2017)
JAMSS	30 g	100 mL NaI (1.6 g/cm^3)	≈25 min	40 MPs (<2 mm)	PET PVC	>92 %	(Nakajima, 2019)
	100 g	1.5 L of $ZnCl_2$ (1.6 g/cm^3)	≈1 h	1-2 mg (≤ 300 µm)	PET PVC LDPE	71% 80% 107%	This work

4.2.5. Application to environmental samples

Once validated, the method was applied to a limited set of beach sediment samples. All sediment samples were extracted according to the given protocol using the density separator setup and analysed by ^{1}H-NMR. The mass concentrations of MP particles are summarised in Table 4.2.6. PET concentrations ranged from 62 to 186 ng/g, LDPE from 91 to 114 ng/g, whereas PVC was below LOQ in all marine samples. RSD values remained below 22%.

Table 4.2.6. Concentration of MPs in sediment samples (n=3) determined by ^{1}H-NMR.

Microplastic	M1	M2	M3
PET	180 ± 10 ng/g	186 ± 43 ng/g	62 ± 16 ng/g
PVC	<LOQ	<LOQ	<LOQ
LDPE	100 ± 20 ng/g	91 ± 10 ng/g	114 ± 23 ng/g

Comparing the outcomes of this study to other studies on beach sand poses challenges given that the majority of the articles reported number-based concentrations (items/kg), as summarised in Table 4.2.7. Most of the studies have extracted the MPs by flotation with NaCl (1.2 g/cm^3) and quantified them by microscopy and FT-IR or Raman spectroscopy. The reported concentrations of MPs were found to be between 2-35 items/kg of PET, 13-22 items/kg of PVC and 20-40 items/kg of LDPE (Godoy et al., 2020; Hayes et al., 2021; Khuyen et al., 2021; Yaranal et al., 2021; Yu et al., 2016). On the other hand, our results of PE and PET present similar levels to those reported in coastal sediment sand from the southern coast of Norway, using density-based separation step with zinc chloride and pyr-GC-MS, reporting concentrations of 32-139 ng/g of PE, 12-136 ng/g of PET and 9-120 ng/g of PVC (Gomiero et al., 2019).

Table 4.2.7. Concentrations of microplastics in different sediment samples.

Location	Extraction	Determination	MPs	Concentrations measured	Reference
Bohai Sea, China	Density separation with NaCl (1.3 g/mL)	Optical microscopy and FT-IR	PET	>5 items/kg	(Yu et al., 2016)
			LDPE	≈40 items /kg	
Karnataka, India	Density separation with NaCl (1.2 g/mL)	Optical fluorescence microscopy and Raman spectroscopy	PET	≈13 items /kg	(Yaranal, 2021)
			PVC	≈13 items /kg	
Vietnam	Density separation with NaCl (1.2 g/mL)	Raman spectroscopy	PET	10-35 items /kg	(Khuyen, 2021)
			PVC	>22 items /kg	
Adelaide, South Australia	Density separation with NaCl (1.2 g/mL)	Optical microscopy and FT-IR	LDPE	<20 items /kg	(Hayes, 2021)
Granada, Spain	Density separation with NaCl (1.2 g/mL)	Optical microscopy and FT-IR	PET	2 items /kg	(Godoy, 2020)
Southern coast, Norway	Density separation with $ZnCl_2$ (1.8 g/cm^3)	Pyr-GC-MS	PE	32 - 139 ng/g	(Gomiero, 2019)
			PET	12 - 136 ng/g	
			PVC	9 - 120 ng/g	

4.3. MIMICKING HUMAN INGESTION OF MICROPLASTICS: ORAL BIOACCESSIBILITY TESTS OF BISPHENOL A AND PHTHALATE ESTERS UNDER FED AND FASTED STATES

The results of this chapter have been published in:

Javier López-Vázquez, Rosario Rodil, María J. Trujillo-Rodríguez, José Benito Quintana, Rafael Cela, Manuel Miró

Science of The Total Environment 2022, 826, 154027-154036

DOI: 10.1016/j.scitotenv.2022.154027

This work was performed in collaboration with Manuel Miró and María J. Trujillo Rodríguez from the Universitat de les Illes Balears.

Science of the Total Environment 826 (2022) 154027

Contents lists available at ScienceDirect

Science of the Total Environment

journal homepage: www.elsevier.com/locate/scitotenv

Mimicking human ingestion of microplastics: Oral bioaccessibility tests of bisphenol A and phthalate esters under fed and fasted states

Javier López-Vázquez [a], Rosario Rodil [a,*], María J. Trujillo-Rodríguez [b], José Benito Quintana [a], Rafael Cela [a], Manuel Miró [b,*]

[a] Department of Analytical Chemistry, Institute of Research on Chemical and Biological Analysis (IAQBUS), Universidade de Santiago de Compostela, E-15782 Santiago de Compostela, Galicia, Spain

[b] FI-TRACE Group, Department of Chemistry, Faculty of Science, University of the Balearic Islands, Carretera de Valldemossa km 7.5, E-07122 Palma de Mallorca, Illes Balears, Spain

4.3.1. Evaluation of the analytical performances of the chromatographic and extraction methods

The liquid and gas chromatographic methods using internal calibration as indicated in Tables 3.3.3, 3.3.4 and 3.3.5 were evaluated in terms of linearity, precision and LOQs for the target compounds.

For GC-MS, the dynamic linear range of all compounds spanned between 1 µg/L and 10 mg/L, except BPA up to 5 mg/L, BzBP and DnOP from 5 µg/L and DiNP and DiDP from 0.5 to 40 mg/L, obtaining determination coefficients in all instances higher than 0.9990. Repeatability, expressed as RSD of 5 replicates at a concentration of 50 µg/L (1 mg/L for DiNP and DiDP), ranged between 5 and 19%, and LOQs, calculated for a S/N ratio of 10, ranged from 0.01 to 1.35 µg/L, except for DiNP and DiDP with LOQs of 500 and 300 µg/L, respectively (Table 3.3.3).

For UHPLC-MS/MS, the dynamic linear range spanned between 1 µg/L and 5 mg/L, except for long-chain PAEs (DiNP and DiDP) up to 10 mg/L, BPA from 0.5-10 mg/L and DnOP from 0.1-10 mg/L, obtaining determination coefficients in all instances higher than 0.9990. Repeatability at 100 µg/L (1 mg/L for BPA) with 5 replicates, was below 19%. LOQs, calculated for a S/N ratio of 10, ranged from 0.10 and 0.70 µg/L, except for DnOP (67 µg/L) and BPA (500 µg/L) (Table 3.3.5).

Based on the above results, GC-MS was used for the determination of BPA and the non-BF of PAEs except for DiNP and DiDP, and UHPLC-MS/MS for the determination of the BF of PAEs and the non-BF of DiNP and DiDP.

For the extraction of the residual PAEs and BPA from MPs to estimate the non-BF, various solvents (AcOEt and DCM) were tested by USE. The results of the analysis of the CRM MPs, expressed as absolute recoveries, are summarized in Table 4.3.1. The extraction recoveries with DCM were improved for BzBP, DnOP and DiDP. Therefore, DCM was selected for the further extraction of non-BF with recoveries from total certified concentrations on LDPE and PVC ranging from 57 to 90% and 77 to 117%, respectively. Repeatability, expressed as RSD, was below 20%. LOQ values, calculated for a S/N ratio of 10, ranged from 0.05 to 7.45 µg/g (see Table 4.3.1).

Matrix effects for the determination of oral bioaccessible PAEs by UHPLC-MS/MS were evaluated by comparing the analytical responses of spiked GIT fluids against those of standards prepared in UPW/MeOH (80/20, v/v) at a concentration level of 400 µg/L. The experimental results revealed that the responses of the long-chain phthalates (DEHP, DnOP, DiNP and DiDP) were those most affected and ranged from 61 to 87% for the gastric fraction, and 73 to 93% for the gastrointestinal fraction as compared to the responses of the standards. Signal suppression was below 40% for all the compounds but compensated with the isotopologues as indicated in Tables 3.3.3 and 3.3.4.

The LLE method for the extraction of BPA from both gastric and gastrointestinal extracts to estimate the BF was performed with different solvents (AcOEt and DCM). To this end, an aliquot of 100 µL of body fluids spiked with BPA (700 µg/L) was extracted with 2 mL of AcOEt or DCM. Recoveries were similar for DCM (111-113%) and AcOEt (108-120%). However, AcOEt was selected for LLE extraction because of its suitability for further analyte derivatization. Repeatability, calculated at 700 µg/L by triplicate and expressed as RSD, was

below 5%. LOQ values, calculated for a S/N ratio of 10, were 0.25 and 0.35 µg/L BPA for gastric and gastrointestinal fluids, respectively.

Table 4.3.1. USE recoveries ± standard deviation and LOQs of PAEs and BPA from CRMs.

Compounds [a]	AcOEt		DCM		LOQs (µg/g) [b]	
	LDPE	PVC	LDPE	PVC	LDPE	PVC
DMP	80 ± 2	83 ± 1	77 ± 1	86 ± 9	0.65	0.50
DEP	74 ± 2	79 ± 1	82 ± 2	97 ± 14	0.40	0.45
BPA	74 ± 2	-	79 ± 2	-	0.05	-
DnBP	110 ± 4	119 ± 1	79 ± 2	90 ± 10	0.45	0.30
BzBP	35 ± 2	37 ± 1	74 ± 4	77 ± 13	1.25	1.45
DEHP	69 ± 5	80 ± 3	63 ± 2	83 ± 16	0.10	0.10
DnOP	41 ± 3	43 ± 2	90 ± 11	117 ± 8	0.35	0.40
DiNP	93 ± 3	110 ± 5	79 ± 3	101 ± 4	2.30	1.80
DiDP	45 ± 16	54 ± 11	57 ± 2	79 ± 5	7.45	6.70

[a]All compounds were analysed by GC-MS, except DiNP and DiDP by UHPLC-MS/MS and [b] Estimated using DCM as extraction solvent

The UHPLC method for the separation and determination of phthalate monoesters has been validated previously by Estévez-Danta et al. (2021) (Table 3.3.5). Briefly, the dynamic liner range spanned from LOQ-1,000 µg/L, LOQs ranged between 0.01 µg/L and 6 µg/L and RSDs at 10 µg/L were below 19%. Matrix effects for metabolites were between 85 and 98% and 72 to 88% for gastric and gastrointestinal fractions, respectively, yet were offset using the deuterated IS as indicated in Table 3.3.5.

4.3.2. Stability of the target PAEs and BPA in GIT fluids

Preliminary tests were performed to investigate the stability of the PAEs and BPA under gastric and gastrointestinal conditions for fed and fasted oral bioaccessibility tests. For that purpose, gastric and gastrointestinal fluids were spiked by triplicate with 7.5 mg/L and 3 mg/L, respectively, of the target PAEs and BPA, to obtain a final concentration of 0.075 mg/L after dilution, and incubated at physiological conditions as described in Section 3.3.2 and determined as Section 3.3.3 Absolute recoveries after gastrointestinal incubation ranged between 82 and 113% (Figure 3.3.3a). Phthalate monoesters were also determined to elucidate their potential generation from the parent phthalate diesters in both gastric and gastrointestinal compartments. Experimental findings demonstrated that MMP, MEP and phthalic acid were the only compounds formed in the incubated samples. Assuming that MMP and MEP are only formed by the hydrolysis of DMP and DEP, respectively, and phthalic acid is equally obtained from both DMP and DEP, the molar conversion percentages are reported in Figure 3.3.3b.

Experimental results indicated that up to a 10% of hydrolysis occurs for DMP and DEP under gastrointestinal extraction with significantly higher percentages under fasted conditions than those of fed conditions (down to 0.5%). This fact could be attributed to the more acidic gastric phase in the UBM test (pH 1.2 ± 0.5) (Figure 3.3.1) since pH affects the hydrolysis rates of PAEs (Harris & Sumpter, 2001). In order to evaluate if the transformation of DMP and DEP is due to the enzymatic activity or the chemical hydrolysis, *in-vitro* digestion was performed under fasted conditions without the addition of enzymes. No statistically significant differences were observed in the extent of generation of MMP, MEP and phthalic acid. This confirms that degradation of DMP and DEP is mainly occasioned by chemical hydrolysis and triggered under fasted conditions.

4.3.3. Fed and fasted human oral bioaccessibility tests

The BFs of PAEs and BPA were calculated related to the certified concentrations provided by the CRMs. The extent of release of the compounds from MPs during human digestion was elucidated by the measurement of the leachable compounds in the respective biorelevant gut fluid (gastric and gastrointestinal phases). Note that the BF represents the maximum amount of compound amenable to be bioavailable and reach the systemic circulation. The percent of bioaccessibility of PAEs and BPA in LDPE and PVC using fed and fasted PBET conditions is presented in Table 4.3.2, and exemplarily summarized in Figure 4.3.1 for DMP and DiDP. Bioaccessibility values ranged between 2% and 83% with the highest bioaccessibility corresponding to DMP, DEP and BPA compared to the other PAEs (Table 4.3.2). Hydrolysis of PAEs during the bioaccessibility tests was also evaluated. MMP, MEP and phthalic acid were the only degradation products identified across the varied GIT fluids as discussed in the previous section, with concentrations of hydrolytic products ranging from 0.7 and 7% (w/w) of the total DMP and from 0.3 and 3% (w/w) of the total DEP (Table 4.3.2 & Figure 4.3.1). Total bioaccessibility (sum of bioaccessible and hydrolysis fractions) ranged between 1.8% for DiDP from PVC in the gastric fraction under fasted conditions to 90% for DMP from LDPE in the gastrointestinal fraction under fed conditions. These results are similar to those previously reported using a dynamic *in-vitro* PBET for PAEs and BPA (Sixto et al., 2021), to those of inhalation (lung) bioaccessibility (Kademoglou et al., 2018) and also to those of GIT bioaccessibility of PAEs in indoor dust (He et al., 2016). Regardless of the polymer type, the % bioaccessibility is inversely correlated with the hydrophobicity of the compounds (log K_{ow}), with Spearman correlation *p-values* <0.0004. The mathematical model that better fits the experimental data is %bioaccessibility = a + b/log K_{ow} (Figure 4.3.2) with correlation coefficients spanning between 0.9087 and 0.9668 for the two types of MPs and PBET methods.

The residual fraction of phthalates and BPA in MPs (non-BF) was evaluated by the analysis of the MPs after the PBET as explained in Experimental. Total non-BFs ranged from 13 to 108% (Table 4.3.2 & Figure 4.3.1).

Finally, a mass balance study was performed by considering the three fractions: BF, non-BF and hydrolysed fraction (see Figure 4.3.1 and Table 4.3.2). The percentages for LPDE under gastric extraction ranged from 78 to 112% and 82 to 117% for the fasted and fed scenarios, respectively. The percentages for LPDE under gastrointestinal extraction spanned from 84 to 118% and 84-126% for the fasted and fed conditions, respectively. As to PVC, the percentages under gastric and gastrointestinal extraction ranged from 68 to 112% and 69-94%, respectively,

for the fasted state and 62-114% and 70-102%, respectively, for the fed state. It should be noted that absolute recoveries down to 70% are encountered, in some instances, for DEP, BzBP, and DINP for all of which congener isotopologues were used.

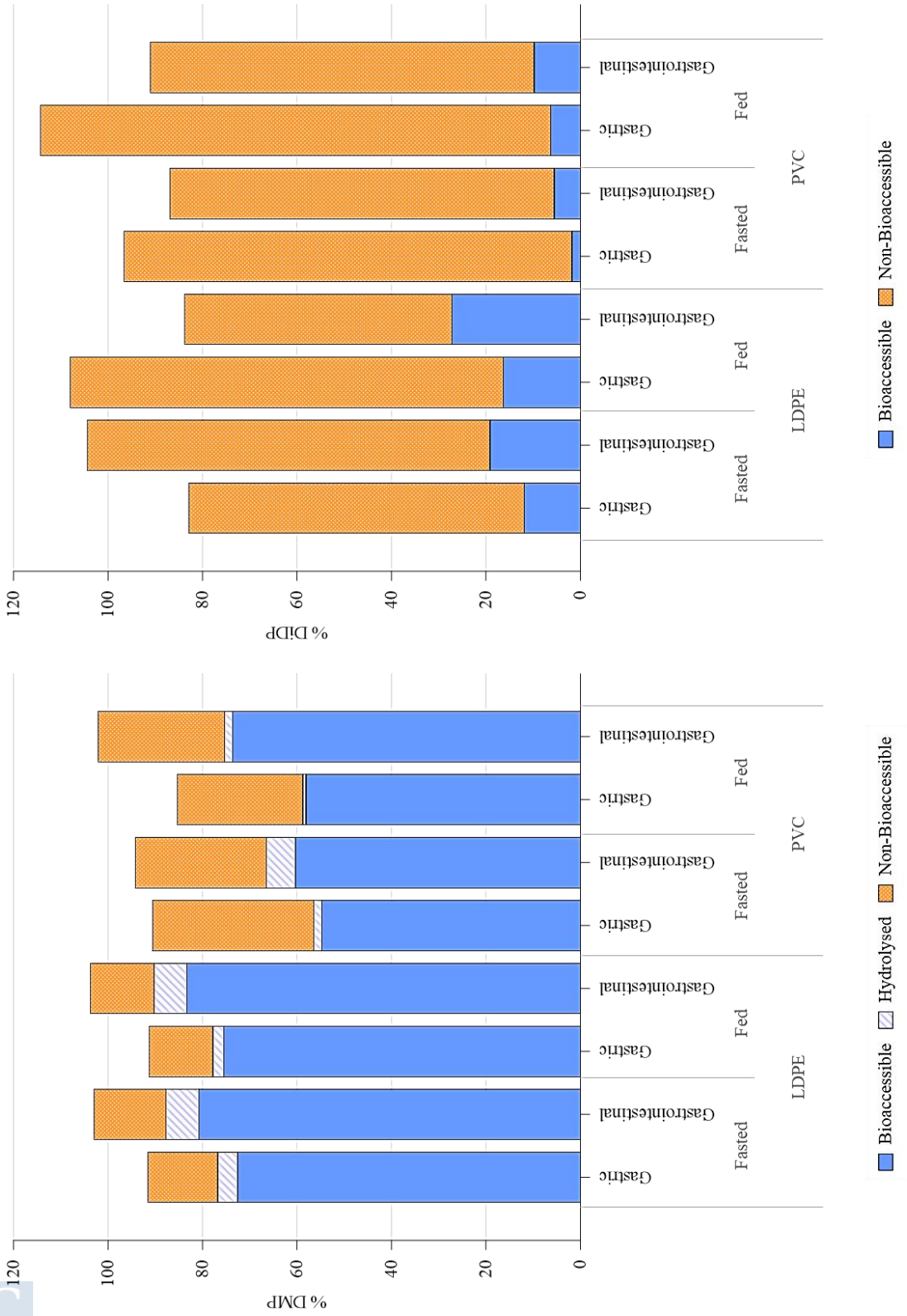

Figure 4.3.1. Stacked barplot of hydrolysed amount, BF and non-BFs for DMP (left) and DiDP (right) based on MP type, PBET model and body fluids.

Table 4.3.2. BF and non-BF (%) of PAEs and BPA in body fluids (n = 3).

Fraction	MPs type	PBET method	GIT fluid	DMP	DEP	BPA	DnBP	BzBP	DEHP	DnOP	DiNP	DiDP
Bioaccessible	LDPE	Fasted	Gastric	73 ± 3	47 ± 2	37 ± 2	14 ± 6	14 ± 3	14 ± 7	15.9 ± 0.4	11.0 ± 0.4	11.9 ± 0.2
Bioaccessible	LDPE	Fasted	Gastrointestinal	81 ± 2	56 ± 2	44 ± 6	31 ± 9	20.9 ± 0.6	18 ± 3	24 ± 2	17.2 ± 0.4	19.1 ± 0.2
Bioaccessible	LDPE	Fed	Gastric	76 ± 4	64 ± 5	53 ± 8	20.0 ± 0.4	19 ± 2	21 ± 2	18 ± 4	15 ± 3	16 ± 3
Bioaccessible	LDPE	Fed	Gastrointestinal	83 ± 1	68 ± 3	67 ± 8	32 ± 3	28 ± 1	32 ± 4	24.9 ± 0.3	22 ± 2	27 ± 3
Bioaccessible	PVC	Fasted	Gastric	55 ± 3	44 ± 3	-	12.5 ± 0.9	4.9 ± 0.5	5 ± 2	6 ± 1	1.9 ± 0.2	1.8 ± 0.2
Bioaccessible	PVC	Fasted	Gastrointestinal	60 ± 2	55 ± 3	-	14 ± 4	8.7 ± 0.8	11 ± 4	9 ± 2	5.3 ± 0.5	5.5 ± 0.3
Bioaccessible	PVC	Fed	Gastric	58.1 ± 0.3	40 ± 2	-	19 ± 2	5.1 ± 0.4	10 ± 4	10 ± 2	6 ± 2	6 ± 2
Bioaccessible	PVC	Fed	Gastrointestinal	74 ± 4	61 ± 2	-	23 ± 2	8.6 ± 0.5	11 ± 4	11 ± 1	8.0 ± 0.6	10 ± 1
Hydrolysis	LDPE	Fasted	Gastric	4.2 ± 0.6	3.0 ± 0.6	-	-	-	-	-	-	-
Hydrolysis	LDPE	Fasted	Gastrointestinal	7.2 ± 0.5	3.4 ± 0.5	-	-	-	-	-	-	-
Hydrolysis	LDPE	Fed	Gastric	2.2 ± 0.7	1.2 ± 0.3	-	-	-	-	-	-	-
Hydrolysis	LDPE	Fed	Gastrointestinal	7 ± 1	1.6 ± 0.2	-	-	-	-	-	-	-
Hydrolysis	PVC	Fasted	Gastric	1.7 ± 0.4	1.3 ± 0.3	-	-	-	-	-	-	-
Hydrolysis	PVC	Fasted	Gastrointestinal	6 ± 1	2.4 ± 0.5	-	-	-	-	-	-	-
Hydrolysis	PVC	Fed	Gastric	0.67 ± 0.08	0.29 ± 0.01	-	-	-	-	-	-	-
Hydrolysis	PVC	Fed	Gastrointestinal	1.7 ± 0.9	0.5 ± 0.1	-	-	-	-	-	-	-
Non-Bioaccessible	LDPE	Fasted	Gastric	14.8 ± 0.1	37 ± 2	52 ± 3	86 ± 3	86 ± 6	98 ± 2	65 ± 4	67 ± 3	71 ± 1
Non-Bioaccessible	LDPE	Fasted	Gastrointestinal	15.2 ± 0.8	34 ± 6	40 ± 2	88 ± 14	71 ± 25	100 ± 17	66 ± 23	88 ± 15	85 ± 9
Non-Bioaccessible	LDPE	Fed	Gastric	13.5 ± 0.1	23.3 ± 0.9	53 ± 4	74 ± 1	63 ± 3	96 ± 5	80 ± 3	84 ± 8	92 ± 9
Non-Bioaccessible	LDPE	Fed	Gastrointestinal	13.5 ± 0.1	19.1 ± 0.7	32 ± 2	65 ± 1	55 ± 2	94 ± 4	77 ± 3	89 ± 6	56 ± 5
Non-Bioaccessible	PVC	Fasted	Gastric	34 ± 1	34.5 ± 0.8	-	72 ± 7	86 ± 13	82 ± 7	105 ± 14	66 ± 3	95 ± 7
Non-Bioaccessible	PVC	Fasted	Gastrointestinal	28 ± 2	25.8 ± 0.6	-	59 ± 1	61 ± 3	62 ± 5	72 ± 9	64 ± 1	81 ± 2

A)

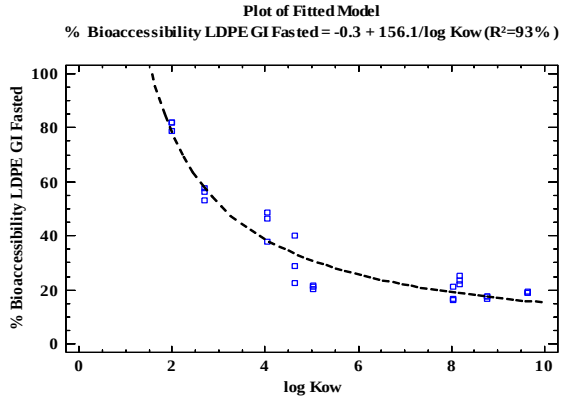

B)

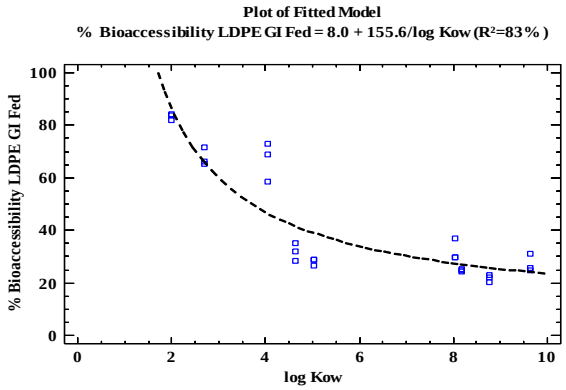

C)

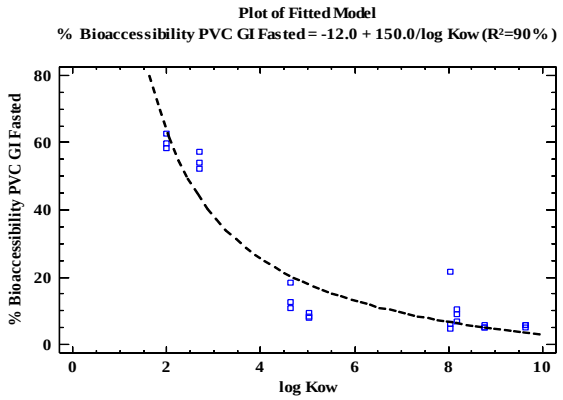

D)

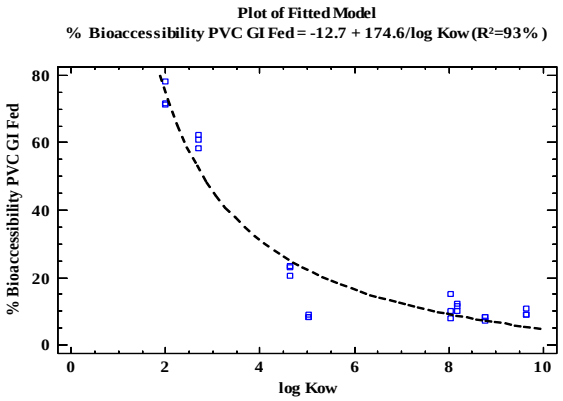

Figure 4.3.2. Regression model of % bioaccessibility of plasticizers in gastrointestinal fluid from A) LDPE under fasted conditions, B) LDPE under fed conditions, C) PVC under fasted conditions, and D) PVC under fed conditions against log K_{ow}.

4.3.4. Evaluation of critical parameters influencing oral bioaccessible fractions

The effect of the polymer type, the *in-vitro* PBET method and the GIT compartment on the magnitude of the BF was investigated using multifactor ANOVA. For BPA, the effect of MP composition could not be evaluated since BPA is only certified in LDPE MPs. As seen in Table 4.3.3, the ANOVA test revealed that all the factors are statistically significant (*p-values* <0.05) for all of the studied compounds. For example, the experimental findings indicated that the lowest bioaccessibility in both gastric and gastrointestinal compartments and both PBETs is encountered for the glassy PVC MPs (Table 4.3.2, Figures 4.3.3 and 4.3.4), which is in good agreement with previous observations for other xenobiotics (Liu et al., 2020). In case of the most polar PAEs, because of the small differences in average particle size of LDPE against PVC MP the lower bioaccessibility from PVC could be attributed to the large heteroatom/C ratio in PVC because of the chloride content of the material as compared to LDPE (only contains alkyl chains) that facilitates strong polar interactions with the less hydrophobic species as previously observed by Liu et al. (2020). Regarding the PBET method, bioaccessibility using fed conditions is significantly higher than that of fasted conditions and, this is likely due to the elevated concentration of enzymes and bile salts acting as surfactants in the gastrointestinal fluids thereby increasing analyte solubility in the gut fluid and triggering displacement from the MP surface. Bioaccessibility also increases whenever the two compartments (gastric + intestinal) are considered as compared to the gastric phase alone (Figure 4.3.3), which is in good agreement with previous literature results (Raffy et al., 2018).

Table 4.3.3. Multifactor ANOVA *p-values*. Statistically significant values (α = 0.05) are given in bold.

Compounds	DMP	DEP	BPA	DnBP	BzBP	DEHP	DnOP	DiNP	DiDP
A: MPs composition	**<0.0001**	**<0.0001**	-	**0.0007**	**<0.0001**	**<0.0001**	**<0.0001**	**<0.0001**	**<0.0001**
B: PBET method	**0.0002**	**<0.0001**	**0.0009**	**0.0049**	**<0.0001**	**0.0063**	**0.0051**	**<0.0001**	**<0.0001**
C: GIT fluid	**<0.0001**	**<0.0001**	**0.0217**	**0.0002**	**<0.0001**	**0.0221**	**<0.0001**	**<0.0001**	**<0.0001**
MP composition-PBET method interaction	**0.0340**	**0.0002**	-	0.2412	**<0.0001**	0.0765	0.2799	0.5374	0.2178
MPs composition-GIT fluid interaction	0.3093	**0.0062**	-	**0.0036**	**0.0007**	0.3519	**0.0015**	**0.0032**	**0.0020**
PBET method - GIT fluid interaction	0.0603	0.4542	0.3523	0.6954	0.4601	0.7556	0.6271	0.9013	0.2681

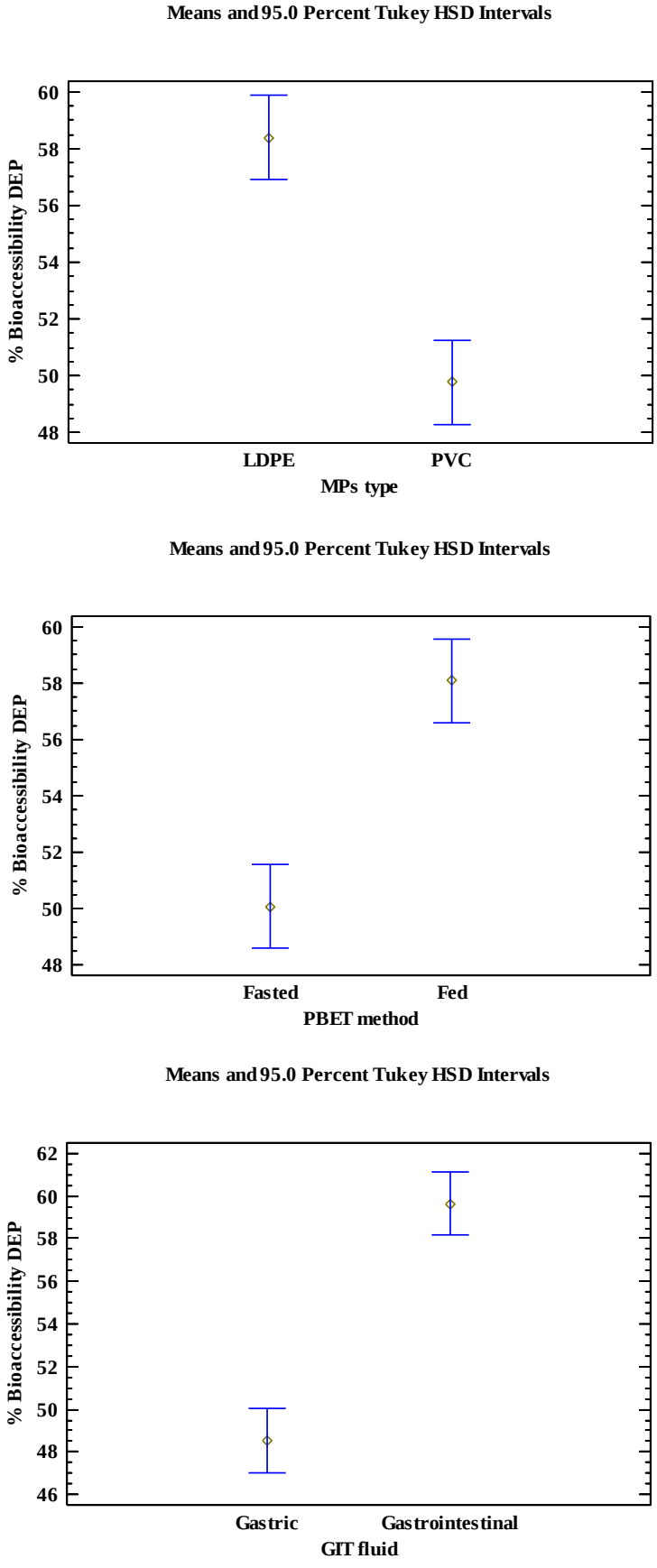

Figure 4.3.3. Multivariate ANOVA means plot including Tukey HSD intervals for DEP.

A)

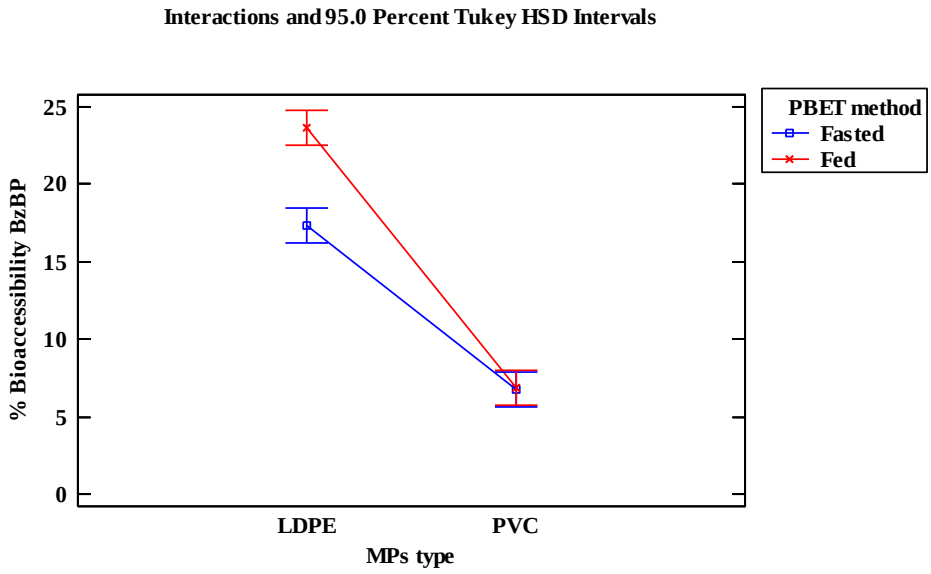

B)

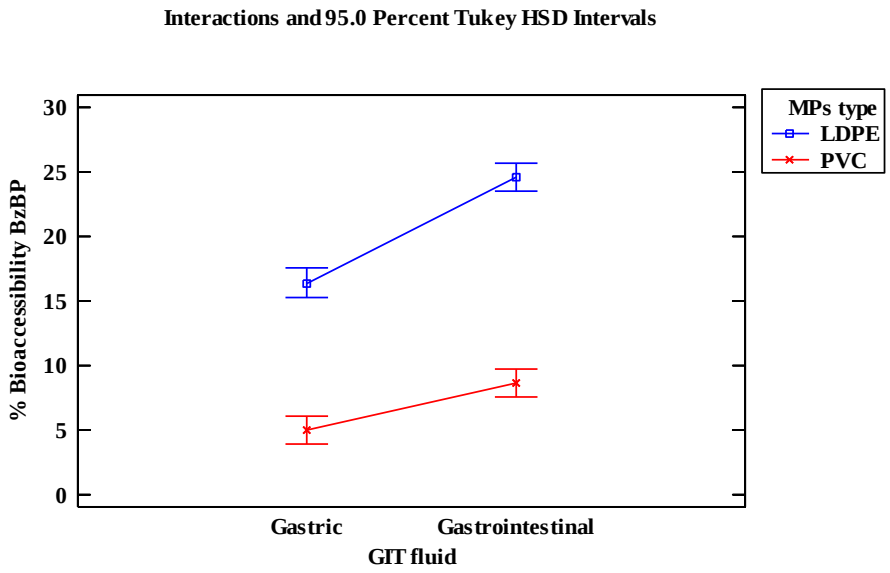

Figure 4.3.4. Interaction plots with Tukey HSD intervals for the statistically significant interactions (α = 0.05) of BzBP as a model analyte: a) MP composition-PBET method and b) GIT fluid-MPs composition.

Two-factor interactions were also studied in this work (Table 4.3.3). Interaction between the MPs composition and the PBET method is significant for DMP, DEP and BzBP (*p-value* <0.05) and shows greater differences between the two PBET methods for LDPE MPs against PVC MPs (see Figure 4.3.5a and 4.3.4a for DEP and BzBP, respectively). Interaction between the MPs composition and the GIT fluid is significant for all the compounds but DMP and DEHP. In the case of DEP, the increase of bioaccessibility during the intestinal step is more acute in PVC than that in LDPE (Figure 4.3.5b). On the contrary, for the other compounds, intestinal bioaccessibility increases more sharply in LDPE (Figure 4.3.4b). However, the interaction between the PBET method and the GIT fluid is not significant for any of the compounds.

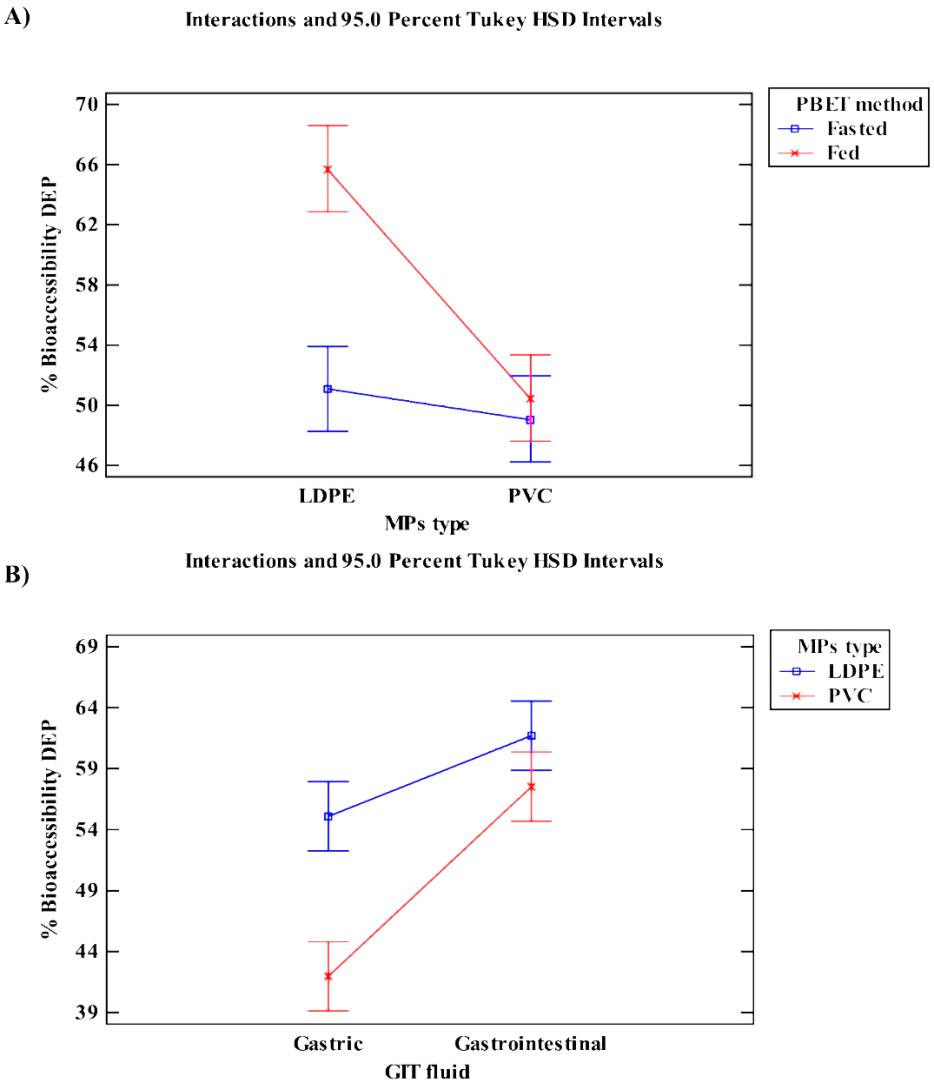

Figure 4.3.5. Interaction plots with Tukey HSD intervals for the statistically significant interactions (α = 0.05) of DEP as a model analyte: (a) MP composition-PBET method and (b) GIT fluid-MPs composition.

4.3.5. Human health risk assessment

To assess the potential human health risks from PAEs and BPA via MPs ingestion, the average daily intake (ADI) of PAEs and BPA per person could be estimated from the average mass of MPs ingested per day (MPM), the total concentration of the PAEs or BPA in the MPs (C) and the oral BF of each compound according to the following equation 6:

$$ADI = MPM \cdot C \cdot BF \text{ (Equation 6)}$$

Previous papers in the literature have estimated the number of MPs ingested by humans per time unit. For example, Cox et al. (2019) estimated that North Americans ingest averagely between 39,000 and 52,000 MPs per year, Zhang et al. (2020) estimated an ingestion rate up to 77,700 MPs per year from salt and water and Senathirajah et al. (2021) between 11,845 and 193,200 MPs/year from shellfish, salt, water and beer. Drinking water (tap and bottled) was deemed the greatest contributor to the number of plastic particles ingested by humans.

However, the number of MPs ingested by an individual will depend on a combination of highly variable parameters, e.g., age, demographics, cultural heritage, geographic location, nature of the development of the surrounding environment and lifestyle options (Rahman et al., 2021). Moreover, Senathirajah et al. (2021) provided a preliminary calculation of the potential mass of MPs that may be ingested by humans. After the estimation of the average number of MPs ingested, they calculated the mass of an individual MP particle using a volume density approach. Considering three scenarios, the global average rate of MP mass ingestion ranged between 7.7 g and 287 g per person per year (0.021-0.786 g per person per day) (Senathirajah et al., 2021).

The concentration of PAEs and BPA in MPs can differ significantly by the origin and ageing of the MPs ranging from the low ng/g in MPs sampled from sea water to mg/g in raw plastic materials (Table 4.3.5). In fact, it is known that plastic materials usually contain 0.1-5% of phthalates as the certified MPs considered in this work (Paluselli et al., 2019). Therefore, three scenarios were considered to calculate the ADI of PAEs and BPA, namely, low (1 ng/g), medium (10 μg/g) and high (3 mg/g) content of PAEs and BPA in MPs.

The BFs used for ADI calculations were the gastrointestinal bioaccessibility data reported in Table 4.3.2, and included the sum of bioaccessible and hydrolysis fractions for each of the two types of MPs. Both UBM and Versantvoort tests were also considered. The human ADI of PAEs and BPA via MPs per person considering a high exposition level (0.786 g MP/(person·day)) ranged from 0.04-0.7 ng/(person·day) under the first scenario, 0.4-7 μg/(person·day) under the second one and 124-2,128 μg/(person·day) under the third one. Results were compared against the human safe reference values based on either the oral reference doses (RfDs) provided by the USEPA, or the tolerable daily intakes (TDI) provided by European Food Safety Authority (EFSA) (EFSA, 2015, 2019) and considering an average adult body weight of 70.8 kg (Walpole et al., 2012). As shown in Table 4.3.4, the levels of exposure to PAEs and BPA were far below the safe reference values even under the third scenario (high level content of additives, viz. 3,000 μg/g), except for DMP, DnBP and BPA. For DMP, the daily intake (DI) at the high-level content of plasticizer is always higher than the safe reference value for adults considering the USEPA RfD regardless of the type of MP and the fed/fasted gastrointestinal digestion conditions. By considering the distinct scenarios for BF calculation, the ADI of DnBP at the high-level content of plasticizer is close to or slightly higher than the safe reference value based on the EFSA TDI but lower if the USEPA RfD is considered. Moreover, the estimated ADI of BPA at the high-level content was between 4 and 6 times higher than the safe reference value based on the EFSA TDI but did not exceed the limit posed by USEPA RfD. Very recently, there is a public consultation about EFSA draft opinion proposing lowering the TDI of BPA to 0.04 ng/(kg·day) (EFSA, 2021), leading to a human safe reference value for an adult of $2.8 \cdot 10^{-3}$ μg/(adult·day), which is far below the ADI under the second scenario. In summary, the human uptake of primary MP might pose severe health risks to humans because of the leachability of the most polar additives, namely, DMP, DnBP and BPA, at expectable concentrations in plastic materials under gastrointestinal digestion conditions.

Table 4.3.4. Concentration of PAEs and BPA reported in MPs.

Compounds	Concentration in MPs (µg/g)	DMP	DEP	BPA	DnBP	BzBP	DEHP	DnOP	DiNP	DiDP
ADI (µg /(adult·day))[a]	1E-03	5E-04 - 7E-04	4E-04 - 5E-04	3E-04 - 5 E-04	1E-04 - 3E-04	7E-05 - 2E-04	8E-05 - 3E-04	7E-05 - 2E-04	4E-05 - 2E-04	4E-05 - 2E-04
	10	5-7	4-5	3-5	1-3	1-2	1-3	1-2	0.4-2	0.4-2
	3,000	**1,574-2,128**	1,342-1,636	**1,043-1,574**	331-**751**	203-666	253-759	207-586	124-517	130-642
USEPA RfD (EPA) (µg/(Kg (BW) day))		20	800	50	100	200	20	-	-	-
EFSA TDI (EFSA, 2015, 2019) (µg/(Kg (BW)·day))		-	-	4	10	500	50	-	150	150
Safe reference values (µg/(adult·day))		1,416[b]/–	56,640[b]/–	3,540[b]/283[c]	7,080[b]/708[c]	14,160[b]/35400[c]	1,416[b]/3540[c]	-	–/10,620[c]	–/10,620[c]

[a]ADI was calculated by considering gastrointestinal bioaccessibility under fed and fasted conditions and also from LDPE and PVC MPs and given in this table as a range for every target species. [b]Safe reference values based on USEPA. RfDs and considering an average adult body weight of 70.8 kg. [c]Safe reference values based on EFSA TDI and considering an average adult body weight of 70.8 kg

Table 4.3.5. Concentration of PAEs and BPA reported in MPs.

Reference	Hirai et al. (2011)	Zhang et al. (2018)	Faure et al. (2015)	Teuten et al. (2009)	Benson and Fred-Ahmadu (2020)	Deng et al. (2021)	Jaworek and Czaplicka (2013)	Pivnenko et al. (2016)
Type of samples	Plastic Fragments collected in open ocean and beaches mainly Pacific (Asia and America)	Beached MPs of the Bohai and the Yellow Sea in north China	MPs from Swiss lakes and rivers	MPs from Ocean in Central Gyre	MPs in sediments of Gulf of Guinea	Plastic samples in Yangtze Estuary wetlands	Polymer material	Residual and source-segregated waste plastics from a municipality in Southern Denmark
MPs type	PE & PP	PE, PP, PS	PE, PP, PS; PE, PVC	PE	PE, PP, PS	PP, PS, PE, PES	PE, PVC, PS	PET, PE, PP, PS, NS
Number of samples	44 samples				27		17 samples	48
DMP		<0.03-1.26 ng/g			[a]nd-15.9 µg/g		nd	<0.08-120 µg/g
DEP		<0.06-16.2 ng/g			nd-0.05 µg/g		nd	<3.4-150 µg/g
BPA	0 - 729.9 ng/g		4.8-28.3 ng/g	5-284 ng/g				
DnBP		<0.02-6.78 ng/g			nd - 4.5 µg/g	32.6-44.6 µg/g	0.9-39.7 µg/g	<0.09-360 µg/g
DiBP		<0.04-7.51 ng/g				10.1-20.5 µg/g		<0.20-460 µg/g
BzBP		<0.002-0.097 ng/g			nd-6.22 µg/g	0.2-2.9 µg/g	nd	<0.02-92 µg/g
DEHP		<0.3-69.9 ng/g			0.19-45.3 µg/g	49.2-840.5 µg/g	nd-3,254.1 µg/g	<0.43-2700 µg/g
DnOP		<0.005-0.17 ng/g			nd-0.13 µg/g	nd-0.5 µg/g		<0.20-99 µg/g
DiNP		<0.007-0.16 ng/g				1.6-64.8 µg/g	nd-16,200 µg/g	
DiDP						1.4-11.6 µg/g		
ΣPAEs			528-111604 ng/g					

[a]nd= not detected

4.4. *IN-VITRO* LEACHING AND PHYSIOLOGICALLY RELEVANT EXTRACTION TESTS FOR PHTHALATE CONGENERS AND BISPHENOL A FROM MICROPLASTICS - ASSESSING THE CONTRIBUTION OF MICROPLASTICS TO THE EXPOSURE OF MARINE VERTEBRATES TOWARDS PLASTIC-RELATED CHEMICALS

4.4.1. Analytical performance of the chromatographic and extraction methods

The LC methods based on external calibration using isotopologues as IS were assessed in terms of linearity, precision and LOQs (see Tables 3.4.1 and 3.3.5) for the target compounds.

For precursors in Table 3.4.1, the dynamic linear range extended from 10 µg/L to 5 mg/L, except for DEP, DnBP and DEHP, which ranged from 2 µg/L to 5 mg/L, and BPA that exhibited a range of 0.05-5 mg/L. In all cases, the determination coefficients were consistently >0.9990. Repeatability at the 100 µg/L level for 5 replicates was below 18% in all cases. The LOQs, calculated for a S/N ratio of 10, ranged from 0.90 and 10 µg/L, thus entailing a significant improvement for BPA and DnOP compared to our previous study (López-Vázquez et al., 2022).

The trueness of the determination of bioaccessible PAEs and BPA in the G and GI (Hamdan's method) phases spiked at a concentration of 400 µg/L ranged from 75 to 118% and 71 to 110%, respectively with an RSD below 18%. The LOQs ranged from 113 and 400 µg/L for G fluid and from 85 and 301 µg/L for GI fluid. Therefore, the bioaccessible fractions for the studied MPs can be quantified above 0.02% (w/w) for the additives at the highest concentration (DiNP and DiDP) and from 0.1-1.1% (w/w) for the remaining compounds.

The method trueness of the total determination of PAEs and BPA in the LDPE and PVC reference materials by USE yielded recoveries ranging from 57 to 90% and 77 to 117%, respectively with RSD < 20% (López-Vázquez et al., 2022) and LOQs spanning from 0.45 to 12 µg/g. Consequently, the non-bioaccessible fraction can be quantified above 0.01% (w/w) for DiNP and DiDP and from 0.06-0.6 % (w/w) for the remainder of the compounds in the MPs analysed.

4.4.2. Leaching of PAEs and BPA in seawater

Leaching tests with single extractants were conducted to investigate the leaching of PAEs and BPA from LDPE and PVC MPs in MQ water and seawater following the analytical procedures described in Section 3.4.2.1.

The experimental results demonstrated that only the most hydrophilic compounds, i.e. DMP, DEP and BPA, were released to a significant extent from both types of MPs in either aqueous milieu with leaching rates ranging from 34 to 81% (w/w) (Table & Figure 4.4.1). In the rest of PAEs, leaching fractions were negligible. These findings align well with previous studies that (i) employed a dynamic on-line leaching test with simulated seawater for PAEs and BPA for the same CRM MPs (Fikarová et al., 2019) and (ii) determined leachable short-chain PAEs from LDPE-bags and PVC-cables (Paluselli et al., 2019). The conversion yields of DMP and DEP into the hydrolysis products (MMP and MEP) were down to 0.8% (w/w) in the leachable fractions of both freshwater and marine water simulating extractants.

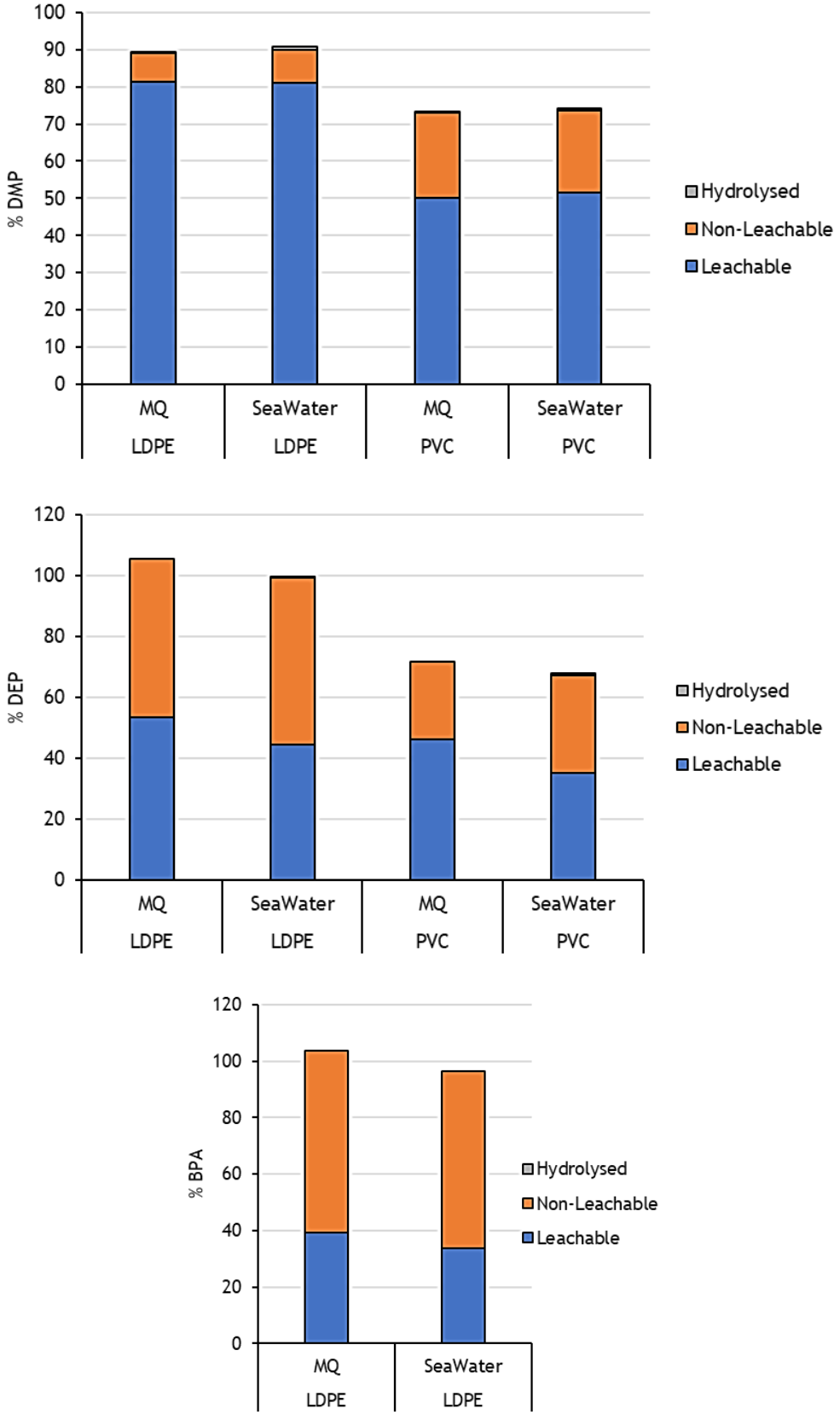

Figure 4.4.1. Leaching of plastic-borne compounds in UPW and seawater, only showing the compounds detectable in the water extractant phase (full data is available in Table 4.4.1).

Table 4.4.1. Leachable and non-leachable fractions (%) of PAEs and BPA using MQ and seawater extractants (n=3).

Fraction	MPs type	Aqueous extractant	DMP	DEP	BPA	DnBP	BzBP	DEHP	DnOP	DiNP	DiDP
Leachable	LDPE	MQ	81 ± 3	53 ± 3	39 ± 4	<0.2	<0.3	<0.1	<1	<0.02	<0.02
Leachable	LDPE	Seawater	81 ± 5	44 ± 3	34 ± 2	<0.2	<0.3	<0.1	<1	<0.02	<0.02
Leachable	PVC	MQ	50 ± 2	46 ± 1	-	<0.2	<0.3	<0.1	<1	<0.02	<0.02
Leachable	PVC	Seawater	52 ± 2	35.2 ± 0.9	-	<0.2	<0.3	<0.1	<1	<0.02	<0.02
Hydrolysis	LDPE	MQ	0.11 ± 0.02	<0.002	-	<0.04	<0.005	<0.02	-	<0.005	-
Hydrolysis	LDPE	Seawater	0.8 ± 0.1	0.2 ± 0.1	-	<0.04	<0.005	<0.02	-	<0.005	-
Hydrolysis	PVC	MQ	0.07 ± 0.02	<0.002	-	<0.04	<0.005	<0.02	-	<0.005	-
Hydrolysis	PVC	Seawater	0.6 ± 0.1	0.42 ± 0.09	-	<0.04	<0.005	<0.02	-	<0.005	-
Non-Leachable	LDPE	MQ	7.9 ± 0.5	52 ± 2	64 ± 4	104 ± 4	104 ± 13	98 ± 13	118 ± 6	93 ± 4	110 ± 10
Non-Leachable	LDPE	Seawater	9 ± 1	55 ± 5	63 ± 5	97 ± 11	99 ± 8	95 ± 11	111 ± 7	91 ± 7	100 ± 7
Non-Leachable	PVC	MQ	23 ± 7	26 ± 8	-	77 ± 17	95 ± 21	83 ± 29	91 ± 12	71 ± 4	73 ± 6
Non-Leachable	PVC	Seawater	22 ± 6	32 ± 7	-	80 ± 12	98 ± 22	95 ± 14	93 ± 7	73 ± 4	82 ± 8

The effects of the MP material and the aqueous extractant onto the leachable fractions of BPA, DMP and DEP were investigated using multifactor ANOVA (Table 4.4.2). Regarding BPA, the effect of MP composition could not be evaluated since BPA is only certified in LDPE MPs. The ANOVA test revealed that the MP material significantly influences the leaching of both DMP and DEP (*p-value* <0.0001), with statistically higher desorption from LDPE MPs for both water extractants, most likely due to the rubbery-like nature of LDPE that is characterized by increased surface hydrophobicity (less prone to retain the most polar additives) compared to glassy PVC (Liu et al., 2020; Shu et al., 2022). The type of aqueous milieu did not exhibit a significant effect on DMP and BPA (*p-value* = 0.7074 and 0.1027, respectively) indicating a similar leaching behaviour in MQ and seawater, as opposed to DEP (*p-value* <0.0001). As to latter, leaching was reduced with the addition of salts, attributed to a salting-out like effect in seawater, thereby suggesting longer residence times of DEP sorbed to MPs in marine settings. Two-factor interactions were not statistically significant for neither DMP and DEP.

The mass balance obtained by the sum of leachable plus residual and hydrolytic fractions for DMP, DEP and BPA rendered absolute recoveries for LDPE and PVC MPs ranging from 89-118% and 68-98%, respectively, for both MQ and seawater.

Table 4.4.2. Multifactor ANOVA *p-values*.

Compounds	DMP	DEP	BPA
A: *MPs material*	**<0.0001**	**0.0001**	-
B: *Aqueous extractant*	0.7074	**<0.0001**	0.1027
MPs composition – Aqueous extractant	0.6543	0.4347	-

Statistically significant values (α=0.05) are given in bold

4.4.3. *In-vitro* fish bioaccessibility tests

The release extent of additives from MPs across the fish GIT was determined by measuring the leachable compounds in biorelevant gut fluids, including gastric, enzyme-solution (Carter's method), intestinal (enzymes + bile salts, Hamdan's method) and gastrointestinal fluids. It is important to note that the bioaccessible fraction represents the maximum amount of compound that can potentially be bioavailable and thus reach the blood stream. The percent of bioaccessibility under different digestive fluids is presented in Table 4.4.3 and Figure 4.4.2. For the most hydrophilic compounds, i.e., DMP, DEP and BPA, fish bioaccessibility values ranged between 34% and 83%, while oral bioaccessibility was always below 8% regardless of the body fluid and type of MP for the remaining compounds. Once again, these results indicate that merely the more hydrophilic PAEs or BPA are substantially bioaccessible (López-Vázquez et al., 2022; Mohamed et al., 2023; Sixto et al., 2021) or leachable (section 3.4.3). The hydrolysis of PAEs in the time course of the oral bioaccessibility tests was also evaluated. MMP, MEP and phthalic acid were the only degradation products identified across the varied GIT fluids, with transformation rates in all cases merely down to 1.6%. Mass balance assessment rendered absolute recoveries spanning from 64 to 117% for all plastic-borne compounds in the various body fluids regardless of the polymer type.

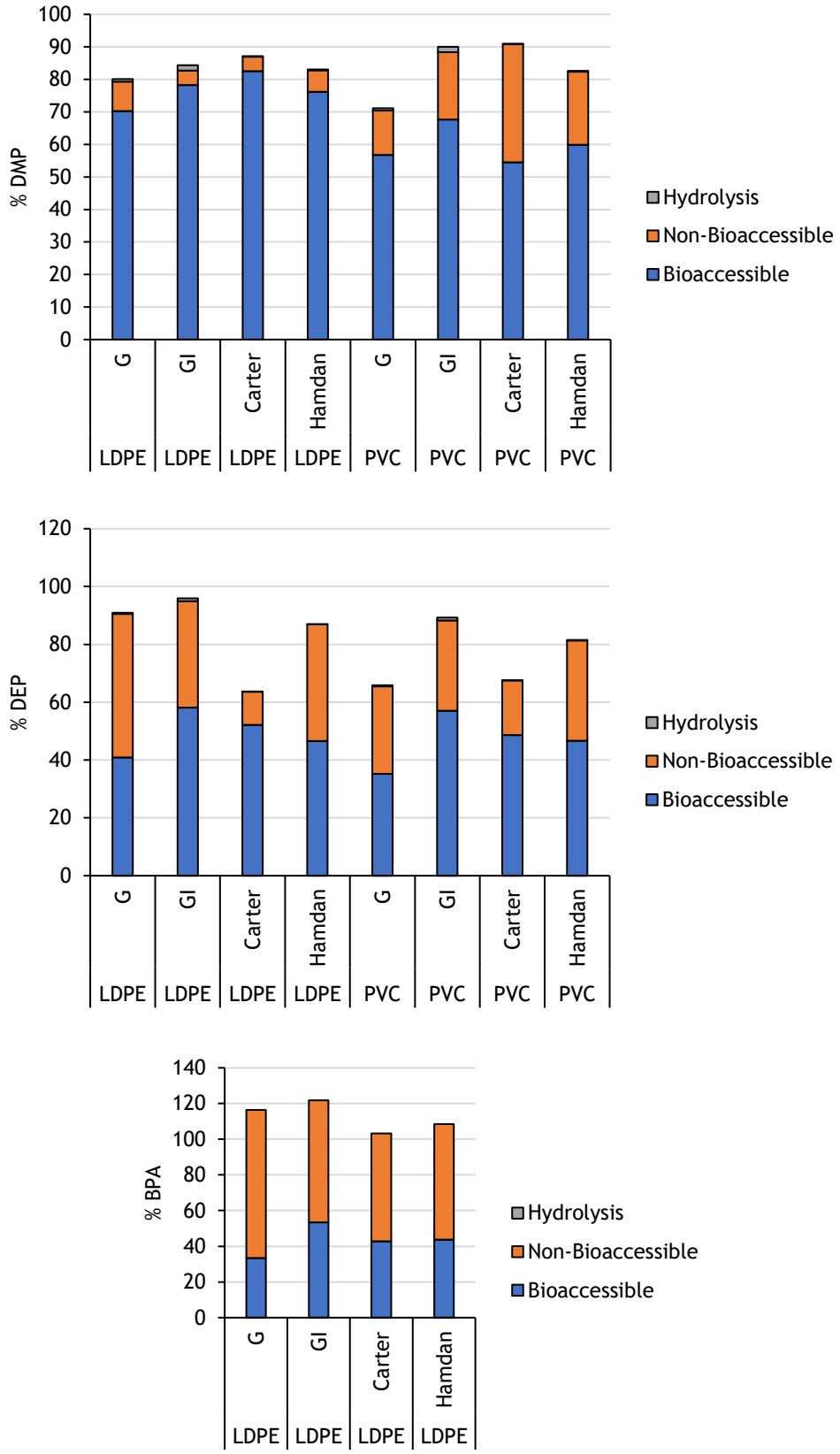

Figure 4.4.2. Comparative assessment of bioaccessible fractions of plastic-borne compounds with a variety of gut fluids, only showing for the three most bioaccessible compounds (full data is available in Table 4.4.3).

Table 4.4.3. Bioaccessible and non-bioaccessible fraction (%) of PAEs and BPA in fish fluids (n=3).

Fraction	MPs type	PBET method	DMP	DEP	BPA	DnBP	BzBP	DEHP	DnOP	DiNP	DiDP
Bioaccessible	LDPE	G	70 ± 2	41 ± 1	34 ± 4	4 ± 2	1.2 ± 0.2	<0.1	<1	0.6 ± 0.1	<0.02
Bioaccessible	LDPE	GI	78 ± 2	58 ± 3	53 ± 4	7.8 ± 0.3	6.6 ± 0.4	<0.1	5 ± 3	<0.02	<0.02
Bioaccessible	LDPE	Carter	83 ± 4	52 ± 5	43 ± 5	2 ± 2	0.8 ± 0.4	<0.1	1.6 ± 0.1	0.7 ± 0.3	<0.02
Bioaccessible	LDPE	Hamdan	76 ± 8	47 ± 6	44 ± 4	2.4 ± 0.2	0.7 ± 0.1	<0.1	<1	1.2 ± 0.6	<0.02
Bioaccessible	PVC	G	57 ± 6	35 ± 5	-	<0.2	0.5 ± 0.2	<0.1	<1	<0.02	<0.02
Bioaccessible	PVC	GI	68 ± 3	57 ± 2	-	<0.2	3.3 ± 0.1	<0.1	5 ± 2	<0.02	5 ± 3
Bioaccessible	PVC	Carter	55 ± 2	49 ± 5	-	2.7 ± 0.6	1.3 ± 0.2	<0.1	1.5 ± 0.3	1.6 ± 0.2	1.1 ± 0.3
Bioaccessible	PVC	Hamdan	60 ± 4	47 ± 6	-	2.1 ± 0.8	0.62 ± 0.04	<0.1	<1	1.4 ± 0.7	<0.02
Hydrolysis	LDPE	G	0.8 ± 0.2	0.3 ± 0.1	-	<0.04	<0.005	<0.02	-	<0.005	-
Hydrolysis	LDPE	GI	1.6 ± 0.2	0.9 ± 0.1	-	<0.04	<0.005	<0.02	-	<0.005	-
Hydrolysis	LDPE	Carter	0.5 ± 0.1	0.10 ± 0.03	-	<0.04	<0.005	<0.02	-	<0.005	-
Hydrolysis	LDPE	Hamdan	0.33 ± 0.04	0.11 ± 0.03	-	<0.04	<0.005	<0.02	-	<0.005	-
Hydrolysis	PVC	G	0.7 ± 0.1	0.36 ± 0.04	-	<0.04	<0.005	<0.02	-	<0.005	-
Hydrolysis	PVC	GI	2 ± 1	1.0 ± 0.5	-	<0.04	<0.005	<0.02	-	<0.005	-
Hydrolysis	PVC	Carter	0.16 ± 0.03	0.11 ± 0.04	-	<0.04	<0.005	<0.02	-	<0.005	-
Hydrolysis	PVC	Hamdan	0.21 ± 0.02	0.22 ± 0.04	-	<0.04	<0.005	<0.02	-	<0.005	-
Non-Bioaccessible	LDPE	G	9 ± 1	50 ± 4	83 ± 7	105 ± 11	104 ± 9	100 ± 25	116 ± 16	89 ± 10	97 ± 22
Non-Bioaccessible	LDPE	GI	4.4 ± 0.2	36.8 ± 0.6	68 ± 10	104 ± 3	108 ± 2	106 ± 4	94 ± 1	90 ± 10	99 ± 3
Non-Bioaccessible	LDPE	Carter	5 ± 2	12 ± 6	61 ± 5	102 ± 4	100 ± 8	117 ± 13	99 ± 7	73 ± 7	103 ± 12
Non-Bioaccessible	LDPE	Hamdan	6.6 ± 0.6	40 ± 2	65 ± 4	96 ± 9	98 ± 8	93 ± 7	98 ± 3	68 ± 8	101 ± 10
Non-Bioaccessible	PVC	G	14 ± 6	30 ± 10	-	98 ± 7	98 ± 9	98 ± 20	81 ± 10	69 ± 5	76 ± 14
Non-Bioaccessible	PVC	GI	21 ± 2	31 ± 4	-	101 ± 10	104 ± 5	93 ± 7	95 ± 9	71 ± 3	84 ± 11
Non-Bioaccessible	PVC	Carter	36.3 ± 0.4	19 ± 1	-	97 ± 5	108 ± 6	109 ± 10	85 ± 1	65 ± 1	84 ± 2
Non-Bioaccessible	PVC	Hamdan	22.5 ± 0.6	35 ± 1	-	78 ± 4	87 ± 4	69 ± 7	71 ± 5	50 ± 1	68.5 ± 0.9

The influence of MP material and the *in-vitro* digestion method on the magnitude of the bioaccessible fractions was investigated using multifactor ANOVA. As shown in Table 4.4.4, the ANOVA test indicated that the digestion method is statistically significant (*p-values* <0.05) for the three most bioaccessible compounds (i.e. DMP, DEP and BPA). The gastric fraction exhibited the lowest bioaccessible fraction, which might be attributed to the shorter contact time and the absence of surface-active biomolecules, while the two-step gastrointestinal digestion incorporating bile acids featured the highest bioaccessibility. It should be noted that fish bioaccessibility of plastic-laden compounds, and thus their risk assessment/exposure, is usually underestimated in the literature because a mere single body fluid extractant is considered in most of the publications (Coffin, Huang, et al., 2019; Coffin, Lee, et al., 2019; Mohamed Nor & Koelmans, 2019). For DMP, the polymer matrix and the interaction between the extraction method and the MP material were also significant. Akin to water leaching, the bioaccessibility of DMP was higher from LDPE MPs, and this effect was more severe for the Carter's method with enzymes only, again indicating the desorption irreversibility of PVC-borne compounds regardless of the complexity of the body fluid. When comparing the oral bioaccessibility results with those of aqueous leaching, only the gastrointestinal bioaccessible fraction was significantly superior to that of leaching in MQ water (Figure 4.4.3) thereby evincing that multiple-step (additive), sequential or dynamic extraction procedures should be called for to enable reliable risk assessment/exposure studies of plastic-borne additives in marine vertebrates.

Table 4.4.4. Multifactor ANOVA *p-values*.

Compounds	DMP	DEP	BPA
A: *MPs material*	**<0.0001**	0.1957	-
B: *Physiologically based extraction test*	**0.0059**	**<0.0001**	**0.0040**
AB interaction	**0.0063**	0.6990	**-**

Statistically significant values (α=0.05) are given in bold

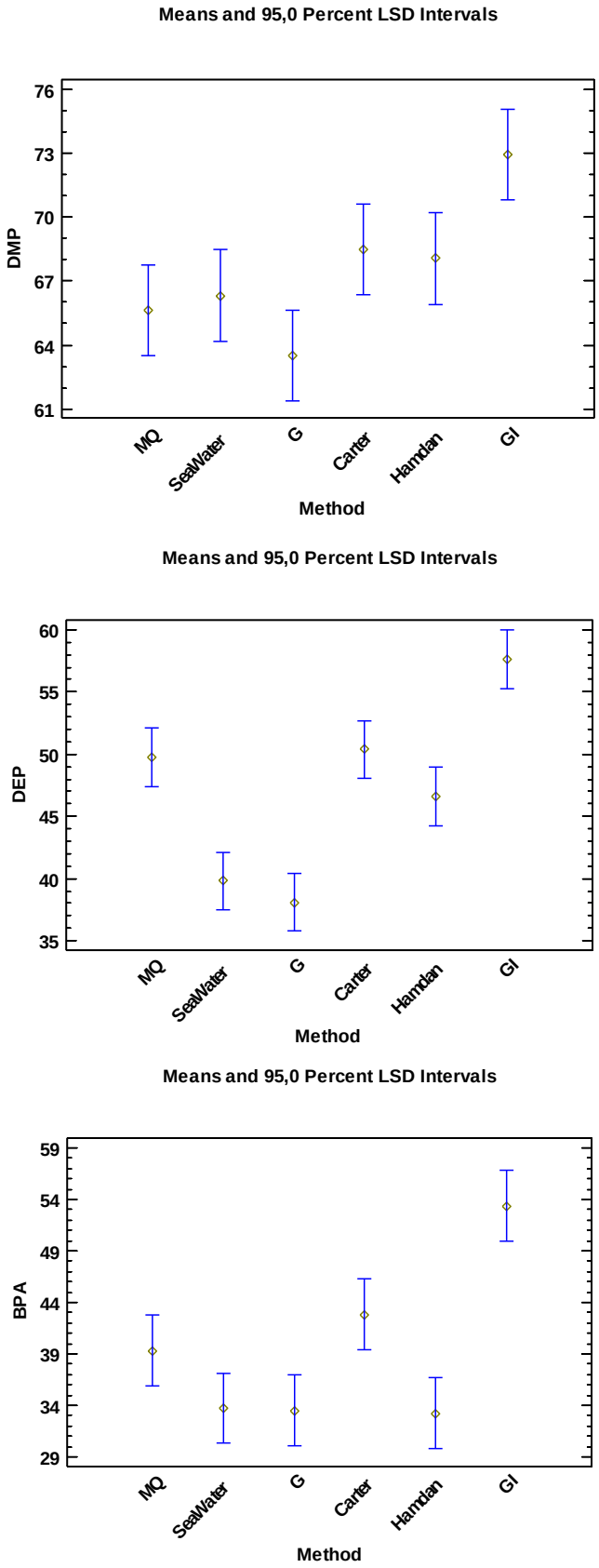

Figure 4.4.3. Comparative assessment of environmental leaching against fish bioaccessibility for DMP, DEP and BPA in MPs.

4.4.4. Microplastic contribution to PAEs and BPA exposure for aquatic marine organisms

PAEs and BPA exposure in aquatic organisms might occur through the ingestion of water and MPs, and thus the contribution of both sources should be elucidated. The DI (µg/kg/day) (Liu et al. (2020) of MP-associated pollutants (see Table 4.4.5) was calculated using equation 7, where $Q_{pollutant}$ (µg/g) stands for the concentration of PAEs or BPA in MPs, F denotes the bioaccessibility (expressed as ratio, instead of %) in the gastrointestinal fluid (worst-case scenario) for PVC or LDPE MPs, C_{MP} (µg/L) is the mass concentration of MPs in the marine environment, V (mL/day) stands for the uptake rate of water and W (kg) is the body (fish) weight.

$$DI_{MP} = \frac{Q_{pollutant}\ x\ F\ x\ C_{MP}\ x\ V}{W} \quad \text{(Equation 7)}$$

Table 4.4.5. Estimated DI_{MP} (µg/BW kg/day) of PAEs and BPA from LDPE and PVC MPs at three concentration levels of chemicals in MPs along with varied concentrations of MPs in the marine environment and different uptake rate of seawater.

			DI (µg/BW kg/day)				
			DMP		DEP		BPA
Q (µg/g MPs)	C (µg MPs/L)	V/W (mL/BW kg/day)	LDPE	PVC	LDPE	PVC	LDPE
1.00E-03	0.15	24	2.88E-12	2.49E-12	2.13E-12	2.09E-12	1.92E-12
10	1	100	7.99E-07	6.92E-07	5.91E-07	5.81E-07	5.34E-07
3000	250	240	0.144	0.12	0.106	0.10	0.096

The concentrations of PAEs and BPA in MPs ($Q_{pollutant}$) vary significantly depending on the source, pursued (micro)plastic application, weathering conditions and polymer chemical nature. It might range from low ng/g in MPs collected from seawater to mg/g in raw plastic materials. Akin to our previous work assessing human exposure (López-Vázquez et al., 2022), three scenarios for Q were considered to calculate the DI of PAEs and BPA, namely, low (1 ng/g), medium (10 µg/g) and high (3 mg/g) concentrations. The F used in DI estimation was the gastrointestinal bioaccessibility data reported in Table 4.4.3, which encompassed the sum of gastrointestinal bioaccessible and hydrolysis fractions in either LDPE or PVC MPs.

Different concentrations of MPs in the marine environment (C_{MP}) have been reported in the literature. Beiras and Schönemann (2020) compiled data on plastic density ranging from <0.0001 to 1.89 mg/L, showing a bell-shaped distribution with the maximum frequency observed at the µg/L level. They reported median values that were similar across all oceans (0.16 µg/L in the North Pacific, 0.17 µg/L in the Arctic, and 0.18 µg/L in the North Atlantic). However, higher concentrations were found in areas more influenced by costal activities (0.92 µg/L in Australia and 1.02 µg/L in the Mediterranean). Further, Isobe et al. (2019) estimated concentrations of MPs in the Pacific Ocean of 0.25 mg/L. Therefore, three scenarios were considered, low (0.15 µg/L) mimicking levels in ocean environments, medium (1 µg/L) for Mediterranean coastal sites and high (250 µg/L) according to exposure predictions.

The uptake rate of water (V) differs significantly among fish species and freshwater/marine environments. Perrott et al. (1992) conducted a study estimating the drinking rate in 12 fish species, ranging from 0.03 to 0.21 mL/kg/h for freshwater fishes and from 1 to 7.76 mL/kg/h for seawater species. In the case of the Japanese medaka (*Oryzias latipes*), Tipsmark et al.

(2020) estimated a drinking rate of 5 mL/kg/h in freshwater, which doubled in seawater. Consequently, the uptake rate per body weight (V/W) for seawater fish ranges from approximately 24 to 240 mL/ BW kg/day. Therefore, three rates were considered: 24, 100 and 240 mL/ BW kg/day.

DI associated to MPs (DI_{MP}) varies greatly depending on the scenario considered. In the worst-case scenario (high level of all the considered parameters), DI_{MP} ranged from 0.1 µg/BW kg/day for BPA to 0.14 µg/BW kg/day for DMP. However, under the best-case scenario, DI_{MP} was ca. 10 orders of magnitude lower, ranging between 2 and 3 ag/BW kg/day (Table 4.4.6).

The contribution of the water ingestion pathway to the fish exposure of DMP, DEP and BPA was estimated according to equation 8, for which $C_{pollutant}$ (µg/L) stands for the concentration of PAEs or BPA in seawater. Different concentrations of DMP, DEP and BPA in the marine environment have been reported in the literature (Tables 4.4.6 and 4.4.7), ranging from <0.001 to ca. 1 µg/L. Therefore, three scenarios were considered, low (0.001 µg/L), medium (0.05 µg/L) and high (1 µg/L).

$$DI_{water} = \frac{C_{pollutant}\, x\, V}{W} \text{ (Equation 8)}$$

Table 4.4.6. Concentrations of DMP and DEP reported in marine/coastal waters.

Reference	Geographical area	Type of sample	DMP (µg/L)	DEP (µg/L)
Prieto et al. (2007)	Spain	Estuarine water	0.21-0.28	0.07
Hadjmohammadi et al. (2011)	Iran	Seawater	0.49	0.52
Sánchez-Avila et al. (2012)	Spain	Seawater	<LOQ – 0.25	0.02 – 0.48
Heo et al. (2020)	South Korea	Seawater	0.02-0.1	0.02 - 0.15
Cao et al. (2022)	China	Seawater	0.0017 – 0.014	<LOQ – 0.032
Paluselli and Kim (2020)	Northwest Pacific	Seawater	<LOQ – 0.004	0.0013 – 0.070
Paluselli et al. (2018)	Marseille Bay	Seawater	0.0008 – 0.012	0.0003 – 0.05
Q. Zhang et al. (2019)	Pacific Ocean	Seawater	<LOQ – 0.0071	<LOQ – 0.0021

DI of DMP, DEP and BPA due to seawater ingestion (DI_{water}) across the different scenarios showed again a large span, ranging from 24 pg/BW kg/day to 0.24 µg/BW kg/day (Table 4.4.8).

Considering an intermediate scenario for both MP and seawater intake, the DIMP of DMP, DEP and BPA represent merely 0.016% of DI_{water}. Therefore, our results signalled that the MPs contribution to the DMP, DEP and BPA exposure to marine fish can be negligible as compared to the waterborne dissolved fraction.

Table 4.4.7. Concentration of BPA reported in seawater.

Reference	Geographical area	BPA (µg/L)
Salgueiro-González et al. (2019)	Spain	<LOQ – 0.48
Basheer and Lee (2004)	Singapore	0.04 – 0.19
Pojana et al. (2007)	Venice lagoon (Italy)	<LOQ – 0.15
Sánchez-Avila et al. (2011)	Catalonia (NE Spain)	0.007 – 0.035
Arditsoglou and Voutsa (2012)	Thermaikos Gulf (Greece)	0.011 – 0.053
Iparraguirre et al. (2012)	Bay of Biscay (Spain)	0.056
Li et al. (2013)	Daliao River Estuary(China)	0.0038 – 0.11
Sánchez-Avila et al. (2013)	Cantabrian coast (Spain)	0.0016 – 0.34
Lisboa et al. (2013)	Santos Bay (Brazil)	<LOQ – 0.077
Salgueiro-González et al. (2015)	Five estuaries (NW Spain)	<LOQ – 0.15
Diao et al. (2017)	Pearl Estuary (China)	0.012 – 0.06
Xu et al. (2018)	Hong Kong (China)	0.003 – 0.11
Staples et al. (2018)	Different locations in Europe and Noth America	<LOQ – 0.90

Table 4.4.8. Estimated DI_{water} (µg/BW kg/day) of PAEs and BPA from seawater ingestion at three concentration levels of chemicals with varied uptake rate of water.

C (µg/L)	V/W (mL/BW kg/day)	DI (µg/BW kg/day)
0.001	24	2.40E-05
0.05	100	0.005
1	240	0.24

4.5. DETERMINATION OF REGULATED PERFLUOROALKYL SUBSTANCES (PFAS) IN DRINKING WATER ACCORDING TO DIRECTIVE 2020/2184/EU

4.5.1. Assessment of blank contamination

A key issue in PFAS determination is the background contamination already reported in the literature (González-Barreiro et al., 2006; Janda et al., 2019). To minimize this limitation, an InfinityLab PFC delay column (or Strata®-X-AW cartridge for on-line SPE) from Agilent was placed before the multisampler valve in order to delay the t_R of PFAS introduced from the solvent, tubing, and the degasser, enabling the chromatographic separation from those PFAS present in the samples. An example of this separation for PFOS is shown in Figure 4.5.1. Subsequently, instrumental blanks were evaluated by running the chromatographic gradient without sample injection (false injection) and also injecting the corresponding solvent MeOH (solvent blank for off-line SPE method) or UPW (solvent blank for on-line SPE and direct injection methods). The results revealed a PFBA background in the false injections from on-line SPE (42.5 ng/L) and in solvent injection (UPW) from on-line SPE and direct injection (57.6 and 12.0 ng/L, respectively). This points to both a potential contamination of the UPW used and the fact that the delay column was not enough to eliminate system blanks in the on-line SPE method since not all the solvents flow through the pre-injector delay column in this configuration. Although other water commercially available water samples were tested, similar results were obtained.

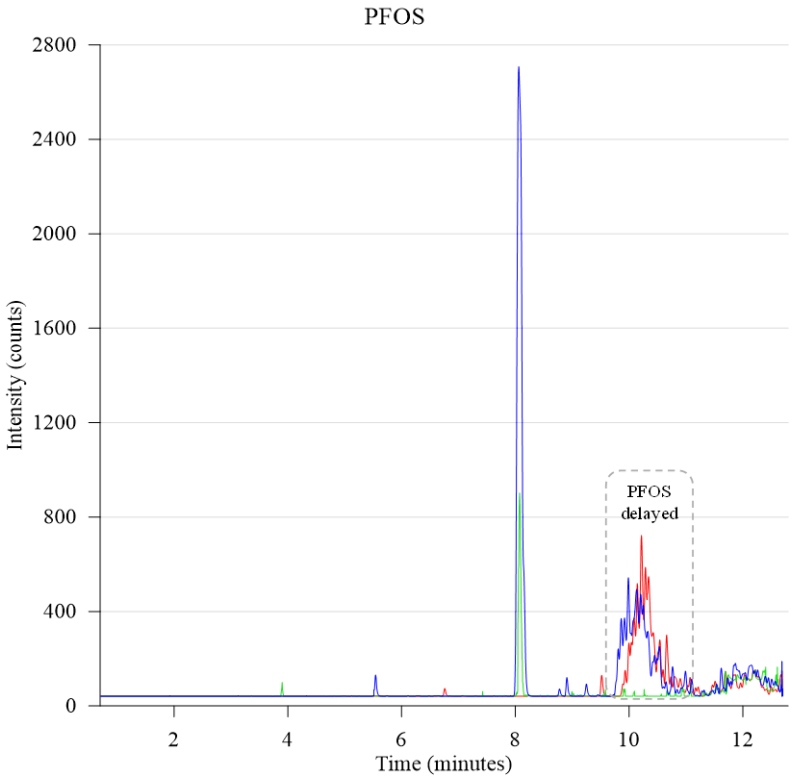

Figure 4.5.1. Comparative chromatograms for native PFOS in MeOH with delay column (red line) and without delay column (green line) and PFOS standard in MeOH (1 µg/L) with delay column (blue line).

In addition, before performing the recovery studies at different levels, several blanks were assessed at the different stages of the sample preparation off-line SPE protocol to check for PFAS contamination. For this purpose, a cartridge blank (entire off-line SPE protocol without sample loading) and an elution solvent blank (10 mL MeOH 5% NH_3 evaporated to dryness and reconstituted) were studied separately (Table 4.5.1). PFBA and PFOA were found in both

elution solvent and cartridge blanks at concentrations below 0.5 ng/mL in the final extract (which would correspond to 0.5 ng/L referred to 200 mL of sample). Thus, for both compounds off-line SPE protocol blanks were performed in each sample batch and their concentrations subtracted from samples.

Table 4.5.1. Concentrations of PFAS in elution solvent and cartridge blanks for the off-line SPE protocol (n=3) referring to the final extract (200 µL).

Compounds	Blank cartridge, ng/mL (%RSD)	Elution solvent, ng/mL (% RSD)
PFBA	0.40 (16)	0.45 (16)
PFPeA	<LOQ	<LOQ
PFHxA	<LOQ	<LOQ
PFHpA	<LOQ	<LOQ
PFOA	0.13 (22)	0.19 (17)
PFNA	<LOQ	<LOQ
PFDA	<LOQ	<LOQ
PFUdA	<LOQ	<LOQ
PFDoA	<LOQ	<LOQ
PFTrDA	<LOQ	<LOQ
PFBS	<LOQ	<LOQ
PFPeS	<LOQ	<LOQ
PFHxS	<LOQ	<LOQ
PFHpS	<LOQ	<LOQ
PFOS	<LOQ	<LOQ
PFNS	<LOQ	<LOQ
PFDS	<LOQ	<LOQ
PFUdS	<LOQ	<LOQ
PFDoS	<LOQ	<LOQ
PFTrDS	<LOQ	<LOQ

4.5.2. Comparison of analytical methods

The validation of the LC-MS/MS methods was performed in terms of linearity, precision and iLOQs (Table 4.5.2). It must be noted that they differ on the column and mobile phases used. Thus, although the off-line SPE and on-line SPE method use the same UHPLC column, the modifier in the case of off-line SPE is ammonium formate (to promote ionization in the negative mode), however this modifier could not be used in the on-line SPE method, since a higher pH is required for elution of the SPE mixed-mode pre-columns, thus 0.05% NH_3 was used instead. Also, a regular C18 3.5-µm LC column was used in the direct injection method, to accommodate a larger injection volume.

Table 4.5.2. Instrumental UHPLC-MS/MS validation parameters for the three evaluated methods.

Compounds	Repeatability n=6 RSD (%)				Determination coefficient (R^2)	iLOQ (ng/L)		
	Off-line SPE 0.5/50 µg/L		On-line SPE 10 ng/L	Direct injection 50 ng/L		Off-line SPE	On-line SPE	Direct injection
PFBA	1	1	7	11	> 0.9981	10	60	1.0
PFPeA	1	1	3	4	> 0.9978	10	2.5	0.7
PFHxA	2	1	1	3	> 0.9988	10	1.5	0.7
PFHpA	1	1	2	3	> 0.9980	10	1.5	0.1
PFOA	1	1	2	6	> 0.9986	10	1.0	0.9
PFNA	2	1	7	12	> 0.9989	5	1.0	0.1
PFDA	1	1	10	18	> 0.9972	20	1.0	0.1
PFUdA	1	1	7	17	> 0.9984	35	1.0	1.0
PFDoA	2	2	20	20	> 0.9975	35	2.0	10
PFTrDA	2	1	3	6	> 0.9953	50	5.0	40
PFBS	1	1	2	1	> 0.9986	10	0.5	0.5
PFPeS	1	1	1	6	> 0.9977	50	0.5	0.1
PFHxS	1	1	1	6	> 0.9988	25	0.5	0.1
PFHpS	1	1	9	7	> 0.9989	10	0.1	0.1
PFOS	2	1	8	9	> 0.9977	30	0.1	0.2
PFNS	2	1	11	5	> 0.9969	15	0.2	0.2
PFDS	2	1	6	10	> 0.9971	20	0.1	1.3
PFUdS	4	3	13	16	> 0.9970	20	5.0	10
PFDoS	2	1	18	20	> 0.9954	10	5.0	15
PFTrDS	3	1	20	20	> 0.9951	25	5.0	50

As presented in Table 4.5.2, linearity was satisfactory with determination coefficients greater than 0.9951. The precision, in terms of intra-day RSD, was evaluated for the chromatographic method used for injecting off-line SPE extracts, through the injection of standards at two concentration levels, 0.5 and 50 µg/L, providing values below 4 and 3%, respectively. For on-line SPE and direct injection where the sample is directly submitted to the instrumental protocol, the repeatability for the injection of standards was satisfactory (below 20%) although a clear worsening in this parameter was observed for longest (C >9) carbon chain congeners. The iLOQs were estimated between 5-50, 0.1-5 and 0.1 to 50 ng/L for off-line SPE, on-line SPE and direct injection instrumental methodologies, respectively. The only exception was PFBA in on-line SPE achieving an iLOQ of 60 ng/L due to the abovementioned blank contamination issues (see section 3.5.1). It must be noted that iLOQs are very close to mLOQs in on-line SPE and direct injection approaches. All methods presented lower mLOQ for short-chain PFAS in comparison with the high-molecular weight congeners.

Table 4.5.3. Trueness, precision and mLOQ for direct injection method in different drinking water samples (n=5).

Compounds	Accuracy (%RSD) [1]		mLOQ (ng/L)	
	Tap water	Bottled water	Tap water	Bottled water
PFBA	119% (17)	156% (17)	9.5	9.0
PFPeA	82% (5)	109% (18)	4.6	1.5
PFHxA	86% (5)	115% (8)	1.2	3.1
PFHpA	88% (10)	110% (16)	1.5	0.7
PFOA	95% (6)	125% (11)	1.1	2.3
PFNA	105% (10)	101% (8)	2.6	1.0
PFDA	78% (2)	83% (10)	1.0	1.9
PFUdA	46% (9)	67% (12)	5.0	1.5
PFDoA	31% (9)	49% (24)	6.0	5.5
PFTrDA	29% (15)	-	10	32
PFBS	94% (6)	93% (4)	1.2	1.2
PFPeS	83% (5)	83% (5)	1.7	1.2
PFHxS	90% (5)	97% (7)	1.3	2.6
PFHpS	106% (6)	96% (7)	2.5	5.5
PFOS	85% (1)	96% (8)	4.5	6.4
PFNS	36% (9)	76% (19)	4.3	5.5
PFDS	41% (11)	52% (11)	6.3	6.5
PFUdS	36% (19)	31% (27)	20	24
PFDoS	51% (28)	-	25	45
PFTrDS	52% (20)	-	70	75

[1]Evaluated at 50 ng/L addition level

In summary, the on-line SPE instrumental method presented some drawbacks due to PFBA contamination and a low sensitivity and repeatability for long-chain PFAS. In direct injection method, the PFBA blank issues were avoided (through the use of the delay column), however

sensitivity was not appropriate for ≥C11 PFAS, which produced iLOQ >1.5 ng/L set as initial objective of this work (i.e. 30% of the result of dividing the total nominal 100 ng/L limit set by Directive 2020/2184/EU by the 20 regulated congeners). The accuracy and mLOQs of both direct injection and on-line SPE methods are provided in supplementary information (Table 4.5.3 and 4.5.4). The evaluated accuracy was not adequate for some congeners using both methods, (<70%) being the lowest values found for the most hydrophobic PFAS. Most of PFASs were corrected with their isotopologues, but the absence of IS for the most hydrophobic PFAS (PFTrDA and PFSAs (C9-C13) together with the low sensitivity of these compounds, may could justify the low accuracies. Nevertheless, direct injection could be particularly useful as a fast-screening method due to its simplicity. Although the iLOQs were the highest for off-line SPE (Table 4.5.2), after a complete sample processing, a concentration factor of 1,000 was achieved allowing the lowest mLOQs. Thus, off-line SPE became the only method that could match the regulatory objectives and was, therefore, fully validated (see section 3.5.3).

Table 4.5.4. Trueness, precision and mLOQ for on-line SPE method in different drinking water samples (n=5).

Compounds	Accuracy (%RSD) [1]		mLOQ (ng/L)	
	Tap water	Bottled water	Tap water	Bottled water
PFBA	-	-	-	-
PFPeA	105% (12)	98% (11)	2.3	2.2
PFHxA	112% (11)	101% (15)	2.5	2.0
PFHpA	106% (9)	92% (8)	3.2	1.5
PFOA	94% (6)	90% (7)	1.6	1.1
PFNA	97% (12)	101% (7)	2.2	2.3
PFDA	104% (16)	88% (5)	3.8	2.3
PFUdA	72% (14)	80% (9)	3.1	2.9
PFDoA	58% (18)	71% (12)	2.0	3.8
PFTrDA	41% (20)	62% (13)	8.6	9.9
PFBS	89% (7)	90% (11)	1.6	1.3
PFPeS	97% (12)	102% (8)	3.9	3.1
PFHxS	112% (8)	101% (13)	4.3	3.0
PFHpS	107% (14)	98% (11)	4.1	4.3
PFOS	92% (12)	87% (16)	5.7	6.9
PFNS	80% (14)	82% (8)	7.3	11
PFDS	74% (16)	90% (9)	7.9	12
PFUdS	71% (20)	75% (17)	8.9	17
PFDoS	48% (18)	53% (12)	9.1	21
PFTrDS	42% (15)	50% (14)	10	26

[1]Evaluated at 50 ng/L addition level

4.5.3. Validation of the off-line SPE-LC-MS/MS methodology

Accuracy, precision and mLOQs were evaluated at 3 concentration levels (1, 10 and 100 ng/L) with real matrices. The experiments at high and medium-levels (10 and 100 ng/L) were performed with tap water, however due to native levels of PFAS in that matrix, experiments at low level (1 ng/L) were performed with bottled water (Table 4.5.5). The chromatogram obtained for bottled water at 1 ng/L is shown in Figure 4.5.2. In all cases, recoveries between 70 and 120% and an RSD <20% were obtained. mLOQs, estimated from the lowest spiking level and considering blanks (see section 2.5), were lower than 0.3 ng/L for all congeners, which implies that the off-line SPE proposed method is suitable to fulfil the sensitivity requirements of the Directive 2020/2184/EU and goes far beyond (lower than 30% of Directive regulation).

Table 4.5.5. Off-line SPE mLOQs and accuracy and precision (n=5) obtained at low (1 ng/L), medium (10 ng/L) and high (100 ng/L) addition level.

Compounds	mLOQ (ng/L)	Accuracy (%RSD)		
		Bottled water [1]	Tap water [1]	
		1 ng/L	10 ng/L	100 ng/L
PFBA	0.15	91 (19)	107 (4)	114 (3)
PFPeA	0.30	113 (8)	107 (1)	106 (3)
PFHxA	0.10	91 (17)	106 (2)	109 (3)
PFHpA	0.20	115 (4)	107 (2)	111 (3)
PFOA	0.05	113 (16)	113 (13)	111 (3)
PFNA	0.15	118 (8)	104 (5)	111 (3)
PFDA	0.15	118 (4)	111 (2)	117 (4)
PFUdA	0.15	115 (8)	109 (2)	118 (6)
PFDoA	0.20	117 (3)	112 (3)	119 (10)
PFTrDA	0.10	112 (13)	71 (13)	90 (14)
PFBS	0.10	109 (7)	116 (2)	119 (5)
PFPeS	0.10	113 (2)	119 (3)	119 (8)
PFHxS	0.20	120 (8)	107 (3)	111 (3)
PFHpS	0.20	101 (4)	110 (2)	111 (3)
PFOS	0.15	112 (10)	90 (4)	119 (9)
PFNS	0.15	100 (15)	113 (9)	119 (11)
PFDS	0.25	104 (14)	105 (6)	108 (11)
PFUdS	0.10	118 (19)	86 (7)	83 (17)
PFDoS	0.10	115 (14)	73 (17)	70 (16)
PFTrDS	0.30	120 (9)	80 (10)	91 (8)

[1]Specific samples used in the validation are shown in Table 3.5.2

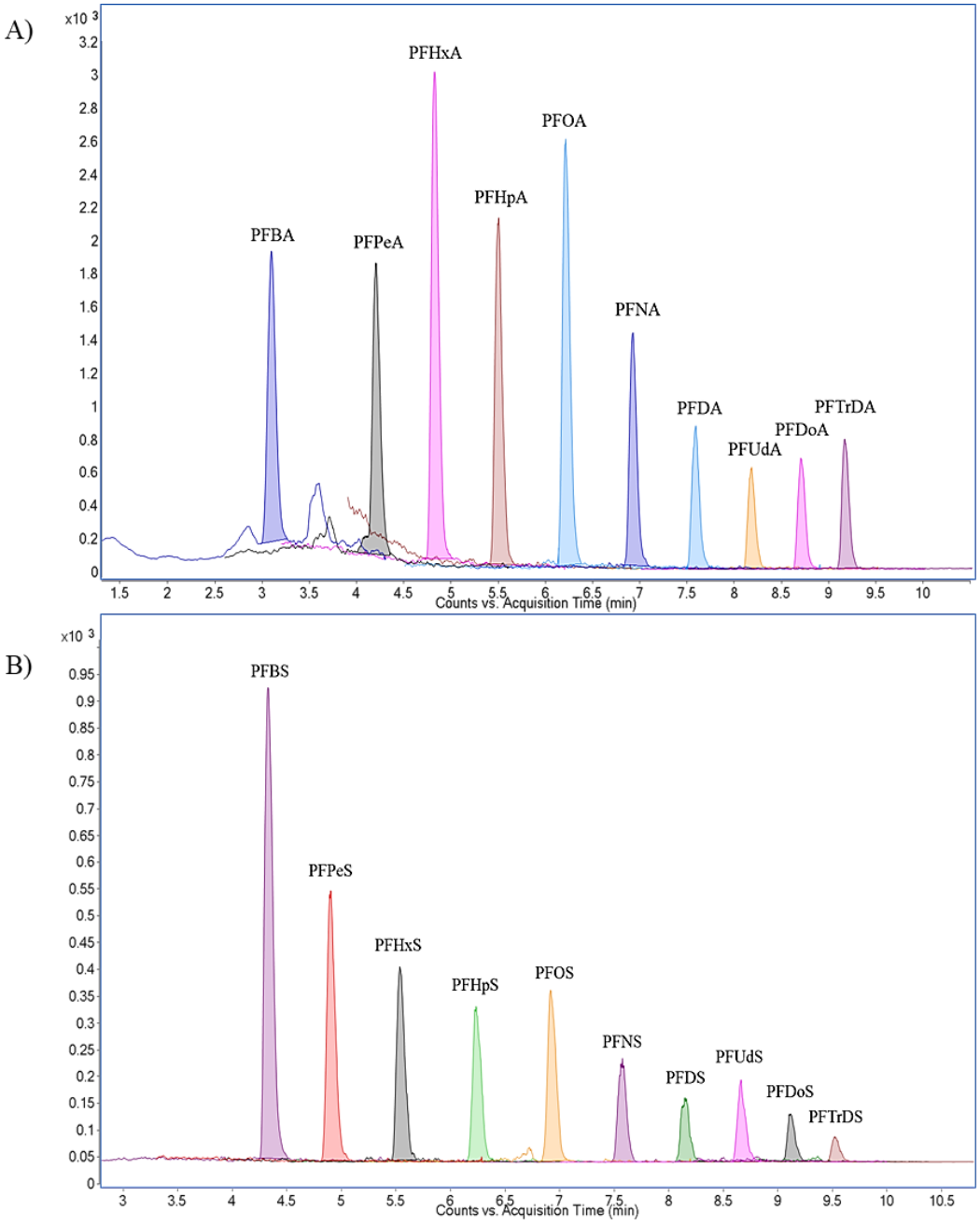

Figure 4.5.2. Chromatograms obtained after submitting bottled water (A) at low addition level (1 ng/L) to the final off-line SPE-LC-MS/MS methodology. A) PFCAs and B) PFSAs.

The influence of the water composition, in terms of salts content (hardness), was evaluated. Thus, matrix effect was calculated for a soft bottled water (A) and hard water (K) (Hessler & Lehner, 2011). Figure 4.5.3 shows the matrix effects evaluated depending on sample hardness. In general, PFCAs were more affected by sample hardness than PFSAs and the matrix effects were higher (signal suppression >30%) for long-chain PFAS (C >11). However, when method accuracy was evaluated for both soft and hard waters the obtained values were satisfactory (>80%) which revealed that the selected IS corrected efficiently these eventual matrix effects.

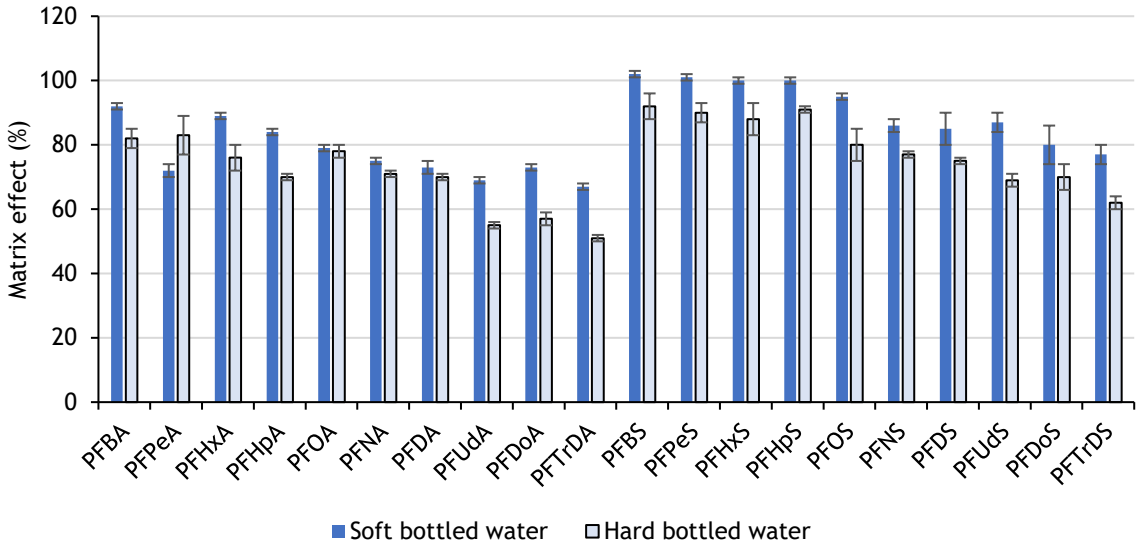

Figure 4.5.3. Influence of sample hardness on method matrix effect. Samples spiked at 100 ng/L (n=3).

4.5.4. Application to tap water and commercial bottled water

The cumulative concentrations of PFAS concentrations found in the samples (data about the samples is presented Table 3.5.3) are shown in Figure 4.5.4 and Figure 4.5.5, individual concentration of PFAS detected in each sample are reported in Table 4.5.6. PFAS were detected in most analysed samples, except in four commercial brands of mineral water where the concentration of PFAS was below mLOQs. In the remaining samples, the total concentrations ranged from 0.4 to 2.2 ng/L for mineral bottled water, and 1.0 to 48 ng/L for tap water samples. Therefore, none of the analysed samples exceed the limits stablished in the Directive 2020/2184/EU (EC, 2020). As expected, due to their high mobility/polarity, short chain PFAS (particularly PFCAs) were the most abundant ones. In fact, PFBA and PFHxA contribute, as average, the 70% of total PFAS concentration. PFBA and PFHxA concentrations ranged between 0.2 and 12 ng/L and 0.3 and 20 ng/L, and their detection frequencies were 83% and 91%, respectively. Regarding long-chain PFCAs (C8-C11), they presented lower detection frequencies (9-78%) and concentrations between 0.1 and 5.1 ng/L, being PFOA the most abundant one. On the other hand, short-chain PFSAs (C4-C7) presented lower detection frequencies (2 to 39%) and were quantified in concentrations ranging between 0.1 and 8.1 ng/L, being the highest values found for PFBS, analogously to what happened with PFBA. Finally, the only long-chain PFSAs detected was PFOS (detection frequency 20%) with concentrations ranging from 0.2 to 9.3 ng/L. These results, in terms of most abundant PFAS and concentration levels are comparable to those found in drinking water from different countries, including Spain (Gao et al., 2019; Kurwadkar et al., 2022; Schwanz et al., 2016; Wang et al., 2016).

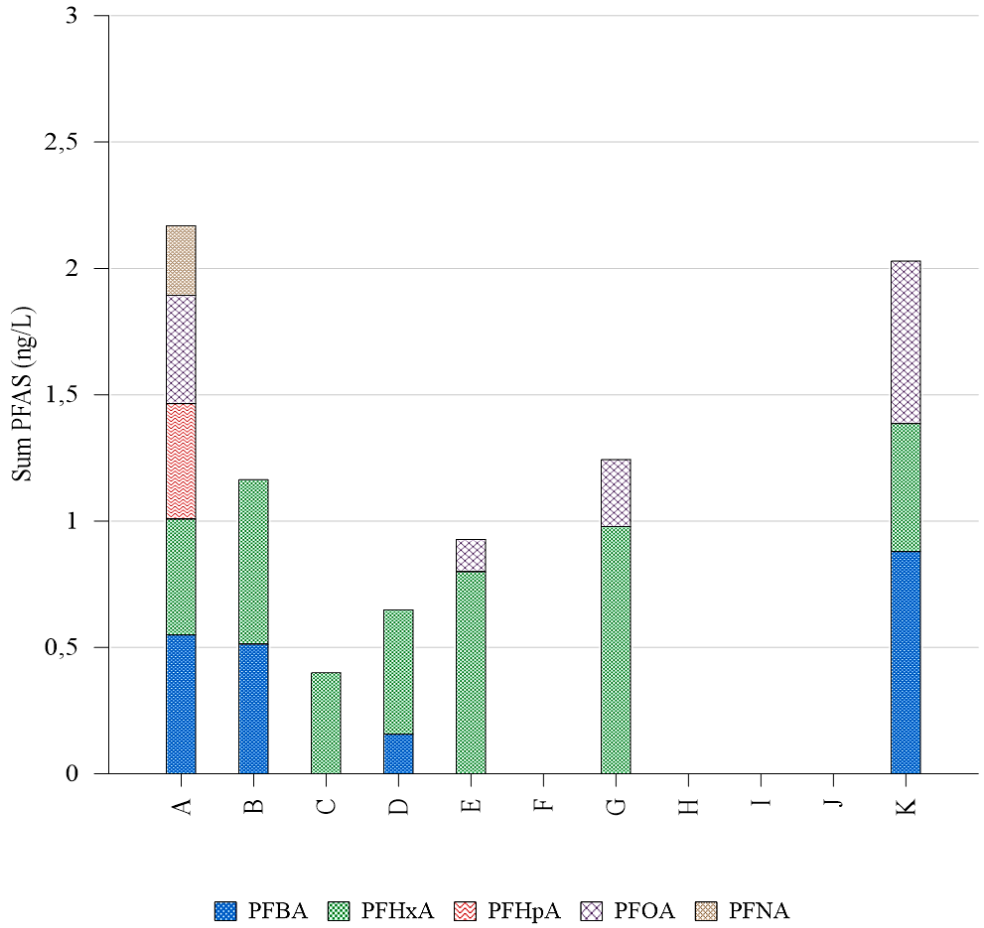

Figure 4.5.4. Stacked barplot of PFAS concentrations (ng/L) in bottled mineral waters.

The PFAS levels in tap water samples (either from Spain or elsewhere) from public facilities were similar with values in general under 20 ng/L (Figure 4.5.5, Table 4.5.6). However, Knoxville (TN), Berlin, Milan and Monterrey (at international level) and Santander and Cartelle (at Spanish level) presented higher values. Berlin, Milan and Monterrey are important metropolitan and industrial cities in their countries, conversely to Knoxville and Santander which are mid-industrialised cities with high tourism influx. Surprisingly, Cartelle which is a scarcely industrialised and populated village in the northwest of Spain, hardly affected by tourism, presented also high values of PFAS concentrations, specially PFHxA and PFHpA. In the city of Milan, where previous studies have reported the presence of PFAS in drinking water (Castiglioni et al., 2015), the concentration values are comparatively high, although below Directive 2020/2184/EU limits, pointing to the ubiquitous contamination by PFAS in the city. Knoxville also sought to improve drinking water treatment due to PFDoA contamination (up to 820 ng/L) in drinking water (UCMR3, 2021), however in our work moderate levels of PFAS, specially PFBA (11 ng/L) were still detected. The levels found in commercial mineral water are significantly lower than in tap water (PFAS levels for bottled water were below 2.2 ng/L), these results are in agreement with reported in literature (Chow et al., 2021; Ünlü Endirlik et al., 2019), pointing to the fact that aquifers used in such cases are much less impacted by PFAS contamination.

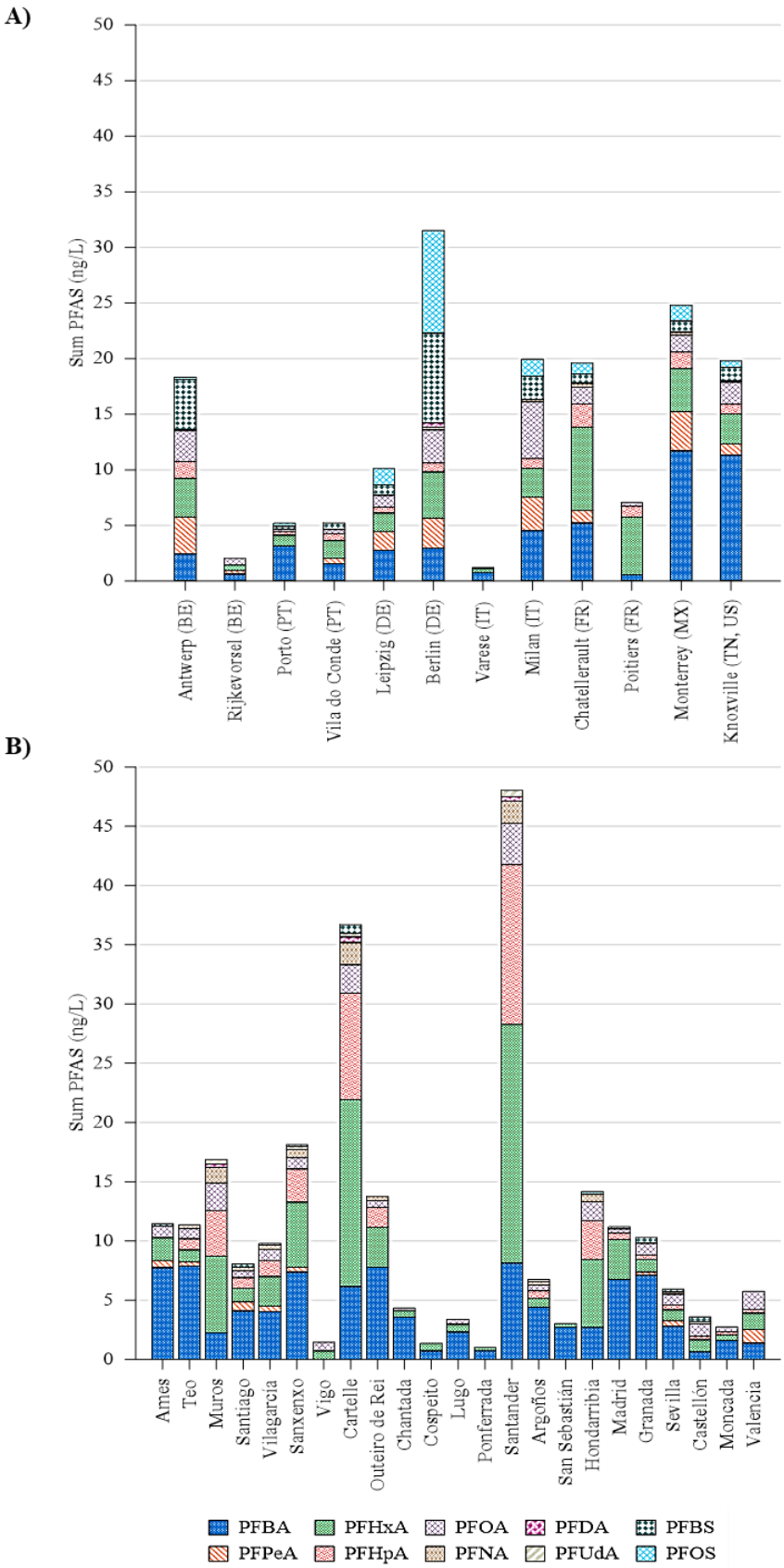

Figure 4.5.5. Stacked barplot of PFAS concentrations (ng/L) on A) international and B) Spanish tap water samples.

Table 4.5.6. Concentrations of PFAS (ng/L) in commercial bottled water (A-K) and tap water samples.

Sample	PFBA	PFPeA	PFHxA	PFHpA	PFOA	PFNA	PFDA	PFUdA	PFBS	PFPeS	PFHxS	PFHpS	PFOS	∑PFAS
A	0.6	<LOQ	0.5	0.5	0.4	0.3	<LOQ	<LOQ	<LOQ	<LOQ	<LOQ	<LOQ	<LOQ	**2.2**
B	0.5	<LOQ	0.7	<LOQ	<LOQ	<LOQ	<LOQ	<LOQ	<LOQ	<LOQ	<LOQ	<LOQ	<LOQ	**1.2**
C	<LOQ	<LOQ	0.4	<LOQ	<LOQ	<LOQ	<LOQ	<LOQ	<LOQ	<LOQ	<LOQ	<LOQ	<LOQ	**0.4**
D	0.2	<LOQ	0.5	<LOQ	<LOQ	<LOQ	<LOQ	<LOQ	<LOQ	<LOQ	<LOQ	<LOQ	<LOQ	**0.7**
E	<LOQ	<LOQ	0.8	<LOQ	0.1	<LOQ	<LOQ	<LOQ	<LOQ	<LOQ	<LOQ	<LOQ	<LOQ	**0.9**
F	<LOQ	<LOQ	<LOQ	<LOQ	<LOQ	<LOQ	<LOQ	<LOQ	<LOQ	<LOQ	<LOQ	<LOQ	<LOQ	**<LOQ**
G	<LOQ	<LOQ	1.0	<LOQ	0.3	<LOQ	<LOQ	<LOQ	<LOQ	<LOQ	<LOQ	<LOQ	<LOQ	**1.2**
H	<LOQ	<LOQ	<LOQ	<LOQ	<LOQ	<LOQ	<LOQ	<LOQ	<LOQ	<LOQ	<LOQ	<LOQ	<LOQ	**<LOQ**
I	<LOQ	<LOQ	<LOQ	<LOQ	<LOQ	<LOQ	<LOQ	<LOQ	<LOQ	<LOQ	<LOQ	<LOQ	<LOQ	**<LOQ**
J	<LOQ	<LOQ	<LOQ	<LOQ	<LOQ	<LOQ	<LOQ	<LOQ	<LOQ	<LOQ	<LOQ	<LOQ	<LOQ	**<LOQ**
K	0.9	<LOQ	0.5	<LOQ	0.6	<LOQ	<LOQ	<LOQ	<LOQ	<LOQ	<LOQ	<LOQ	<LOQ	**2.0**
Ames (ES)	7.7	0.6	1.9	<LOQ	1.0	<LOQ	<LOQ	<LOQ	0.2	<LOQ	<LOQ	<LOQ	<LOQ	**11.5**
Teo (ES)	7.9	0.3	1.0	0.9	0.9	0.3	<LOQ	<LOQ	<LOQ	<LOQ	<LOQ	<LOQ	<LOQ	**11.4**
Muros (ES)	2.3	<LOQ	6.4	3.9	2.3	1.3	0.3	0.4	<LOQ	<LOQ	<LOQ	<LOQ	<LOQ	**16.9**
Santiago (ES)	4.1	0.8	1.1	0.9	0.6	0.3	<LOQ	<LOQ	0.3	<LOQ	<LOQ	<LOQ	<LOQ	**8.1**
Vilagarcía (ES)	4.0	0.5	2.5	1.4	0.9	0.4	<LOQ	<LOQ	0.1	<LOQ	<LOQ	<LOQ	<LOQ	**9.8**
Sanxenxo (ES)	7.3	0.5	5.5	2.8	1.0	0.7	<LOQ	0.3	0.2	<LOQ	<LOQ	<LOQ	<LOQ	**18.1**
Vigo (ES)	<LOQ	<LOQ	0.70	<LOQ	0.8	<LOQ	<LOQ	<LOQ	<LOQ	<LOQ	<LOQ	<LOQ	<LOQ	**1.5**
Cartelle (ES)	6.1	<LOQ	15.8	9.0	2.4	1.9	0.5	0.3	0.7	<LOQ	<LOQ	<LOQ	<LOQ	**36.7**
Outeiro de Rei (ES)	7.8	<LOQ	3.4	1.7	0.6	0.3	<LOQ	<LOQ	<LOQ	<LOQ	<LOQ	<LOQ	<LOQ	**13.7**
Chantada (ES)	3.6	<LOQ	0.5	<LOQ	0.2	<LOQ	<LOQ	<LOQ	<LOQ	<LOQ	<LOQ	<LOQ	<LOQ	**4.3**
Cospeito (ES)	0.7	<LOQ	0.7	<LOQ	<LOQ	<LOQ	<LOQ	<LOQ	<LOQ	<LOQ	<LOQ	<LOQ	<LOQ	**1.4**
Lugo (ES)	2.3	<LOQ	0.7	<LOQ	0.4	<LOQ	<LOQ	<LOQ	<LOQ	<LOQ	<LOQ	<LOQ	<LOQ	**3.4**
Ponferrada (ES)	0.7	<LOQ	0.3	<LOQ	<LOQ	<LOQ	<LOQ	<LOQ	<LOQ	<LOQ	<LOQ	<LOQ	<LOQ	**1.0**
Santander (ES)	8.1	<LOQ	20.1	13.5	3.5	1.9	0.4	0.5	<LOQ	<LOQ	<LOQ	<LOQ	<LOQ	**48.0**
Argoños (ES)	4.4	<LOQ	0.7	0.6	0.5	0.3	<LOQ	0.2	<LOQ	<LOQ	<LOQ	<LOQ	<LOQ	**6.8**
San Sebastián (ES)	2.7	<LOQ	0.3	<LOQ	<LOQ	<LOQ	<LOQ	<LOQ	<LOQ	<LOQ	<LOQ	<LOQ	<LOQ	**3.0**
Hondarribia (ES)	2.7	<LOQ	5.8	3.3	1.6	0.6	<LOQ	<LOQ	<LOQ	<LOQ	<LOQ	<LOQ	0.2	**14.2**
Madrid (ES)	6.8	<LOQ	3.4	0.5	0.3	<LOQ	<LOQ	<LOQ	0.2	<LOQ	<LOQ	<LOQ	<LOQ	**11.2**
Granada (ES)	7.1	0.3	1.1	0.4	1.0	<LOQ	<LOQ	<LOQ	0.5	<LOQ	<LOQ	<LOQ	<LOQ	**10.3**
Sevilla (ES)	2.8	0.5	0.9	0.4	0.9	0.2	<LOQ	<LOQ	0.3	<LOQ	<LOQ	<LOQ	<LOQ	**5.9**
Castellón (ES)	0.6	<LOQ	1.0	0.3	1.1	<LOQ	<LOQ	0.2	0.4	<LOQ	<LOQ	<LOQ	<LOQ	**3.6**
Moncada (ES)	1.6	<LOQ	0.5	0.2	0.4	<LOQ	<LOQ	<LOQ	<LOQ	<LOQ	<LOQ	<LOQ	<LOQ	**2.7**
Valencia (ES)	1.4	1.2	1.3	0.4	1.5	<LOQ	<LOQ	<LOQ	<LOQ	<LOQ	<LOQ	<LOQ	<LOQ	**5.7**
Antwerp (BE)	2.4	3.3	3.4	1.6	2.7	0.2	<LOQ	<LOQ	4.5	<LOQ	0.4	<LOQ	0.2	**18.7**
Rijkevorsel (BE)	0.6	0.3	0.5	<LOQ	0.6	<LOQ	<LOQ	<LOQ	<LOQ	<LOQ	<LOQ	<LOQ	<LOQ	**2.0**
Porto (PT)	3.2	<LOQ	0.9	0.3	0.3	<LOQ	<LOQ	<LOQ	0.3	<LOQ	0.2	<LOQ	0.3	**5.4**
Vila do Conde (PT)	1.6	0.5	1.6	0.6	0.4	<LOQ	<LOQ	<LOQ	0.6	<LOQ	<LOQ	<LOQ	<LOQ	**5.2**
Leipzig (DE)	2.8	1.7	1.6	0.6	1.1	<LOQ	<LOQ	<LOQ	1.0	<LOQ	0.3	<LOQ	1.4	**10.4**
Berlin (DE)	3.0	2.7	4.1	0.8	3.0	0.3	0.4	<LOQ	8.1	1.8	6.8	0.3	9.3	**40.3**
Varese (IT)	0.8	<LOQ	0.3	<LOQ	0.1	<LOQ	<LOQ	<LOQ	<LOQ	<LOQ	<LOQ	<LOQ	<LOQ	**1.2**
Milan (IT)	4.5	3.1	2.6	0.9	5.1	0.2	<LOQ	<LOQ	2.1	0.2	1.1	<LOQ	1.5	**21.2**
Chatellerault (FR)	5.2	1.2	7.5	2.1	1.5	0.3	<LOQ	<LOQ	0.8	0.1	1.6	<LOQ	1.0	**21.4**
Poitiers (FR)	0.6	<LOQ	5.2	0.9	0.4	<LOQ	<LOQ	<LOQ	<LOQ	<LOQ	<LOQ	<LOQ	<LOQ	**7.1**
Monterrey (MX)	11.7	3.6	3.8	1.5	1.5	0.3	<LOQ	<LOQ	1.0	0.4	2.1	<LOQ	1.4	**27.3**
Knoxville (USA)	11.3	1.0	2.7	0.8	2.0	0.2	<LOQ	<LOQ	1.1	<LOQ	0.4	<LOQ	0.6	**20.2**

PFDOA, PFTrDA, PFNS, PFDS, PFUdS, PFDoS and PFTrDS concentrations were below mLOQ in all samples

4.6. INSIGHTS INTO THE APPLICATION OF THE ANODIC OXIDATION PROCESS FOR THE REMOVAL OF PER- AND POLYFLUOROALKYL SUBSTANCES (PFAS) IN WATER MATRICES

4.6.1. Degradation of ultrashort- to long-chain PFAS (C1-C13)

A mixture of 24 C1-C13 PFAS in UPW, each one with a content of 0.2 µg/L (total PFAS content of 4.8 µg/L), was subjected to the AO-BDD process at a current density of 100 mA/cm^2.

4.6.1.1. Considerations on the initial PFAS removal

Of the 24 PFAS under analysis, 7 of them, namely PFNS (C9), PFDS (C10), PFUdS (C11), PFDoA (C12), PFDoS (C12), PFTrDA (C13), and PFTrDS (C13), were not detected in solution at a reaction time of 0 min, i.e., just after solution recirculation in the system for ~20 min before the supply of electrical current. In addition, the content of other long-chain PFAS, namely PFOA (C8), PFOS (C8), PFNA (C9), and PFUdA (C11), was diminished at t = 0 min by ~53-69%. Because of these initial decreases of PFAS concentration, the relative total PFAS content at t = 0 min was ~62% and not the nominal spiked value (Figure 4.6.1a). A control test involving the recirculation of the PFAS solution in the system for 4h without applying current revealed that the PFAS decay at t = 0 min was similar to that obtained in the remaining trials. This PFAS content persisted throughout the entire duration of the test, with a maximum variation of ±5%.

The initial PFAS removal can be attributed to the total or partial physisorption/chemisorption of PFAS to the hydrophobic hydrogenated BDD surface (Ferro & De Battisti, 2002), as well as to the glass vessel acting as homogenization reservoir, although the latter may play a minor role due to the hydrophilic nature of the glass (Bernett & Zisman, 1969). The tendency of PFAS to adsorb is affected by their chain length and headgroup (i.e., carboxylic *versus* sulfonic moieties). Long-chain PFAS with ≥8 total carbon atoms in their structure, or ≥7 carbon atoms in the perfluoroalkyl chain for PFCA, were the ones that absorbed. Note that in a PFSA, the perfluoroalkyl chain length (PCL) has the same number of C atoms as the whole molecular structure. By contrast, the PCL is 1 C shorter (1 CF_2 group shorter) in a PFCA with the same total number of C atoms. Generally, the longer the chain length of a PFAS, the higher its adsorption ability. This can be attributed to a growing hydrophobicity of PFAS as the chain length increases, as illustrated by the increasing n-octanol-water distribution coefficients (D_{ow}) (Table 4.6.1), ultimately favouring PFAS adsorption on hydrophobic surfaces. PFDA (C10) was an exception, for which the initial content was not diminished, but this result cannot be explained in the light of its D_{ow}. The gain of PFAS-BDD interactions for longer-chain PFAS was confirmed in Nienhauser et al. (2022) by the determination of a higher wettability (measurement of the contact angle) of the hydrophobic BDD electrode in the presence of longer-chain PFAS. It should also be mentioned that the higher adsorption capacity of long-chain PFAS compared to short-chain PFAS has been observed regardless of the adsorbent (Gagliano et al., 2020). A higher interaction between glass and PFAS for longer-chain PFAS is also expected. Point et al. (2019) observed a high adsorption of PFAS with 10 or more carbons in their backbone to the walls of glass in contrast to shorter-chain PFAS, and Lath et al. (2019); Zenobio et al. (2022) observed the adsorption of PFOA (C8) and PFOS (C8) to the glass vessel walls, although typically by <23%. With regard to PFAS headgroup, it is possible to infer that PFSA underwent a stronger physisorption/chemisorption than their PFCA counterparts since C9-C13 PFSA were totally

adsorbed before the reaction start, and this happened only for C12-C13 PFCA. Nevertheless, the log D_{ow} values in Table 4.6.1 point to the fact that PFSA are more hydrophilic than their PFCA analogues regardless of the chain length, which is corroborated by shorter retention of PFSA on the reversed-phase LC column (Table 3.6.4). Therefore, PFAS initial sorption seems to be influenced by other mechanisms besides hydrophobicity.

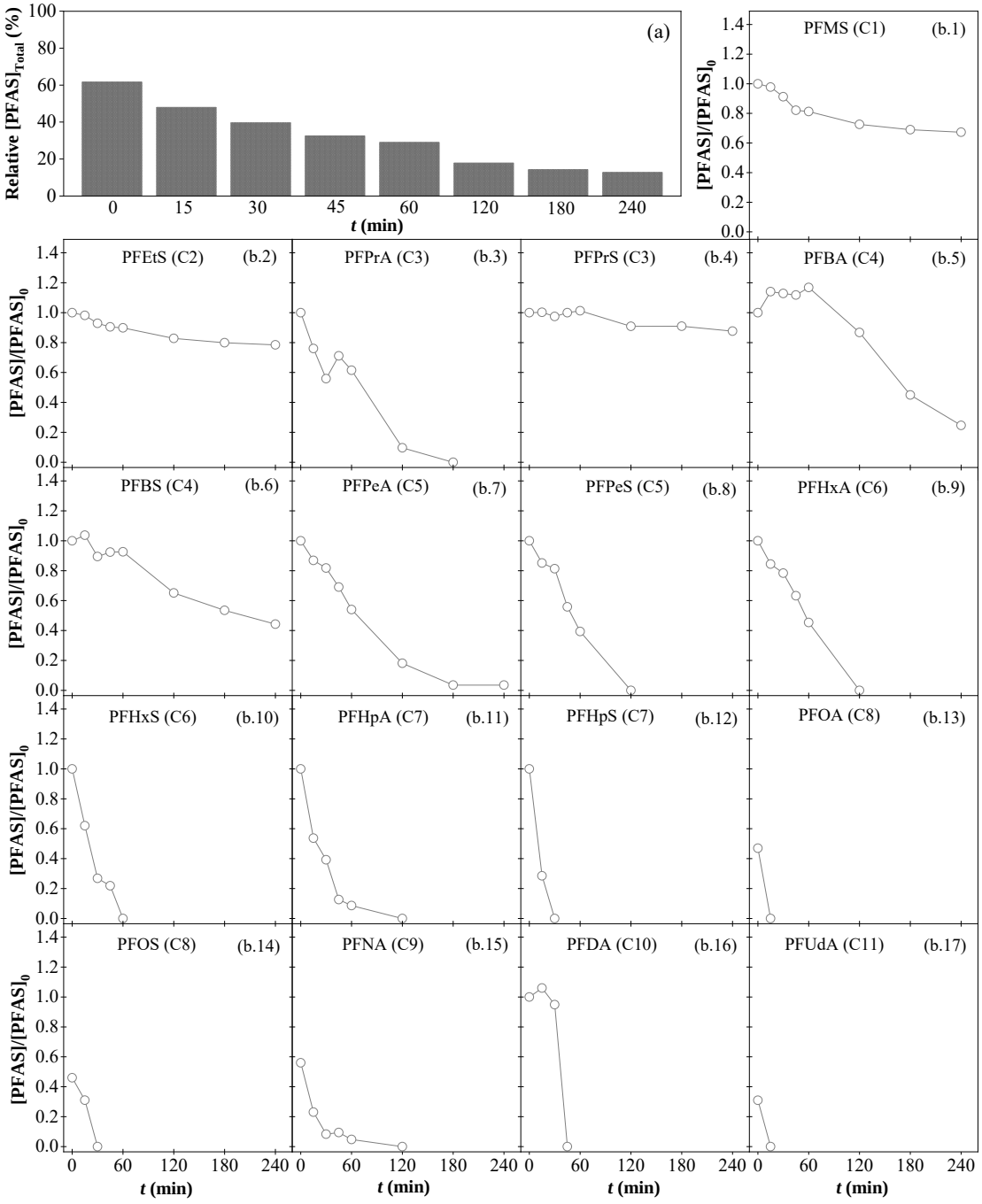

Figure 4.6.1. Degradation of a mixture of 24 C1-C13 PFAS (0.2 µg/L each) in UPW by the AO-BDD process at a current density of 100 mA/cm^2 with the conditions of [Na_2SO_4] = 30mM, pH = 7.0±0.2 and T = 25±1°C. (a) relative concentration decay of total PFAS, and (b) normalized individual PFAS concentration decay. PFNS (C9), PFDS (C10), PFUdS (C11), PFDoA (C12), PFDoS (C12), PFTrDA (C13), and PFTrDS (C13) are not displayed since they were not detected in the solution at t = 0 min.

Table 4.6.1. Summary of physicochemical properties of PFAS under study.

Compound	Acronym	Total no. C atoms [a]	PCL no. C atoms [b]	MW [c] (g/mol)	Log D_{ow} (pH 7.4) (Radjenovic et al, 2020)	α_p anion (C m^2/V)	α_p acid (C m^2/V)	E_{LUMO} - E_{HOMO} (Hartrees)	D [d] ($\times 10^{-6}$ cm^2/s)	pK_a [e]	E^o anion (V/SHE)	E^o acid (V/SHE)
Perfluoromethanesulfonic acid	PFMS	C1	C1	150.08	-3.88	-	-	-	8.3	-3.43 (Marselli et al, 2003)	-	-
Perfluoroethanesulfonic acid	PFEtS	C2	C2	200.09	-3.12	-	-	-	7.0	-3.31 (Marselli et al, 2003)	-	-
Perfluoropropanoic acid	PFPrA	C3	C2	164.03	-2.24	-	-	-	7.8	0.37 (Marselli et al, 2003)	-	-
Perfluoropropanesulfonic acid	PFPrS	C3	C3	250.09	-2.37	-	-	-	6.1	-3.31 (Marselli et al, 2003)	-	-
Perfluorobutanoic acid	PFBA	C4	C3	214.04	-1.13	77.5 (Harris, 2009)	82.4 (Harris, 2009) or 50 (Panizza et al, 2009)	0.235 (Panizza et al, 2009)	6.7	0.05 to 0.7 (Duinslaeger et al, 2022; Lin et al, 2018)	2.96 (Harris, 2009)	3.65 (Harris, 2009)
Perfluorobutanesulfonic acid	PFBS	C4	C4	300.10	-1.56	107 (Harris, 2009)	115 (Harris, 2009) or 73 (Panizza et al, 2009)	0.242 (Panizza et al, 2009)	5.5	-3.32 to 0.14 (Marselli et al, 2003; Lin et al, 2018; Liu et al, 2019)	3.71 (Harris, 2009)	3.96 (Harris, 2009)
Perfluoropentanoic acid	PFPeA	C5	C4	264.05	-0.34	-	62 (Panizza et al, 2009)	0.221 (Panizza et al, 2009)	5.9	-0.10 (Lin et al. 2018)	-	-
Perfluoropentanesulfonic acid	PFPeS	C5	C5	350.10	-1.08	-	-	-	5.0	-3.32 to 0.3 (Marsell et al, 2003; Nienhauser et al, 2022)	-	-
Perfluorohexanoic acid	PFHxA	C6	C5	298.06	0.15	109 (Niu et al, 2012)	113 (Harris, 2009) or 72 (Panizza et al, 2009)	0.198 (Panizza et al, 2009)	5.5	-0.17 to 0.16 (Lin et al, 2018; Liu et al, 2019)	2.97 (Harris, 2009)	3.70 (Harris, 2009)
Perfluorohexanesulfonic acid	PFHxS	C6	C6	400.11	-0.54	138 (Harris, 2009)	146 (Harris, 2009) or 115 (Panizza et al, 2009)	0.192 (Panizza et al, 2009)	4.7	-3.32 to 0.14 (Marselli et al, 2003; Lin et al, 2018; Liu et al, 2019)	3.72 (Harris, 2009)	4.00 (Harris, 2009)
Perfluoroheptanoic acid	PFHpA	C7	C6	364.06	1.11	124 (Harris, 2009)	129 (Harris, 2009) or 85 (Panizza et al, 2009)	0.172 (Panizza et al, 2009)	4.9	-0.20 to -0.19 (Lin et al, 2018; Liu et al, 2019)	2.96 (Harris, 2009)	3.58 (Harris, 2009)
Perfluoroheptanesulfonic acid	PFHpS	C7	C7	450.12	0.10	-	-	-	4.3	-3.32 to 0.3 (Harris, 2009)	-	-

[a]Total no. C atoms: total number of C atoms in the structure. [b]PCL no. C atoms: number of C atoms in the perfluoroalkyl chain length. [c]MW: Molecular weight. [d]Diffusion coefficient calculated by the Hayduk-Laudie equation (Hayduk & Laudie, 1974). [e]Both experimental and theoretically predicted values were considered

Table 4.6.1. Summary of physicochemical properties of PFAS under study (cont.).

Compound	Acronym	Total no. C atoms [a]	PCL no. C atoms [b]	MW [c] (g/mol)	Log D_{ow} (pH 7.4) (Radjenovic et al, 2020)	α_p anion (C m^2/V)	α_p acid (C m^2/V)	E_{LUMO} - E_{HOMO} (Hartrees)	D [d] ($\times 10^{-6}$ cm^2/s)	pK_a [e]	$E°$ anion (V/SHE)	$E°$ acid (V/SHE)
Perfluorooctanoic acid	PFOA	C8	C7	414.07	1.82	140 (Harris, 2009)	144 (Harris, 2009) or 97 (Panizza et al, 2009)	0.155 (Panizza et al, 2009)	4.6	-0.21 to 0.7 (Duinslaeger et al, 2022; Lin et al, 2018; Liu et al, 2019)	2.91 (Harris, 2009)	3.71 (Harris, 2009)
Perfluorooctanesulfonic acid	PFOS	C8	C8	500.13	0.66	170 (Harris, 2009)	177 (Harris, 2009) or 117 (Panizza et al, 2009)	0.165 (Panizza et al, 2009)	4.1	-3.32 to 0.14 (Marselli et al, 2003; Lin et al, 2018; Liu et al, 2019; Niu et al, 2013)	3.74 (Harris, 2009)	4.02 (Harris, 2009)
Perfluorononanoic acid	PFNA	C9	C8	464.08	2.84	155 (Harris, 2009)	145 (Harris, 2009)	-	4.3	-0.21 to 0.52 (Marselli et al, 2003; Lin et al, 2018; Liu et al, 2019)	3.12 (Harris, 2009)	3.76 (Harris, 2009)
Perfluorononanesulfonic acid	PFNS	C9	C9	550.14	1.35	-	-	-	3.9	<-3.24 (Marselli et al, 2003)	-	-
Perfluorodecanoic acid	PFDA	C10	C9	514.08	3.62	-	-	-	4.0	-0.22 to -0.21 (Lin et al, 2018; Liu et al, 2019)	-	-
Perfluorodecanesulfonic acid	PFDS	C10	C10	600.15	2.13	-	-	-	3.7	-3.24 to 0.14 (Marselli et al, 2003; Lin et al, 2018; Liu et al, 2019)	-	-
Perfluoroundecanoic acid	PFUdA	C11	C10	564.09	4.23	-	-	-	3.8	-0.21 to 0.52 (Marselli et al, 2003)	-	-
Perfluoroundecanesulfonic acid	PFUdS	C11	C11	600.15	2.98	-	-	-	3.7	< -3.24 (Marselli et al, 2003)	-	-
Perfluorododecanoic acid	PFDoA	C12	C11	614.10	4.58	-	-	-	3.6	-0.21 to 0.8 (Duinslaeger et al, 2022; Liu et al, 2019)	-	-
Perfluorododecanesulfonic acid	PFDoS	C12	C12	700.16	3.55	-	-	-	3.4	> -3.24 (Marselli et al, 2003)	-	-
Perfluorotridecanoic acid	PFTrDA	C13	C12	664.10	4.97	-	-	-	3.5	-3.24 to -0.22 (Marselli et al, 2003; Lin et al, 2018)	-	-
Perfluorotridecanesulfonic acid	PFTrDS	C13	C13	750.17	3.93	-	-	-	3.2	> -3.24 (Marselli et al, 2003)	-	-

[a]Total no. C atoms: total number of C atoms in the structure. [b]PCL no. C atoms: number of C atoms in the perfluoroalkyl chain length. [c]MW: Molecular weight. [d]Diffusion coefficient calculated by the Hayduk-Laudie equation (Hayduk & Laudie, 1974). [e]Both experimental and theoretically predicted values were considered

PFAS potentially adsorbed on the BDD surface before the reaction began may have been readily degraded upon the start of the AO-BDD process. The PFAS adsorption to the glass walls may have been irreversible (Zenobio et al., 2022). The non-adsorbed PFAS underwent different degradation rates highly influenced by their chain length and headgroup, as follows.

4.6.1.2. Degradation of ultrashort- to long-chain PFAS (C1-C13) as a function of perfluoroalkyl chain length

The global PFAS decay was steeper during the first 120 min of reaction (Figure 4.6.1) and can be attributed to faster degradation of PFAS with a longer PCL (≥PCL C5) (Figures 4.6.1b.7-b.17). In turn, the total PFAS removal was low for reaction times >120 min (Figure 4.6.1a) and can be related to the slow or null removal of PFAS with a shorter PCL (≤PCL C4), in some cases affected by the generation of shorter-chain PFAS from the breakage of longer-chain PFAS (Figures 4.6.1b.1-b.6). Overall, the larger the PCL of a PFAS, the higher its degradation rate, considering PFAS with the same headgroup. For example, the k was about 1.4, 3.9, 5.0, and 7.8-fold larger for PFNA (PCL C8) compared to PFHpA (PCL C6), PFHxA (PCL C5), PFPeA (PCL C4), and PFBA (PCL C3), respectively, and about 2.8 and 8.7-fold higher for PFHxS (PCL C6) compared to PFPeS (PCL C5) and PFBS (PCL C4), respectively (Table 4.6.2). The higher degradability of longer-chain PFAS may be intimately related to the higher affinity of these PFAS to be physiosorbed/chemisorbed/electrosorbed on the hydrophobic BDD surface due to their higher hydrophobicity according to the K_{ow} values (Table 4.6.1). The higher degradability of PFAS with longer PCL may be intimately related to the higher affinity of these PFAS to be physisorbed/chemisorbed/electrosorbed on the hydrophobic BDD surface due to their higher hydrophobicity according to the D_{ow} values. This may have enhanced PFAS concentration at the BDD surface, ultimately promoting their oxidation. Furthermore, the molecular polarizability (αp) and the frontier molecular orbital energies, which are good indicators of the reactivity of a molecule, can also explain the higher ability of longer-PCL PFAS to oxidation. Table 4.6.1 shows an increase in the αp of PFAS (deprotonated (αp anion) and protonated (αp acid)) as their PCL increases. In detail, the αp measures the ability of compounds to form a dipole in response to an external electric field (Kušić et al., 2009), and thus this trend indicates a higher capability of longer-PCL PFAS to transfer electrons faster and ultimately oxidize more quickly. With regard to the frontier molecular orbital energies, the gap between the energy of the highest occupied molecular orbital (E_{HOMO}) and the energy of the lowest unoccupied molecular orbital (E_{LUMO}), referred to as E_{LUMO} - E_{HOMO}, is analysed. E_{HOMO} and E_{LUMO} represent the ability of a molecule to donate or gain an electron, respectively. Consequently, E_{LUMO} - E_{HOMO} implies the molecule's stability in terms of redox reactivity (Kušić et al., 2009). The greater the E_{LUMO} - E_{HOMO}, the higher the molecule's stability. Table 4.6.1 shows lower E_{LUMO} - E_{HOMO} values for increasing chain lengths, thus supporting the faster degradation for longer-chain PFAS.

Table 4.6.2. Pseudo-first-order kinetic constants (k) of PFAS and corresponding residual variance (S^2_R) and coefficient of determination (R^2) for the degradation of PFAS in UPW by the AO-BDD process at a current density of 100 mA/cm^2 using different PFAS solutions: mixture of 24 C1-C13 PFAS (0.2 µg/L each), mixture of 8 C1-C8 PFAS (2.0 µg/L each), and individual solutions (2.0 µg/L each).

	UPW - j = 100 mA/cm^2														
	24 C1-C13 PFAS with 0.2 µg/L					8 C1-C8 PFAS with 2.0 µg/L					Individual PFAS with 2.0 µg/L				
	Time interval (min)	k (×10^{-3} /min)	S^2_R (µg^2/L^2)	R^2	C_0 (µg/L)	Time interval (min)	k (×10^{-3} /min)	S^2_R (µg^2/L^2)	R^2	C_0 (µg/L)	Time interval (min)	k (×10^{-3} /min)	S^2_R (µg^2/L^2)	R^2	C_0 (µg/L)
PFMS (C1)	Not adjusted					Not adjusted					Not adjusted				
PFEtS (C2)	Not adjusted					Not adjusted					Not adjusted				
PFPrA (C3)	**45-180** [a]	**21±5**	**5.4×10^{-4}**	**0.965**	**0.14**	**60-240** [a]	**4.7±0.9**	**1.2×10^{-1}**	**0.905**	**2.3**	**0-30**	**62±19**	**1.6×10^{-1}**	**0.920**	**2.0**
PFPrS (C3)	Not adjusted					Not adjusted					Not adjusted				
PFBA (C4)	**60-240** [a]	**7±1**	**7.5×10^{-4}**	**0.964**	**0.23**	**0-180**	**12±1**	**1.2×10^{-1}**	**0.963**	**2.0**	**0-120**	**26±2**	**4.7×10^{-2}**	**0.983**	**2.0**
PFBS (C4)	60-240 [a]	4.5±0.3	1.6×10^{-4}	0.969	0.19	0-240	3.3±0.2	2.1×10^{-2}	0.977	2.0	Not adjusted				
PFPeA (C5)	**0-240**	**11±1**	**1.5×10^{-3}**	**0.965**	**0.20**	-					-				
PFPeS (C5)	0-120	14±2	2.5×10^{-3}	0.907	0.20	-					-				
PFHxA (C6)	**0-180**	**14±2**	**2.4×10^{-3}**	**0.937**	**0.20**	-					-				
PFHxS (C6)	0-60	39±4	6.8×10^{-4}	0.972	0.20	-					-				
PFHpA (C7)	**0-120**	**38±3**	**3.7×10^{-4}**	**0.987**	**0.20**	-					-				
PFHpS (C7)	Not adjusted					-					-				
PFOA (C8)	**Not adjusted**					**Not adjusted**					**Not adjusted**				
PFOS (C8)	Not adjusted					Totally adsorbed before the beginning of the reaction					Totally adsorbed before the beginning of the reaction				
PFNA (C9)	**0-120**	**55±5**	**2.6×10^{-4}**	**0.982**	**0.15**	-					-				
PFNS (C9)	Totally adsorbed before the beginning of the reaction					-					-				
PFDA (C10)	**Not adjusted**					-					-				
PFDS (C10)	Totally adsorbed before the beginning of the reaction					-					-				
PFUdA (C11)	**Not adjusted**					-					-				
PFUdS (C11)	Totally adsorbed before the beginning of the reaction					-					-				
PFDoA (C12)	**Totally adsorbed before the beginning of the reaction**					-					-				
PFDoAS(C12)	Totally adsorbed before the beginning of the reaction					-					-				
PFTrDA (C13)	**Totally adsorbed before the beginning of the reaction**					-					-				
PFTrDS (C13)	Totally adsorbed before the beginning of the reaction					-					-				

[a]The fitting was performed only considering the reaction after the evident generation of the PFAS

Besides log D_{ow}, α_p, and E_{LUMO} - E_{HOMO}, Table 4.6.1 compiles other molecular descriptors of PFAS, including: the diffusion coefficient (D), the acid dissociation constant (pK_a), and the standard reduction potential for protonated (E^o *anion*) and deprotonated (E^o *acid*) PFAS. These descriptors, however, do not support the observed higher degradation rates for higher chain lengths. The D decreases with increasing chain lengths, going against the achieved results. Its contradictory effect may have been mitigated by the high mass transfer in the MicroFlowCell® at a Re of 1750 (maximum Re permitted by this electrochemical cell). Alternatively, the effect of other factors, such as D_{ow}, α_p, and E_{LUMO} - E_{HOMO}, may have upstaged the impact of D. Regarding the pK_a, it is difficult to make any definite statement since the pK_a values of PFAS are often concentration-dependent (Burns et al., 2008). A trend cannot be observed in Table 4.6.1. But it is possible to state that the presented pK_a values were always very low, ≤0.52, indicating that PFAS existed almost entirely in the anionic form at the solution pH (~7). This may have caused some electrostatic repulsion of PFAS from the negatively charged BDD anode surface. As regards the E^o values, they exhibit minor variations for PFAS as a function of PCL, likely not contributing to the observed differences.

The results obtained are in line with those reported in the literature for C4-C8 PFAS resorting not only to BDD anodes (Nienhauser et al., 2022; Trautmann et al., 2015; Zhuo et al., 2012) but also to titanium suboxide Ti_4O_7 anode (Wang et al., 2020), cerium (Ce)-doped lead dioxide (PbO_2) anode (Niu et al., 2012), and ruthenium (IV) oxide (RuO_2) anode (Schaefer et al., 2017).

Despite the general rule, there was a major exception: PFPrA (PCL C2) was more easily oxidized than some longer-PCL PFCA (PCL C3, C4, and C5), even upon generation of this PFAS from the breakage of longer-chain PFAS. This exception cannot be explained based on the molecular descriptors of Table 4.6.1. Some data are lacking and those available do not support the achieved results.

It is worth mentioning that the formation of some PFAS from the breakdown of longer-chain PFAS likely occurred for PFPrA (PCL C2), PFBA (PCL C3), and PFBS (PCL C4) since there was an evident rise in their content along the reaction (Figure 4.6.1). Notwithstanding, the generation of other PFAS in lower amounts not capable of causing a visible formation during the reaction should not be dismissed. Their formation may have led only to a deceleration of the degradation rate. This is valid for all the results obtained in this study.

4.6.1.3. Degradation of ultrashort- to long-chain PFAS (C1-C13) as a function of PFAS headgroup

Concerning PFAS headgroup, it is only possible to carry out a proper comparison for PFAS with C2, C3, C4, C5, and C6 PCL since: (i) PFCA with C1 PCL were not tested, (ii) minimal differences were found for C7 and C8-PCL PFAS, and (iii) no conclusions could be inferred for C9 and C10-PCL because PFSA with these chain lengths were totally sorbed on the system at t = 0 min (see Section 4.6.1.3).

Figures 4.6.1b.1-b.17 and Table 4.6.2 show that PFCA were more easily degraded than their PFSA counterparts for C2, C3, and C4 PCL, while no difference was observed for C5 and C6 PCL. The D_{ow} values are in line with the results for the C2-C4 PCL PFAS as Table 4.6.1 indicates that PFCA are more hydrophobic than PFSA regardless of the PCL. The *pKa* and *D*

values (Table 4.6.1) also support the results for C2-C4 PCL PFAS. Lower *pKa* values seem to be attributed to PFSA, even considering all the limitations of the presented *pKa* values, thereby contributing to a higher electrostatic repulsion of PFSA from the negatively charged BDD surface. The *D* values are higher for PFCA irrespective of the chain length, which might have promoted PFCA degradation. However, it is unlikely that *D* contributed to the achieved degradation kinetics taking into consideration the previous discussion on this parameter. For C6 PCL PFAS, the higher αp and E^o values (Table 4.6.1) for PFSA compared to PFCA may have improved the ability of PFSA for degradation, thereby contributing for the similar degradation rates of PFCA and PFSA. As concerns E_{LUMO} - E_{HOMO}, no differences were observed as a function of PFAS headgroup. The existence of other factors affecting the reactivity of PFAS besides those considered here should not be disregarded.

In the literature, the effect PFAS headgroup on the degradation rate is contradictory and has been inaccurately carried out for PFAS with the same number of total C in their structure instead of number of C in the perfluoroalkyl chain. The most common trend points to a faster degradation of PFCA compared to their PFSA counterparts with the total number of C atoms - C4, C6, and C8 (Le et al., 2019; H. Lin et al., 2018; Nienhauser et al., 2022; Trautmann et al., 2015; Wang et al., 2020; Zhuo et al., 2012), but the opposite was also observed for C4 and C6 chain lengths (Nienhauser et al., 2022; Trautmann et al., 2015).

4.6.2. Degradation of multi-solute systems with different content and diversity of PFAS and of single-solute systems

In the first approach, a multi-solute system composed of 8 C1-C8 PFAS in UPW, each one with a content of 2.0 µg/L, was exposed to the AO-BDD process at 100 mA/cm^2 for comparison with the previous 24 C1-C13 PFAS multi-solute system. These two systems differed in terms of content of each PFAS (2.0 µg/L *versus* 0.2 µg/L) and number and nature of PFAS (8 PFAS with C1-C8 chain lengths *versus* 24 PFAS with C1-C13 chain lengths), giving rise to different total contents of PFAS (16 µg/L *versus* 4.8 µg/L). In a second approach, the UPW was spiked with 2.0 µg/L of each C1-C8 PFAS individually and subjected to the AO-BDD process at 100 mA/cm^2 for comparison with the 8 C1-C8 PFAS multi-solute system.

4.6.2.1. 8 C1-C8 PFAS system *versus* 24 C1-C13 PFAS system

4.6.2.1.1. Considerations on the initial PFAS removal in the 8 C1-C8 PFAS system versus the 24 C1-C13 PFAS system

At t = 0 min, the total PFAS content decreased from 100% to ~81% in the 8 C1-C8 PFAS mixture (Figure 4.6.2a) due to a total removal of PFOS (C8) and ~54% removal of PFOA (C8). This corresponded to an initial decay of ~3.0 µg/L of PFAS. Comparable reductions were noted in a control test where the PFAS solution circulated within the system for 4h without the application of current. These achievements can probably be attributed to the total (for PFOS) or partial (for PFOA) physisorption/chemisorption of PFAS to the hydrophobic BDD surface

and glass vessel walls. The complete initial PFOS (C8) decay in the 8 C1-C8 PFAS mixture contrasted with an initial decay of ~54% in the 24 C1-C13 PFAS mixture. For PFOA (C8), the decay was similar in both mixtures. The poorer abatement of PFOS (C8) in the 24 C1-C13 PFAS multi-solute system can be mainly ascribed to a stronger competition between PFAS for the adsorption sites on the BDD surface in this system due to the presence of longer-chain PFAS (>C8), which have higher hydrophobicity and thus higher affinity to adsorb on the BDD surface.

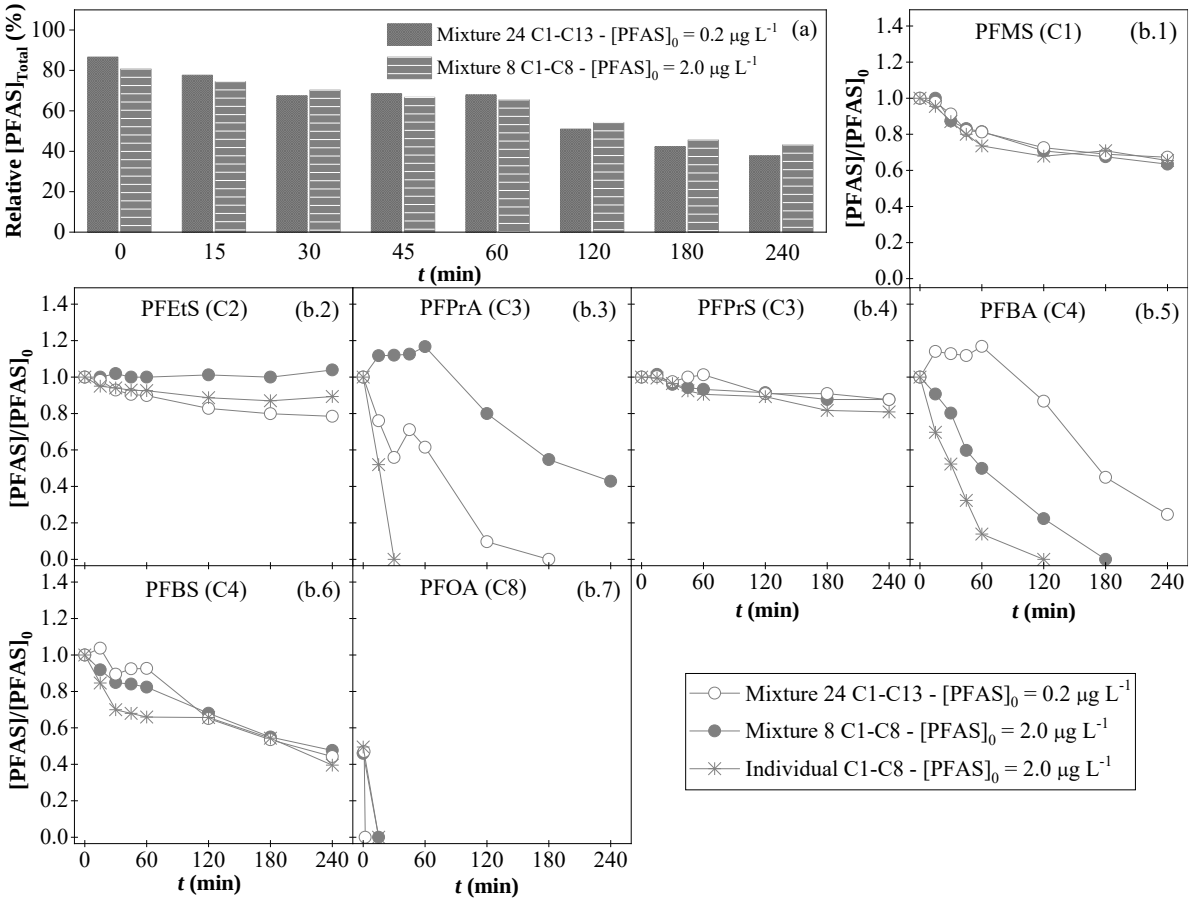

Figure 4.6.2. Degradation of a mixture of 24 C1-C13 PFAS (0.2 μg/L each) *versus* a mixture of 8 C1-C8 PFAS (2.0 μg/L each) *versus* individual solutions with 2.0 μg/L of each PFAS in UPW by the AO-BDD process at a current density of 100 mA/cm^2 with the conditions of [Na_2SO_4] = 30mM, pH = 7.0±0.2 and T = 25±1°C. (a) relative concentration decay of C1-C8 PFAS, and (b) normalized individual PFAS concentration decay. PFOS (C8) is not displayed since it was not detected in the solution at t = 0 min in the 8 C1-C8 PFAS mixture and in the individual solution.

4.6.2.1.2. Degradation of PFAS in the 8 C1-C8 PFAS system versus the 24 C1-C13 PFAS system

Figure 4.6.2 illustrates the abatement of the 7 PFAS not initially physiosorbed/chemisorbed (omission of PFOS) during the AO-BDD process in the 8 C1-C8 PFAS mixture compared to that in the 24 C1-C13 PFAS mixture for the same PFAS. The total PFAS decay was ~3-5% lower in the 8 C1-C8 PFAS mixture for long reaction times (≥120 min) (Figure 4.6.2a). After 240 min of reaction, the total of the PFAS decayed by ~57% in the 8 C1-C8 PFAS mixture and

~62% in the 24 C1-C13 PFAS mixture. The slightly lower PFAS removal in the 8 C1-C8 PFAS mixture can be mainly attributed to distinct behaviours of PFEtS (C2), PFPrA (C3), and PFBA (C4) (Figures 4.6.2b.1-b.7). PFEtS (C2) was visibly formed in the 8 C1-C8 PFAS system, contrasting with its continuous decay in the 24 C1-C13 PFAS system, and PFPrA (C3) was generated in much higher amount in the 8 C1-C8 PFAS mixture. These outcomes indicate that these two compounds are intermediates of PFAS with chain length ≤C8, as formerly pointed out in Section 4.6.1.2, and, moreover, that they were subjected to stronger coadsorption effects in the 8 C1-C8 PFAS mixture, delaying their degradation. These stronger coadsorption effects taking place in the 8 C1-C8 PFAS mixture may have been a consequence of the presence of larger amounts of more hydrophobic PFAS competing with shorter-chain PFAS for adsorption sites (total at t = 0 min of 14 µg/L of PFAS with ≥C2 in the 8 C1-C8 PFAS mixture *versus* 4.6 µg/L of PFAS with ≥C2 in the 24 C1-C13 PFAS mixture). For PFBA (C4), there was no visible formation in the 8 C1-C8 PFAS mixture, in contrast with a noticeable formation in the 24 C1-C13 PFAS mixture, which suggests that the PFBA (C4) is likely a by-product of the degradation of PFAS with chain lengths >C8.

4.6.2.2. Single-solute systems *versus* multi-solute systems

4.6.2.2.1. Considerations on the initial PFAS removal in the single-solute systems versus the 8 C1-C8 PFAS system

In single-solute systems, PFOS (C8) was not detected in solution and PFOA (C8) was removed by ~50% at t = 0 min, probably due to physisorption/chemisorption mechanisms at the hydrophobic BDD surface and glass reservoir walls. These results were similar to those achieved in the 8 C1-C8 PFAS mixture, which reveals that the presence of PFAS with chains lengths <C8 did not affect the initial adsorption of C8-PFAS on the anode surface.

4.6.2.2.2. Degradation of PFAS in the single-solute systems versus the 8 C1-C8 PFAS system

Figures 4.6.2b.1-b.7 show the decay of each PFAS in the single-solute solutions and compare this with the decay of each PFAS in the 8 C1-C8 PFAS mixture (and in the 24 C1-C13 PFAS mixture as well). PFPrA (C3) and PFBA (C4) were degraded much faster in the individual PFAS solutions than in the 8 C1-C8 PFAS mixture. The *k* values were about 13.2-fold and 2.2-fold higher, respectively (Table 4.6.2). The faster degradations of these C3 and C4 PFCA in the individual PFAS solutions can be attributed to: (i) the absence of competitive adsorption effects, with other PFAS not having more affinity with the anode surface compared to these PFCA, and (ii) the absence of the generation of these PFCA as intermediates of the degradation of PFAS with larger chain lengths. The degradation of the remaining PFAS was quite similar regardless of the solution composition. This can be related to the absence of the two abovementioned phenomena and, for PFMS (C1), PFEtS (C2), PFPrS (C3), and PFBS (C4), this can also be ascribed to their recalcitrant character, with the oxidative species in the AO-BDD process being unable to oxidize them whatever their concentration at the anode surface.

4.6.3. Effect of water/wastewater matrix

As for the UPW, the four additional water matrices (DW, UWW, NF, and RO) were spiked with the mixture of 0.2 µg/L of 24 C1-C13 PFAS and with the mixture of 2.0 µg/L of 8 C1-C8 PFAS and exposed to the AO-BDD process at 100 mA/cm^2.

4.6.3.1. Characteristics of water/wastewater matrices

The original PFAS content in all the matrices was below the limits of quantification of the LC-MS/MS method (Table 3.6.5). However, the presence of PFAS precursor compounds should not be disregarded since a total oxidizable precursor assay (TOPA) approach was not performed (Simon et al., 2023)

From Table 3.6.3, it is possible to discuss in detail the physicochemical characteristics of the four real water/wastewater matrices and of the UPW. As regards the total organic content (inferred from the COD measurement, which considers dissolved and suspended organics), the different matrices can be arranged in the following descending order: RO >> NF > UWW (COD was not detected in the DW and UPW matrices). But if one considers the dissolved organic matter (inferred from the DOC), the RO and NF present a similar value, and the order changes to RO ~ NF > UWW > DW > UPW since a major part of the organics in the RO were in suspension.

In terms of total content of ions, the conductivity allows to organize the water/wastewater matrices in the following descending order: RO >> NF >> UWW >> DW > UPW. The lower ionic content of the UPW, DW, and UWW matrices (conductivity <1.5 mS/cm) resulted in the need for adding a supporting electrolyte to ensure that the cell potential did not provide excessive energy consumption and did not overcome the maximum permitted by the power supply (30 V). The Na_2SO_4 was the selected supporting electrolyte after a set of tests to minimize the negative effects of the added ions in PFAS determination by LC-MS/MS. A content of 30mM of Na_2SO_4 was added to the UPW and DW, and 10mM of Na_2SO_4 were added to the UWW. Upon this addition, the total conductivity in all the water/wastewater matrices ranged from 3.1 to 5.8 mS/cm. This contributed to the sequencing of the matrices as follows in terms of conductivity: RO > UPW ~ DW > UWW > NF.

With respect to the individual analysis of ions, one can highlight the content of the main ions from which strong oxidants can be formed. According to Eqs. (11)-(20), these ions would include Cl^-, SO_4^{2-}, PO_4^{3-}, and CO_3^{2-}. However, it is possible to exclude PO_4^{3-} and CO_3^{2-} because the PO_4^{3-} oxidation is only expected at alkaline pH and not at the reaction pH (pH 7) (Sánchez et al., 2013) and the content of CO_3^{2-} may have been null at pH 7 since the speciation of inorganic carbon indicates that this ion emerges for pH values above ~7.5-8.5 (Yimin Chen et al., 2016). The original content of Cl^- and SO_4^{2-} followed the same trend as the original content of total ions in all the waters/wastewaters, i.e., RO >> NF >> UWW >> DW > UPW. But this scenario changed for SO_4^{2-} upon the addition of Na_2SO_4 since the content of this ion dramatically increased in the UPW, DW, and UWW matrices. The water/wastewater matrices

can be arranged in the following descending order in terms of SO_4^{2-} content upon Na_2SO_4 addition: UPW ~ DW >> UWW >> RO > NF.

$$R \rightarrow (R^{\bullet})^{+} + e^{-} \text{ (Equation 9)}$$

$$M + H_2O \rightarrow M(^{\bullet}OH) + H^{+} + e^{-} \text{ (Equation 10)}$$

$$2M(^{\bullet}OH) \rightarrow 2MO + H_2O_2 \text{ (Equation 11)}$$

$$3H_2O \rightarrow O_3 + 6H^{+} + 6e^{-} \text{ (Equation 12)}$$

$$2Cl^{-} \rightarrow Cl_2 + 2e^{-} \text{ (Equation 13)}$$

$$Cl_2 + H_2O \leftrightarrow HClO + Cl^{-} + H^{+} \text{ (Equation 14)}$$

$$HClO \leftrightarrow ClO^{-} + H^{+} \text{ (Equation 15)}$$

$$2SO_4^{2-} \rightarrow S_2O_8^{2-} + 2e^{-} \text{ (Equation 16)}$$

$$SO_4^{2-} \rightarrow SO_4^{\bullet-} + e^{-} \text{ (Equation 17)}$$

$$S_2O_8^{2-} + {}^{\bullet}OH \rightarrow HSO_4^{-} + SO_4^{\bullet-} + 1/2O_2 \text{ (Equation 18)}$$

$$S_2O_8^{2-} + R \rightarrow 2SO_4^{\bullet-} + R^{\bullet} \text{ (Equation 19)}$$

$$S_2O_8^{2-} + e^{-} \rightarrow SO_4^{2-} + SO_4^{\bullet-} \text{ (Equation 20)}$$

$$2PO_4^{3-} \rightarrow P_2O_8^{4-} + 2e^{-} \text{ (Equation 21)}$$

$$2CO_3^{2-} \rightarrow C_2O_6^{2-} + 2e^{-} \text{ (Equation 22)}$$

The matrices were also characterized in terms of total amount of oxidants accumulated in the solution during electrolysis at 100 mA/cm^2. The content of accumulated oxidants depends on their generation, as well as on their consumption typically by the organic compounds available in the matrices, transfer to the bulk solution, and storage ability. Accumulated oxidants in the solution (determined right after sampling) may have mostly included H_2O_2, $S_2O_8^{2-}$, HClO, and ClO^{-} despite the expected formation and action of $^{\bullet}OH$, $SO4^{\bullet-}$ and O_3. This is because (i) $^{\bullet}OH$ interact with the anode surface, thus only acting in the anode vicinity, and have short lifetimes in water of few ns (Janzen et al., 1992), (ii) $SO4^{\bullet-}$ have lifetimes of some dozens of µs (Araújo et al., 2022), and (iii) unreacted O_3 may have been quickly release into the atmosphere. Cl_2, $P_2O_8^{4-}$, and $C_2O_6^{2-}$ are not expected to be formed/present at pH 7 (Araújo et al., 2022; Yimin Chen et al., 2016; Janzen et al., 1992; Sánchez et al., 2013; Wang et al., 2007). Figure 4.6.3a shows an accumulation of oxidants for long reaction times (≥180 min) in the different water/wastewater matrices in the following decreasing order: RO >> NF >> UWW > DW > UPW. The matrices were arranged in this same order as regards Cl^{-} content, thus pointing to a major formation of HClO and ClO^{-} oxidants compared to H_2O_2 and $S_2O_8^{2-}$. From Figure 4.6.3b, it is possible to confirm that the generated oxidants were used to oxidize the

organics available in the solution. The degradation of organics was very pronounced in the RO (removal of 161 mg O_2/L of COD), followed by the NF (removal of 105 mg O_2/L of COD) and the UWW (removal of 32 mg O_2/L of COD). The oxidants may have been produced in much larger amounts than those presented, especially in the RO. In fact, it is observed a decay in the total oxidants content in the RO at reaction times <120 min, which can be related to the consumption of large amounts of oxidants by the organics in this matrix.

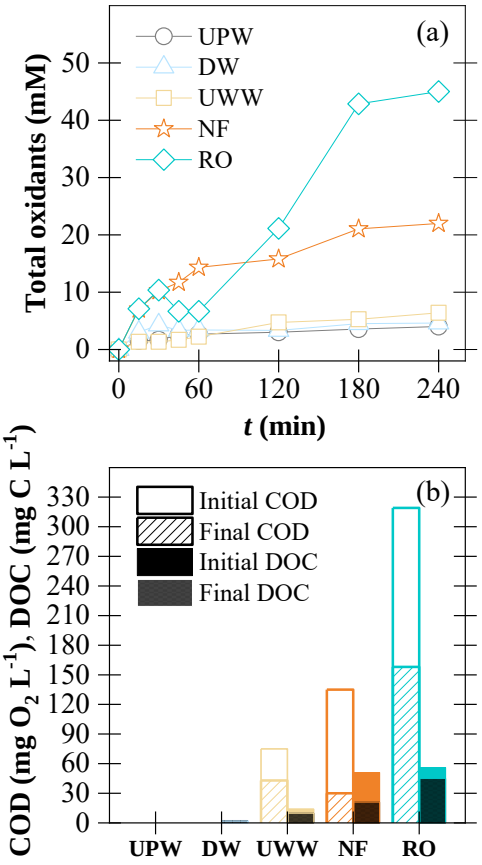

Figure 4.6.3. (a) Total oxidants content in the various water/wastewater matrices during electrolysis with a BDD anode and a Pt cathode at a current density of 100 mA/cm^2 with the conditions of [Na_2SO_4] = 30mM for UPW and DW, 10mM for UWW, and 0mM for NF and RO, pH = 7.0±0.2 and T = 25±1°C. (b) Initial and final COD and DOC contents (final contents correspond to the application of 240 min of electrolysis) in each water/wastewater matrix.

4.6.3.2. Considerations on the initial PFAS removal in the different water/wastewater matrices

In the 24 C1-C13 PFAS system, PFNS (C9), PFDS (C10), PFUdS (C11), PFDoA (C12), PFDoS (C12), PFTrDA (C13), and PFTrDS (C13) were not detected in solution at t = 0 min in all the new matrices, similarly to what happened in the UPW. Furthermore, the content of PFOA (C8), PFOS (C8), PFNA (C9), and PFUdA (C11) decreased in the five water/wastewater matrices. This decrease was generally quite similar in the UPW, DW, and UWW solutions (44-69%), and higher (by 5-52%) in the NF and RO matrices. This higher initial decline in the NF and RO

matrices came along with the removal of PFPeS (C5), PFHxS (C6), and PFHpS (C7) exclusively for these matrices (45-63%).

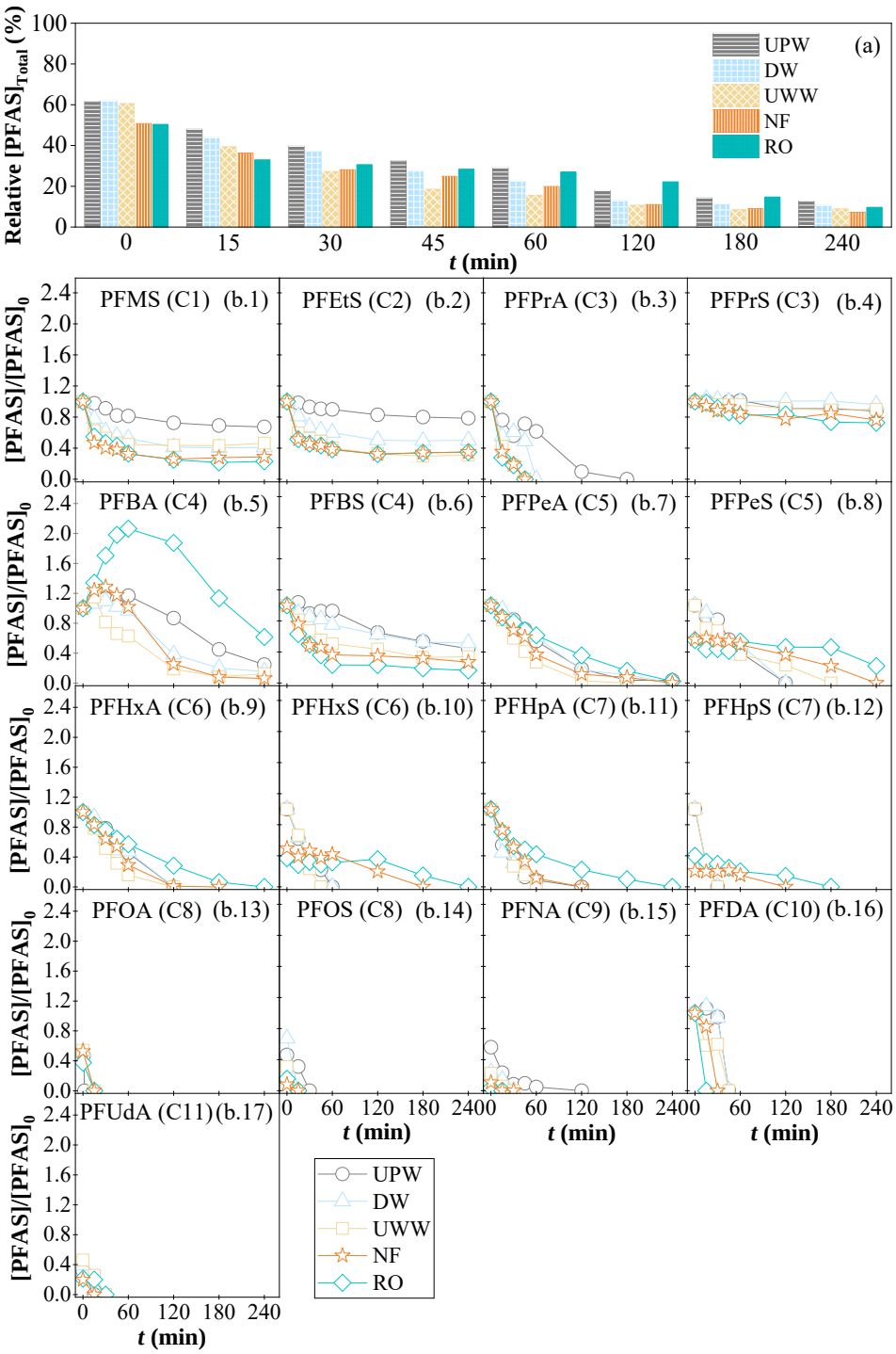

Figure 4.6.4. Degradation of a mixture of 24 C1-C13 PFAS (0.2 µg/L each) in the various water/wastewater matrices by the AO-BDD process at a current density of 100 mA/cm^2 with the conditions of [Na_2SO_4] = 30mM for UPW and DW, 10mM for UWW, and 0mM for NF and RO, pH = 7.0±0.2 and T = 25±1°C. (a) relative concentration decay of total PFAS, and (b) normalized individual PFAS concentration decay. PFNS (C9), PFDS (C10), PFUdS (C11), PFDoA (C12), PFDoS (C12), PFTrDA (C13), and PFTrDS (C13) are not displayed since they were not detected in the solution at t = 0 min.

In Figure 4.6.4a, the higher initial decay of PFAS in the NF and RO matrices is clearly illustrated, where one can observe at t = 0 min a relative total PFAS content of ~62% in the UPW, DW, and UWW solutions, and of ~50% in the RO and NF solutions. Comparable removal patterns were noted in control test for each water matrix, wherein the PFAS solution was recirculated in the system for 240 min without the application of current. It is conceivable that one may observe an augmented physisorption/chemisorption of PFAS in matrices with higher loadings. A possible explanation for this can build on the higher organic contents in the more loaded matrices since organic matter may positively affect the adsorption of PFAS on the surface of active materials by the formation of PFAS aggregates and organic matter-PFAS complexes (Gagliano et al., 2020; McCleaf et al., 2017). Note that this goes against the competitive role in the adsorption process often played by organic matter in some studies (Appleman et al., 2013; Kothawala et al., 2017).

In the 8 C1-C8 PFAS system, there were no differences between the initial PFAS removal in the UPW and in the other matrices: PFOS (C8) was not detected for any water/wastewater matrix, and PFOA (C8) was removed by ~50-60% in all the matrices. Since the removal of these two PFAS can correspond to the adsorption of ~3 μg/L of PFAS on the BDD surface, the initial adsorption of other PFAS by the formation of PFAS aggregates and organic matter-PFAS complexes may have been hindered.

4.6.3.3. Degradation of PFAS in the different water/wastewater matrices

The degradation of PFAS was distinct in the various water/wastewater matrices. Regarding the 24 C1-C13 PFAS system, Figure 4.6.4a shows that for reaction times ≥45 min, PFAS were in general degraded to a lesser extent in the UPW and RO matrices. For the other water matrices, i.e., DW, UWW, and NF, the relative extent of the decay varied with reaction time but was typically higher for more loaded matrices at longer reaction times. After 240 min of reaction, the total PFAS was reduced by ~87%, ~90%, ~91%, and ~93% in the UPW, RO/DW, UWW, and NF matrices, respectively. Thus, it may be said that a sharper PFAS decay was obtained for water/wastewater matrices with higher contents of ions and organic matter up to a given content of organics, such as that in the RO (COD of 319 mg O_2/L). The results for the NF, UWW, DW, and UPW can be mainly attributed to the production of higher amounts of oxidants in solutions with higher content of ions, mostly Cl^- as previously mentioned. In addition, the presence of a moderate content of organics may have contributed to the adsorption of PFAS on the BDD surface by the formation of PFAS aggregates and organic matter-PFAS complexes, as suggested by the results on the initial PFAS decay. In the RO, the PFAS removal was lower, likely due to the competition of PFAS with organics for active sites on the BDD surface and for oxidants.

The analysis of the decay of each PFAS in the 24 C1-C13 PFAS system (Figures 4.6.4b.1-b.17) allows to infer that the remaining PFAS after 240 min of reaction comprised those with total chain length ≤C4 (excluding the C3-PFPrA) in all the water/wastewater matrices. Furthermore, it was perceived an accumulation of large amounts of PFBA (C4) in the RO, and C5-C7 PFAS were degraded very slowly in this matrix (e.g., the *k* for PFPeA (C5) was approximately 1.1-1.8-fold lower in the RO compared to the other matrices (Table 4.6.3)). Additionally, it is worth mentioning that an abrupt decay was observed in the first instants of reaction for PFMS (C1), PFEtS (C2), and PFPrA (C3) in the UWW, NF, and RO matrices, and

to a lower extent in the DW. Likely, this can be attributed to the formation of complexes between these PFAS and initially oxidized or reduced compounds, which were readily adsorbed on the BDD surface and degraded.

PFAS abatement during the AO-BDD process in the 8 C1-C8 PFAS mixture corroborate the results achieved in the 24 C1-C13 PFAS mixture. Once again, inferior total PFAS removals were achieved in the UPW and RO solutions for reaction times ≥45 min, and the total removals in the other water/wastewater solutions varied with the reaction time (Figure 4.6.5a). After 240 min of reaction, the total PFAS were degraded by ~63%, ~66%, ~67%, and ~68% in the UPW/RO, UWW, NF, and DW matrices, respectively. The remaining PFAS refer to those with chain lengths ≤C4, excluding C3-PFPrA for all water matrices except the UPW, and C4-PFBA for all the waters/wastewaters (Figures 4.6.5b.1-b.7). In the 24 C1-C13 PFAS mixture, C3-PFPrA did not contribute to the final PFAS content for none of the waters/wastewaters. But this PFAS was perceptibly formed and suffered a much slower decay in most of the waters/wastewaters spiked with the 8 C1-C8 PFAS mixture. This confirms the previous assumption (Section 4.6.2.1.2), which proposes that PFPrA (C3) is an intermediate of PFAS with chain length ≤C8 competing with the large amounts of hydrophobic PFAS for adsorption sites at the BDD surface in the 8 C1-C8 PFAS mixture.

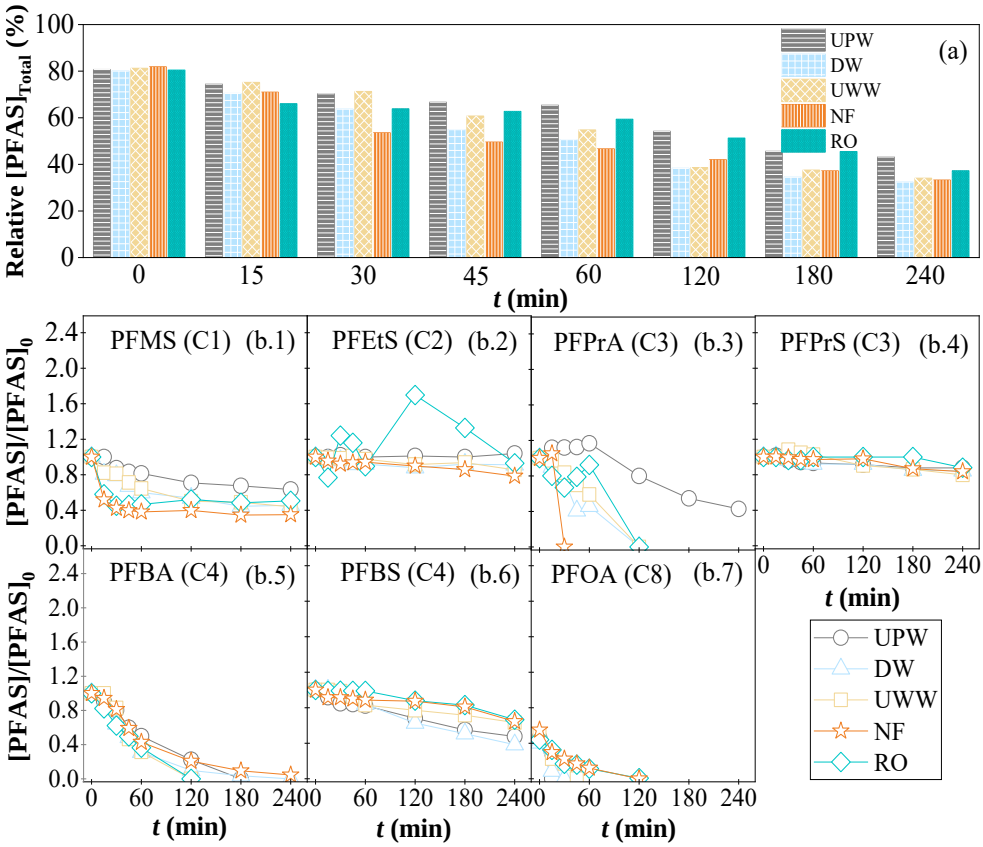

Figure 4.6.5. Degradation of a mixture of 8 C1-C8 PFAS (2.0 µg/L each) in various water matrices by the AO-BDD process at a current density of 100 mA/cm² with the conditions of [Na_2SO_4] = 30mM for UPW and DW, 10mM for UWW, and 0mM for NF and RO, pH = 7.0±0.2 and T = 25±1°C. (a) relative concentration decay of total PFAS, and (b) normalized individual PFAS concentration decay. PFOS (C8) is not displayed since it was not detected in the solution at t = 0 min.

Table 4.6.3. Pseudo-first-order kinetic constants (k) of PFAS and corresponding residual variance (S^2_R) and coefficient of determination (R^2) for the degradation of PFAS in the various water matrices (UPW, DW, UWW, NF, and RO) by the AO-BDD process at a current density of 100 mA/cm² using a mixture of 24 C1-C13 PFAS (0.2 µg/L each).

	24 C1-C13 PFAS with 0.2 µg/L - j = 100 mA/cm²														
	UPW					DW					UWW				
	Time interval (min)	k ($\times10^{-3}$ /min)	S^2_R (µg²/L²)	R^2	C_0 (µg/L)	Time interval (min)	k ($\times10^{-3}$ /min)	S^2_R (µg²/L²)	R^2	C_0 (µg/L)	Time interval (min)	k ($\times10^{-3}$ /min)	S^2_R (µg²/L²)	R^2	C_0 (µg/L)
PFMS (C1)	Not adjusted					Not adjusted					Not adjusted				
PFEtS (C2)	Not adjusted					Not adjusted					Not adjusted				
PFPrA (C3)	**45-180** [a]	**21±5**	**5.4×10^{-4}**	**0.965**	**0.14**	**Not adjusted**					**Not adjusted**				
PFPrS (C3)	Not adjusted					Not adjusted					Not adjusted				
PFBA (C4)	**60-240** [a]	**7±1**	**7.5×10^{-4}**	**0.964**	**0.23**	**Not adjusted**					**15-240** [a]	**16±1**	**9.8×10^{-4}**	**0.975**	**0.23**
PFBS (C4)	60-240 [a]	4.5±0.3	1.6×10^{-4}	0.969	0.19	Not adjusted					Not adjusted				
PFPeA (C5)	**0-240**	**11±1**	**1.5×10^{-3}**	**0.965**	**0.20**	**0-240**	**11±1**	**1.6×10^{-3}**	**0.964**	**0.20**	**0-180**	**20±1**	**4.5×10^{-4}**	**0.987**	**0.20**
PFPeS (C5)	0-120	14±2	2.5×10^{-3}	0.907	0.20	0-240	15±2	2.0×10^{-3}	0.954	0.20	0-180	16±1	8.6×10^{-4}	0.968	0.20
PFHxA (C6)	**0-180**	**14±2**	**2.4×10^{-3}**	**0.937**	**0.20**	**0-120**	**15±2**	**2.0×10^{-3}**	**0.923**	**0.20**	**0-120**	**25±2**	**6.9×10^{-4}**	**0.976**	**0.20**
PFHxS (C6)	0-60	39±4	6.8×10^{-4}	0.972	0.20	0-60	33±4	1.1×10^{-3}	0.951	0.20	Not adjusted				
PFHpA (C7)	**0-120**	**38±3**	**3.7×10^{-4}**	**0.987**	**0.20**	**0-60**	**47±4**	**4.3×10^{-4}**	**0.982**	**0.20**	**0-60**	**38±6**	**1.5×10^{-3}**	**0.946**	**0.20**
PFHpS (C7)	Not adjusted					Not adjusted					Not adjusted				
PFOA (C8)	**Not adjusted**					**Not adjusted**					**Not adjusted**				
PFOS (C8)	Not adjusted					Not adjusted					Not adjusted				
PFNA (C9)	**0-120**	**55±5**	**2.6×10^{-4}**	**0.982**	**0.15**	**Not adjusted**					**Not adjusted**				
PFNS (C9)	Totally adsorbed before the beginning of the reaction					Totally adsorbed before the beginning of the reaction					Totally adsorbed before the beginning of the reaction				
PFDA (C10)	**Not adjusted**					**Not adjusted**					**Not adjusted**				
PFDS (C10)	Totally adsorbed before the beginning of the reaction					Totally adsorbed before the beginning of the reaction					Totally adsorbed before the beginning of the reaction				
PFUdA (C11)	**Not adjusted**					**Not adjusted**					**Not adjusted**				
PFUdS (C11)	Totally adsorbed before the beginning of the reaction					Totally adsorbed before the beginning of the reaction					Totally adsorbed before the beginning of the reaction				
PFDoA (C12)	**Totally adsorbed before the beginning of the reaction**					**Totally adsorbed before the beginning of the reaction**					**Totally adsorbed before the beginning of the reaction**				
PFDoAS(C12)	Totally adsorbed before the beginning of the reaction					Totally adsorbed before the beginning of the reaction					Totally adsorbed before the beginning of the reaction				
PFTrDA (C13)	**Totally adsorbed before the beginning of the reaction**					**Totally adsorbed before the beginning of the reaction**					**Totally adsorbed before the beginning of the reaction**				
PFTrDS (C13)	Totally adsorbed before the beginning of the reaction					Totally adsorbed before the beginning of the reaction					Totally adsorbed before the beginning of the reaction				

[a]The fitting was performed only considering the reaction after the evident generation of the PFAS

The absence of PFBA (C4) at final reaction times for all water/wastewater matrices spiked with the 8 C1-C8 PFAS contrasts with the remaining amounts of this PFAS in the RO and UPW matrices spiked with the 24 C1-C13 PFAS. This corroborates the assumption in Section 4.6.2.1.2 that suggests that PFBA (C4) is a by-product of the degradation of PFAS with chain length >C8. Besides these differences in the decay of C3-PFPrA and C4-PFBA in the various waters/wastewaters spiked with the distinct PFAS mixtures, highlight can also be given to the distinct decays of C2-PFEtS and C4-PFBS in these two mixtures. In the C1-C8 PFAS mixture, these two last PFAS exhibited slower decays, mostly null decays, and PFEtS (C2) was visibly formed in the RO. These results point to the formation of PFEtS (C2) and PFBS (C4) as intermediates of the degradation of PFAS with chain lengths ≤C8, an output that was not evident in the UPW analysis.

4.6.4. Effect of current density

j is a crucial parameter since it regulates the extent/amount of direct oxidation and indirect oxidation via Eqs. (10), (12), (13), (16), (17), (20), (21), and (22). The effect of *j* on the degradation of PFAS by the AO-BDD process was assessed for a broad range of *j* from 20 mA/cm^2 to 250 mA/cm^2 in the UPW applying a mixture of 8 C1-C8 PFAS with 2.0 µg/L of each PFAS. Furthermore, the impact of *j* of 20 mA/cm^2 *versus* 100 mA/cm^2 was assessed in all the real water/wastewater matrices using the same multi-solute system.

4.6.4.1. Degradation of PFAS at different current densities

In the UPW, the applied *j* values provided average cell potentials during reactions of ~5.8-27 V. Figure 4.6.6a shows an increase in the total decay of PFAS for increasing *j* from 20 mA/cm^2 to 250 mA/cm^2. However, the differences were slight for j values of 80-250 mA/cm^2 at reaction times ≥180 min, at which only the content of PFPrA (C3) was distinct at these *j* (Figures 4.6.6c.1-c.7). In general, PFPrA (C3) benefitted from *j* at all the j range. The same was achieved for PFBA (C4), but this PFAS was totally removed at reaction times ≤180 min applying *j* of 80-250 mA/cm^2, thereby not contributing to the reported slight differences. The *k* was ~1.8-fold and ~2.8-fold larger for PFPrA (C3) and PFBA (C4), respectively, at mA/cm^2 compared to 80 mA/cm^2 (the pseudo-first-order kinetic model was not adjusted at lower *j*) (Table 4.6.4). The incessant positive influence of j for PFPrA (C3) and PFBA (C4) indicates that the degradation of these two PFAS was controlled by charge transfer even for very high *j*, thereby pointing to their willingness to degrade whether enough oxidants are provided. The decay of PFMS (C1), PFBS (C4), and PFOA (C8) also benefited from the *j* but not up to 250 mA/cm^2. This benefit ceased at *j* ≥40 mA/cm^2 for PFMS (C1) and at *j* ≥80 mA/cm^2 for PFBS (C4) and PFOA (C8). In the case of PFMS (C1) and PFBS (C4), the stop of the reaction improvement with *j* came along with a maximum degradation of ~37% and ~52% after 240 min of reaction, respectively. For PFOA (C8), this came along with an instantaneous degradation. These outcomes suggest that PFMS (C1) and PFBS (C4) are very recalcitrant, with finite reactivity, while PFOA (C8) is responsive to the oxidants generated during the AO-BDD process. The decay of PFEtS (C2) and PFPrS (C3) was null regardless of the *j*, pointing to an even higher recalcitrant character of these compounds compared to PFMS (C1) and PFBS (C4). Note that the decays of PFMS (C1), PFEtS (C2), PFPrS (C3), and PFBS (C4) were null or very small for single-solute UPW systems

(see Section 4.6.2.2.2), which reinforces their persistence since it allows to exclude the presence of competitive adsorption effects and high impact of the formation of these PFAS along reaction on the degradation kinetics.

Table 4.6.4. Pseudo-first-order kinetic constants (k) of PFAS and corresponding residual variance (S^2_R) and coefficient of determination (R^2) for the degradation of a mixture of 8 C1-C8 PFAS (2.0 µg/L each) in UPW by the AO-BDD process at different current densities (20, 40, 80, 100, and 250 mA/cm^2).

	UPW - 8 C1-C8 PFAS with 2.0 µg/L															
	j = 20 mA/cm^2					j = 40 mA/cm^2					j = 80 mA/cm^2					
	Time interval (min)	k (×10^{-3} /min)	S^2_R (µg^2/L^2)	R^2	C_0 (µg/L)	Time interval (min)	k (×10^{-3} /min)	S^2_R (µg^2/L^2)	R^2	C_0 (µg/L)	Time interval (min)	k (×10^{-3} /min)	S^2_R (µg^2/L^2)	R^2	C_0 (µg/L)	
PFMS (C1)		Not adjusted					Not adjusted					Not adjusted				
PFEtS (C2)		Not adjusted					Not adjusted					Not adjusted				
PFPrA (C3)		**Not adjusted**					**Not adjusted**				**60-240** [a]	**6.4±0.2**	1.5×10^{-3}	**0.997**	**2.3**	
PFPrS (C3)		Not adjusted					Not adjusted					Not adjusted				
PFBA (C4)		**Not adjusted**					**Not adjusted**				**0-180**	**10±1**	2.4×10^{-1}	**0.926**	**2.0**	
PFBS (C4)		Not adjusted					Not adjusted				0-240	3.3±0.2	2.1×10^{-2}	0.977	2.0	
PFOA (C8)	**0-60**	**42±7**	3.8×10^{-2}	**0.946**	**0.98**		**Not adjusted**					**Not adjusted**				
PFOS (C8)	Totally adsorbed before the beginning of the reaction					Totally adsorbed before the beginning of the reaction					Totally adsorbed before the beginning of the reaction					

	j = 100 mA/cm^2					j = 250 mA/cm^2				
	Time interval (min)	k (×10^{-3} /min)	S^2_R (µg^2/L^2)	R^2	C_0 (µg/L)	Time interval (min)	k (×10^{-3} /min)	S^2_R (µg^2/L^2)	R^2	C_0 (µg/L)
PFMS (C1)		Not adjusted					Not adjusted			
PFEtS (C2)		Not adjusted					Not adjusted			
PFPrA (C3)	**60-240** [a]	**4.7±0.9**	1.2×10^{-1}	**0.905**	**2.3**	**15-180** [a]	**18±1**	4.2×10^{-2}	**0.989**	**2.2**
PFPrS (C3)		Not adjusted					Not adjusted			
PFBA (C4)	**0-180**	**12±1**	1.2×10^{-1}	**0.963**	**2.0**	**0-120**	**28±2**	3.3×10^{-2}	**0.988**	**2.0**
PFBS (C4)	0-240	3.3±0.2	2.1×10^{-2}	0.977	2.0	0-240	3.9±0.2	2.9×10^{-2}	0.974	2.0
PFOA (C8)	**Not adjusted**					**Not adjusted**				
PFOS (C8)	Totally adsorbed before the beginning of the reaction					Totally adsorbed before the beginning of the reaction				

[a]The fitting was performed only considering the reaction after the evident generation of the PFAS

Figures 4.6.7-4.6.10 illustrate the impact of *j* (20 mA/cm^2 *versus* 100 mA/cm^2) in the real water/wastewater matrices. The respective *k* values are displayed in Tables 4.6.5 and 4.6.6. A *j* of 20 mA/cm^2 caused average cell potentials of ~5.9-7.6 V, and 100 mA/cm^2 led to average cell potentials of ~14.6-22.0 V. For all the matrices, the application of 100 mA/cm^2 was beneficial compared to 20 mA/cm^2. After 240 min of reaction, the total PFAS decay was 15-34% larger at 100 mA/cm^2 compared to 20 mA/cm^2 in all waters/wastewaters mainly due to a higher decline of PFMS (C1), PFPrA (C3), PFBA (C4), PFBS (C4), and PFOA (C8). It is only worth highlighting the abrupt decay of PFPrA (C3) up to complete vanishing in the NF at 20 mA/cm^2 after 180 min of reaction, which contrasts with a null decay or even formation of this PFAS in the other water/wastewater matrices. The sharp decay of PFPrA (C3) also occurred in the NF solution at 100 mA/cm^2, although after a short reaction time (30 min). This can indicate a total PFPrA (C3) degradation or complexation with some compounds in solution, likely organics generated from the oxidation of starting organics present in the NF.

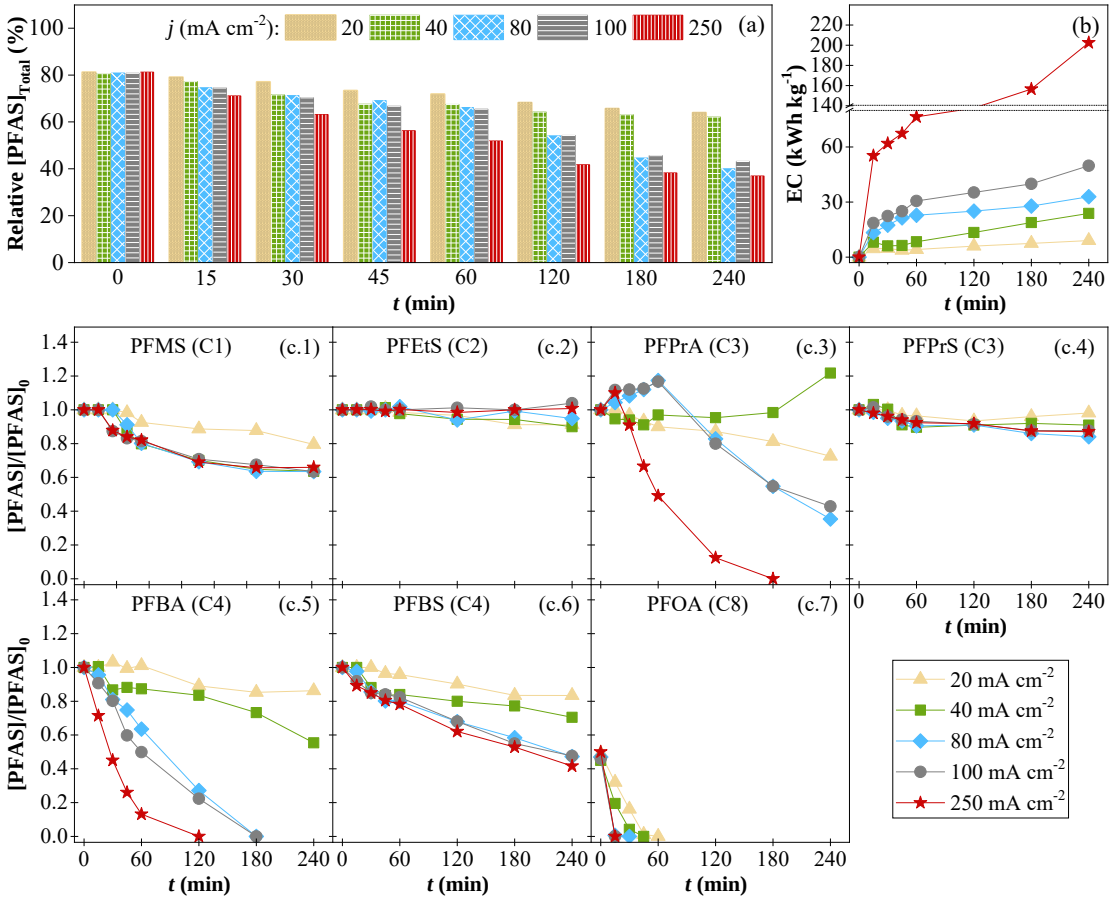

Figure 4.6.6. Degradation of a mixture of a mixture of 8 C1-C8 PFAS (2.0 µg/L each) in UPW by the AO-BDD process at different current densities (20, 40, 80, 100, and 250 mA/cm^2) with the conditions of [Na_2SO_4] = 30mM, pH = 7.0±0.2 and T = 25±1°C. (a) relative concentration decay, (b) energy consumption for electrochemical cell operation, and (c) normalized individual PFAS concentration decay. PFOS (C8) is not displayed since it was not detected in the solution at t = 0 min.

In all water matrices, it is noteworthy that the release of hydrogen (H_2) and oxygen (O_2) bubbles from the hydrogen evolution reaction (HER) and oxygen evolution reaction (OER), respectively, may have potentially led to the escape of some PFAS (Cao et al., 2019). This effect may have been more pronounced at higher current densities, where these side reactions become more relevant. It is also worth noting that despite the requirement of large *j* values to

improve the removal of some PFAS, the energy consumption for electrochemical cell operation dramatically increases (Figure 4.6.6b) and the Joule heating also increases.

Ultimately, the observed outcomes showed that most studies on the degradation PFAS, which employ *j* of 20 mA/cm^2 or lower (Duinslaeger & Radjenovic, 2022; Y. Liu et al., 2019; Schaefer et al., 2015), should be examined cautiously since PFAS decay may have been under charge transfer control. In these studies, it is usual to achieve increasing degradation rates for higher *j* in the whole tested range, which corroborate with the current results. It is also worth noting that despite the requirement of large *j* values for some PFAS to hinder limitations related to charge transfer, the energy consumption for electrochemical cell operation can dramatically increase (Figure 4.6.6b).

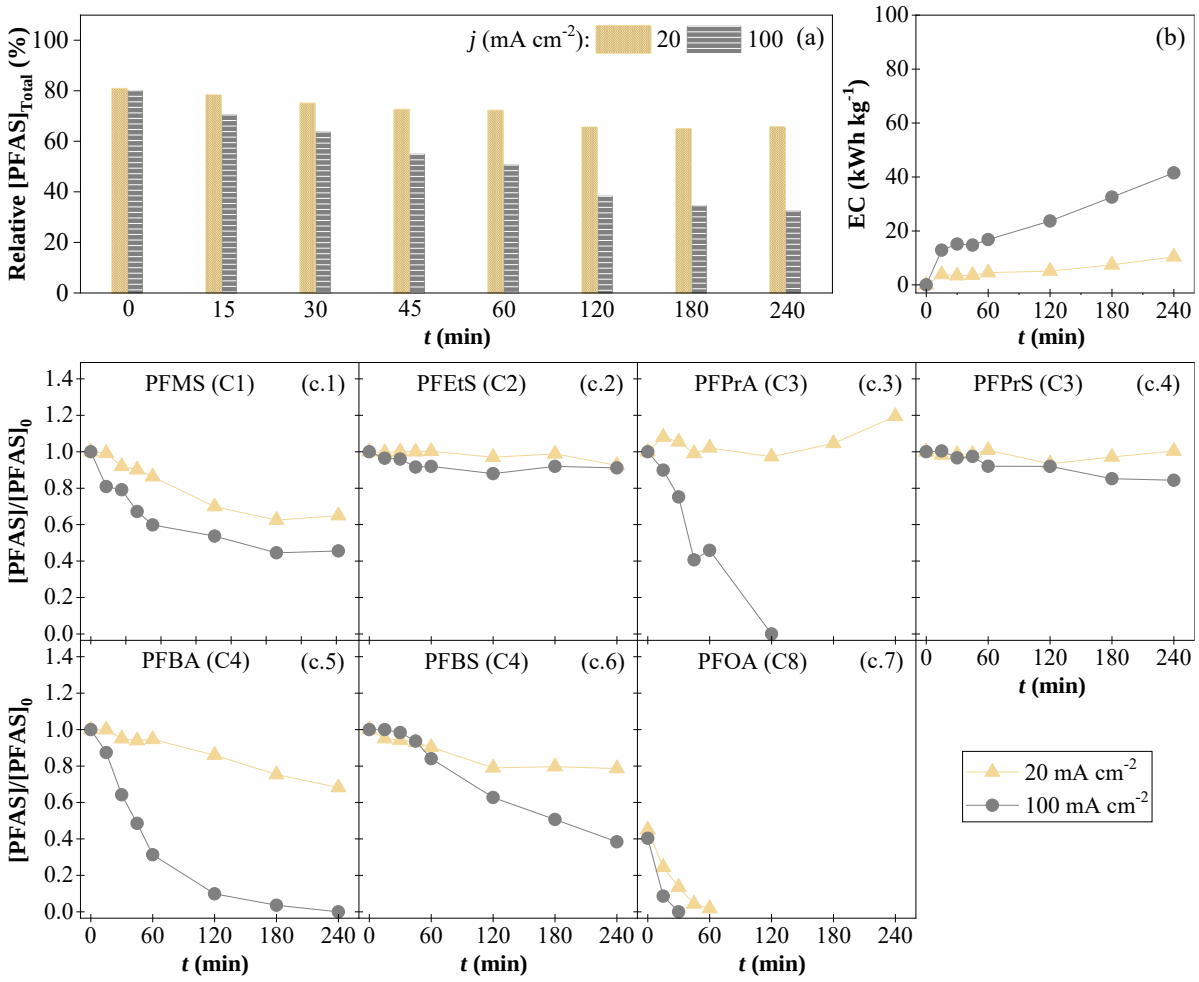

Figure 4.6.7. Degradation of a mixture of a mixture of 8 C1-C8 PFAS (2.0 µg/L each) in DW by the AO-BDD process at different current densities (20 and 100 mA/cm^2) with the conditions of [Na_2SO_4] = 30mM, pH = 7.0±0.2 and T = 25±1ºC. (a) relative concentration decay, (b) energy consumption for electrochemical cell operation, and (c) normalized individual PFAS concentration decay. PFOS (C8) is not displayed since it was not detected in the solution at t = 0 min.

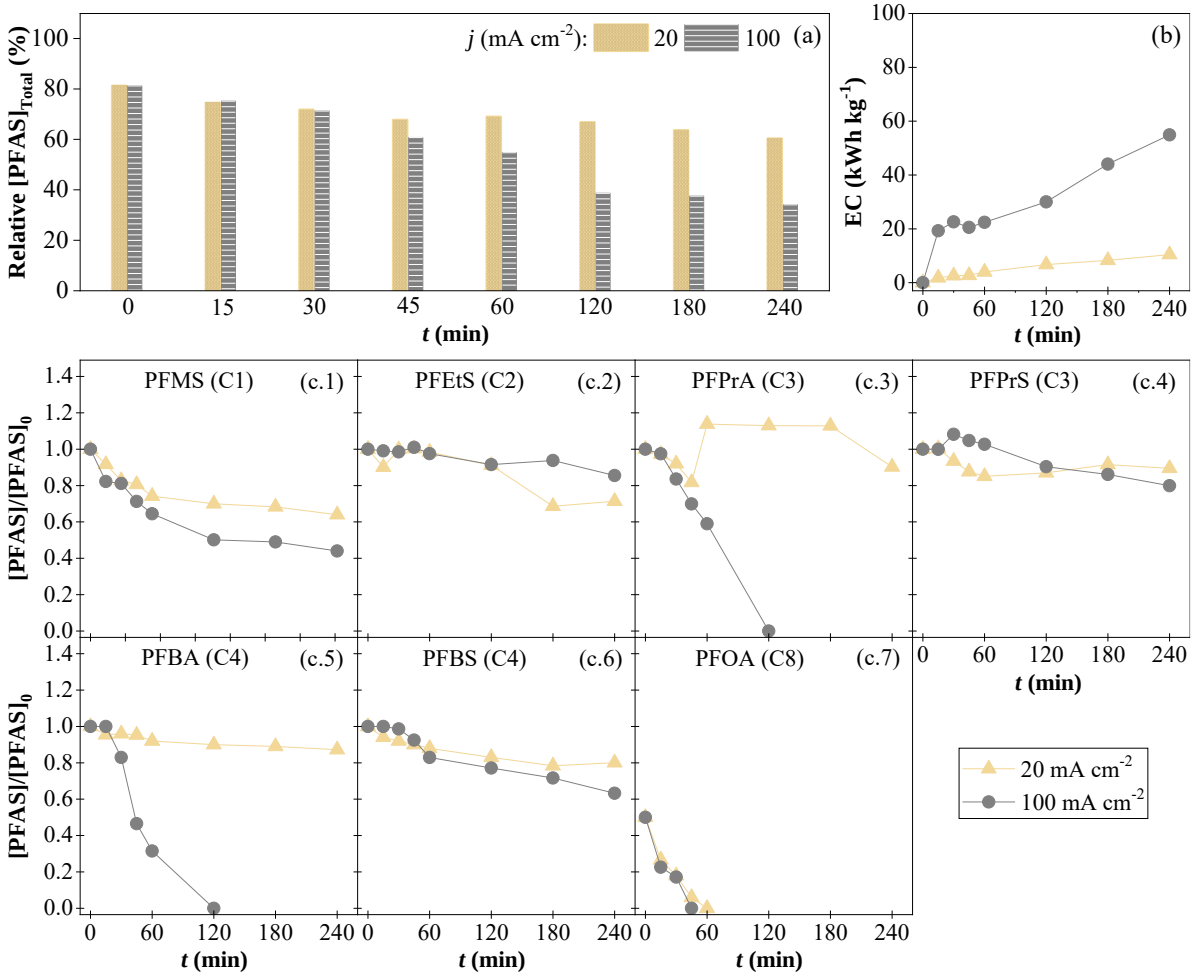

Figure 4.6.8. Degradation of a mixture of a mixture of 8 C1-C8 PFAS (2.0 µg/L each) in UWW by the AO-BDD process at different current densities (20 and 100 mA/cm^2) with the conditions of [Na_2SO_4] = 10mM, pH = 7.0±0.2 and T = 25±1°C. (a) relative concentration decay, (b) energy consumption for electrochemical cell operation, and (c) normalized individual PFAS concentration decay. PFOS (C8) is not displayed since it was not detected in the solution at t = 0 min.

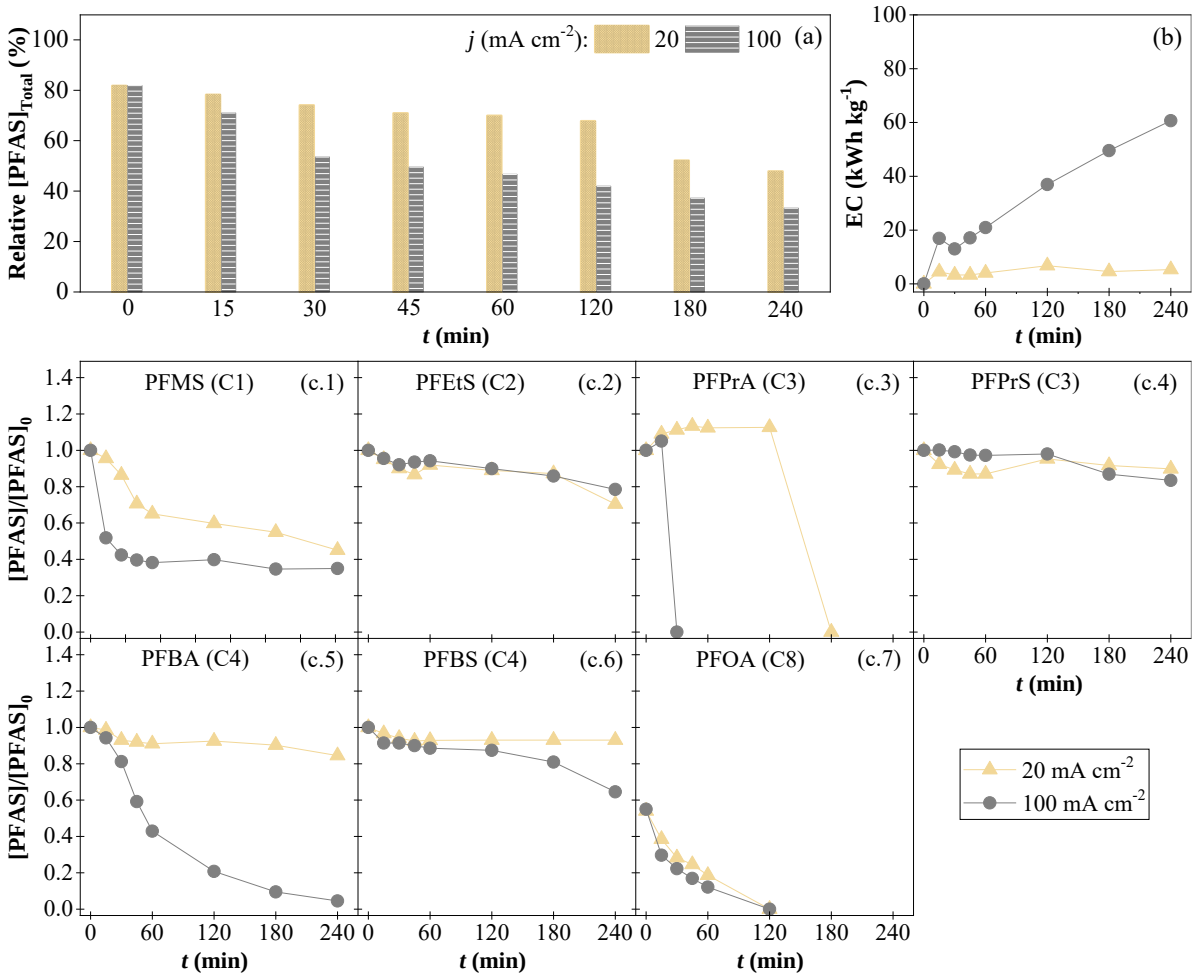

Figure 4.6.9. Degradation of a mixture of a mixture of 8 C1-C8 PFAS (2.0 µg/L each) in NF by the AO-BDD process at different current densities (20 and 100 mA/cm^2) with the conditions of [Na_2SO_4] = 0mM, pH = 7.0±0.2 and T = 25±1°C. (a) relative concentration decay, (b) energy consumption for electrochemical cell operation, and (c) normalized individual PFAS concentration decay. PFOS (C8) is not displayed since it was not detected in the solution at t = 0 min.

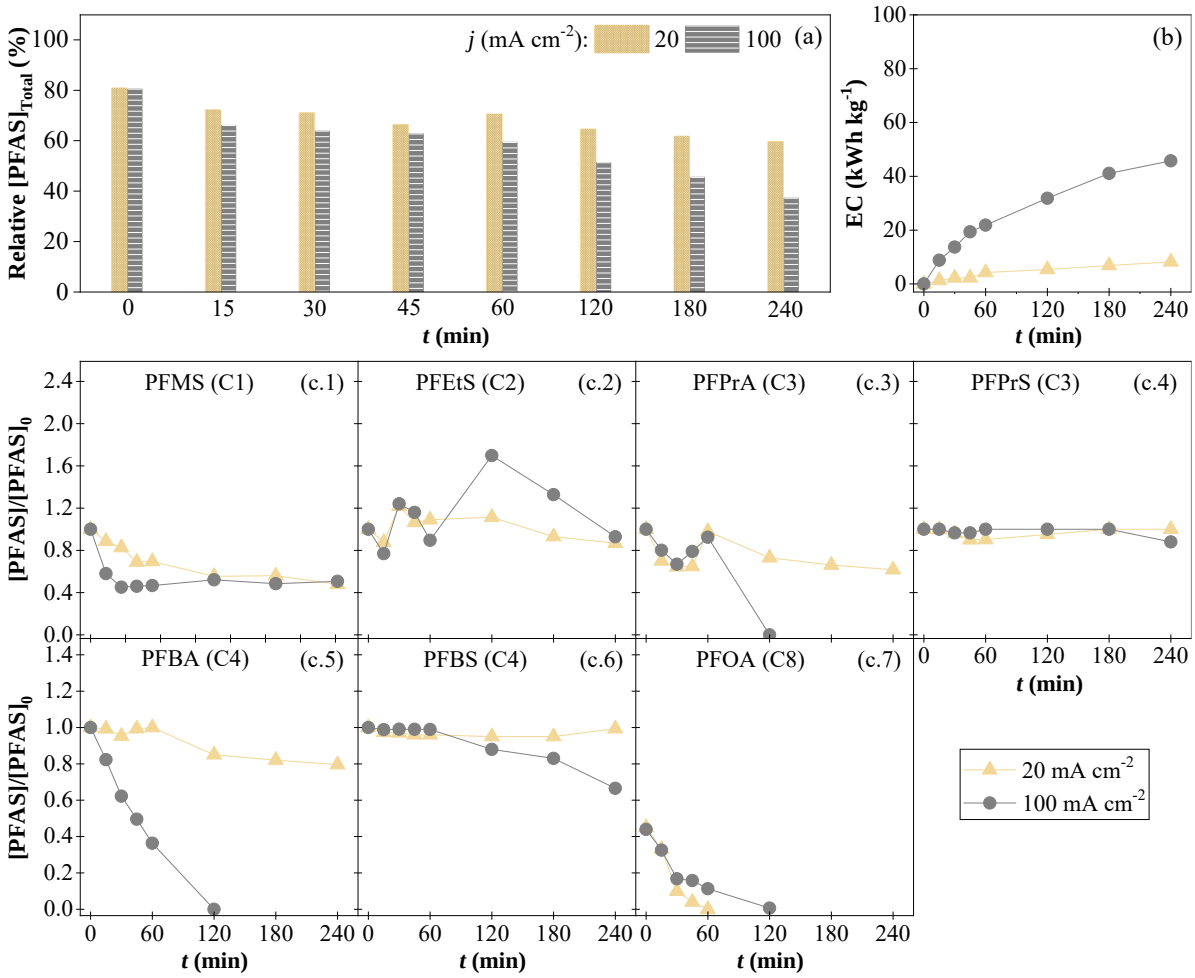

Figure 4.6.10. Degradation of a mixture of a mixture of 8 C1-C8 PFAS (2.0 µg/L each) in RO by the AO-BDD process at different current densities (20 and 100 mA/cm^2) with the conditions of [Na_2SO_4] = 0mM, pH = 7.0±0.2 and T = 25±1°C. (a) relative concentration decay, (b) energy consumption for electrochemical cell operation, and (c) normalized individual PFAS concentration decay. PFOS (C8) is not displayed since it was not detected in the solution at t = 0 min.

Table 4.6.5. Pseudo-first-order kinetic constants (k) of PFAS and corresponding residual variance (S^2_R) and coefficient of determination (R^2) for the degradation of a mixture of 8 C1-C8 PFAS (2.0 µg/L each) in the various water matrices (UPW, DW, UWW, NF, and RO) by the AO process with a BDD anode at 20 mA/cm².

	8 C1-C8 PFAS with 2.0 µg/L - j = 20 mA/cm²														
	UPW					DW					UWW				
	Time interval (min)	k ($\times10^{-3}$ /min)	S^2_R (µg²/L²)	R^2	C_0 (µg/L)	Time interval (min)	k ($\times10^{-3}$ /min)	S^2_R (µg²/L²)	R^2	C_0 (µg/L)	Time interval (min)	k ($\times10^{-3}$ /min)	S^2_R (µg²/L²)	R^2	C_0 (µg/L)
PFMS (C1)	Not adjusted					0-240	2.3±0.2	4.4×10^{-2}	0.931	2.0	Not adjusted				
PFEtS (C2)	Not adjusted					Not adjusted					Not adjusted				
PFPrA (C3)	**Not adjusted**					**Not adjusted**					**Not adjusted**				
PFPrS (C3)	Not adjusted					Not adjusted					Not adjusted				
PFBA (C4)	**Not adjusted**					**15-240** [a]	**1.66±0.07**	**6.5×10^{-3}**	**0.980**	**2.0**	**Not adjusted**				
PFBS (C4)	Not adjusted					Not adjusted					Not adjusted				
PFOA (C8)	**0-60**	**42±7**	**3.8×10^{-2}**	**0.946**	**0.98**	**0-240**	**44±2**	**3.7×10^{-3}**	**0.995**	**0.9**	**0-60**	**42±4**	**1.3×10^{-2}**	**0.979**	**1.0**
PFOS (C8)	Totally adsorbed before the beginning of the reaction					Totally adsorbed before the beginning of the reaction					Totally adsorbed before the beginning of the reaction				

	NF					RO				
	Time interval (min)	k ($\times10^{-3}$ /min)	S^2_R (µg²/L²)	R^2	C_0 (µg/L)	Time interval (min)	k ($\times10^{-3}$ /min)	S^2_R (µg²/L²)	R^2	C_0 (µg/L)
PFMS (C1)	Not adjusted					Not adjusted				
PFEtS (C2)	Not adjusted					Not adjusted				
PFPrA (C3)	**Not adjusted**					**Not adjusted**				
PFPrS (C3)	Not adjusted					Not adjusted				
PFBA (C4)	**Not adjusted**					**Not adjusted**				
PFBS (C4)	Not adjusted					Not adjusted				
PFOA (C8)	**0-120**	**30±3**	**1.9×10^{-2}**	**0.973**	**1.1**	**0-60**	**41±8**	**4.4×10^{-2}**	**0.928**	**0.9**
PFOS (C8)	Not adjusted					Totally adsorbed before the beginning of the reaction				

[a]The fitting was performed only considering the reaction after the evident generation of the PFAS

Table 4.6.6. Pseudo-first-order kinetic constants (k) of PFAS and corresponding residual variance (S^2_R) and coefficient of determination (R^2) for the degradation of a mixture of 8 C1-C8 PFAS (2.0 μg/L each) in the various water matrices (UPW, DW, UWW, NF, and RO) by the AO-BDD process at 100 mA/cm².

	8 C1-C8 PFAS with 2.0 μg/L - j = 100 mA/cm²														
	UPW					DW					UWW				
	Time interval (min)	k ($\times10^{-3}$ /min)	S^2_R (μg²/L²)	R^2	C_0 (μg/L)	Time interval (min)	k ($\times10^{-3}$ /min)	S^2_R (μg²/L²)	R^2	C_0 (μg/L)	Time interval (min)	k ($\times10^{-3}$ /min)	S^2_R (μg²/L²)	R^2	C_0 (μg/L)
PFMS (C1)	Not adjusted					Not adjusted					Not adjusted				
PFEtS (C2)	Not adjusted					Not adjusted					Not adjusted				
PFPrA (C3)	**60-240** [a]	**4.7±0.9**	**1.2×10^{-1}**	**0.905**	**2.3**	**0-120**	**15±3**	**2.5×10^{-1}**	**0.908**	**2.0**	**Not adjusted**				
PFPrS (C3)	Not adjusted					Not adjusted					Not adjusted				
PFBA (C4)	**0-180**	**12±1**	**1.2×10^{-1}**	**0.963**	**2.0**	**0-240**	**17±1**	**6.2×10^{-2}**	**0.985**	**2.0**	**15-120** [a]	**24±3**	**9.9×10^{-2}**	**0.961**	**2.0**
PFBS (C4)	0-240	3.3±0.2	2.1×10^{-2}	0.977	2.0	0-240	3.6±0.3	8.4×10^{-2}	0.950	2.0	15-240 [a]	2.2±0.2	3.1×10^{-2}	0.934	2.0
PFOA (C8)	**Not adjusted**					**Not adjusted**					**Not adjusted**				
PFOS (C8)	Totally adsorbed before the beginning of the reaction					Totally adsorbed before the beginning of the reaction					Totally adsorbed before the beginning of the reaction				

	NF					RO				
	Time interval (min)	k ($\times10^{-3}$ /min)	S^2_R (μg²/L²)	R^2	C_0 (μg/L)	Time interval (min)	k ($\times10^{-3}$ /min)	S^2_R (μg²/L²)	R^2	C_0 (μg/L)
PFMS (C1)	Not adjusted					Not adjusted				
PFEtS (C2)	Not adjusted					Not adjusted				
PFPrA (C3)	**Not adjusted**					**Not adjusted**				
PFPrS (C3)	Not adjusted					Not adjusted				
PFBA (C4)	**0-240**	**12±1**	**1.2×10^{-1}**	**0.971**	**2.0**	**0-120**	**17±2**	**8.2×10^{-2}**	**0.967**	**2.0**
PFBS (C4)	Not adjusted					Not adjusted				
PFOA (C8)	**0-120**	**30±1**	**1.9×10^{-2}**	**0.973**	**1.1**	**0-180**	**25±2**	**1.1×10^{-2}**	**0.982**	**0.9**
PFOS (C8)	Not adjusted					Totally adsorbed before the beginning of the reaction				

[a]The fitting was performed only considering the reaction after the evident generation of the PFAS

4.6.5. Degradation mechanism of PFAS

From all the previous results, it is possible to state that PFEtS (C2), PFPrA (C3), and PFBS (C4) are for sure intermediates of PFAS with total chain length ≤C8 (and can also be intermediates of PFAS with chain length >C8), while PFBA (C4) is certainly intermediate of PFAS with chain length >C8 (and can also be intermediate of PFAS with chain length ≤C8). In an attempt to scrutinize the electrooxidation mechanism of PFAS, the amount of all PFAS was followed during the degradation of each PFAS in UPW (2.0 µg/L of each C1-C8 PFAS) at 100 mA/cm^2. However, the formation of shorter-chain PFAS was never detected. A possible explanation for these results is that PFAS generated as intermediates may have been much faster oxidized at the BDD surface in the single-solute solutions than in the multi-solute solutions due to the absence of competitive adsorption and oxidation. Furthermore, the low formation yields may have hindered the detection of intermediates.

It has been proposed that the electrooxidation of PFCA and PFSA is initiated by direct electron transfer to the anode surface followed by the cleavage of the $-COO^-$ and $-SO_3$ functional groups, respectively, resulting in a C_nF_{2n+1} radical that can react with oxidants to form shorter-chain PFAS via repetitive CF_2-unzipping cycles, ultimately yielding CO_2 and HF (Carter & Farrell, 2008; H. Lin et al., 2018; Niu et al., 2013; Radjenovic et al., 2020; Wang et al., 2020). Various studies report the conversion of long-chain PFAS into ultrashort- and short-chain PFAS using BDD anodes, similarly to what happened in the current study, and some studies also detected the formation of medium-chain PFAS from the degradation of long-chain PFAS, which were not detected in the present study (Carter & Farrell, 2008; Nienhauser et al., 2022; Trautmann et al., 2015). Nienhauser et al. (2022) detected PFBA (C4) and PFBS (C4) as intermediates of multi-solute solutions contaminated with 92-1,650 µg/L of C4-C8 PFAS. Trautmann et al. (2015) detected PFBA (C4), PFPeA (C5), PFHxA (C6), and PFHpA (C7) from the degradation of RO polluted with an extensive content (4.0-19 mg/L) of C4-C8 PFAS. The generation of PFBS (C4) from the degradation of PFAS ≤C8 found in Nienhauser et al. (2022) is in agreement with the findings of the current study, while the results found in Trautmann et al. (2015) are in contrast. These differences can be related to the dissimilar employed PFAS contents since the competition between PFAS for active anode adsorption sites may have been much more relevant for more concentrated solutions. Concerning single-solute solutions, Nienhauser et al. (2022) detected the formation of PFBA (C4) during the degradation of C8-PFOA (137 µg/L) but were unable to notice the generation of shorter-chain PFAS during the degradation of 165 µg/L of PFOS (C8). The results regarding the PFOS (C8) are in line with those obtained in the current study, but those regarding PFOA (C8) differ. The ~70-fold larger C8-PFOA content employed in Nienhauser et al. (2022) may have contributed to this discrepancy. Carter and Farrell (2008) degraded a solution contaminated with PFOS (C8) at ~200 mg/L and detected TFA (C2) as a by-product, which is a compound that was not assessed in the current study.

CONCLUSIONS

5. CONCLUSIONS

Given the surge in plastics and chemicals production in recent years, there is a pressing need to comprehend the quantity of MPs, PFAS, and plastic-related chemicals reaching the environment and ultimately human health.

To address these challenges, this thesis makes a valuable contribution to the global analytical landscape by developing novel analytical methods and finally applying them to investigate the presence of MPs, PFAS and other chemicals, as well as their bioaccessibility from MPs and the improvement of water treatment technologies.

The main conclusions of each individual research project included in this thesis are presented below.

1. **Screening of organic chemicals associated to virgin low-density polyethylene microplastic pellets exposed to the Mediterranean Sea environment by combining gas chromatography and liquid chromatography coupled to quadrupole-time-of-flight mass spectrometry.**

This research has demonstrated that the synergistic combination of various complementary chromatographic techniques coupled with HRMS allows for the expansion of the range of chemicals associated with LDPE MPs that can be identified in marine environments. In our investigation, utilizing different workflows, we were able to detect up to 50 organic chemicals within an 8-week exposure period in a port area in Mallorca (East of Spain).

Even in the case of primary production pellets, which are not anticipated to contain significant amounts of additives, our findings reveal that they may indeed contain chemicals that are rapidly released into the environment, such as melamine or EHS. Additionally, chemicals with moderate to non-polar characteristics, commonly found in marine environments, tend to partition to LDPE MPs, resulting in accumulated concentrations ranging from approximately 100 to 300 μg/kg (e.g., BPA). Consequently, LDPE MPs can function both as carriers of pollutants (additives) released into the environment and as vectors of other anthropogenic chemicals into aquatic organisms.

2. **Combination of a novel cost-effective glass density separator followed by quantitative ^{1}H-nuclear magnetic resonance spectroscopy for the determination of microplastics in marine sediments.**

This research led to the design of a novel glass device for extracting MPs from sediment samples using relatively small amounts of saline solutions. This device offers a cost-effective solution, reducing the use of toxic saline solutions, which can also be reused. Additionally, the identification of MP particles through ^{1}H-NMR spectroscopy has been demonstrated for various

types of MPs (PET, PVC, and LDPE) with particle sizes ≤300 μm and realistic concentrations from sediment samples.

This approach proved to be both time- and cost-efficient while it yields quantitative information for the entire sample. Alternative methods such as FT-IR or Raman are challenging to automate within a reasonable analysis time, while pyrolysis-GC-MS methods have limitations in sample capacity. In our proposed method, recoveries ranged from 71 to 107%, demonstrating good sensitivity with LOQs ranging from 15 to 245 ng/g. The method was applied to analyse three marine sediment samples from Galicia (NW Spain), showcasing PET and LDPE quantification in the approximate range of 50-200 ng/g as a proof-of-principle application.

3. Mimicking human ingestion of microplastics: oral bioaccessibility tests of bisphenol A and phthalate esters under fed and fasted states.

The human oral bioaccessibility study of PAEs and BPA with different range of polarities (log K_{ow} 1.98-9.65) from LDPE and PVC MPs by *in-vitro* PBETs tests using fed and fasted conditions has concluded that the gastric compartment usually accounts for more than 65% of overall bioaccessibility and increases significantly for those compounds with log K_{ow} <4.0, with the highest leachability values for DMP, DEP and BPA. It is important to note that DMP and DEP underwent partial hydrolysis under gastrointestinal conditions, resulting in the formation of MMP, MEP, and phthalic acid. Furthermore, the release of PAEs and BPA was more prominent from LDPE compared to PVC, likely due to the distinct chemical sorptive properties of PVC *versus* LDPE. This includes the structural rigidity of glassy PVC, leading to significant and irreversible sorption and low diffusion kinetics of highly hydrophobic compounds from rigid pores. Additionally, the increased surface polarity of PVC compared to rubbery LDPE promotes the adherence of more polar additives. The larger surface area in contact with body fluids of LDPE, attributed to its higher density and lower average particle size (110 μm for LDPE vs 140 μm for PVC), may contribute to the greater oral bioaccessibility of plastic additives from LDPE MPs. Moreover, the results indicate that higher amounts of enzymes in suspension and bile salts under fed state conditions, leading to the formation of micelles, enhance the bioaccessibility of plastic-borne organic compounds compared to fasted state conditions.

The estimated human ADI, considering the overall oral bioaccessibility data obtained, suggests that the accidental ingestion of MPs exceeding 3,000 μg/g (i.e., 0.3% (w/w)) of DMP, DnBP, or BPA could pose a genuine risk to human health based on USEPA RfD and/or EFSA TDI values.

4. *In-vitro* leaching and physiologically relevant extraction tests for phthalate congeners and bisphenol A from microplastics - Assessing the contribution of microplastics to the exposure of marine vertebrates towards plastic-related chemicals.

Our results indicate that, owing to their increased hydrophobicity, DMP, DEP, and BPA are the compounds within the plastic-related chemicals investigated here that exhibit the highest bioaccessibility in fish upon ingestion, regardless of the composition of gut fluids and the number of gastrointestinal compartments.

These same compounds, known for their rapid and extensive leaching from plastic materials into the environment, both in freshwater and saltwater, can be detected in the aquatic environment at significant concentrations, especially in areas prone to plastic debris accumulation. When assessing the daily intake of PAEs and BPA through water and MP ingestion, our findings reveal that MP ingestion is not the primary source of exposure to these plastic-associated compounds. However, it is worth noting that due to the facile leaching of these three chemicals into water, they also contribute to an increasing concentration of such substances in both freshwater and marine environments.

5. Determination of regulated perfluoroalkyl substances (PFAS) in drinking water according to Directive 2020/2184/EU.

A comparison of three methods (direct injection, on-line, and offline SPE, combined with LC-MS/MS in all cases) developed for the analysis of a total of 20 PFAS ranging from C4 to C13, as specified in Directive 2020/2184/EU, was conducted. Among these methods, on-line SPE demonstrated the poorest performance due to issues related to blank contamination. In contrast, direct injection approached the required mLOQs, except for longer-chain PFAS congeners, and could serve as a cost-effective and less labour-intensive screening method. Consequently, only offline SPE met the specified mLOQs to comply with the Directive requirements. This method achieved mLOQs between 5 and 10 times lower than those mandated by current legislation, demonstrating its capability to address potentially more stringent future regulations and delivering satisfactory performance in the 1-100 ng/L range (referring to individual PFAS).

When applied to 46 samples, from across Spain, Europe and North America, the method detected 13 PFAS (10 short-chain and 3 long-chain PFAS). Notably, the most polar PFAS, namely PFBA, PFHxA, and PFBS, were the most frequently identified congeners within each group (PFCAs and PFSAs), also exhibiting the highest concentrations. In contrast, PFOS and PFOA, well-known and extensively studied PFAS, were detected in the samples but at lower concentrations than short-chain congeners. This underscores concern about mobile and persistent chemicals as potential contaminants in drinking water and the potential substitution of longer-chain PFAS by shorter-chain alternatives. While bottled mineral water contamination was lower than tap water from public facilities, none of the samples exceeded the total limit stipulated in Directive 2020/2184/EU.

6. Insights into the application of the anodic oxidation process for the removal of per- and polyfluoroalkyl substances (PFAS) in water matrices.

The developed method for assessing the removal degradation of 23 PFAS (C2-C13) using an electrochemical advanced oxidation process, specifically anodic oxidation, exhibited distinct characteristics based on the perfluoroalkyl chain length and headgroup of the PFAS. PFSA compounds with chain lengths C1-C4 proved to be the most recalcitrant, posing greater challenges for decomposition compared to their PFCA counterparts. Conversely, PFSA compounds with chain lengths C5-C7 demonstrated a higher degradation ability than their PFCA counterparts, and PFSA ≥C9 were readily adsorbed on the hydrophobic BDD surface, potentially undergoing instantaneous degradation, in contrast to a similar behaviour observed only for PFCA ≥C12. Notably, PFPrA exhibited a higher degradation rate compared to some

longer-chain PFCA, deviating from the expected norm that longer-chain PFAS with the same headgroup typically show higher degradation rates.

The degradation kinetics of certain PFAS, particularly PFEtS, PFPrA, and PFBA, were influenced by PFAS content (0.2 µg/L *versus* 2.0 µg/L) and diversity (24 C1-C13 PFAS *versus* 8 C1-C8 PFAS *versus* individual PFAS). This influence was attributed to competitive adsorption effects in the presence of PFAS with varying perfluoroalkyl chain lengths and the generation of PFAS as intermediates during the oxidation of longer-chain PFAS.

In real water/wastewater matrices, PFAS removal generally occurred more rapidly compared to UPW due to a higher ion content (mostly Cl^-) and the subsequent electrogeneration of a greater quantity of oxidants (mostly HClO and ClO^-). However, the higher ion content also brought a higher ionic content, creating competition with PFAS for oxidants, which proved detrimental, particularly in the presence of a COD of 319 mg O_2/L in the RO system.

Lastly, it was identified that applying a *j* greater than 20 mA/cm^2 was necessary to eliminate charge transfer limitations for most PFAS in all water/wastewater matrices. In UPW, the degradation rate of PFPrA and PFBA was maximized for $j \geq 250$ mA/cm^2, the degradation rate of PFBS and PFOA was maximized for a *j* of 80 mA/cm^2, and the degradation rate of PFMS was maximized for a *j* of 40 mA/cm^2.

REFERENCES

6. REFERENCES

Abdallah, M. A.-E., Tilston, E., Harrad, S., & Collins, C. (2012). In vitro assessment of the bioaccessibility of brominated flame retardants in indoor dust using a colon extended model of the human gastrointestinal tract. *Journal of Environmental Monitoring*, *14*(12), 3276-3283. https://doi.org/10.1039/C2EM30690E

The age of plastic: from Parkesine to pollution. (2019). Retrieved 24 Oct from https://www.sciencemuseum.org.uk/objects-and-stories/chemistry/age-plastic-parkesine-pollution

Agustina, T. E., Ang, H. M., & Vareek, V. K. (2005). A review of synergistic effect of photocatalysis and ozonation on wastewater treatment. *Journal of Photochemistry and Photobiology C: Photochemistry Reviews*, *6*(4), 264-273. https://doi.org/10.1016/j.jphotochemrev.2005.12.003

Al-Odaini, N. A., Shim, W. J., Han, G. M., Jang, M., & Hong, S. H. (2015). Enrichment of hexabromocyclododecanes in coastal sediments near aquaculture areas and a wastewater treatment plant in a semi-enclosed bay in South Korea. *Science of The Total Environment*, *505*, 290-298. https://doi.org/10.1016/j.scitotenv.2014.10.019

Al Amin, M., Sobhani, Z., Liu, Y., Dharmaraja, R., Chadalavada, S., Naidu, R., Chalker, J. M., & Fang, C. (2020). Recent advances in the analysis of per- and polyfluoroalkyl substances (PFAS)—A review. *Environmental Technology & Innovation*, *19*, 100879. https://doi.org/10.1016/j.eti.2020.100879

Alfonso, M. B., Arias, A. H., & Piccolo, M. C. (2020). Microplastics integrating the zooplanktonic fraction in a saline lake of Argentina: influence of water management. *Environmental Monitoring and Assessment*, *192*(2), 117. https://doi.org/10.1007/s10661-020-8080-1

Allinson, M., Yamashita, N., Taniyasu, S., Yamazaki, E., & Allinson, G. (2019). Occurrence of perfluoroalkyl substances in selected Victorian rivers and estuaries: An historical snapshot. *Heliyon*, *5*(9), e02472. https://doi.org/10.1016/j.heliyon.2019.e02472

Ambrogi, V., Carfagna, C., Cerruti, P., & Marturano, V. (2017). 4 - Additives in Polymers. In C. F. Jasso-Gastinel & J. M. Kenny (Eds.), *Modification of Polymer Properties* (pp. 87-108). William Andrew Publishing. https://doi.org/10.1016/B978-0-323-44353-1.00004-X

Amelia, T. S. M., Khalik, W. M. A. W. M., Ong, M. C., Shao, Y. T., Pan, H.-J., & Bhubalan, K. (2021). Marine microplastics as vectors of major ocean pollutants and its hazards to the marine ecosystem and humans. *Progress in Earth and Planetary Science*, *8*(1), 12. https://doi.org/10.1186/s40645-020-00405-4

Andrady, A. L. (2011). Microplastics in the marine environment. *Marine Pollution Bulletin*, *62*(8), 1596-1605. https://doi.org/10.1016/j.marpolbul.2011.05.030

Appleman, T. D., Dickenson, E. R. V., Bellona, C., & Higgins, C. P. (2013). Nanofiltration and granular activated carbon treatment of perfluoroalkyl acids. *Journal of Hazardous Materials*, *260*, 740-746. https://doi.org/10.1016/j.jhazmat.2013.06.033

Aragaw, T. A. (2021). Microplastic pollution in African countries' water systems: a review on findings, applied methods, characteristics, impacts, and managements. *SN Applied Sciences*, *3*(6), 629. https://doi.org/10.1007/s42452-021-04619-z

Araujo, C. F., Nolasco, M. M., Ribeiro, A. M. P., & Ribeiro-Claro, P. J. A. (2018). Identification of microplastics using Raman spectroscopy: Latest developments and future prospects. *Water Research*, *142*, 426-440. https://doi.org/10.1016/j.watres.2018.05.060

Araújo, K. C. F., dos Santos, E. V., Nidheesh, P. V., & Martínez-Huitle, C. A. (2022). Fundamentals and advances on the mechanisms of electrochemical generation of persulfate and sulfate radicals in aqueous medium. *Current Opinion in Chemical Engineering*, *38*, 100870. https://doi.org/10.1016/j.coche.2022.100870

Arditsoglou, A., & Voutsa, D. (2012). Occurrence and partitioning of endocrine-disrupting compounds in the marine environment of Thermaikos Gulf, Northern Aegean Sea, Greece. *Marine Pollution Bulletin*, *64*(11), 2443-2452. https://doi.org/10.1016/j.marpolbul.2012.07.048

Arinaitwe, K., Keltsch, N., Taabu-Munyaho, A., Reemtsma, T., & Berger, U. (2021). Perfluoroalkyl substances (PFASs) in the Ugandan waters of Lake Victoria: Spatial distribution, catchment release and public exposure risk via municipal water consumption. *Science of The Total Environment*, *783*, 146970. https://doi.org/10.1016/j.scitotenv.2021.146970

Arthur, C., Baker, J. E., & Bamford, H. A. (2009). Proceedings of the International Research Workshop on the Occurrence, Effects, and Fate of Microplastic Marine Debris, September 9-11, 2008, University of Washington Tacoma, Tacoma, WA, USA [Technical Memorandum]. https://repository.library.noaa.gov/view/noaa/2509 (NOAA technical memorandum NOS-OR&R 30)

Ašmonaitė, G., Tivefälth, M., Westberg, E., Magnér, J., Backhaus, T., & Carney Almroth, B. (2020). Microplastics as a Vector for Exposure to Hydrophobic Organic Chemicals in Fish: A Comparison of Two Polymers and Silica Particles Spiked With Three Model Compounds [Original Research]. *Frontiers in Environmental Science*, *8*. https://doi.org/10.3389/fenvs.2020.00087

Avio, C. G., Gorbi, S., & Regoli, F. (2015). Experimental development of a new protocol for extraction and characterization of microplastics in fish tissues: First observations in commercial species from Adriatic Sea. *Marine Environmental Research*, *111*, 18-26. https://doi.org/10.1016/j.marenvres.2015.06.014

Babayev, M., Capozzi, S. L., Miller, P., McLaughlin, K. R., Medina, S. S., Byrne, S., Zheng, G., & Salamova, A. (2022). PFAS in drinking water and serum of the people of a southeast Alaska community: A pilot study. *Environmental Pollution*, *305*, 119246. https://doi.org/10.1016/j.envpol.2022.119246

Baekeland, L. H. (1909). The synthesis, constitution, and uses of bakelite. *Industrial & Engineering Chemistry*, *1*(3), 149-161. https://doi.org/10.1021/ie50003a004

Bai, X., & Son, Y. (2021). Perfluoroalkyl substances (PFAS) in surface water and sediments from two urban watersheds in Nevada, USA. *Science of The Total Environment*, *751*, 141622. https://doi.org/10.1016/j.scitotenv.2020.141622

Bakir, A., Rowland, S. J., & Thompson, R. C. (2014a). Enhanced desorption of persistent organic pollutants from microplastics under simulated physiological conditions. *Environmental Pollution*, *185*, 16-23. https://doi.org/10.1016/j.envpol.2013.10.007

Bakir, A., Rowland, S. J., & Thompson, R. C. (2014b). Transport of persistent organic pollutants by microplastics in estuarine conditions. *Estuarine, Coastal and Shelf Science*, *140*, 14-21. https://doi.org/10.1016/j.ecss.2014.01.004

Bao, Z.-Z., Lu, S.-Q., Wang, G., Cai, Z., & Chen, Z.-F. (2023). Adsorption of 2-hydroxynaphthalene, naphthalene, phenanthrene, and pyrene by polyvinyl chloride microplastics in water and their bioaccessibility under in vitro human gastrointestinal system. *Science of The Total Environment*, *871*, 162157. https://doi.org/10.1016/j.scitotenv.2023.162157

BARGE. (2011). UBM procedure for the measurement of inorganic contaminant bioaccessibility from solid matrices. https://www2.bgs.ac.uk/barge/docs/BARGE_UBM_DEC_2010.pdf

Basheer, C., & Lee, H. K. (2004). Analysis of endocrine disrupting alkylphenols, chlorophenols and bisphenol-A using hollow fiber-protected liquid-phase microextraction coupled with injection port-derivatization gas chromatography–mass spectrometry. *Journal of Chromatography A*, *1057*(1), 163-169. https://doi.org/10.1016/j.chroma.2004.09.083

Beiras, R., & Schönemann, A. M. (2020). Currently monitored microplastics pose negligible ecological risk to the global ocean. *Scientific Reports*, *10*(1), 22281. https://doi.org/10.1038/s41598-020-79304-z

Bernett, M. K., & Zisman, W. A. (1969). Effect of adsorbed water on wetting properties of borosilicate glass, quartz, and sapphire. *Journal of Colloid and Interface Science*, *29*(3), 413-423. https://doi.org/10.1016/0021-9797(69)90120-9

Bertoldi, C., Lara, L. Z., Mizushima, F. A. d. L., Martins, F. C. G., Battisti, M. A., Hinrichs, R., & Fernandes, A. N. (2021). First evidence of microplastic contamination in the freshwater of Lake Guaíba, Porto Alegre, Brazil. *Science of The Total Environment*, *759*, 143503. https://doi.org/10.1016/j.scitotenv.2020.143503

Bharath K, M., S, S., Natesan, U., Ayyamperumal, R., Kalam S, N., S, A., K, S., & C, A. (2021). Microplastics as an emerging threat to the freshwater ecosystems of Veeranam lake in south India: A multidimensional approach. *Chemosphere*, *264*, 128502. https://doi.org/10.1016/j.chemosphere.2020.128502

Boiteux, V., Dauchy, X., Bach, C., Colin, A., Hemard, J., Sagres, V., Rosin, C., & Munoz, J.-F. (2017). Concentrations and patterns of perfluoroalkyl and polyfluoroalkyl substances in a river and three drinking water treatment plants near and far from a major production source. *Science of The Total Environment*, *583*, 393-400. https://doi.org/10.1016/j.scitotenv.2017.01.079

Boiteux, V., Dauchy, X., Rosin, C., & Munoz, J.-F. (2012). National Screening Study on 10 Perfluorinated Compounds in Raw and Treated Tap Water in France. *Archives of Environmental Contamination and Toxicology*, *63*(1), 1-12. https://doi.org/10.1007/s00244-012-9754-7

Bolgar, M., Hubball, J., Groeger, J., & Meronek, S. (2007). *Handbook for the chemical analysis of plastic and polymer additives*. CRC Press. https://doi.org/10.1201/9781420044881

Bolobajev, J., Trapido, M., & Dulova, N. (2015). Application of Different Techniques for Activation of H2O2/Fe3+ System: A Comparative Study. *Journal of Advanced Oxidation Technologies*, *18*(2), 347-352. https://doi.org/10.1515/jaots-2015-0222

Bordós, G., Urbányi, B., Micsinai, A., Kriszt, B., Palotai, Z., Szabó, I., Hantosi, Z., & Szoboszlay, S. (2019). Identification of microplastics in fish ponds and natural freshwater environments of the Carpathian basin, Europe. *Chemosphere*, *216*, 110-116. https://doi.org/10.1016/j.chemosphere.2018.10.110

Bosker, T., Guaita, L., & Behrens, P. (2018). Microplastic pollution on Caribbean beaches in the Lesser Antilles. *Marine Pollution Bulletin*, *133*, 442-447. https://doi.org/10.1016/j.marpolbul.2018.05.060

Boulanger, B., Vargo, J., Schnoor, J. L., & Hornbuckle, K. C. (2004). Detection of Perfluorooctane Surfactants in Great Lakes Water. *Environmental Science & Technology*, *38*(15), 4064-4070. https://doi.org/10.1021/es0496975

Brennecke, D., Duarte, B., Paiva, F., Caçador, I., & Canning-Clode, J. (2016). Microplastics as vector for heavy metal contamination from the marine environment. *Estuarine, Coastal and Shelf Science*, *178*, 189-195. https://doi.org/10.1016/j.ecss.2015.12.003

Burns, D. C., Ellis, D. A., Li, H., McMurdo, C. J., & Webster, E. (2008). Experimental pKa Determination for Perfluorooctanoic Acid (PFOA) and the Potential Impact of pKa Concentration Dependence on Laboratory-Measured Partitioning Phenomena and Environmental Modeling. *Environmental Science & Technology*, *42*(24), 9283-9288. https://doi.org/10.1021/es802047v

Cabañero, A. I., Madrid, Y., & Cámara, C. (2004). Selenium and mercury bioaccessibility in fish samples: an in vitro digestion method. *Analytica Chimica Acta*, *526*(1), 51-61. https://doi.org/10.1016/j.aca.2004.09.039

Cabañero, A. I., Madrid, Y., & Cámara, C. (2007). Mercury–Selenium Species Ratio in Representative Fish Samples and Their Bioaccessibility by an In Vitro Digestion Method. *Biological Trace Element Research*, *119*(3), 195-211. https://doi.org/10.1007/s12011-007-8007-5

Campo, J., Lorenzo, M., Pérez, F., Picó, Y., Farré, M. l., & Barceló, D. (2016). Analysis of the presence of perfluoroalkyl substances in water, sediment and biota of the Jucar River (E Spain). Sources, partitioning and relationships with water physical characteristics. *Environmental Research*, *147*, 503-512. https://doi.org/10.1016/j.envres.2016.03.010

Cao, Y., Lee, C., Davis, E. T. J., Si, W., Wang, F., Trimpin, S., & Luo, L. (2019). 1000-Fold Preconcentration of Per- and Polyfluorinated Alkyl Substances within 10 Minutes via Electrochemical Aerosol Formation. *Analytical Chemistry*, *91*(22), 14352-14358. https://doi.org/10.1021/acs.analchem.9b02758

Cao, Y., Li, J., Wu, R., Lin, H., Lao, J.-Y., Ruan, Y., Zhang, K., Wu, J., Leung, K. M. Y., & Lam, P. K. S. (2022). Phthalate esters in seawater and sediment of the northern South China Sea: Occurrence, distribution, and ecological risks. *Science of The Total Environment*, *811*, 151412. https://doi.org/10.1016/j.scitotenv.2021.151412

Carbery, M., O'Connor, W., & Palanisami, T. (2018). Trophic transfer of microplastics and mixed contaminants in the marine food web and implications for human health. *Environment International*, *115*, 400-409. https://doi.org/10.1016/j.envint.2018.03.007

Carter, C. G., Bransden, M. P., van Barneveld, R. J., & Clarke, S. M. (1999). Alternative methods for nutrition research on the southern bluefin tuna, Thunnus maccoyii: in vitro digestibility. *Aquaculture*, *179*(1), 57-70. https://doi.org/10.1016/S0044-8486(99)00152-0

Carter, K. E., & Farrell, J. (2008). Oxidative Destruction of Perfluorooctane Sulfonate Using Boron-Doped Diamond Film Electrodes. *Environmental Science & Technology*, *42*(16), 6111-6115. https://doi.org/10.1021/es703273s

Caruso, G. (2019). Microplastics as vectors of contaminants. *Marine Pollution Bulletin*, *146*, 921-924. https://doi.org/10.1016/j.marpolbul.2019.07.052

Castiglioni, S., Valsecchi, S., Polesello, S., Rusconi, M., Melis, M., Palmiotto, M., Manenti, A., Davoli, E., & Zuccato, E. (2015). Sources and fate of perfluorinated compounds in the aqueous environment and in drinking water of a highly urbanized and industrialized area in Italy. *Journal of Hazardous Materials*, *282*, 51-60. https://doi.org/10.1016/j.jhazmat.2014.06.007

Castro, V., Quintana, J. B., Carpinteiro, I., Cobas, J., Carro, N., Cela, R., & Rodil, R. (2021). Combination of different chromatographic and sampling modes for high-resolution mass spectrometric screening of organic microcontaminants in water. *Analytical and Bioanalytical Chemistry*, *413*(22), 5607-5618. https://doi.org/10.1007/s00216-021-03226-6

Castro, V., Quintana, J. B., López-Vázquez, J., Carro, N., Cobas, J., Bilbao, D., Cela, R., & , & Rodil, R. (2021). *EI-HRMS library of spectra aquired on a GC-QTOF* https://doi.org/10.5281/zenodo.5647960

Castro, V., Quintana, J. B., López-Vázquez, J., Carro, N., Cobas, J., Bilbao, D., Cela, R., & Rodil, R. (2022). Development and application of an in-house library and workflow for gas chromatography–electron ionization–accurate-mass/high-resolution mass spectrometry screening of environmental samples. *Analytical and Bioanalytical Chemistry*, *414*(21), 6327-6340. https://doi.org/10.1007/s00216-021-03810-w

Catarino, A. I., Thompson, R., Sanderson, W., & Henry, T. B. (2017). Development and optimization of a standard method for extraction of microplastics in mussels by enzyme digestion of soft tissues. *Environmental Toxicology and Chemistry*, *36*(4), 947-951. https://doi.org/10.1002/etc.3608

Cave, M. R., Wragg, J., Harrison, I., Vane, C. H., Wiele, T. V. d., Groeve, E. D., Nathanail, C. P., Ashmore, M., Thomas, R., Robinson, J., & Daly, P. (2010). Comparison of Batch Mode and Dynamic Physiologically Based Bioaccessibility Tests for PAHs in Soil Samples. *Environmental Science & Technology*, *44*(7), 2654-2660. https://doi.org/10.1021/es903258v

Chen, D., Sharma, S. K., & Mudhoo, A. (2011). *Handbook on applications of ultrasound: sonochemistry for sustainability*. CRC press.

Chen, X.-j., Ma, J.-j., Yu, R.-l., Hu, G.-r., & Yan, Y. (2022). Bioaccessibility of microplastic-associated heavy metals using an in vitro digestion model and its implications for human health risk assessment. *Environmental Science and Pollution Research*, *29*(51), 76983-76991. https://doi.org/10.1007/s11356-022-20983-8

Chen, Y., Shu, L., Qiu, Z., Lee, D. Y., Settle, S. J., Que Hee, S., Telesca, D., Yang, X., & Allard, P. (2016). Exposure to the BPA-Substitute Bisphenol S Causes Unique Alterations of Germline Function. *PLOS Genetics*, *12*(7), e1006223. https://doi.org/10.1371/journal.pgen.1006223

Chen, Y., Zhang, L., Xu, C., & Vaidyanathan, S. (2016). Dissolved inorganic carbon speciation in aquatic environments and its application to monitor algal carbon uptake. *Science of The Total Environment*, *541*, 1282-1295. https://doi.org/10.1016/j.scitotenv.2015.10.025

Chiaia-Hernández, A. C., Scheringer, M., Müller, A., Stieger, G., Wächter, D., Keller, A., Pintado-Herrera, M. G., Lara-Martin, P. A., Bucheli, T. D., & Hollender, J. (2020). Target and suspect screening analysis reveals persistent emerging organic contaminants in soils and sediments. *Science of The Total Environment*, *740*, 140181. https://doi.org/10.1016/j.scitotenv.2020.140181

Chindarkar, N. S., Wakefield, M. R., Stone, J. A., & Fitzgerald, R. L. (2014). Liquid Chromatography High-Resolution TOF Analysis: Investigation of MSE for Broad-Spectrum Drug Screening. *Clinical Chemistry*, *60*(8), 1115-1125. https://doi.org/10.1373/clinchem.2014.222976

Choi, Y., Lee, J.-H., Kim, K., Mun, H., Park, N., & Jeon, J. (2021). Identification, quantification, and prioritization of new emerging pollutants in domestic and industrial effluents, Korea: Application of LC-HRMS based suspect and non-target screening.

Journal of Hazardous Materials, *402*, 123706. https://doi.org/10.1016/j.jhazmat.2020.123706

Chow, S. J., Ojeda, N., Jacangelo, J. G., & Schwab, K. J. (2021). Detection of ultrashort-chain and other per- and polyfluoroalkyl substances (PFAS) in U.S. bottled water. *Water Research*, *201*, 117292. https://doi.org/10.1016/j.watres.2021.117292

Choy, C. A., Robison, B. H., Gagne, T. O., Erwin, B., Firl, E., Halden, R. U., Hamilton, J. A., Katija, K., Lisin, S. E., Rolsky, C., & S. Van Houtan, K. (2019). The vertical distribution and biological transport of marine microplastics across the epipelagic and mesopelagic water column. *Scientific Reports*, *9*(1), 7843. https://doi.org/10.1038/s41598-019-44117-2

Ciofi, L., Renai, L., Rossini, D., Ancillotti, C., Falai, A., Fibbi, D., Bruzzoniti, M. C., Santana-Rodriguez, J. J., Orlandini, S., & Del Bubba, M. (2018). Applicability of the direct injection liquid chromatographic tandem mass spectrometric analytical approach to the sub-ngL−1 determination of perfluoro-alkyl acids in waste, surface, ground and drinking water samples. *Talanta*, *176*, 412-421. https://doi.org/10.1016/j.talanta.2017.08.052

Coffin, S., Huang, G.-Y., Lee, I., & Schlenk, D. (2019). Fish and Seabird Gut Conditions Enhance Desorption of Estrogenic Chemicals from Commonly-Ingested Plastic Items. *Environmental Science & Technology*, *53*(8), 4588-4599. https://doi.org/10.1021/acs.est.8b07140

Coffin, S., Lee, I., Gan, J., & Schlenk, D. (2019). Simulated digestion of polystyrene foam enhances desorption of diethylhexyl phthalate (DEHP) and In vitro estrogenic activity in a size-dependent manner. *Environmental Pollution*, *246*, 452-462. https://doi.org/10.1016/j.envpol.2018.12.011

Cole, M., Webb, H., Lindeque, P. K., Fileman, E. S., Halsband, C., & Galloway, T. S. (2014). Isolation of microplastics in biota-rich seawater samples and marine organisms. *Scientific Reports*, *4*(1), 1-8. https://doi.org/10.1038/srep04528

Convention, S. (2016). *Listing of POPs in the Stockholm Convention*. Retrieved 21 Apr from http://chm.pops.int/TheConvention/ThePOPs/ListingofPOPs/tabid/2509/Default.aspx

Coppock, R. L., Cole, M., Lindeque, P. K., Queirós, A. M., & Galloway, T. S. (2017). A small-scale, portable method for extracting microplastics from marine sediments. *Environmental Pollution*, *230*, 829-837. https://doi.org/10.1016/j.envpol.2017.07.017

Courtene-Jones, W., Quinn, B., Murphy, F., Gary, S. F., & Narayanaswamy, B. E. (2017). Optimisation of enzymatic digestion and validation of specimen preservation methods for the analysis of ingested microplastics [10.1039/C6AY02343F]. *Analytical Methods*, *9*(9), 1437-1445. https://doi.org/10.1039/C6AY02343F

Cox, K. D., Covernton, G. A., Davies, H. L., Dower, J. F., Juanes, F., & Dudas, S. E. (2019). Human Consumption of Microplastics. *Environmental Science & Technology*, *53*(12), 7068-7074. https://doi.org/10.1021/acs.est.9b01517

Crichton, E. M., Noël, M., Gies, E. A., & Ross, P. S. (2017). A novel, density-independent and FTIR-compatible approach for the rapid extraction of microplastics from aquatic sediments [10.1039/C6AY02733D]. *Analytical Methods*, *9*(9), 1419-1428. https://doi.org/10.1039/C6AY02733D

Cruz, R., Cunha, S. C., & Casal, S. (2015). Brominated flame retardants and seafood safety: A review. *Environment International*, *77*, 116-131. https://doi.org/10.1016/j.envint.2015.01.001

Cui, D., Li, X., & Quinete, N. (2020). Occurrence, fate, sources and toxicity of PFAS: What we know so far in Florida and major gaps. *TrAC Trends in Analytical Chemistry*, *130*, 115976. https://doi.org/10.1016/j.trac.2020.115976

Cuñat, A., Álvarez-Ruiz, R., Morales Suarez-Varela, M. M., & Pico, Y. (2022). Suspected-screening assessment of the occurrence of organic compounds in sewage sludge. *Journal of Environmental Management*, *308*, 114587. https://doi.org/10.1016/j.jenvman.2022.114587

Da Costa, J. P., ROCHA-SANTOS, T., & DUARTE, A. C. (2020). *The environmental impacts of plastics and micro-plastics use, waste and pollution: EU and national measures*. EPRS: European Parliamentary Research Service. Retrieved 18 Jan from https://policycommons.net/artifacts/1426661/the-environmental-impacts-of-plastics-and-micro-plastics-use-waste-and-pollution/2041108/

Dalahmeh, S., Tirgani, S., Komakech, A. J., Niwagaba, C. B., & Ahrens, L. (2018). Per- and polyfluoroalkyl substances (PFASs) in water, soil and plants in wetlands and agricultural areas in Kampala, Uganda. *Science of The Total Environment*, *631-632*, 660-667. https://doi.org/10.1016/j.scitotenv.2018.03.024

Dang, T. T., Do, V. M., & Trinh, V. T. (2020). Nano-Catalysts in Ozone-Based Advanced Oxidation Processes for Wastewater Treatment. *Current Pollution Reports*, *6*(3), 217-229. https://doi.org/10.1007/s40726-020-00147-3

Dean, J. R., & Ma, R. (2007). Approaches to assess the oral bioaccessibility of persistent organic pollutants: A critical review. *Chemosphere*, *68*(8), 1399-1407. https://doi.org/10.1016/j.chemosphere.2007.03.054

Dehaut, A., Cassone, A.-L., Frère, L., Hermabessiere, L., Himber, C., Rinnert, E., Rivière, G., Lambert, C., Soudant, P., Huvet, A., Duflos, G., & Paul-Pont, I. (2016). Microplastics in seafood: Benchmark protocol for their extraction and characterization. *Environmental Pollution*, *215*, 223-233. https://doi.org/10.1016/j.envpol.2016.05.018

Dekiff, J. H., Remy, D., Klasmeier, J., & Fries, E. (2014). Occurrence and spatial distribution of microplastics in sediments from Norderney. *Environmental Pollution*, *186*, 248-256. https://doi.org/10.1016/j.envpol.2013.11.019

Deng, Z.-H., Cheng, C.-G., Wang, X.-L., Shi, S.-H., Wang, M.-L., & Zhao, R.-S. (2018). Preconcentration and Determination of Perfluoroalkyl Substances (PFASs) in Water Samples by Bamboo Charcoal-Based Solid-Phase Extraction Prior to Liquid Chromatography–Tandem Mass Spectrometry. *Molecules*, *23*(4), 902. https://doi.org/10.3390/molecules23040902

Derco, J., Dudáš, J., Valičková, M., Šimovičová, K., & Kecskés, J. (2015). Removal of micropollutants by ozone based processes. *Chemical Engineering and Processing - Process Intensification*, *94*, 78-84. https://doi.org/10.1016/j.cep.2015.03.014

Diao, P., Chen, Q., Wang, R., Sun, D., Cai, Z., Wu, H., & Duan, S. (2017). Phenolic endocrine-disrupting compounds in the Pearl River Estuary: Occurrence, bioaccumulation and risk assessment. *Science of The Total Environment*, *584-585*, 1100-1107. https://doi.org/10.1016/j.scitotenv.2017.01.169

Ding, L., Mao, R. f., Guo, X., Yang, X., Zhang, Q., & Yang, C. (2019). Microplastics in surface waters and sediments of the Wei River, in the northwest of China. *Science of The Total Environment*, *667*, 427-434. https://doi.org/10.1016/j.scitotenv.2019.02.332

Dioses-Salinas, D. C., Pizarro-Ortega, C. I., & De-la-Torre, G. E. (2020). A methodological approach of the current literature on microplastic contamination in terrestrial environments: Current knowledge and baseline considerations. *Science of The Total Environment*, *730*, 139164. https://doi.org/10.1016/j.scitotenv.2020.139164

Dodiuk, H. (2021). *Handbook of thermoset plastics*. William Andrew.

Domingo, J. L., & Nadal, M. (2019). Human exposure to per- and polyfluoroalkyl substances (PFAS) through drinking water: A review of the recent scientific literature. *Environmental Research*, *177*, 108648. https://doi.org/10.1016/j.envres.2019.108648

Dou, W., Zhang, Z., Huang, W., Wang, X., Zhang, R., Wu, Y., Sun, A., Shi, X., & Chen, J. (2022). Contaminant occurrence, spatiotemporal variation, and ecological risk of organophosphorus flame retardants (OPFRs) in Hangzhou Bay and east China sea ecosystem. *Chemosphere*, *303*, 135032. https://doi.org/10.1016/j.chemosphere.2022.135032

Du, J., Li, H., Xu, S., Zhou, Q., Jin, M., & Tang, J. (2019). A review of organophosphorus flame retardants (OPFRs): occurrence, bioaccumulation, toxicity, and organism exposure. *Environmental Science and Pollution Research*, *26*(22), 22126-22136. https://doi.org/10.1007/s11356-019-05669-y

Duinslaeger, N., & Radjenovic, J. (2022). Electrochemical degradation of per- and polyfluoroalkyl substances (PFAS) using low-cost graphene sponge electrodes. *Water Research*, *213*, 118148. https://doi.org/10.1016/j.watres.2022.118148

Dümichen, E., Eisentraut, P., Bannick, C. G., Barthel, A.-K., Senz, R., & Braun, U. (2017). Fast identification of microplastics in complex environmental samples by a thermal degradation method. *Chemosphere*, *174*, 572-584. https://doi.org/10.1016/j.chemosphere.2017.02.010

Eaton, A. D., Clesceri, L. S., Franson, M. A. H., Rice, E. W., & Greenberg, A. E. (Eds.). (2005). *Standard Methods for Examination of Water and Wastewater, 21st Edition*. American Public Health Association (APHA) - American Water Works Association (AWWA) - Water Environment Federation (WEF).

EC. (2003). Directive 2003/11/EC of the European Parliament and of the Council of 6 February 2003 Amending for the 24th Time Council Directive 76/769/EEC Relating to Restrictions on the Marketing and Use of Certain Dangerous Substances and Preparations (Pentabromodiphenyl Ether, Octabromo-diphenyl Ether). *Official Journal of the European Union*, *66*, 1-44. https://eur-lex.europa.eu/LexUriServ/LexUriServ.do?uri=OJ:L:2003:042:0045:0046:EN:PDF

EC. (2006). European Commission Regulation No.1907/2006 Concerning the Registration Evaluation Authorisation and Restriction of Chemicals (REACH) Establishing a European Chemicals Agency Amending Directive 1999/45/EC and Repealing Council Regulation (EEC) No.793/93 and Commission Regulation (EC) No.1488/94 as Well as Council Directive 76/769/EEC and Commission Directives 91/155/EEC93/67/EEC93/105/EC and 2000/21/EC. *Official Journal of the European Union* *107*, 1-44. https://eur-lex.europa.eu/legal-content/EN/TXT/PDF/?uri=CELEX:02006R1907-20140410

EC. (2009). Decision 2005/717/EC-exemption of Deca BDE from the Prohibition on Use. *Official Journal of the European Union*, *66*, 1-44. https://eur-lex.europa.eu/LexUriServ/LexUriServ.do?uri=OJ:L:2005:271:0048:0050:EN:PDF

EC. (2011). Commission regulation (EU) no 10/2011 on plastic materials and articles intended to come into contact with food. *Official Journal of the European Union*, *12*, 1-44. https://eur-lex.europa.eu/legal-content/EN/TXT/PDF/?uri=CELEX:32011R0010

EC. (2013). Directive 2013/39/EU of the European Parliament and of the Council of 12 August 2013 amending Directives 2000/60/EC and 2008/105/EC as regards priority substances in the field of water policy Text with EEA relevance. *Official Journal of the European*

Union, *226*, 1-17. https://eur-lex.europa.eu/LexUriServ/LexUriServ.do?uri=OJ:L:2013:226:0001:0017:en:PDF

EC. (2014a). European Commission, REACH - Restrictions Commission conclusions on the review clause of REACH Annex XVII, entry 52 (DINP, DIDP and DNOP). https://ec.europa.eu/docsroom/documents/13172/attachments/1/translations

EC. (2014b). European Commission. Commission conclusions on the review clause of REACH Annex XVII, entry 51 (DEHP, DBP, BBP), CA/42/2014. https://ec.europa.eu/docsroom/documents/5765/attachments/1/translations

EC. (2016). Commission Regulation (EU) 2016/2235 of 12 December 2016 amending Annex XVII to Regulation (EC) No 1907/2006 of the European Parliament and of the Council concerning the Registration, Evaluation, Authorisation and Restriction of Chemicals (REACH) as regards bisphenol A (Text with EEA relevance). *Official Journal European Union*, *337*, 3-5. https://eur-lex.europa.eu/eli/reg/2016/2235/oj

EC. (2020). Directive (EU) 2020/2184 of the European Parliament and of the Council of 16 December 2020 on the quality of water intended for human consumption. *Official Journal of the European Union*, *435*, 1-62. https://eur-lex.europa.eu/eli/dir/2020/2184/oj

EC. (2021). Guidance Document on Analytical Quality Control and Method Validation for Pesticide Residues Analysis in Food and Feed SANTE 11312/2021. *Sante/11312/2021*, 1-57. https://ec.europa.eu/food/system/files/2022-02/pesticides_mrl_guidelines_wrkdoc_2021-11312.pdf

ECHA. (2006). *2-ethylhexyl salicylate REACH dossier*. Retrieved 26 Oct from https://echa.europa.eu/es/registration-dossier/-/registered-dossier/14203/3/1/6

ECHA. (2021a). *Describing the uses of additives in plastic material for articles and estimating the related exposure : practical guide for industry*. Retrieved 25 Oct from https://echa.europa.eu/documents/10162/17228/expo_plastic_addives_guide_en.pdf/ef63b255-6ea2-5645-a553-9408057eb4fd

ECHA. (2021b). *Mapping exercise – Plastic additives initiative*. Retrieved 18 Jan from https://echa.europa.eu/pt/mapping-exercise-plastic-additives-initiative

ECHA. (2022). *REACH*. Retrieved 19 Jan from https://echa.europa.eu/regulations/reach

ECPI. (2022). *Plasticizers*. Retrieved 20 Jan from http://www.plasticisers.org/en_GB/plasticisers

EESC. (2023). Opinion of the European Economic and Social Committee on the proposal for a Directive of the European Parliament and of the Council amending Directive 2000/60/EC establishing a framework for Community action in the field of water policy, Directive 2006/118/EC on the protection of groundwater against pollution and deterioration and Directive 2008/105/EC on environmental quality standards in the field of water policy. *Official Journal of the European Union*, *146*, 1-5.

EFSA. (2015). Scientific Opinion on the risks to public health related to the presence of bisphenol A (BPA) in foodstuffs. *EFSA Journal*, *13*(1), 3978. https://doi.org/10.2903/j.efsa.2015.3978

EFSA. (2019). Update of the risk assessment of di-butylphthalate (DBP), butyl-benzyl-phthalate (BBP), bis(2-ethylhexyl)phthalate (DEHP), di-isononylphthalate (DINP) and di-isodecylphthalate (DIDP) for use in food contact materials. *EFSA Journal*, *17*(12), e05838. https://doi.org/10.2903/j.efsa.2019.5838

EFSA. (2021). Bisphenol A: EFSA draft opinion proposes lowering the tolerable daily intake. *ESFA J*. https://www.efsa.europa.eu/en/news/bisphenol-efsa-draft-opinion-proposes-lowering-tolerable-daily-intake

Eo, S., Hong, S. H., Song, Y. K., Han, G. M., & Shim, W. J. (2019). Spatiotemporal distribution and annual load of microplastics in the Nakdong River, South Korea. *Water Research*, *160*, 228-237. https://doi.org/10.1016/j.watres.2019.05.053

Erni-Cassola, G., Gibson, M. I., Thompson, R. C., & Christie-Oleza, J. A. (2017). Lost, but Found with Nile Red: A Novel Method for Detecting and Quantifying Small Microplastics (1 mm to 20 μm) in Environmental Samples. *Environmental Science & Technology*, *51*(23), 13641-13648. https://doi.org/10.1021/acs.est.7b04512

Estévez-Danta, A., Rodil, R., Pérez-Castaño, B., Cela, R., Quintana, J. B., & González-Mariño, I. (2021). Comprehensive determination of phthalate, terephthalate and di-iso-nonyl cyclohexane-1,2-dicarboxylate metabolites in wastewater by solid-phase extraction and ultra(high)-performance liquid chromatography-tandem mass spectrometry. *Talanta*, *224*, 121912. https://doi.org/10.1016/j.talanta.2020.121912

Felsing, S., Kochleus, C., Buchinger, S., Brennholt, N., Stock, F., & Reifferscheid, G. (2018). A new approach in separating microplastics from environmental samples based on their electrostatic behavior. *Environmental Pollution*, *234*, 20-28. https://doi.org/10.1016/j.envpol.2017.11.013

Ferro, S., & De Battisti, A. (2002). Electron transfer reactions at conductive diamond electrodes. *Electrochimica Acta*, *47*(10), 1641-1649. https://doi.org/10.1016/S0013-4686(01)00898-2

Fikarová, K., Cocovi-Solberg, D. J., Rosende, M., Horstkotte, B., Sklenářová, H., & Miró, M. (2019). A flow-based platform hyphenated to on-line liquid chromatography for automatic leaching tests of chemical additives from microplastics into seawater. *Journal of Chromatography A*, *1602*, 160-167. https://doi.org/10.1016/j.chroma.2019.06.041

Fries, E., Dekiff, J. H., Willmeyer, J., Nuelle, M.-T., Ebert, M., & Remy, D. (2013). Identification of polymer types and additives in marine microplastic particles using pyrolysis-GC/MS and scanning electron microscopy. *Environmental science: processes & impacts*, *15*(10), 1949-1956. https://doi.org/10.1039/C3EM00214D

Fuller, S., & Gautam, A. (2016). A Procedure for Measuring Microplastics using Pressurized Fluid Extraction. *Environmental Science & Technology*, *50*(11), 5774-5780. https://doi.org/10.1021/acs.est.6b00816

Fulmer, G. R., Miller, A. J. M., Sherden, N. H., Gottlieb, H. E., Nudelman, A., Stoltz, B. M., Bercaw, J. E., & Goldberg, K. I. (2010). NMR Chemical Shifts of Trace Impurities: Common Laboratory Solvents, Organics, and Gases in Deuterated Solvents Relevant to the Organometallic Chemist. *Organometallics*, *29*(9), 2176-2179. https://doi.org/10.1021/om100106e

Gagliano, E., Sgroi, M., Falciglia, P. P., Vagliasindi, F. G. A., & Roccaro, P. (2020). Removal of poly- and perfluoroalkyl substances (PFAS) from water by adsorption: Role of PFAS chain length, effect of organic matter and challenges in adsorbent regeneration. *Water Research*, *171*, 115381. https://doi.org/10.1016/j.watres.2019.115381

Gao, P., Cui, J., & Deng, Y. (2021). Direct regeneration of ion exchange resins with sulfate radical-based advanced oxidation for enabling a cyclic adsorption – regeneration treatment approach to aqueous perfluorooctanoic acid (PFOA). *Chemical Engineering Journal*, *405*, 126698. https://doi.org/10.1016/j.cej.2020.126698

Gao, Y., Liang, Y., Gao, K., Wang, Y., Wang, C., Fu, J., Wang, Y., Jiang, G., & Jiang, Y. (2019). Levels, spatial distribution and isomer profiles of perfluoroalkyl acids in soil, groundwater and tap water around a manufactory in China. *Chemosphere*, *227*, 305-314. https://doi.org/10.1016/j.chemosphere.2019.04.027

García-de-Vinuesa, A., Demestre, M., & Lloret, J. (2022). Fatty acids as trophic markers and indicators of the quality of benthic habitats: The example of maerl and crinoid beds in the Northwestern Mediterranean. *Journal of Sea Research*, *187*, 102254. https://doi.org/10.1016/j.seares.2022.102254

Geer Wallace, M. A., & McCord, J. P. (2020). Chapter 16 - High-resolution mass spectrometry. In J. Beauchamp, C. Davis, & J. Pleil (Eds.), *Breathborne Biomarkers and the Human Volatilome (Second Edition)* (pp. 253-270). Elsevier. https://doi.org/10.1016/B978-0-12-819967-1.00016-5

GEF. (2012). Secretariat of the Convention on Biological Diversity and Scientific and Technical Advisory Panel GEF. *Impacts of Marine Debris on Biodiversity: Current Status and Potential Solutuions*, *67*, 1-9.

Geyer, R., Jambeck, J. R., & Law, K. L. (2017). Production, use, and fate of all plastics ever made. *Science Advances*, *3*(7), e1700782. https://doi.org/10.1126/sciadv.1700782

Ghosh, U., Kane Driscoll, S., Burgess, R. M., Jonker, M. T., Reible, D., Gobas, F., Choi, Y., Apitz, S. E., Maruya, K. A., Gala, W. R., Mortimer, M., & Beegan, C. (2014). Passive sampling methods for contaminated sediments: Practical guidance for selection, calibration, and implementation. *Integrated Environmental Assessment and Management*, *10*(2), 210-223. https://doi.org/10.1002/ieam.1507

Gilannejad, N., Martínez-Rodríguez, G., Yúfera, M., & Moyano, F. J. (2018). Modelling digestive hydrolysis of nutrients in fish using factorial designs and desirability function. *PloS one*, *13*(11), e0206556. https://doi.org/10.1371/journal.pone.0206556

Gobelius, L., Hedlund, J., Dürig, W., Tröger, R., Lilja, K., Wiberg, K., & Ahrens, L. (2018). Per- and Polyfluoroalkyl Substances in Swedish Groundwater and Surface Water: Implications for Environmental Quality Standards and Drinking Water Guidelines. *Environmental Science & Technology*, *52*(7), 4340-4349. https://doi.org/10.1021/acs.est.7b05718

Godoy, V., Prata, J. C., Blázquez, G., Almendros, A. I., Duarte, A. C., Rocha-Santos, T., Calero, M., & Martín-Lara, M. Á. (2020). Effects of distance to the sea and geomorphological characteristics on the quantity and distribution of microplastics in beach sediments of Granada (Spain). *Science of The Total Environment*, *746*, 142023. https://doi.org/10.1016/j.scitotenv.2020.142023

Gomiero, A., Øysæd, K. B., Agustsson, T., van Hoytema, N., van Thiel, T., & Grati, F. (2019). First record of characterization, concentration and distribution of microplastics in coastal sediments of an urban fjord in south west Norway using a thermal degradation method. *Chemosphere*, *227*, 705-714. https://doi.org/10.1016/j.chemosphere.2019.04.096

Gomiero, A., Øysæd, K. B., Palmas, L., & Skogerbø, G. (2021). Application of GCMS-pyrolysis to estimate the levels of microplastics in a drinking water supply system. *Journal of Hazardous Materials*, *416*, 125708. https://doi.org/10.1016/j.jhazmat.2021.125708

Gonkowski, S., & Makowska, K. (2022). Environmental Pollution with Bisphenol A and Phthalates—A Serious Risk to Human and Animal Health. *International Journal of Environmental Research and Public Health*, *19*(21), 13983. 10.3390/ijerph192113983

González-Barreiro, C., Martínez-Carballo, E., Sitka, A., Scharf, S., & Gans, O. (2006). Method optimization for determination of selected perfluorinated alkylated substances in water samples. *Analytical and Bioanalytical Chemistry*, *386*(7), 2123-2132. https://doi.org/10.1007/s00216-006-0902-7

González-Mariño, I., Montes, R., Quintana, J. B., & Rodil, R. (2019). Plasticizers | Environmental Analysis. In P. Worsfold, C. Poole, A. Townshend, & M. Miró (Eds.), *Encyclopedia of Analytical Science (Third Edition)* (pp. 309-317). Academic Press. https://doi.org/10.1016/B978-0-12-409547-2.14009-0

Goodman, J. E., & Peterson, M. K. (2014). Bisphenol A. In P. Wexler (Ed.), *Encyclopedia of Toxicology (Third Edition)* (pp. 514-518). Academic Press. https://doi.org/10.1016/B978-0-12-386454-3.00366-3

Gorman, D., Moreira, F. T., Turra, A., Fontenelle, F. R., Combi, T., Bícego, M. C., & de Castro Martins, C. (2019). Organic contamination of beached plastic pellets in the South Atlantic: Risk assessments can benefit by considering spatial gradients. *Chemosphere*, *223*, 608-615. https://doi.org/10.1016/j.chemosphere.2019.02.094

Gouin, T., Roche, N., Lohmann, R., & Hodges, G. (2011). A Thermodynamic Approach for Assessing the Environmental Exposure of Chemicals Absorbed to Microplastic. *Environmental Science & Technology*, *45*(4), 1466-1472. https://doi.org/10.1021/es1032025

Gouliarmou, V., Collins, C. D., Christiansen, E., & Mayer, P. (2013). Sorptive Physiologically Based Extraction of Contaminated Solid Matrices: Incorporating Silicone Rod As Absorption Sink for Hydrophobic Organic Contaminants. *Environmental Science & Technology*, *47*(2), 941-948. https://doi.org/10.1021/es303165u

Graham, E. R., & Thompson, J. T. (2009). Deposit- and suspension-feeding sea cucumbers (Echinodermata) ingest plastic fragments. *Journal of Experimental Marine Biology and Ecology*, *368*(1), 22-29. https://doi.org/10.1016/j.jembe.2008.09.007

Guerra, A., Etienne-Mesmin, L., Livrelli, V., Denis, S., Blanquet-Diot, S., & Alric, M. (2012). Relevance and challenges in modeling human gastric and small intestinal digestion. *Trends in Biotechnology*, *30*(11), 591-600. https://doi.org/10.1016/j.tibtech.2012.08.001

Guo, X., Pang, J., Chen, S., & Jia, H. (2018). Sorption properties of tylosin on four different microplastics. *Chemosphere*, *209*, 240-245. https://doi.org/10.1016/j.chemosphere.2018.06.100

Guo, Z., Zhu, Z., Huang, S., & Wang, J. (2020). Non-targeted screening of pesticides for food analysis using liquid chromatography high-resolution mass spectrometry-a review. *Food Additives & Contaminants: Part A*, *37*(7), 1180-1201. https://doi.org/10.1080/19440049.2020.1753890

Haave, M., Lorenz, C., Primpke, S., & Gerdts, G. (2019). Different stories told by small and large microplastics in sediment - first report of microplastic concentrations in an urban recipient in Norway. *Marine Pollution Bulletin*, *141*, 501-513. https://doi.org/10.1016/j.marpolbul.2019.02.015

Habib, R. Z., Thiemann, T., & Kendi, R. A. (2020). Microplastics and Wastewater Treatment Plants-A Review. *Journal of Water Resource and Protection*, *12*, 1-35, Article 97637. https://doi.org/10.4236/jwarp.2020.121001

Hadjmohammadi, M. R., Fatemi, M. H., & Taneh, T. (2011). Coacervative extraction of phthalates from water and their determination by high performance liquid chromatography. *Journal of the Iranian Chemical Society*, *8*(1), 100-106. https://doi.org/10.1007/BF03246206

Hamdan, M., Moyano, F. J., & Schuhardt, D. (2009). Optimization of a gastrointestinal model applicable to the evaluation of bioaccessibility in fish feeds. *Journal of the Science of Food and Agriculture*, *89*(7), 1195-1201. https://doi.org/10.1002/jsfa.3574

Hanke, G., Galgani, F., Werner, S., Oosterbaan, L., Nilsson, P., Fleet, D., Kinsey, S., Thompson, R., Palatinus, A., & Van Franeker, J. (2013). Guidance on Monitoring of Marine Litter in European Seas: a guidance document within the Common Implementation Strategy for the Marine Strategy Framework Directive. *Publications Office of the European Union Luxembourg*, 128. https://doi.org/10.2788/99475

Hansen, K. J., Johnson, H. O., Eldridge, J. S., Butenhoff, J. L., & Dick, L. A. (2002). Quantitative Characterization of Trace Levels of PFOS and PFOA in the Tennessee River. *Environmental Science & Technology*, *36*(8), 1681-1685. https://doi.org/10.1021/es010780r

Harrad, S., Wemken, N., Drage, D. S., Abdallah, M. A.-E., & Coggins, A.-M. (2019). Perfluoroalkyl Substances in Drinking Water, Indoor Air and Dust from Ireland: Implications for Human Exposure. *Environmental Science & Technology*, *53*(22), 13449-13457. https://doi.org/10.1021/acs.est.9b04604

Harris, C. A., & Sumpter, J. P. (2001). The Endocrine Disrupting Potential of Phthalates. In M. Metzler (Ed.), *Endocrine Disruptors – Part I* (pp. 169-201). Springer Berlin Heidelberg. https://doi.org/10.1007/10690734_9

Harrison, J. P., Ojeda, J. J., & Romero-González, M. E. (2012). The applicability of reflectance micro-Fourier-transform infrared spectroscopy for the detection of synthetic microplastics in marine sediments. *Science of The Total Environment*, *416*, 455-463. https://doi.org/10.1016/j.scitotenv.2011.11.078

Hayduk, W., & Laudie, H. (1974). Prediction of diffusion coefficients for nonelectrolytes in dilute aqueous solutions. *AIChE Journal*, *20*(3), 611-615. https://doi.org/10.1002/aic.690200329

Hayes, A., Kirkbride, K. P., & Leterme, S. C. (2021). Variation in polymer types and abundance of microplastics from two rivers and beaches in Adelaide, South Australia. *Marine Pollution Bulletin*, *172*, 112842. https://doi.org/10.1016/j.marpolbul.2021.112842

He, R., Li, Y., Xiang, P., Li, C., Zhou, C., Zhang, S., Cui, X., & Ma, L. Q. (2016). Organophosphorus flame retardants and phthalate esters in indoor dust from different microenvironments: Bioaccessibility and risk assessment. *Chemosphere*, *150*, 528-535. https://doi.org/10.1016/j.chemosphere.2015.10.087

Heo, H., Choi, M.-J., Park, J., Nam, T., & Cho, J. (2020). Anthropogenic Occurrence of Phthalate Esters in Beach Seawater in the Southeast Coast Region, South Korea. *Water*, *12*(1), 122. https://doi.org/10.3390/w12010122

Hernández, F., Fabregat-Safont, D., Campos-Mañas, M., & Quintana, J. B. (2023). Efficient Validation Strategies in Environmental Analytical Chemistry: A Focus on Organic Micropollutants in Water Samples. *Annual Review of Analytical Chemistry*, *16*(1), 401-428. https://doi.org/10.1146/annurev-anchem-091222-112115

Hessler, J., & Lehner, N. (2011). *Planning and designing research animal facilities*. Academic Press.

Hidalgo-Ruz, V., Gutow, L., Thompson, R. C., & Thiel, M. (2012). Microplastics in the Marine Environment: A Review of the Methods Used for Identification and Quantification. *Environmental Science & Technology*, *46*(6), 3060-3075. https://doi.org/10.1021/es2031505

Hopkins, Z. R., Sun, M., DeWitt, J. C., & Knappe, D. R. U. (2018). Recently Detected Drinking Water Contaminants: GenX and Other Per- and Polyfluoroalkyl Ether Acids. *Journal AWWA*, *110*(7), 13-28. https://doi.org/10.1002/awwa.1073

Hori, H., Hayakawa, E., Einaga, H., Kutsuna, S., Koike, K., Ibusuki, T., Kiatagawa, H., & Arakawa, R. (2004). Decomposition of Environmentally Persistent Perfluorooctanoic

Acid in Water by Photochemical Approaches. *Environmental Science & Technology*, *38*(22), 6118-6124. https://doi.org/10.1021/es049719n

Hori, H., Yamamoto, A., Koike, K., Kutsuna, S., Osaka, I., & Arakawa, R. (2007). Photochemical decomposition of environmentally persistent short-chain perfluorocarboxylic acids in water mediated by iron(II)/(III) redox reactions. *Chemosphere*, *68*(3), 572-578. https://doi.org/10.1016/j.chemosphere.2006.12.038

Horton, A. A., Walton, A., Spurgeon, D. J., Lahive, E., & Svendsen, C. (2017). Microplastics in freshwater and terrestrial environments: Evaluating the current understanding to identify the knowledge gaps and future research priorities. *Science of The Total Environment*, *586*, 127-141. https://doi.org/10.1016/j.scitotenv.2017.01.190

Hou, X., Huang, X., Ai, Z., Zhao, J., & Zhang, L. (2016). Ascorbic acid/Fe@Fe2O3: A highly efficient combined Fenton reagent to remove organic contaminants. *Journal of Hazardous Materials*, *310*, 170-178. https://doi.org/10.1016/j.jhazmat.2016.01.020

Huang, Y., Li, H., Bai, M., & Huang, X. (2018). Efficient extraction of perfluorocarboxylic acids in complex samples with a monolithic adsorbent combining fluorophilic and anion-exchange interactions. *Analytica Chimica Acta*, *1011*, 50-58. https://doi.org/10.1016/j.aca.2018.01.032

Hurdzan, C. M., Basta, N. T., Hatcher, P. G., & Tuovinen, O. H. (2008). Phenanthrene release from natural organic matter surrogates under simulated human gastrointestinal conditions. *Ecotoxicology and Environmental Safety*, *69*(3), 525-530. https://doi.org/10.1016/j.ecoenv.2007.02.006

Hurley, R. R., Lusher, A. L., Olsen, M., & Nizzetto, L. (2018). Validation of a Method for Extracting Microplastics from Complex, Organic-Rich, Environmental Matrices. *Environmental Science & Technology*, *52*(13), 7409-7417. https://doi.org/10.1021/acs.est.8b01517

ICB. (2008). *Bisphenol A (BPA Uses and Market Data*. Retrieved 23 Jan from http://www.icis.com/v2/chemicals/9075165/bisphenol-a/uses.html2008

Imhof, H. K., Schmid, J., Niessner, R., Ivleva, N. P., & Laforsch, C. (2012). A novel, highly efficient method for the separation and quantification of plastic particles in sediments of aquatic environments. *Limnology and Oceanography: Methods*, *10*(7), 524-537. https://doi.org/10.4319/lom.2012.10.524

Iparraguirre, A., Navarro, P., Prieto, A., Rodil, R., Olivares, M., Fernández, L.-Á., & Zuloaga, O. (2012). Membrane-assisted solvent extraction coupled to large volume injection–gas chromatography–mass spectrometry for the determination of a variety of endocrine disrupting compounds in environmental water samples. *Analytical and Bioanalytical Chemistry*, *402*(9), 2897-2907. https://doi.org/10.1007/s00216-012-5717-0

Isaev, A. B., & Magomedova, A. G. (2022). Advanced Oxidation Processes Based Emerging Technologies for Dye Wastewater Treatment. *Moscow University Chemistry Bulletin*, *77*(4), 181-196. https://doi.org/10.3103/S0027131422040046

Isobe, A., Azuma, T., Cordova, M. R., Cózar, A., Galgani, F., Hagita, R., Kanhai, L. D., Imai, K., Iwasaki, S., Kako, S. i., Kozlovskii, N., Lusher, A. L., Mason, S. A., Michida, Y., Mituhasi, T., Morii, Y., Mukai, T., Popova, A., Shimizu, K., Tokai, T., Uchida, K., Yagi, M., & Zhang, W. (2021). A multilevel dataset of microplastic abundance in the world's upper ocean and the Laurentian Great Lakes. *Microplastics and Nanoplastics*, *1*(1), 16. https://doi.org/10.1186/s43591-021-00013-z

Isobe, A., Iwasaki, S., Uchida, K., & Tokai, T. (2019). Abundance of non-conservative microplastics in the upper ocean from 1957 to 2066. *Nature Communications*, *10*(1), 417. https://doi.org/10.1038/s41467-019-08316-9

Iyare, P. U., Ouki, S. K., & Bond, T. (2020). Microplastics removal in wastewater treatment plants: a critical review [10.1039/D0EW00397B]. *Environmental Science: Water Research & Technology*, *6*(10), 2664-2675. https://doi.org/10.1039/D0EW00397B

James, K., Peters, R. E., Laird, B. D., Ma, W. K., Wickstrom, M., Stephenson, G. L., & Siciliano, S. D. (2011). Human Exposure Assessment: A Case Study of 8 PAH Contaminated Soils Using in Vitro Digestors and the Juvenile Swine Model. *Environmental Science & Technology*, *45*(10), 4586-4593. https://doi.org/10.1021/es1039979

Janda, J., Nödler, K., Brauch, H.-J., Zwiener, C., & Lange, F. T. (2019). Robust trace analysis of polar (C2-C8) perfluorinated carboxylic acids by liquid chromatography-tandem mass spectrometry: method development and application to surface water, groundwater and drinking water. *Environmental Science and Pollution Research*, *26*(8), 7326-7336. https://doi.org/10.1007/s11356-018-1731-x

Janzen, E. G., Kotake, Y., & Randall D, H. (1992). Stabilities of hydroxyl radical spin adducts of PBN-type spin traps. *Free Radical Biology and Medicine*, *12*(2), 169-173. https://doi.org/10.1016/0891-5849(92)90011-5

Jiang, L., Hong, Y., Xie, G., Zhang, J., Zhang, H., & Cai, Z. (2021). Comprehensive multi-omics approaches reveal the hepatotoxic mechanism of perfluorohexanoic acid (PFHxA) in mice. *Science of The Total Environment*, *790*, 148160. https://doi.org/10.1016/j.scitotenv.2021.148160

Jin, L., Zhang, P., Shao, T., & Zhao, S. (2014). Ferric ion mediated photodecomposition of aqueous perfluorooctane sulfonate (PFOS) under UV irradiation and its mechanism. *Journal of Hazardous Materials*, *271*, 9-15. https://doi.org/10.1016/j.jhazmat.2014.01.061

Juhasz, A. L., Herde, P., & Smith, E. (2016). Oral relative bioavailability of Dichlorodiphenyltrichloroethane (DDT) in contaminated soil and its prediction using in vitro strategies for exposure refinement. *Environmental Research*, *150*, 482-488. https://doi.org/10.1016/j.envres.2016.06.039

Juhasz, A. L., Weber, J., Stevenson, G., Slee, D., Gancarz, D., Rofe, A., & Smith, E. (2014). In vivo measurement, in vitro estimation and fugacity prediction of PAH bioavailability in post-remediated creosote-contaminated soil. *Science of The Total Environment*, *473-474*, 147-154. https://doi.org/10.1016/j.scitotenv.2013.12.031

Kaboré, H. A., Vo Duy, S., Munoz, G., Méité, L., Desrosiers, M., Liu, J., Sory, T. K., & Sauvé, S. (2018). Worldwide drinking water occurrence and levels of newly-identified perfluoroalkyl and polyfluoroalkyl substances. *Science of The Total Environment*, *616-617*, 1089-1100. https://doi.org/10.1016/j.scitotenv.2017.10.210

Kademoglou, K., Giovanoulis, G., Palm-Cousins, A., Padilla-Sanchez, J. A., Magnér, J., de Wit, C. A., & Collins, C. D. (2018). In Vitro Inhalation Bioaccessibility of Phthalate Esters and Alternative Plasticizers Present in Indoor Dust Using Artificial Lung Fluids. *Environmental Science & Technology Letters*, *5*(6), 329-334. https://doi.org/10.1021/acs.estlett.8b00113

Kane, I. A., & Clare, M. A. (2019). Dispersion, accumulation, and the ultimate fate of microplastics in deep-marine environments: a review and future directions. *Frontiers in earth science*, *7*, 80. https://doi.org/10.3389/feart.2019.00080

Karami, A., Golieskardi, A., Choo, C. K., Romano, N., Ho, Y. B., & Salamatinia, B. (2017). A high-performance protocol for extraction of microplastics in fish. *Science of The Total Environment*, *578*, 485-494. https://doi.org/10.1016/j.scitotenv.2016.10.213

Karlsson, T. M., Vethaak, A. D., Almroth, B. C., Ariese, F., van Velzen, M., Hassellöv, M., & Leslie, H. A. (2017). Screening for microplastics in sediment, water, marine invertebrates and fish: Method development and microplastic accumulation. *Marine Pollution Bulletin*, *122*(1), 403-408. https://doi.org/10.1016/j.marpolbul.2017.06.081

Kelley, M. E., Brauning, S., Schoof, R., & Ruby, M. (2002). *Assessing oral bioavailability of metals in soil*. Battelle Press.

Kester, D. R., Duedall, I. W., Connors, D. N., & Pytkowicz, R. M. (1967). Preparation of artificial seawater. *Limnology and Oceanography*, *12*(1), 176-179. https://doi.org/10.4319/lo.1967.12.1.0176

Khuyen, V. T. K., Le, D. V., Fischer, A. R., & Dornack, C. (2021). Comparison of Microplastic Pollution in Beach Sediment and Seawater at UNESCO Can Gio Mangrove Biosphere Reserve. *Global Challenges*, *5*(11), 2100044. https://doi.org/10.1002/gch2.202100044

Kim, K. Y., Ekpe, O. D., Lee, H.-J., & Oh, J.-E. (2020). Perfluoroalkyl substances and pharmaceuticals removal in full-scale drinking water treatment plants. *Journal of Hazardous Materials*, *400*, 123235. https://doi.org/10.1016/j.jhazmat.2020.123235

Koelmans, A. A., Bakir, A., Burton, G. A., & Janssen, C. R. (2016). Microplastic as a Vector for Chemicals in the Aquatic Environment: Critical Review and Model-Supported Reinterpretation of Empirical Studies. *Environmental Science & Technology*, *50*(7), 3315-3326. https://doi.org/10.1021/acs.est.5b06069

Kolthoff, I., & Carr, E. (1953). Volumetric determination of persulfate in presence of organic substances. *Analytical Chemistry*, *25*(2), 298-301. https://doi.org/10.1021/ac60074a024

Kothawala, D. N., Köhler, S. J., Östlund, A., Wiberg, K., & Ahrens, L. (2017). Influence of dissolved organic matter concentration and composition on the removal efficiency of perfluoroalkyl substances (PFASs) during drinking water treatment. *Water Research*, *121*, 320-328. https://doi.org/10.1016/j.watres.2017.05.047

Kováts, E. (1958). Gas-chromatographische Charakterisierung organischer Verbindungen. Teil 1: Retentionsindices aliphatischer Halogenide, Alkohole, Aldehyde und Ketone. *Helvetica Chimica Acta*, *41*(7), 1915-1932. https://doi.org/10.1002/hlca.19580410703

Krasowska, K., Dereszewska, A., & Popek, M. (2022). Preliminary approach to ecological risk assessment of microplastics in selected coastal regions of Baltic Sea. *Safety and Reliability of Systems and Processes*, 133-142. https://doi.org/10.26408/srsp-2022-08

Kühn, S., van Werven, B., van Oyen, A., Meijboom, A., Bravo Rebolledo, E. L., & van Franeker, J. A. (2017). The use of potassium hydroxide (KOH) solution as a suitable approach to isolate plastics ingested by marine organisms. *Marine Pollution Bulletin*, *115*(1), 86-90. https://doi.org/10.1016/j.marpolbul.2016.11.034

Kurwadkar, S., Dane, J., Kanel, S. R., Nadagouda, M. N., Cawdrey, R. W., Ambade, B., Struckhoff, G. C., & Wilkin, R. (2022). Per- and polyfluoroalkyl substances in water and wastewater: A critical review of their global occurrence and distribution. *Science of The Total Environment*, *809*, 151003. https://doi.org/10.1016/j.scitotenv.2021.151003

Kušić, H., Rasulev, B., Leszczynska, D., Leszczynski, J., & Koprivanac, N. (2009). Prediction of rate constants for radical degradation of aromatic pollutants in water matrix: A QSAR study. *Chemosphere*, *75*(8), 1128-1134. https://doi.org/10.1016/j.chemosphere.2009.01.019

Laglbauer, B. J. L., Franco-Santos, R. M., Andreu-Cazenave, M., Brunelli, L., Papadatou, M., Palatinus, A., Grego, M., & Deprez, T. (2014). Macrodebris and microplastics from beaches in Slovenia. *Marine Pollution Bulletin*, *89*(1), 356-366. https://doi.org/10.1016/j.marpolbul.2014.09.036

Laist, D. W. (1997). Impacts of Marine Debris: Entanglement of Marine Life in Marine Debris Including a Comprehensive List of Species with Entanglement and Ingestion Records. In J. M. Coe & D. B. Rogers (Eds.), *Marine Debris: Sources, Impacts, and Solutions* (pp. 99-139). Springer New York. https://doi.org/10.1007/978-1-4613-8486-1_10

Lashuk, B. (2021). *Photocatalytic Ozonation for the Degradation of Per- and Poly-Fluoroalkyl Substances (PFAS) in Water* (Publication Number 29274292) [M.Sc., McGill University (Canada)]. ProQuest Dissertations & Theses Global. Canada -- Quebec, CA. https://www.proquest.com/dissertations-theses/photocatalytic-ozonation-degradation-per-poly/docview/2701132949/se-2?accountid=17253

Lath, S., Knight, E. R., Navarro, D. A., Kookana, R. S., & McLaughlin, M. J. (2019). Sorption of PFOA onto different laboratory materials: Filter membranes and centrifuge tubes. *Chemosphere*, *222*, 671-678. https://doi.org/10.1016/j.chemosphere.2019.01.096

Lavers, J. L., Oppel, S., & Bond, A. L. (2016). Factors influencing the detection of beach plastic debris. *Marine Environmental Research*, *119*, 245-251. https://doi.org/10.1016/j.marenvres.2016.06.009

Le, T. X. H., Haflich, H., Shah, A. D., & Chaplin, B. P. (2019). Energy-Efficient Electrochemical Oxidation of Perfluoroalkyl Substances Using a Ti4O7 Reactive Electrochemical Membrane Anode. *Environmental Science & Technology Letters*, *6*(8), 504-510. https://doi.org/10.1021/acs.estlett.9b00397

Lebreton, L., Slat, B., Ferrari, F., Sainte-Rose, B., Aitken, J., Marthouse, R., Hajbane, S., Cunsolo, S., Schwarz, A., Levivier, A., Noble, K., Debeljak, P., Maral, H., Schoeneich-Argent, R., Brambini, R., & Reisser, J. (2018). Evidence that the Great Pacific Garbage Patch is rapidly accumulating plastic. *Scientific Reports*, *8*(1), 4666. https://doi.org/10.1038/s41598-018-22939-w

Lebreton, L. C. M., van der Zwet, J., Damsteeg, J.-W., Slat, B., Andrady, A., & Reisser, J. (2017). River plastic emissions to the world's oceans. *Nature Communications*, *8*(1), 15611. https://doi.org/10.1038/ncomms15611

Lechner, A., Keckeis, H., Lumesberger-Loisl, F., Zens, B., Krusch, R., Tritthart, M., Glas, M., & Schludermann, E. (2014). The Danube so colourful: A potpourri of plastic litter outnumbers fish larvae in Europe's second largest river. *Environmental Pollution*, *188*, 177-181. https://doi.org/10.1016/j.envpol.2014.02.006

Lee, H., Shim, W. J., & Kwon, J.-H. (2014). Sorption capacity of plastic debris for hydrophobic organic chemicals. *Science of The Total Environment*, *470-471*, 1545-1552. https://doi.org/10.1016/j.scitotenv.2013.08.023

Lee, Y.-C., Lo, S.-L., Chiueh, P.-T., Liou, Y.-H., & Chen, M.-L. (2010). Microwave-hydrothermal decomposition of perfluorooctanoic acid in water by iron-activated persulfate oxidation. *Water Research*, *44*(3), 886-892. https://doi.org/10.1016/j.watres.2009.09.055

Lee, Y., Lo, S., Kuo, J., & Hsieh, C. (2012). Decomposition of perfluorooctanoic acid by microwaveactivated persulfate: Effects of temperature, pH, and chloride ions. *Frontiers of Environmental Science & Engineering*, *6*(1), 17-25. https://doi.org/10.1007/s11783-011-0371-x

Lei, Y.-J., Tian, Y., Sobhani, Z., Naidu, R., & Fang, C. (2020). Synergistic degradation of PFAS in water and soil by dual-frequency ultrasonic activated persulfate. *Chemical Engineering Journal*, *388*, 124215. https://doi.org/10.1016/j.cej.2020.124215

Li, C., Sun, H., Juhasz, A. L., Cui, X., & Ma, L. Q. (2016). Predicting the Relative Bioavailability of DDT and Its Metabolites in Historically Contaminated Soils Using a

Tenax-Improved Physiologically Based Extraction Test (TI-PBET). *Environmental Science & Technology*, *50*(3), 1118-1125. https://doi.org/10.1021/acs.est.5b03891

Li, F., Duan, J., Tian, S., Ji, H., Zhu, Y., Wei, Z., & Zhao, D. (2020). Short-chain per- and polyfluoroalkyl substances in aquatic systems: Occurrence, impacts and treatment. *Chemical Engineering Journal*, *380*, 122506. https://doi.org/10.1016/j.cej.2019.122506

Li, H., Junker, A. L., Wen, J., Ahrens, L., Sillanpää, M., Tian, J., Cui, F., Vergeynst, L., & Wei, Z. (2023). A recent overview of per- and polyfluoroalkyl substances (PFAS) removal by functional framework materials. *Chemical Engineering Journal*, *452*, 139202. https://doi.org/10.1016/j.cej.2022.139202

Li, J., Fu, J., Zhang, H., Li, Z., Ma, Y., Wu, M., & Liu, X. (2013). Spatial and seasonal variations of occurrences and concentrations of endocrine disrupting chemicals in unconfined and confined aquifers recharged by reclaimed water: A field study along the Chaobai River, Beijing. *Science of The Total Environment*, *450-451*, 162-168. https://doi.org/10.1016/j.scitotenv.2013.01.089

Li, J., Zhang, H., Zhang, K., Yang, R., Li, R., & Li, Y. (2018). Characterization, source, and retention of microplastic in sandy beaches and mangrove wetlands of the Qinzhou Bay, China. *Marine Pollution Bulletin*, *136*, 401-406. https://doi.org/10.1016/j.marpolbul.2018.09.025

Li, J., Zhang, K., & Zhang, H. (2018). Adsorption of antibiotics on microplastics. *Environmental Pollution*, *237*, 460-467. https://doi.org/10.1016/j.envpol.2018.02.050

Lin, H., Niu, J., Liang, S., Wang, C., Wang, Y., Jin, F., Luo, Q., & Huang, Q. (2018). Development of macroporous Magnéli phase Ti4O7 ceramic materials: As an efficient anode for mineralization of poly- and perfluoroalkyl substances. *Chemical Engineering Journal*, *354*, 1058-1067. https://doi.org/10.1016/j.cej.2018.07.210

Lin, J., Xu, X.-P., Yue, B.-Y., Li, Y., Zhou, Q.-Z., Xu, X.-M., Liu, J.-Z., Wang, Q.-Q., & Wang, J.-H. (2021). A novel thermoanalytical method for quantifying microplastics in marine sediments. *Science of The Total Environment*, *760*, 144316. https://doi.org/10.1016/j.scitotenv.2020.144316

Lin, L., Zuo, L.-Z., Peng, J.-P., Cai, L.-Q., Fok, L., Yan, Y., Li, H.-X., & Xu, X.-R. (2018). Occurrence and distribution of microplastics in an urban river: A case study in the Pearl River along Guangzhou City, China. *Science of The Total Environment*, *644*, 375-381. https://doi.org/10.1016/j.scitotenv.2018.06.327

Lisboa, N. S., Fahning, C. S., Cotrim, G., dos Anjos, J. P., de Andrade, J. B., Hatje, V., & da Rocha, G. O. (2013). A simple and sensitive UFLC-fluorescence method for endocrine disrupters determination in marine waters. *Talanta*, *117*, 168-175. https://doi.org/10.1016/j.talanta.2013.08.006

Liu, G., Zhu, Z., Yang, Y., Sun, Y., Yu, F., & Ma, J. (2019). Sorption behavior and mechanism of hydrophilic organic chemicals to virgin and aged microplastics in freshwater and seawater. *Environmental Pollution*, *246*, 26-33. https://doi.org/10.1016/j.envpol.2018.11.100

Liu, L., Qu, Y., Huang, J., & Weber, R. (2021). Per- and polyfluoroalkyl substances (PFASs) in Chinese drinking water: risk assessment and geographical distribution. *Environmental Sciences Europe*, *33*(1), 6. https://doi.org/10.1186/s12302-020-00425-3

Liu, X., Gharasoo, M., Shi, Y., Sigmund, G., Hüffer, T., Duan, L., Wang, Y., Ji, R., Hofmann, T., & Chen, W. (2020). Key Physicochemical Properties Dictating Gastrointestinal Bioaccessibility of Microplastics-Associated Organic Xenobiotics: Insights from a Deep Learning Approach. *Environmental Science & Technology*, *54*(19), 12051-12062. https://doi.org/10.1021/acs.est.0c02838

Liu, Y., Fan, X., Quan, X., Fan, Y., Chen, S., & Zhao, X. (2019). Enhanced Perfluorooctanoic Acid Degradation by Electrochemical Activation of Sulfate Solution on B/N Codoped Diamond. *Environmental Science & Technology*, *53*(9), 5195-5201. https://doi.org/10.1021/acs.est.8b06130

Liu, Y., Pereira, A. D. S., & Martin, J. W. (2015). Discovery of C5–C17 Poly- and Perfluoroalkyl Substances in Water by In-Line SPE-HPLC-Orbitrap with In-Source Fragmentation Flagging. *Analytical Chemistry*, *87*(8), 4260-4268. https://doi.org/10.1021/acs.analchem.5b00039

Löder, M. G. J., Imhof, H. K., Ladehoff, M., Löschel, L. A., Lorenz, C., Mintenig, S., Piehl, S., Primpke, S., Schrank, I., Laforsch, C., & Gerdts, G. (2017). Enzymatic Purification of Microplastics in Environmental Samples. *Environmental Science & Technology*, *51*(24), 14283-14292. https://doi.org/10.1021/acs.est.7b03055

Loewen, M., Halldorson, T., Wang, F., & Tomy, G. (2005). Fluorotelomer Carboxylic Acids and PFOS in Rainwater from an Urban Center in Canada. *Environmental Science & Technology*, *39*(9), 2944-2951. https://doi.org/10.1021/es048635b

Loos, R., Tavazzi, S., Mariani, G., Suurkuusk, G., Paracchini, B., & Umlauf, G. (2017). Analysis of emerging organic contaminants in water, fish and suspended particulate matter (SPM) in the Joint Danube Survey using solid-phase extraction followed by UHPLC-MS-MS and GC–MS analysis. *Science of The Total Environment*, *607-608*, 1201-1212. https://doi.org/10.1016/j.scitotenv.2017.07.039

López-Vázquez, J., Rodil, R., Trujillo-Rodríguez, M. J., Quintana, J. B., Cela, R., & Miró, M. (2022). Mimicking human ingestion of microplastics: Oral bioaccessibility tests of bisphenol A and phthalate esters under fed and fasted states. *Science of The Total Environment*, *826*, 154027. https://doi.org/10.1016/j.scitotenv.2022.154027

Lorenzo, M., Campo, J., Morales Suárez-Varela, M., & Picó, Y. (2019). Occurrence, distribution and behavior of emerging persistent organic pollutants (POPs) in a Mediterranean wetland protected area. *Science of The Total Environment*, *646*, 1009-1020. https://doi.org/10.1016/j.scitotenv.2018.07.304

Loyo-Rosales, J. E., Rosales-Rivera, G. C., Lynch, A. M., Rice, C. P., & Torrents, A. (2004). Migration of Nonylphenol from Plastic Containers to Water and a Milk Surrogate. *Journal of Agricultural and Food Chemistry*, *52*(7), 2016-2020. https://doi.org/10.1021/jf0345696

Lu, M., Li, G., Yang, Y., & Yu, Y. (2021). A review on in-vitro oral bioaccessibility of organic pollutants and its application in human exposure assessment. *Science of The Total Environment*, *752*, 142001. https://doi.org/10.1016/j.scitotenv.2020.142001

Mafuta, C., Baker, E., Rucevska, I., Thygesen, K., Appelquist, L. R., Westerveld, L., Tsakona, M., Macmillan-Lawler, M., Harris, P., & Sevaldsen, P. (2021). *Drowning in Plastics: Marine Litter and Plastic Waste Vital Graphics*. Secretariats of the Basel, Rotterdam and Stockholm Secretariats and GRID-Arendal. Retrieved 18 Jan from https://policycommons.net/artifacts/2390247/drowning-in-plastics/3411476/

Mahamuni, N. N., & Adewuyi, Y. G. (2010). Advanced oxidation processes (AOPs) involving ultrasound for waste water treatment: A review with emphasis on cost estimation. *Ultrasonics Sonochemistry*, *17*(6), 990-1003. https://doi.org/10.1016/j.ultsonch.2009.09.005

Mahat, S. (2017). *Separation and quantification of Microplastics from Beach and Sediment samples using the Bauta microplastic-sediment separator* Norwegian University of Life Sciences]. http://hdl.handle.net/11250/2459114

Mai, L., Bao, L.-J., Shi, L., Liu, L.-Y., & Zeng, E. Y. (2018). Polycyclic aromatic hydrocarbons affiliated with microplastics in surface waters of Bohai and Huanghai Seas, China. *Environmental Pollution*, *241*, 834-840. https://doi.org/10.1016/j.envpol.2018.06.012

Mani, T., Primpke, S., Lorenz, C., Gerdts, G., & Burkhardt-Holm, P. (2019). Microplastic Pollution in Benthic Midstream Sediments of the Rhine River. *Environmental Science & Technology*, *53*(10), 6053-6062. https://doi.org/10.1021/acs.est.9b01363

Manna, M., & Sen, S. (2023). Advanced oxidation process: a sustainable technology for treating refractory organic compounds present in industrial wastewater. *Environmental Science and Pollution Research*, *30*(10), 25477-25505. https://doi.org/10.1007/s11356-022-19435-0

Martín, J., Santos, J. L., Aparicio, I., & Alonso, E. (2022). Microplastics and associated emerging contaminants in the environment: Analysis, sorption mechanisms and effects of co-exposure. *Trends in Environmental Analytical Chemistry*, *35*, e00170. https://doi.org/10.1016/j.teac.2022.e00170

Masset, T., Ferrari, B. J. D., Dudefoi, W., Schirmer, K., Bergmann, A., Vermeirssen, E., Grandjean, D., Harris, L. C., & Breider, F. (2022). Bioaccessibility of Organic Compounds Associated with Tire Particles Using a Fish In Vitro Digestive Model: Solubilization Kinetics and Effects of Food Coingestion. *Environmental Science & Technology*, *56*(22), 15607-15616. https://doi.org/10.1021/acs.est.2c04291

Masura, J., Baker, J., Foster, G., & Arthur, C. (2015). Laboratory Methods for the Analysis of Microplastics in the Marine Environment: Recommendations for quantifying synthetic particles in waters and sediments. *NOAA Marine Debris Division Silver Spring, MD*, 31. https://doi.org/10.25607/OBP-604

Mato, Y., Isobe, T., Takada, H., Kanehiro, H., Ohtake, C., & Kaminuma, T. (2001). Plastic Resin Pellets as a Transport Medium for Toxic Chemicals in the Marine Environment. *Environmental Science & Technology*, *35*(2), 318-324. https://doi.org/10.1021/es0010498

Mazariegos-Ortíz, C., de los Ángeles Rosales, M., Carrillo-Ovalle, L., Cardoso, R. P., Muniz, M. C., & dos Anjos, R. M. (2020). First evidence of microplastic pollution in the El Quetzalito sand beach of the Guatemalan Caribbean. *Marine Pollution Bulletin*, *156*, 111220. https://doi.org/10.1016/j.marpolbul.2020.111220

Mazur, D. M., Detenchuk, E. A., Sosnova, A. A., Artaev, V. B., & Lebedev, A. T. (2021). GC-HRMS with Complementary Ionization Techniques for Target and Non-target Screening for Chemical Exposure: Expanding the Insights of the Air Pollution Markers in Moscow Snow. *Science of The Total Environment*, *761*, 144506. https://doi.org/10.1016/j.scitotenv.2020.144506

McCleaf, P., Englund, S., Östlund, A., Lindegren, K., Wiberg, K., & Ahrens, L. (2017). Removal efficiency of multiple poly- and perfluoroalkyl substances (PFASs) in drinking water using granular activated carbon (GAC) and anion exchange (AE) column tests. *Water Research*, *120*, 77-87. https://doi.org/10.1016/j.watres.2017.04.057

Mohamed, D. F. M. S., Kim, D. Y., An, J., Kim, M., Chun, S.-H., & Kwon, J.-H. (2023). Simplified Unified BARGE Method to Assess Migration of Phthalate Esters in Ingested PVC Consumer Products. *International Journal of Environmental Research and Public Health*, *20*(3), 1907. https://doi.org/10.3390/ijerph20031907

Mohamed Nor, N. H., & Koelmans, A. A. (2019). Transfer of PCBs from Microplastics under Simulated Gut Fluid Conditions Is Biphasic and Reversible. *Environmental Science & Technology*, *53*(4), 1874-1883. https://doi.org/10.1021/acs.est.8b05143

Möller, J. N., Heisel, I., Satzger, A., Vizsolyi, E. C., Oster, S. D. J., Agarwal, S., Laforsch, C., & Löder, M. G. J. (2022). Tackling the Challenge of Extracting Microplastics from Soils: A Protocol to Purify Soil Samples for Spectroscopic Analysis. *Environmental Toxicology and Chemistry*, *41*(4), 844-857. https://doi.org/10.1002/etc.5024

Molly, K., Vande Woestyne, M., & Verstraete, W. (1993). Development of a 5-step multi-chamber reactor as a simulation of the human intestinal microbial ecosystem. *Applied Microbiology and Biotechnology*, *39*(2), 254-258. https://doi.org/10.1007/BF00228615

Montes, R., Rodil, R., Placer, L., Wilms, J. M., Cela, R., & Quintana, J. B. (2020). Applicability of mixed-mode chromatography for the simultaneous analysis of C1-C18 perfluoroalkylated substances. *Analytical and Bioanalytical Chemistry*, *412*(20), 4849-4856. https://doi.org/10.1007/s00216-020-02434-w

Moody, C. A., & Field, J. A. (1999). Determination of Perfluorocarboxylates in Groundwater Impacted by Fire-Fighting Activity. *Environmental Science & Technology*, *33*(16), 2800-2806. https://doi.org/10.1021/es981355+

Morales, G. A., & Moyano, F. J. (2010). Application of an in vitro gastrointestinal model to evaluate nitrogen and phosphorus bioaccessibility and bioavailability in fish feed ingredients. *Aquaculture*, *306*(1), 244-251. https://doi.org/10.1016/j.aquaculture.2010.05.014

Moreira, F. C., Boaventura, R. A. R., Brillas, E., & Vilar, V. J. P. (2015). Remediation of a winery wastewater combining aerobic biological oxidation and electrochemical advanced oxidation processes. *Water Research*, *75*, 95-108. https://doi.org/10.1016/j.watres.2015.02.029

Moyano, F. J., Saénz de Rodrigáñez, M. A., Díaz, M., & Tacon, A. G. J. (2015). Application of in vitro digestibility methods in aquaculture: constraints and perspectives. *Reviews in Aquaculture*, *7*(4), 223-242. https://doi.org/10.1111/raq.12065

Mudumbi, J. B. N., Ntwampe, S. K. O., Muganza, F. M., & Okonkwo, J. O. (2013). Perfluorooctanoate and perfluorooctane sulfonate in South African river water. *Water Science and Technology*, *69*(1), 185-194. https://doi.org/10.2166/wst.2013.566

Naidoo, T., Goordiyal, K., & Glassom, D. (2017). Are Nitric Acid (HNO3) Digestions Efficient in Isolating Microplastics from Juvenile Fish? *Water, Air, & Soil Pollution*, *228*(12), 470. https://doi.org/10.1007/s11270-017-3654-4

Nakajima, R., Tsuchiya, M., Lindsay, D. J., Kitahashi, T., Fujikura, K., & Fukushima, T. (2019). A new small device made of glass for separating microplastics from marine and freshwater sediments. *PeerJ*, *7*, e7915. https://doi.org/10.7717/peerj.7915

Net, S., Sempéré, R., Delmont, A., Paluselli, A., & Ouddane, B. (2015). Occurrence, Fate, Behavior and Ecotoxicological State of Phthalates in Different Environmental Matrices. *Environmental Science & Technology*, *49*(7), 4019-4035. https://doi.org/10.1021/es505233b

Nienhauser, A. B., Ersan, M. S., Lin, Z., Perreault, F., Westerhoff, P., & Garcia-Segura, S. (2022). Boron-doped diamond electrodes degrade short- and long-chain per- and polyfluorinated alkyl substances in real industrial wastewaters. *Journal of Environmental Chemical Engineering*, *10*(2), 107192. https://doi.org/10.1016/j.jece.2022.107192

Niu, J., Lin, H., Gong, C., & Sun, X. (2013). Theoretical and Experimental Insights into the Electrochemical Mineralization Mechanism of Perfluorooctanoic Acid. *Environmental Science & Technology*, *47*(24), 14341-14349. https://doi.org/10.1021/es402987t

Niu, J., Lin, H., Xu, J., Wu, H., & Li, Y. (2012). Electrochemical Mineralization of Perfluorocarboxylic Acids (PFCAs) by Ce-Doped Modified Porous Nanocrystalline

PbO2 Film Electrode. *Environmental Science & Technology*, *46*(18), 10191-10198. https://doi.org/10.1021/es302148z

Nuelle, M.-T., Dekiff, J. H., Remy, D., & Fries, E. (2014). A new analytical approach for monitoring microplastics in marine sediments. *Environmental Pollution*, *184*, 161-169. https://doi.org/10.1016/j.envpol.2013.07.027

Nzeribe, B. N., Crimi, M., Mededovic Thagard, S., & Holsen, T. M. (2019). Physico-Chemical Processes for the Treatment of Per- And Polyfluoroalkyl Substances (PFAS): A review. *Critical Reviews in Environmental Science and Technology*, *49*(10), 866-915. https://doi.org/10.1080/10643389.2018.1542916

Odoardi, S., Valentini, V., De Giovanni, N., Pascali, V. L., & Strano-Rossi, S. (2017). High-throughput screening for drugs of abuse and pharmaceutical drugs in hair by liquid-chromatography-high resolution mass spectrometry (LC-HRMS). *Microchemical Journal*, *133*, 302-310. https://doi.org/10.1016/j.microc.2017.03.050

OECD. (2018). Considerations for Assessing the Risks of Combined Exposure to Multiple Chemicals, Series on Testing and Assessment No. 296, Environment, Health and Safety Division, Environment Directorate. https://www.oecd.org/chemicalsafety/risk-assessment/considerations-for-assessing-the-risks-of-combined-exposure-to-multiple-chemicals.pdf

OECD. (2022). The current plastics lifecycle is far from circular. *OECD Publishing*. https://www.oecd.org/environment/plastics/plastics-lifecycle-is-far-from-circular.htm

Oehlmann, J., Schulte-Oehlmann, U., Kloas, W., Jagnytsch, O., Lutz, I., Kusk, K. O., Wollenberger, L., Santos, E. M., Paull, G. C., Van Look, K. J. W., & Tyler, C. R. (2009). A critical analysis of the biological impacts of plasticizers on wildlife. *Philosophical Transactions of the Royal Society B: Biological Sciences*, *364*(1526), 2047-2062. https://doi.org/10.1098/rstb.2008.0242

Ololade, I. A. (2014). Spatial distribution of perfluorooctane sulfonate (PFOS) in major rivers in southwest Nigeria. *Toxicological & Environmental Chemistry*, *96*(9), 1356-1365. https://doi.org/10.1080/02772248.2015.1028409

Paluselli, A., Aminot, Y., Galgani, F., Net, S., & Sempéré, R. (2018). Occurrence of phthalate acid esters (PAEs) in the northwestern Mediterranean Sea and the Rhone River. *Progress in Oceanography*, *163*, 221-231. https://doi.org/10.1016/j.pocean.2017.06.002

Paluselli, A., Fauvelle, V., Galgani, F., & Sempéré, R. (2019). Phthalate Release from Plastic Fragments and Degradation in Seawater. *Environmental Science & Technology*, *53*(1), 166-175. https://doi.org/10.1021/acs.est.8b05083

Paluselli, A., & Kim, S.-K. (2020). Horizontal and vertical distribution of phthalates acid ester (PAEs) in seawater and sediment of East China Sea and Korean South Sea: Traces of plastic debris? *Marine Pollution Bulletin*, *151*, 110831. https://doi.org/10.1016/j.marpolbul.2019.110831

Pan, C.-G., Ying, G.-G., Liu, Y.-S., Zhang, Q.-Q., Chen, Z.-F., Peng, F.-J., & Huang, G.-Y. (2014). Contamination profiles of perfluoroalkyl substances in five typical rivers of the Pearl River Delta region, South China. *Chemosphere*, *114*, 16-25. https://doi.org/10.1016/j.chemosphere.2014.04.005

Pan, W., Kang, Y., Zeng, L., Zhang, Q., Luo, J., & Wong, M. H. (2016). Comparison of in vitro digestion model with in vivo relative bioavailability of BDE-209 in indoor dust and combination of in vitro digestion/Caco-2 cell model to estimate the daily intake of BDE-209 via indoor dust. *Environmental Pollution*, *218*, 497-504. https://doi.org/10.1016/j.envpol.2016.07.029

Panchangam, S. C., Lin, A. Y.-C., Shaik, K. L., & Lin, C.-F. (2009). Decomposition of perfluorocarboxylic acids (PFCAs) by heterogeneous photocatalysis in acidic aqueous medium. *Chemosphere*, *77*(2), 242-248. https://doi.org/10.1016/j.chemosphere.2009.07.003

Peez, N., Janiska, M.-C., & Imhof, W. (2019). The first application of quantitative 1H NMR spectroscopy as a simple and fast method of identification and quantification of microplastic particles (PE, PET, and PS). *Analytical and Bioanalytical Chemistry*, *411*(4), 823-833. https://doi.org/10.1007/s00216-018-1510-z

Perrott, M. N., Grierson, C. E., Hazon, N., & Balment, R. J. (1992). Drinking behaviour in sea water and fresh water teleosts, the role of the renin-angiotensin system. *Fish Physiology and Biochemistry*, *10*(2), 161-168. https://doi.org/10.1007/BF00004527

Peters, C. A., Hendrickson, E., Minor, E. C., Schreiner, K., Halbur, J., & Bratton, S. P. (2018). Pyr-GC/MS analysis of microplastics extracted from the stomach content of benthivore fish from the Texas Gulf Coast. *Marine Pollution Bulletin*, *137*, 91-95. https://doi.org/10.1016/j.marpolbul.2018.09.049

Pétré, M.-A., Genereux, D. P., Koropeckyj-Cox, L., Knappe, D. R. U., Duboscq, S., Gilmore, T. E., & Hopkins, Z. R. (2021). Per- and Polyfluoroalkyl Substance (PFAS) Transport from Groundwater to Streams near a PFAS Manufacturing Facility in North Carolina, USA. *Environmental Science & Technology*, *55*(9), 5848-5856. https://doi.org/10.1021/acs.est.0c07978

Point, A. D., Holsen, T. M., Fernando, S., Hopke, P. K., & Crimmins, B. S. (2019). Towards the development of a standardized method for extraction and analysis of PFAS in biological tissues [10.1039/C9EW00765B]. *Environmental Science: Water Research & Technology*, *5*(11), 1876-1886. https://doi.org/10.1039/C9EW00765B

Pojana, G., Gomiero, A., Jonkers, N., & Marcomini, A. (2007). Natural and synthetic endocrine disrupting compounds (EDCs) in water, sediment and biota of a coastal lagoon. *Environment International*, *33*(7), 929-936. https://doi.org/10.1016/j.envint.2007.05.003

Poyatos, J. M., Muñio, M. M., Almecija, M. C., Torres, J. C., Hontoria, E., & Osorio, F. (2010). Advanced Oxidation Processes for Wastewater Treatment: State of the Art. *Water, Air, and Soil Pollution*, *205*(1), 187-204. https://doi.org/10.1007/s11270-009-0065-1

Pozo, K., Urbina, W., Gómez, V., Torres, M., Nuñez, D., Přibylová, P., Audy, O., Clarke, B., Arias, A., Tombesi, N., Guida, Y., & Klánová, J. (2020). Persistent organic pollutants sorbed in plastic resin pellet — "Nurdles" from coastal areas of Central Chile. *Marine Pollution Bulletin*, *151*, 110786. https://doi.org/10.1016/j.marpolbul.2019.110786

Prata, J. C., da Costa, J. P., Duarte, A. C., & Rocha-Santos, T. (2019). Methods for sampling and detection of microplastics in water and sediment: A critical review. *TrAC Trends in Analytical Chemistry*, *110*, 150-159. https://doi.org/10.1016/j.trac.2018.10.029

Prieto, A., Zuloaga, O., Usobiaga, A., Etxebarria, N., & Fernández, L. A. (2007). Development of a stir bar sorptive extraction and thermal desorption–gas chromatography–mass spectrometry method for the simultaneous determination of several persistent organic pollutants in water samples. *Journal of Chromatography A*, *1174*(1), 40-49. https://doi.org/10.1016/j.chroma.2007.07.054

Quinn, B., Murphy, F., & Ewins, C. (2017). Validation of density separation for the rapid recovery of microplastics from sediment [10.1039/C6AY02542K]. *Analytical Methods*, *9*(9), 1491-1498. https://doi.org/10.1039/C6AY02542K

Quintana, J. B., Rosende, M., Montes, R., Rodríguez-Álvarez, T., Rodil, R., Cela, R., & Miró, M. (2017). In-vitro estimation of bioaccessibility of chlorinated organophosphate flame

retardants in indoor dust by fasting and fed physiologically relevant extraction tests. *Science of The Total Environment*, *580*, 540-549. https://doi.org/10.1016/j.scitotenv.2016.11.210

Radjenovic, J., Duinslaeger, N., Avval, S. S., & Chaplin, B. P. (2020). Facing the Challenge of Poly- and Perfluoroalkyl Substances in Water: Is Electrochemical Oxidation the Answer? *Environmental Science & Technology*, *54*(23), 14815-14829. https://doi.org/10.1021/acs.est.0c06212

Radjenovic, J., & Sedlak, D. L. (2015). Challenges and Opportunities for Electrochemical Processes as Next-Generation Technologies for the Treatment of Contaminated Water. *Environmental Science & Technology*, *49*(19), 11292-11302. https://doi.org/10.1021/acs.est.5b02414

Raffy, G., Mercier, F., Glorennec, P., Mandin, C., & Le Bot, B. (2018). Oral bioaccessibility of semi-volatile organic compounds (SVOCs) in settled dust: A review of measurement methods, data and influencing factors. *Journal of Hazardous Materials*, *352*, 215-227. https://doi.org/10.1016/j.jhazmat.2018.03.035

Rafieenia, R., Sulonen, M., Mahmoud, M., El-Gohary, F., & Rossa, C. A. (2022). Integration of microbial electrochemical systems and photocatalysis for sustainable treatment of organic recalcitrant wastewaters: Main mechanisms, recent advances, and present prospects. *Science of The Total Environment*, *824*, 153923. https://doi.org/10.1016/j.scitotenv.2022.153923

Rahman, A., Sarkar, A., Yadav, O. P., Achari, G., & Slobodnik, J. (2021). Potential human health risks due to environmental exposure to nano- and microplastics and knowledge gaps: A scoping review. *Science of The Total Environment*, *757*, 143872. https://doi.org/10.1016/j.scitotenv.2020.143872

Rahman, M. F., Peldszus, S., & Anderson, W. B. (2014). Behaviour and fate of perfluoroalkyl and polyfluoroalkyl substances (PFASs) in drinking water treatment: A review. *Water Research*, *50*, 318-340. https://doi.org/10.1016/j.watres.2013.10.045

Rani, M., Shim, W. J., Han, G. M., Jang, M., Al-Odaini, N. A., Song, Y. K., & Hong, S. H. (2015). Qualitative Analysis of Additives in Plastic Marine Debris and Its New Products. *Archives of Environmental Contamination and Toxicology*, *69*(3), 352-366. https://doi.org/10.1007/s00244-015-0224-x

Real Decreto 1/2016, de 8 de enero, por el que se aprueba la revisión de los Planes Hidrológicos de las demarcaciones hidrográficas del Cantábrico Occidental, Guadalquivir, Ceuta, Melilla, Segura y Júcar, y de la parte española de las demarcaciones hidrográficas del Cantábrico Oriental, Miño-Sil, Duero, Tajo, Guadiana y Ebro., 2972-4301 16.

Remya, N., & Lin, J.-G. (2011). Current status of microwave application in wastewater treatment—A review. *Chemical Engineering Journal*, *166*(3), 797-813. https://doi.org/10.1016/j.cej.2010.11.100

Renner, G., Nellessen, A., Schwiers, A., Wenzel, M., Schmidt, T. C., & Schram, J. (2020). Hydrophobicity–water/air–based enrichment cell for microplastics analysis within environmental samples: A proof of concept. *MethodsX*, *7*, 100732. https://doi.org/10.1016/j.mex.2019.11.006

Rios-Fuster, B., Alomar, C., Paniagua González, G., Garcinuño Martínez, R. M., Soliz Rojas, D. L., Fernández Hernando, P., & Deudero, S. (2022). Assessing microplastic ingestion and occurrence of bisphenols and phthalates in bivalves, fish and holothurians from a Mediterranean marine protected area. *Environmental Research*, *214*, 114034. https://doi.org/10.1016/j.envres.2022.114034

Rios, L. M., Moore, C., & Jones, P. R. (2007). Persistent organic pollutants carried by synthetic polymers in the ocean environment. *Marine Pollution Bulletin*, *54*(8), 1230-1237. https://doi.org/10.1016/j.marpolbul.2007.03.022

Ritchie, H., Roser, M. (2018). *Plastic Pollution*. Retrieved 24 Oct from https://ourworldindata.org/plastic-pollution#citation

Roch, S., & Brinker, A. (2017). Rapid and Efficient Method for the Detection of Microplastic in the Gastrointestinal Tract of Fishes. *Environmental Science & Technology*, *51*(8), 4522-4530. https://doi.org/10.1021/acs.est.7b00364

Rochman, C. M. (2015). The complex mixture, fate and toxicity of chemicals associated with plastic debris in the marine environment. *Marine anthropogenic litter*, 117-140. https://doi.org/10.1007/978-3-319-16510-3_5

Rochman, C. M., Hoh, E., Kurobe, T., & Teh, S. J. (2013). Ingested plastic transfers hazardous chemicals to fish and induces hepatic stress. *Scientific Reports*, *3*(1), 3263. https://doi.org/10.1038/srep03263

Rosende, M., Prieto, A., Etxebarria, N., Martorell, G., & Miró, M. (2019). Automatic Mesofluidic System Combining Dynamic Gastrointestinal Bioaccessibility with Lab-on-Valve-Based Sorptive Microextraction for Risk Exposure of Organic Emerging Contaminants in Filter-Feeding Organisms. *Analytical Chemistry*, *91*(9), 5739-5746. https://doi.org/10.1021/acs.analchem.8b05870

Ruby, M. V., Davis, A., Schoof, R., Eberle, S., & Sellstone, C. M. (1996). Estimation of Lead and Arsenic Bioavailability Using a Physiologically Based Extraction Test. *Environmental Science & Technology*, *30*(2), 422-430. https://doi.org/10.1021/es950057z

Ruby, M. V., Fehling, K. A., Paustenbach, D. J., Landenberger, B. D., & Holsapple, M. P. (2002). Oral Bioaccessibility of Dioxins/Furans at Low Concentrations (50−350 ppt Toxicity Equivalent) in Soil. *Environmental Science & Technology*, *36*(22), 4905-4911. https://doi.org/10.1021/es020636l

Saadati, N., Abdullah, M. P., Zakaria, Z., Sany, S. B., Rezayi, M., & Hassonizadeh, H. (2013). Limit of detection and limit of quantification development procedures for organochlorine pesticides analysis in water and sediment matrices. *Chem Cent J*, *7*(1), 63. https://doi.org/10.1186/1752-153x-7-63

Saeidnia, S. (2014). Phthalates. *Encyclopedia of Toxicology*, *3*, 928-933. https://doi.org/10.1016/B978-0-12-386454-3.00963-5

Salgueiro-González, N., Campillo, J. A., Viñas, L., Beiras, R., López-Mahía, P., & Muniategui-Lorenzo, S. (2019). Occurrence of selected endocrine disrupting compounds in Iberian coastal areas and assessment of the environmental risk. *Environmental Pollution*, *249*, 767-775. https://doi.org/10.1016/j.envpol.2019.03.107

Salgueiro-González, N., Turnes-Carou, I., Viñas-Diéguez, L., Muniategui-Lorenzo, S., López-Mahía, P., & Prada-Rodríguez, D. (2015). Occurrence of endocrine disrupting compounds in five estuaries of the northwest coast of Spain: Ecological and human health impact. *Chemosphere*, *131*, 241-247. https://doi.org/10.1016/j.chemosphere.2014.12.062

Salihovic, S., Mattioli, L., Lindström, G., Lind, L., Monica Lind, P., & Bavel, B. v. (2012). A rapid method for screening of the Stockholm Convention POPs in small amounts of human plasma using SPE and HRGC/HRMS. *Chemosphere*, *86*(7), 747-753. https://doi.org/10.1016/j.chemosphere.2011.11.006

Sánchez-Avila, J., Fernandez-Sanjuan, M., Vicente, J., & Lacorte, S. (2011). Development of a multi-residue method for the determination of organic micropollutants in water,

sediment and mussels using gas chromatography–tandem mass spectrometry. *Journal of Chromatography A*, *1218*(38), 6799-6811. https://doi.org/10.1016/j.chroma.2011.07.056

Sánchez-Avila, J., Tauler, R., & Lacorte, S. (2012). Organic micropollutants in coastal waters from NW Mediterranean Sea: Sources distribution and potential risk. *Environment International*, *46*, 50-62. https://doi.org/10.1016/j.envint.2012.04.013

Sánchez-Avila, J., Vicente, J., Echavarri-Erasun, B., Porte, C., Tauler, R., & Lacorte, S. (2013). Sources, fluxes and risk of organic micropollutants to the Cantabrian Sea (Spain). *Marine Pollution Bulletin*, *72*(1), 119-132. https://doi.org/10.1016/j.marpolbul.2013.04.010

Sánchez, A., Llanos, J., Sáez, C., Cañizares, P., & Rodrigo, M. A. (2013). On the applications of peroxodiphosphate produced by BDD-electrolyses. *Chemical Engineering Journal*, *233*, 8-13. https://doi.org/10.1016/j.cej.2013.08.022

Santos, L. H. M. L. M., Insa, S., Arxé, M., Buttiglieri, G., Rodríguez-Mozaz, S., & Barceló, D. (2023). Analysis of microplastics in the environment: Identification and quantification of trace levels of common types of plastic polymers using pyrolysis-GC/MS. *MethodsX*, *10*, 102143. https://doi.org/10.1016/j.mex.2023.102143

Schaefer, C. E., Andaya, C., Burant, A., Condee, C. W., Urtiaga, A., Strathmann, T. J., & Higgins, C. P. (2017). Electrochemical treatment of perfluorooctanoic acid and perfluorooctane sulfonate: Insights into mechanisms and application to groundwater treatment. *Chemical Engineering Journal*, *317*, 424-432. https://doi.org/10.1016/j.cej.2017.02.107

Schaefer, C. E., Andaya, C., Urtiaga, A., McKenzie, E. R., & Higgins, C. P. (2015). Electrochemical treatment of perfluorooctanoic acid (PFOA) and perfluorooctane sulfonic acid (PFOS) in groundwater impacted by aqueous film forming foams (AFFFs). *Journal of Hazardous Materials*, *295*, 170-175. https://doi.org/10.1016/j.jhazmat.2015.04.024

Schlesinger, D. R., McDermott, C., Le, N. Q., Ko, J. S., Johnson, J. K., Demirev, P. A., & Xia, Z. (2022). Destruction of per/poly-fluorinated alkyl substances by magnetite nanoparticle-catalyzed UV-Fenton reaction. *Environmental Science: Water Research & Technology*, *8*(11), 2732-2743. https://doi.org/10.1039/D2EW00058J

Schwanz, T. G., Llorca, M., Farré, M., & Barceló, D. (2016). Perfluoroalkyl substances assessment in drinking waters from Brazil, France and Spain. *Sci Total Environ*, *539*, 143-152. https://doi.org/10.1016/j.scitotenv.2015.08.034

Schymanski, E. L., Jeon, J., Gulde, R., Fenner, K., Ruff, M., Singer, H. P., & Hollender, J. (2014). Identifying Small Molecules via High Resolution Mass Spectrometry: Communicating Confidence. *Environmental Science & Technology*, *48*(4), 2097-2098. https://doi.org/10.1021/es5002105

Schymanski, E. L., Singer, H. P., Slobodnik, J., Ipolyi, I. M., Oswald, P., Krauss, M., Schulze, T., Haglund, P., Letzel, T., Grosse, S., Thomaidis, N. S., Bletsou, A., Zwiener, C., Ibáñez, M., Portolés, T., de Boer, R., Reid, M. J., Onghena, M., Kunkel, U., Schulz, W., Guillon, A., Noyon, N., Leroy, G., Bados, P., Bogialli, S., Stipaničev, D., Rostkowski, P., & Hollender, J. (2015). Non-target screening with high-resolution mass spectrometry: critical review using a collaborative trial on water analysis. *Analytical and Bioanalytical Chemistry*, *407*(21), 6237-6255. https://doi.org/10.1007/s00216-015-8681-7

Scott, B. F., Moody, C. A., Spencer, C., Small, J. M., Muir, D. C. G., & Mabury, S. A. (2006). Analysis for Perfluorocarboxylic Acids/Anions in Surface Waters and Precipitation

Using GC−MS and Analysis of PFOA from Large-Volume Samples. *Environmental Science & Technology*, *40*(20), 6405-6410. https://doi.org/10.1021/es061131o

Senathirajah, K., Attwood, S., Bhagwat, G., Carbery, M., Wilson, S., & Palanisami, T. (2021). Estimation of the mass of microplastics ingested – A pivotal first step towards human health risk assessment. *Journal of Hazardous Materials*, *404*, 124004. https://doi.org/10.1016/j.jhazmat.2020.124004

Sgier, L., Freimann, R., Zupanic, A., & Kroll, A. (2016). Flow cytometry combined with viSNE for the analysis of microbial biofilms and detection of microplastics. *Nature Communications*, *7*(1), 11587. https://doi.org/10.1038/ncomms11587

Sharma, B. M., Bharat, G. K., Tayal, S., Larssen, T., Bečanová, J., Karásková, P., Whitehead, P. G., Futter, M. N., Butterfield, D., & Nizzetto, L. (2016). Perfluoroalkyl substances (PFAS) in river and ground/drinking water of the Ganges River basin: Emissions and implications for human exposure. *Environmental Pollution*, *208*, 704-713. https://doi.org/10.1016/j.envpol.2015.10.050

Shen, Y.-S., & Wang, D.-K. (2002). Development of photoreactor design equation for the treatment of dye wastewater by UV/H2O2 process. *Journal of Hazardous Materials*, *89*(2), 267-277. https://doi.org/10.1016/S0304-3894(01)00317-X

Shimizu, K., Sokolov, S. V., Kätelhön, E., Holter, J., Young, N. P., & Compton, R. G. (2017). In situ Detection of Microplastics: Single Microparticle-electrode Impacts. *Electroanalysis*, *29*(10), 2200-2207. https://doi.org/10.1002/elan.201700213

Shu, S., Shuo, M., & Zhenfeng, Z. (2022). Adsorption of Polyethylene and Polyvinyl Chloride to Phthalate Esters. *Environmental Science & Technology (10036504)*, *45*(8), 9-16. https://doi.org/10.19672/j.cnki.1003-6504.0105.22.338

Silva, A. S., García, R. S., Cooper, I., Franz, R., & Losada, P. P. (2006). Compilation of analytical methods and guidelines for the determination of selected model migrants from plastic packaging. *Trends in Food Science & Technology*, *17*(10), 535-546. https://doi.org/10.1016/j.tifs.2006.04.009

Simcik, M. F., & Dorweiler, K. J. (2005). Ratio of Perfluorochemical Concentrations as a Tracer of Atmospheric Deposition to Surface Waters. *Environmental Science & Technology*, *39*(22), 8678-8683. https://doi.org/10.1021/es0511218

Simon-Sánchez, L., Grelaud, M., Garcia-Orellana, J., & Ziveri, P. (2019). River Deltas as hotspots of microplastic accumulation: The case study of the Ebro River (NW Mediterranean). *Science of The Total Environment*, *687*, 1186-1196. https://doi.org/10.1016/j.scitotenv.2019.06.168

Simon, F., Gehrenkemper, L., Becher, S., Dierkes, G., Langhammer, N., Cossmer, A., von der Au, M., Göckener, B., Fliedner, A., Rüdel, H., Koschorreck, J., & Meermann, B. (2023). Quantification and characterization of PFASs in suspended particulate matter (SPM) of German rivers using EOF, dTOPA, (non-)target HRMS. *Sci Total Environ*, *885*, 163753. https://doi.org/10.1016/j.scitotenv.2023.163753

Sixto, A., El-Morabit, B., Trujillo-Rodríguez, M. J., Carrasco-Correa, E. J., & Miró, M. (2021). An automatic flow-through system for exploration of the human bioaccessibility of endocrine disrupting compounds from microplastics [10.1039/D1AN00446H]. *Analyst*, *146*(12), 3858-3870. https://doi.org/10.1039/D1AN00446H

Skaggs, C. S., & Logue, B. A. (2021). Ultratrace analysis of per- and polyfluoroalkyl substances in drinking water using ice concentration linked with extractive stirrer and high performance liquid chromatography – tandem mass spectrometry. *Journal of Chromatography A*, *1659*, 462493. https://doi.org/10.1016/j.chroma.2021.462493

Smith, E., Weber, J., Rofe, A., Gancarz, D., Naidu, R., & Juhasz, A. L. (2012). Assessment of DDT Relative Bioavailability and Bioaccessibility in Historically Contaminated Soils Using an in Vivo Mouse Model and Fed and Unfed Batch in Vitro Assays. *Environmental Science & Technology*, *46*(5), 2928-2934. https://doi.org/10.1021/es203030q

Staples, C., van der Hoeven, N., Clark, K., Mihaich, E., Woelz, J., & Hentges, S. (2018). Distributions of concentrations of bisphenol A in North American and European surface waters and sediments determined from 19 years of monitoring data. *Chemosphere*, *201*, 448-458. https://doi.org/10.1016/j.chemosphere.2018.02.175

Staples, C. A., Dome, P. B., Klecka, G. M., Oblock, S. T., & Harris, L. R. (1998). A review of the environmental fate, effects, and exposures of bisphenol A. *Chemosphere*, *36*(10), 2149-2173. https://doi.org/10.1016/S0045-6535(97)10133-3

Steenland, K., & Winquist, A. (2021). PFAS and cancer, a scoping review of the epidemiologic evidence. *Environmental Research*, *194*, 110690. https://doi.org/10.1016/j.envres.2020.110690

Stock, F., Kochleus, C., Bänsch-Baltruschat, B., Brennholt, N., & Reifferscheid, G. (2019). Sampling techniques and preparation methods for microplastic analyses in the aquatic environment – A review. *TrAC Trends in Analytical Chemistry*, *113*, 84-92. https://doi.org/10.1016/j.trac.2019.01.014

Sujathan, S., Kniggendorf, A.-K., Kumar, A., Roth, B., Rosenwinkel, K.-H., & Nogueira, R. (2017). Heat and Bleach: A Cost-Efficient Method for Extracting Microplastics from Return Activated Sludge. *Archives of Environmental Contamination and Toxicology*, *73*(4), 641-648. https://doi.org/10.1007/s00244-017-0415-8

Sundkvist, A. M., Olofsson, U., & Haglund, P. (2010). Organophosphorus flame retardants and plasticizers in marine and fresh water biota and in human milk [10.1039/B921910B]. *Journal of Environmental Monitoring*, *12*(4), 943-951. https://doi.org/10.1039/B921910B

Szabo, D., Coggan, T. L., Robson, T. C., Currell, M., & Clarke, B. O. (2018). Investigating recycled water use as a diffuse source of per- and polyfluoroalkyl substances (PFASs) to groundwater in Melbourne, Australia. *Science of The Total Environment*, *644*, 1409-1417. https://doi.org/10.1016/j.scitotenv.2018.07.048

Tagg, A., Harrison, J. P., Ju-Nam, Y., Sapp, M., Bradley, E. L., Sinclair, C. J., & Ojeda, J. J. (2017). Fenton's reagent for the rapid and efficient isolation of microplastics from wastewater. *Chemical Communications*, *53*(2), 372-375. https://doi.org/10.1039/C6CC08798A

Takagi, S., Adachi, F., Miyano, K., Koizumi, Y., Tanaka, H., Mimura, M., Watanabe, I., Tanabe, S., & Kannan, K. (2008). Perfluorooctanesulfonate and perfluorooctanoate in raw and treated tap water from Osaka, Japan. *Chemosphere*, *72*(10), 1409-1412. https://doi.org/10.1016/j.chemosphere.2008.05.034

Takemine, S., Matsumura, C., Yamamoto, K., Suzuki, M., Tsurukawa, M., Imaishi, H., Nakano, T., & Kondo, A. (2014). Discharge of perfluorinated compounds from rivers and their influence on the coastal seas of Hyogo prefecture, Japan. *Environmental Pollution*, *184*, 397-404. https://doi.org/10.1016/j.envpol.2013.09.016

Talsness, C. E., Andrade, A. J. M., Kuriyama, S. N., Taylor, J. A., & vom Saal, F. S. (2009). Components of plastic: experimental studies in animals and relevance for human health. *Philosophical Transactions of the Royal Society B: Biological Sciences*, *364*(1526), 2079-2096. https://doi.org/10.1098/rstb.2008.0281

Tamminga, M., Stoewer, S.-C., & Fischer, E. K. (2019). On the representativeness of pump water samples versus manta sampling in microplastic analysis. *Environmental Pollution*, *254*, 112970. https://doi.org/10.1016/j.envpol.2019.112970

Tan, X., Yu, X., Cai, L., Wang, J., & Peng, J. (2019). Microplastics and associated PAHs in surface water from the Feilaixia Reservoir in the Beijiang River, China. *Chemosphere*, *221*, 834-840. https://doi.org/10.1016/j.chemosphere.2019.01.022

Tang, K. H. D., & Luo, Y. (2023). Abundance and Characteristics of Microplastics in the Soil of a Higher Education Institution in China. *Tropical Aquatic and Soil Pollution*, *3*(1), 1-14. https://doi.org/10.53623/tasp.v3i1.152

Tao, S., Li, L., Ding, J., Zhong, J., Zhang, D., Lu, Y., Yang, Y., Wang, X., Li, X., Cao, J., Lu, X., & Liu, W. (2011). Mobilization of Soil-Bound Residue of Organochlorine Pesticides and Polycyclic Aromatic Hydrocarbons in an in vitro Gastrointestinal Model. *Environmental Science & Technology*, *45*(3), 1127-1132. https://doi.org/10.1021/es1025849

Telving, R., Hasselstrøm, J. B., & Andreasen, M. F. (2016). Targeted toxicological screening for acidic, neutral and basic substances in postmortem and antemortem whole blood using simple protein precipitation and UPLC-HR-TOF-MS. *Forensic Science International*, *266*, 453-461. https://doi.org/10.1016/j.forsciint.2016.07.004

Teuten, E. L., Rowland, S. J., Galloway, T. S., & Thompson, R. C. (2007). Potential for Plastics to Transport Hydrophobic Contaminants. *Environmental Science & Technology*, *41*(22), 7759-7764. https://doi.org/10.1021/es071737s

Thompson, J., Eaglesham, G., & Mueller, J. (2011). Concentrations of PFOS, PFOA and other perfluorinated alkyl acids in Australian drinking water. *Chemosphere*, *83*(10), 1320-1325. https://doi.org/10.1016/j.chemosphere.2011.04.017

Thompson, R. C., Olsen, Y., Mitchell, R. P., Davis, A., Rowland, S. J., John, A. W. G., McGonigle, D., & Russell, A. E. (2004). Lost at Sea: Where Is All the Plastic? *Science*, *304*(5672), 838-838. https://doi.org/10.1126/science.1094559

Tilston, E. L., Gibson, G. R., & Collins, C. D. (2011). Colon Extended Physiologically Based Extraction Test (CE-PBET) Increases Bioaccessibility of Soil-Bound PAH. *Environmental Science & Technology*, *45*(12), 5301-5308. https://doi.org/10.1021/es2004705

Tipsmark, C. K., Nielsen, A. M., Bossus, M. C., Ellis, L. V., Baun, C., Andersen, T. L., Dreier, J., Brewer, J. R., & Madsen, S. S. (2020). Drinking and Water Handling in the Medaka Intestine: A Possible Role of Claudin-15 in Paracellular Absorption? *International Journal of Molecular Sciences*, *21*(5), 1853. https://doi.org/10.3390/ijms21051853

Trautmann, A. M., Schell, H., Schmidt, K. R., Mangold, K.-M., & Tiehm, A. (2015). Electrochemical degradation of perfluoroalkyl and polyfluoroalkyl substances (PFASs) in groundwater. *Water Science and Technology*, *71*(10), 1569-1575. https://doi.org/10.2166/wst.2015.143

Turner, A. (2017). In situ elemental characterisation of marine microplastics by portable XRF. *Marine Pollution Bulletin*, *124*(1), 286-291. https://doi.org/10.1016/j.marpolbul.2017.07.045

UCMR3. (2021). *PFAS Sampling in TN*. Retrieved 18 Mar from

Ünlü Endirlik, B., Bakır, E., Boşgelmez, İ. İ., Eken, A., Narin, İ., & Gürbay, A. (2019). Assessment of perfluoroalkyl substances levels in tap and bottled water samples from Turkey. *Chemosphere*, *235*, 1162-1171. https://doi.org/10.1016/j.chemosphere.2019.06.228

Uriakhil, M. A., Sidnell, T., De Castro Fernández, A., Lee, J., Ross, I., & Bussemaker, M. (2021). Per- and poly-fluoroalkyl substance remediation from soil and sorbents: A review of adsorption behaviour and ultrasonic treatment. *Chemosphere*, *282*, 131025. https://doi.org/10.1016/j.chemosphere.2021.131025

USEPA. (2010). *Hexabromocyclododecane (HBCD) Action Plan*. Retrieved 21 Apr from https://www.epa.gov/assessing-and-managing-chemicals-under-tsca/hexabromocyclododecane-hbcd-action-plan

USEPA. (2012). *Certain Polybrominated Diphenylethers; Significant New Use Rule and Test Rule*. Retrieved 21 Apr from http://blogs.edf.org/health/files/2012/07/EDF_Earthjustice-Comments-on-Proposed-PBDE-test-rule-and-SNUR-FINAL-7-31-12.pdf

USEPA. (2016a). *Drinking Water Health Advisory for Perfluorooctane Sulfonate (PFOS). EPA 822R16004*. Retrieved 28 Mar from https://www.epa.gov/safewater

USEPA. (2016b). *Drinking Water Health Advisory for Perfluorooctanoic Acid (PFOA). EPA 822R16005*. Retrieved 28 Mar from https://www.epa.gov/safewater

USEPA. (2020). *Method 537.1: Determination of Selected Per- and Polyfluorinated Alkyl Substances in Drinking Water by Solid Phase Extraction and Liquid Chromatography/Tandem Mass Spectrometry (LC/MS/MS).* Retrieved 05 Sept from https://cfpub.epa.gov/si/si_public_record_Report.cfm?dirEntryId=348508&Lab=CESER

USEPA. (2023). *PFAS National Primary Drinking Water Regulation Rulemaking* Pre-publication. Retrieved 28 Mar from https://www.epa.gov/system/files/documents/2023-03/Pre-Publication%20Federal%20Register%20Notice_PFAS%20NPDWR_NPRM_Final_3.13.23.pdf

Valsecchi, S., Rusconi, M., Mazzoni, M., Viviano, G., Pagnotta, R., Zaghi, C., Serrini, G., & Polesello, S. (2015). Occurrence and sources of perfluoroalkyl acids in Italian river basins. *Chemosphere*, *129*, 126-134. https://doi.org/10.1016/j.chemosphere.2014.07.044

Van Cauwenberghe, L., Claessens, M., Vandegehuchte, M. B., Mees, J., & Janssen, C. R. (2013). Assessment of marine debris on the Belgian Continental Shelf. *Marine Pollution Bulletin*, *73*(1), 161-169. https://doi.org/10.1016/j.marpolbul.2013.05.026

Van Den Dool, H., & Kratz, P. D. (1963). A generalization of the retention index system including linear temperature programmed gas-liquid partition chromatography. *Journal of Chromatographic*, *11*, 463-471. https://doi.org/10.1016/S0021-9673(01)80947-X

Vasiluk, L., Pinto, L. J., Walji, Z. A., Tsang, W. S., Gobas, F. A. P. C., Eickhoff, C., & Moore, M. M. (2007). Benzo[a]pyrene bioavailability from pristine soil and contaminated sediment assessed using two in vitro models. *Environmental Toxicology and Chemistry*, *26*(3), 387-393. https://doi.org/10.1897/06-343R.1

Vedolin, M. C., Teophilo, C. Y. S., Turra, A., & Figueira, R. C. L. (2018). Spatial variability in the concentrations of metals in beached microplastics. *Marine Pollution Bulletin*, *129*(2), 487-493. https://doi.org/10.1016/j.marpolbul.2017.10.019

Velzeboer, I., Kwadijk, C. J. A. F., & Koelmans, A. A. (2014). Strong Sorption of PCBs to Nanoplastics, Microplastics, Carbon Nanotubes, and Fullerenes. *Environmental Science & Technology*, *48*(9), 4869-4876. https://doi.org/10.1021/es405721v

Versantvoort, C. H. M., Oomen, A. G., Van de Kamp, E., Rompelberg, C. J. M., & Sips, A. J. A. M. (2005). Applicability of an in vitro digestion model in assessing the

bioaccessibility of mycotoxins from food. *Food and Chemical Toxicology*, *43*(1), 31-40. https://doi.org/10.1016/j.fct.2004.08.007

Vethaak, A. D., & Leslie, H. A. (2016). Plastic Debris Is a Human Health Issue. *Environmental Science & Technology*, *50*(13), 6825-6826. https://doi.org/10.1021/acs.est.6b02569

Vialkova, E., Obukhova, M., & Belova, L. (2021). Microwave Irradiation in Technologies of Wastewater and Wastewater Sludge Treatment: A Review. *Water*, *13*(13), 1784. https://doi.org/10.3390/w13131784

von Gunten, U. (2003). Ozonation of drinking water: Part I. Oxidation kinetics and product formation. *Water Research*, *37*(7), 1443-1467. https://doi.org/10.1016/S0043-1354(02)00457-8

Wagner, S., & Schlummer, M. (2020). Legacy additives in a circular economy of plastics: Current dilemma, policy analysis, and emerging countermeasures. *Resources, Conservation and Recycling*, *158*, 104800. https://doi.org/10.1016/j.resconrec.2020.104800

Walpole, S. C., Prieto-Merino, D., Edwards, P., Cleland, J., Stevens, G., & Roberts, I. (2012). The weight of nations: an estimation of adult human biomass. *BMC Public Health*, *12*(1), 439. https://doi.org/10.1186/1471-2458-12-439

Wang, F., Shih, K. M., & Li, X. Y. (2015). The partition behavior of perfluorooctanesulfonate (PFOS) and perfluorooctanesulfonamide (FOSA) on microplastics. *Chemosphere*, *119*, 841-847. https://doi.org/10.1016/j.chemosphere.2014.08.047

Wang, J., Shi, Y., & Cai, Y. (2018). A highly selective dispersive liquid–liquid microextraction approach based on the unique fluorous affinity for the extraction and detection of per- and polyfluoroalkyl substances coupled with high performance liquid chromatography tandem–mass spectrometry. *Journal of Chromatography A*, *1544*, 1-7. https://doi.org/10.1016/j.chroma.2018.02.047

Wang, J., & Wang, S. (2018). Activation of persulfate (PS) and peroxymonosulfate (PMS) and application for the degradation of emerging contaminants. *Chemical Engineering Journal*, *334*, 1502-1517. https://doi.org/10.1016/j.cej.2017.11.059

Wang, L., Bassiri, M., Najafi, R., Najafi, K., Yang, J., Khosrovi, B., Hwong, W., Barati, E., Belisle, B., Celeri, C., & Robson, M. C. (2007). Hypochlorous acid as a potential wound care agent: part I. Stabilized hypochlorous acid: a component of the inorganic armamentarium of innate immunity. *J Burns Wounds*, *6*, e5. https://www.ncbi.nlm.nih.gov/pmc/articles/PMC1853323/pdf/jobw06e5.pdf

Wang, P., Lu, Y., Wang, T., Zhu, Z., Li, Q., Meng, J., Su, H., Johnson, A. C., & Sweetman, A. J. (2016). Coupled production and emission of short chain perfluoroalkyl acids from a fast developing fluorochemical industry: Evidence from yearly and seasonal monitoring in Daling River Basin, China. *Environ Pollut*, *218*, 1234-1244. https://doi.org/10.1016/j.envpol.2016.08.079

Wang, S., Cai, Y., Ma, L., Lin, X., Li, Q., Li, Y., & Wang, X. (2022). Perfluoroalkyl substances in water, sediment, and fish from a subtropical river of China: Environmental behaviors and potential risk. *Chemosphere*, *288*, 132513. https://doi.org/10.1016/j.chemosphere.2021.132513

Wang, Y., Pierce, R. D., Shi, H., Li, C., & Huang, Q. (2020). Electrochemical degradation of perfluoroalkyl acids by titanium suboxide anodes [10.1039/C9EW00759H]. *Environmental Science: Water Research & Technology*, *6*(1), 144-152. https://doi.org/10.1039/C9EW00759H

Wang, Y., Zhang, P., Pan, G., & Chen, H. (2008). Ferric ion mediated photochemical decomposition of perfluorooctanoic acid (PFOA) by 254nm UV light. *Journal of Hazardous Materials*, *160*(1), 181-186. https://doi.org/10.1016/j.jhazmat.2008.02.105

Weissermel, K., Arpe, H. (1981). *Química orgánica industrial: productos de partida e intermedios más importantes*. Reverté.

Wilson, E. W., Castro, V., Chaves, R., Espinosa, M., Rodil, R., Quintana, J. B., Vieira, M. N., & Santos, M. M. (2021). Using zebrafish embryo bioassays combined with high-resolution mass spectrometry screening to assess ecotoxicological water bodies quality status: A case study in Panama rivers. *Chemosphere*, *272*, 129823. https://doi.org/10.1016/j.chemosphere.2021.129823

Wilson, S. R., Malerød, H., Holm, A., Molander, P., Lundanes, E., & Greibrøkk, T. (2007). On-line SPE—Nano-LC—Nanospray-MS for Rapid and Sensitive Determination of Perfluorooctanoic Acid and Perfluorooctane Sulfonate in River Water. *Journal of Chromatographic Science*, *45*(3), 146-152. https://doi.org/10.1093/chromsci/45.3.146

Wolf, S., Schmidt, S., Müller-Hannemann, M., & Neumann, S. (2010). In silico fragmentation for computer assisted identification of metabolite mass spectra. *BMC Bioinformatics*, *11*(1), 148. https://doi.org/10.1186/1471-2105-11-148

Wong, S. L., Ngadi, N., & Abdullah, T. A. T. (2015). Study on Dissolution of Low Density Polyethylene (LDPE). *Applied Mechanics and Materials*, *695*, 170-173. https://doi.org/10.4028/www.scientific.net/AMM.695.170

Wu, C., Zhang, K., Huang, X., & Liu, J. (2016). Sorption of pharmaceuticals and personal care products to polyethylene debris. *Environmental Science and Pollution Research*, *23*(9), 8819-8826. https://doi.org/10.1007/s11356-016-6121-7

Xu, E. G., Chan, S. N., Choi, K. W., Lee, J. H. W., & Leung, K. M. Y. (2018). Tracking major endocrine disruptors in coastal waters using an integrative approach coupling field-based study and hydrodynamic modeling. *Environmental Pollution*, *233*, 387-394. https://doi.org/10.1016/j.envpol.2017.10.086

Yang, S., Cheng, J., Sun, J., Hu, Y., & Liang, X. (2013). Defluorination of aqueous perfluorooctanesulfonate by activated persulfate oxidation. *PloS one*, *8*(10), e74877. https://doi.org/10.1371/journal.pone.0074877

Yaranal, N. A., Subbiah, S., & Mohanty, K. (2021). Distribution and characterization of microplastics in beach sediments from Karnataka (India) coastal environments. *Marine Pollution Bulletin*, *169*, 112550. https://doi.org/10.1016/j.marpolbul.2021.112550

Yin, H., Chen, R., Wang, H., Schwarz, C., Hu, H., Shi, B., & Wang, Y. (2023). Co-occurrence of phthalate esters and perfluoroalkyl substances affected bacterial community and pathogenic bacteria growth in rural drinking water distribution systems. *Science of The Total Environment*, *856*, 158943. https://doi.org/10.1016/j.scitotenv.2022.158943

Yu, X., Peng, J., Wang, J., Wang, K., & Bao, S. (2016). Occurrence of microplastics in the beach sand of the Chinese inner sea: the Bohai Sea. *Environmental Pollution*, *214*, 722-730. https://doi.org/10.1016/j.envpol.2016.04.080

Yu, Y.-X., Chen, L., Yang, D., Pang, Y.-P., Zhang, S.-H., Zhang, X.-Y., Yu, Z.-Q., Wu, M.-H., & Fu, J.-M. (2012). Polycyclic aromatic hydrocarbons in animal-based foods from Shanghai: bioaccessibility and dietary exposure. *Food Additives & Contaminants: Part A*, *29*(9), 1465-1474. https://doi.org/10.1080/19440049.2012.694121

Yu, Y., Yang, D., Wang, X., Huang, N., Zhang, X., Zhang, D., & Fu, J. (2013). Factors influencing on the bioaccessibility of polybrominated diphenyl ethers in size-specific dust from air conditioner filters. *Chemosphere*, *93*(10), 2603-2611. https://doi.org/10.1016/j.chemosphere.2013.09.085

Yuan, W., Liu, X., Wang, W., Di, M., & Wang, J. (2019). Microplastic abundance, distribution and composition in water, sediments, and wild fish from Poyang Lake, China. *Ecotoxicology and Environmental Safety*, *170*, 180-187. https://doi.org/10.1016/j.ecoenv.2018.11.126

Zada, L., Leslie, H. A., Vethaak, A. D., Tinnevelt, G. H., Jansen, J. J., de Boer, J. F., & Ariese, F. (2018). Fast microplastics identification with stimulated Raman scattering microscopy. *Journal of Raman Spectroscopy*, *49*(7), 1136-1144. https://doi.org/10.1002/jrs.5367

Zaharia, C., Suteu, D., Muresan, A., Muresan, R., & Popescu, A. (2009). Textile wastewater treatment by homogenous oxidation with hydrogen peroxide. *Environmental Engineering and Management Journal*, *8*(6), 1359-1369. https://doi.org/10.30638/eemj.2009.199

Zenobio, J. E., Salawu, O. A., Han, Z., & Adeleye, A. S. (2022). Adsorption of per- and polyfluoroalkyl substances (PFAS) to containers. *Journal of Hazardous Materials Advances*, *7*, 100130. https://doi.org/10.1016/j.hazadv.2022.100130

Zhang, B., Wu, D., Yang, X., Teng, J., Liu, Y., Zhang, C., Zhao, J., Yin, X., You, L., Liu, Y., & Wang, Q. (2019). Microplastic pollution in the surface sediments collected from Sishili Bay, North Yellow Sea, China. *Marine Pollution Bulletin*, *141*, 9-15. https://doi.org/10.1016/j.marpolbul.2019.02.021

Zhang, Q., Song, J., Li, X., Peng, Q., Yuan, H., Li, N., Duan, L., & Ma, J. (2019). Concentrations and distribution of phthalate esters in the seamount area of the Tropical Western Pacific Ocean. *Marine Pollution Bulletin*, *140*, 107-115. https://doi.org/10.1016/j.marpolbul.2019.01.015

Zhang, Q., Xu, E. G., Li, J., Chen, Q., Ma, L., Zeng, E. Y., & Shi, H. (2020). A Review of Microplastics in Table Salt, Drinking Water, and Air: Direct Human Exposure. *Environmental Science & Technology*, *54*(7), 3740-3751. https://doi.org/10.1021/acs.est.9b04535

Zhang, W., Zhang, Q., & Liang, Y. (2022). Ineffectiveness of ultrasound at low frequency for treating per- and polyfluoroalkyl substances in sewage sludge. *Chemosphere*, *286*, 131748. https://doi.org/10.1016/j.chemosphere.2021.131748

Zhuo, Q., Deng, S., Yang, B., Huang, J., Wang, B., Zhang, T., & Yu, G. (2012). Degradation of perfluorinated compounds on a boron-doped diamond electrode. *Electrochimica Acta*, *77*, 17-22. https://doi.org/10.1016/j.electacta.2012.04.145

Ziajahromi, S., Neale, P. A., Rintoul, L., & Leusch, F. D. L. (2017). Wastewater treatment plants as a pathway for microplastics: Development of a new approach to sample wastewater-based microplastics. *Water Research*, *112*, 93-99. https://doi.org/10.1016/j.watres.2017.01.042

Ziccardi, L. M., Edgington, A., Hentz, K., Kulacki, K. J., & Kane Driscoll, S. (2016). Microplastics as vectors for bioaccumulation of hydrophobic organic chemicals in the marine environment: A state-of-the-science review. *Environmental Toxicology and Chemistry*, *35*(7), 1667-1676. https://doi.org/10.1002/etc.3461

Zincke, T. (1905). Ueber die Einwirkung von Brom und von Chlor auf Phenole: Substitutionsproducte, Pseudobromide und Pseudochloride. *Justus Liebigs Annalen der Chemie*, *343*(1), 75-99. https://doi.org/10.1002/jlac.19053430106

Zobkov, M., Zobkova, M., Galakhina, N., & Efremova, T. (2020). Method for microplastics extraction from Lake sediments. *MethodsX*, *7*, 101140. https://doi.org/10.1016/j.mex.2020.101140

ANNEX

ANNEX: LIST OF PUBLICATIONS AND CONTRIBUTION STATEMENT

Data are compiled from Web of Science (Clarivate Analytics) as on November, 1st 2023.

1. Javier López-Vázquez, Rosario Rodil, María J. Trujillo-Rodríguez, José Benito Quintana, Rafael Cela and Manuel Miró. Mimicking human ingestion of microplastics: Oral bioaccessibility tests of bisphenol A and phthalate esters under fed and fasted states. Science of the Total Environment (2022). DOI: 10.1016/j.scitotenv.2022.154027.
   Impact factor (2022): 9.8

   Journal ranking (2022): Environmental Sciences, 26 of 275.

   Citations: 3

   Contribution statement: I was responsible for performing all laboratory experiments, chromatographic analysis and data processing and treatment related to the corresponding chemical analyses described in the manuscript. I wrote the original draft of the manuscript and provided critical feedback during subsequent manuscript elaboration. All authors provided critical feedback and helped shape to the final version of the manuscript.

Publications related to other chapters of this thesis are currently under development.

This thesis investigates the determination of microplastics (MPs), per- and poly luoroalkyl substances (PFAS), and plastic-related chemicals and their potential effects on environmental and human health. It presents new methods for the determination of MPs in marine sediment, the dynamics of MPs-chemicals association in the marine environment, and further in-vitro bioaccessibility of phthalate compounds and bisphenol A from MPs. Furthermore, this thesis introduces a novel method for PFAS determination in drinking water in response to Directive 2020/2184/EU and it explores a new electrochemical oxidation-based remediation technology.